

Award Number: W81XWH-04-1-0106

TITLE: Glutamate Receptor Aptamers and ALS

PRINCIPAL INVESTIGATOR: Li Niu

CONTRACTING ORGANIZATION: University at Albany, SUNY
Albany, New York 12222

REPORT DATE: January 2008

TYPE OF REPORT: Annual

PREPARED FOR: U.S. Army Medical Research and Materiel Command
Fort Detrick, Maryland 21702-5012

DISTRIBUTION STATEMENT: Approved for Public Release;
Distribution Unlimited

The views, opinions and/or findings contained in this report are those of the author(s) and should not be construed as an official Department of the Army position, policy or decision unless so designated by other documentation.

REPORT DOCUMENTATION PAGE

Form Approved
OMB No. 0704-0188

Public reporting burden for this collection of information is estimated to average 1 hour per response, including the time for reviewing instructions, searching existing data sources, gathering and maintaining the data needed, and completing and reviewing this collection of information. Send comments regarding this burden estimate or any other aspect of this collection of information, including suggestions for reducing this burden to Department of Defense, Washington Headquarters Services, Directorate for Information Operations and Reports (0704-0188), 1215 Jefferson Davis Highway, Suite 1204, Arlington, VA 22202-4302. Respondents should be aware that notwithstanding any other provision of law, no person shall be subject to any penalty for failing to comply with a collection of information if it does not display a currently valid OMB control number. **PLEASE DO NOT RETURN YOUR FORM TO THE ABOVE ADDRESS.**

1. REPORT DATE 07-01-2008		2. REPORT TYPE Annual		3. DATES COVERED 8 DEC 2006 - 7 DEC 2007	
4. TITLE AND SUBTITLE Glutamate Receptor Aptamers and ALS				5a. CONTRACT NUMBER	
				5b. GRANT NUMBER W81XWH-04-1-0106	
				5c. PROGRAM ELEMENT NUMBER	
6. AUTHOR(S) Li Niu Email: lniu@albany.edu				5d. PROJECT NUMBER	
				5e. TASK NUMBER	
				5f. WORK UNIT NUMBER	
7. PERFORMING ORGANIZATION NAME(S) AND ADDRESS(ES) University at Albany, SUNY Albany, New York 12222				8. PERFORMING ORGANIZATION REPORT NUMBER	
9. SPONSORING / MONITORING AGENCY NAME(S) AND ADDRESS(ES) U.S. Army Medical Research and Materiel Command Fort Detrick, Maryland 21702-5012				10. SPONSOR/MONITOR'S ACRONYM(S)	
				11. SPONSOR/MONITOR'S REPORT NUMBER(S)	
12. DISTRIBUTION / AVAILABILITY STATEMENT Approved for Public Release; Distribution Unlimited					
13. SUPPLEMENTARY NOTES					
14. ABSTRACT Excitotoxicity is one of the leading causes for amyotrophic lateral sclerosis (ALS). Our goal was to develop a novel class of powerful aptamer-based, anti-excitotoxic inhibitors against GluR2Qflip, a key AMPA receptor subunit that controls the calcium permeability and mediates excitotoxicity. An aptamer is a single-stranded nucleic acid that directly inhibits a protein's function by folding into a specific tertiary structure that dictates high-affinity binding to the target protein. To date, we have identified two classes of aptamers (i.e. competitive and noncompetitive aptamers) against GluR2Qflip, by using a molecular biology approach called systematic evolution of ligands by exponential enrichment (SELEX). These aptamers are water soluble and have a nanomolar affinity against GluR2Qflip. Their inhibitory properties rival those of any existing small, chemical inhibitors. We are continuing to work with these aptamers towards developing them into anti-excitotoxic drugs for treating patients with ALS, including those Gulf War veterans suffering from ALS.					
15. SUBJECT TERMS ALS, anti-excitotoxic drugs, aptamers, glutamate receptors					
16. SECURITY CLASSIFICATION OF:			17. LIMITATION OF ABSTRACT	18. NUMBER OF PAGES	19a. NAME OF RESPONSIBLE PERSON USAMRMC
a. REPORT U	b. ABSTRACT U	c. THIS PAGE U			19b. TELEPHONE NUMBER (include area code)
			UU	101	

Table of Contents

	<u>Page</u>
Introduction	3
Body	3
Key Research Accomplishments	16
Reportable Outcomes	17
Conclusions	18
References	19
Appendices	22

1. INTRODUCTION

Studies of Gulf War veterans with ALS have suggested a link of Gulf War service to this fatal neurodegenerative disease. Although the pathogenesis of the war-related ALS is unknown, the excitotoxicity or excessive excitatory neurotransmission, mainly mediated by the AMPA-type (α -amino-3-hydroxy-5-methyl-4-isoxazole propionate) glutamate receptors, may play a central role in the selective motor neuron death in ALS. Thus, developing AMPA receptor inhibitors to control the receptor-mediated neurodegeneration has been a long-pursued therapeutic effort. To date, virtually all inhibitors are chemically synthesized. The majority of these compounds, however, show poor water solubility and cross activity with other glutamate receptor subtypes. Furthermore, no kinetic method is available to screen inhibitors against functional receptor states, which are formed after glutamate binding, but only exist for no more than a few milliseconds. All these problems have significantly hindered design of inhibitors/drugs for an effective ALS therapy. The goal of this project was to develop water soluble, more potent and specific inhibitors, which are aptamers (i.e., RNA inhibitors), as a novel class of anti-excitotoxic drugs. The hypothesis to be tested is that potent and selective AMPA receptor inhibitors (aptamers) can be developed by a novel combination of two approaches, namely, an *in vitro* iteration procedure or systematic evolution of ligands by exponential enrichment (SELEX) to select aptamers from a combinatorial RNA library and a laser-pulse photolysis technique that has a microsecond time resolution to screen the RNAs against the *functional* forms (i.e., non-desensitized) of the receptors.

The aptamers we propose to develop is of novelty in both strategy and outcome of drug design. First, aptamers are different from chemically synthesized compounds in that an aptamer is a single-stranded nucleic acid that directly inhibits a protein's function. The inhibitory property of the aptamer is through its uniquely folded three-dimensional structure that confers a high affinity. Furthermore, aptamers are water soluble by nature. Second, the use of SELEX (see Fig. 1 below) to evolve aptamers does not require the knowledge of the structure of the target protein. Third, the laser-pulse photolysis technique we developed previously will be used as a critical method to screen the aptamers against the GluR2Q_{flip} open-channel conformation that exists less than a few milliseconds after binding of glutamate. To test this hypothesis, I proposed three Tasks.

In Task 1, high affinity RNA aptamers that target GluR2 AMPA receptors will be selected from an RNA library consisting of $\sim 10^{13}$ sequences using SELEX. Three AMPA receptor inhibitors (NBQX, philanthotoxin-343 and GYKI 47261) were proposed to displace RNAs previously bound to the receptor sites. By our design, two types of aptamers, competitive (using NBQX, a classic competitive antagonist) and noncompetitive (using philanthotoxin and GYKI inhibitor), are expected. This is because RNA molecules bound to the same site and/or to site mutually exclusive as a compound listed above are eluted during the selection.

In Task 2, each of the four AMPA receptor subunits, i.e., GluR1 to GluR4, will be expressed in HEK-293 cells. The channel opening kinetics of the homomeric channel will be characterized using the laser-pulse photolysis and caged glutamate. The channel-opening and the channel-closing rate constants as well as the dissociation equilibrium constant for glutamate will be determined. Likewise, two representative kainate receptor subunits, GluR5Q and GluR6Q, both of which can form the corresponding homomeric receptor channel respectively, will be characterized.

In Task 3, the affinity of an aptamer for both the closed and open forms of a homomeric AMPA receptor channel will be measured. The selectivity of each aptamer for all AMPA receptor subunits will also be determined. The use of the kainate receptors ensures that the desired aptamers will be selective to AMPA receptors, while the use of individual AMPA receptors further ensures that subunit-specific aptamers within the AMPA receptor subtype will be identified.

2. BODY

To date, we have identified two classes of aptamers, both of which have apparent K_I in the nanomolar region for inhibiting the GluR2Q_{flip} receptor channel. These two classes are competitive and noncompetitive aptamers. In the noncompetitive category, we further identified two groups of aptamers specific towards unique receptor conformations. One group shows specificity towards the open-channel form whereas the other shows the higher affinity for the closed-channel receptor conformation. I should emphasize that aptamers as high

affinity, water soluble compounds have been never been reported previously. Furthermore, there is no known inhibitor targeting specific AMPA receptor conformations. Therefore, our work not only represents a conceptual advance in development of inhibitors but also materialization of some unique inhibitors ready to be developed into potential therapeutics. Below I wish to introduce the methodology we have used before describe specific accomplishments.

2.1. Methods

2.1.1. Selection of Aptamers as Inhibitors Using SELEX

The first main approach in our research is SELEX. The principle and the experimental procedure of using SELEX for aptamer discovery have been described in detail in my proposal and are illustrated in Fig. 1 below (2, 3). As shown, an RNA library was mixed with the GluR2Q_{flip} AMPA receptors expressed in HEK-293 cells (this is the binding step). Then, a chemical inhibitor, such as NBQX, was used to elute competitive aptamers bound to the same site and/or different site(s) that were mutually exclusive (i.e., NBQX or 1,2,3,4-tetrahydro-6-nitro-2,3-dioxo-benzol[f]quinoxaline-7-sulfonamide disodium is a classic competitive inhibitor for AMPA receptor). The eluted RNA molecules were reverse-transcribed and PCR-amplified. The new, enriched pool of RNAs was made by *in vitro* transcription. The new RNA pool was used for a new round of selection. After 14 rounds of selections, the SELEX was terminated. The DNA pool from the 11th, 12th and 14th rounds were cloned and sequenced. Consensus sequences were then identified by sequence alignment.

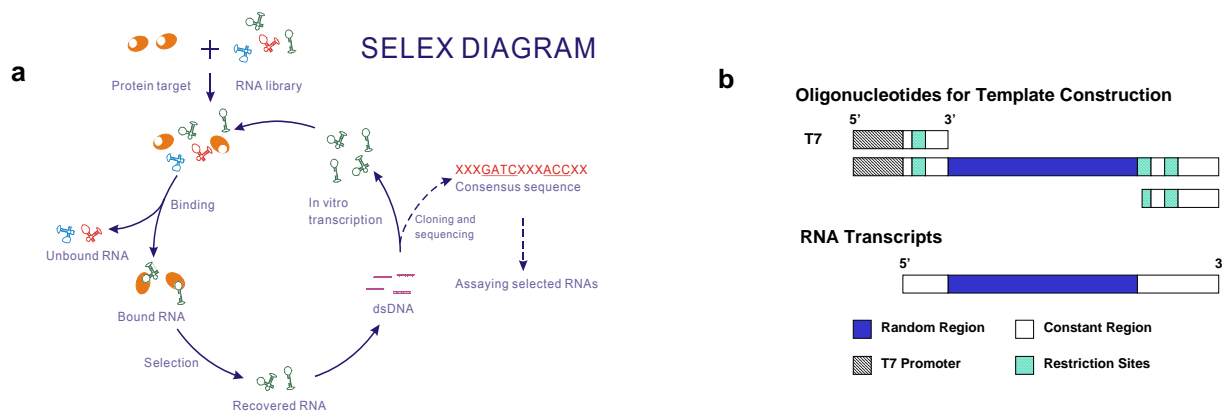


Fig. 1. (a) Flow chart of SELEX. The library we used for SELEX contains a sequence degeneracy of $\sim 10^{15}$. The DNA template contains 118 nucleotides. (b) The combinatorial RNA library is made by transcribing the DNA templates. Each template consists of 108 bases with a 40-base randomized segment. This segment is flanked by two constant regions for primer annealing. The 5' constant sequence includes a promoter for T7 RNA polymerase. The two restriction sites are *EcoRI* located in the 5' constant region and *HindIII* located in the 3' constant region, respectively.

2.1.2. Measuring the Glutamate Receptor Channel-opening Kinetics Using Laser-Pulse Photolysis Technique

Understanding of inhibitor-receptor interactions within the microsecond (μ s)-to-millisecond (ms) time domain is currently lacking, due to the fact that the time resolution of the conventional kinetic techniques is not sufficient to measure the channel opening kinetics of the AMPA and kainate receptor channels. For instance, an AMPA receptor opens its channel in the μ s time scale and desensitizes within a few ms in the continued presence of glutamate. Competitive and noncompetitive inhibitors, for instance, are presumed to interact with the channels within this time domain. However, as one of the most commonly used assays, equilibrium binding using radioligand is relevant to the desensitized receptors in general. Single channel recording can measure rapid kinetics, but has not worked well with AMPA and kainate receptors, because of an intrinsic short lifetime or a rapid channel closing rate constant.

The laser-pulse photolysis technique using caged neurotransmitters has been developed to measure the receptor channel opening kinetics and inhibitor-receptor interaction with a μ s time resolution (4, 5). Caged neurotransmitters are biologically inert, but photolabile precursors of neurotransmitters. This technique utilizes a rapid photolytic release of a neurotransmitter from the caged precursor within the μ s time domain to overcome the otherwise slow diffusion and mixing of free neurotransmitters with the receptor on the surface of a cell. Using this technique, the opening of a receptor channel can be measured prior to receptor desensitization (6). To

study glutamate receptors, we have synthesized a caged glutamate (4). The structure of the caged glutamate and the set-up of the laser-pulse photolysis technique are shown in Fig. 2.

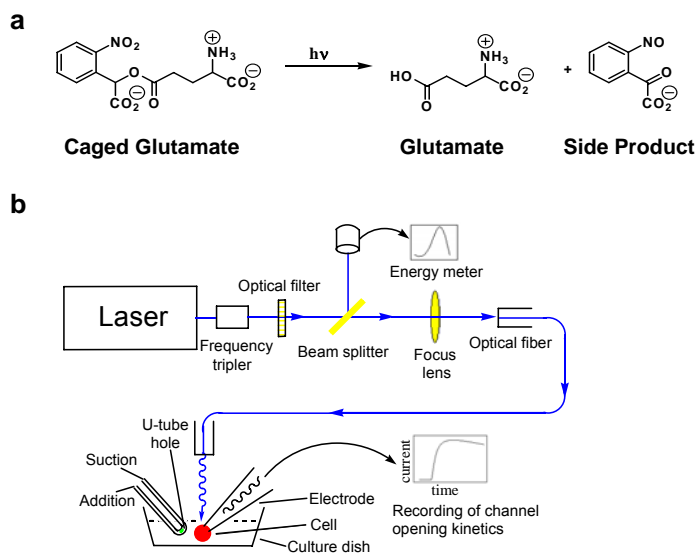


Fig. 2 (a) Photolysis of the caged glutamate. (b) Schematic drawing of the laser-pulse photolysis setup and a U-tube device for delivering caged neurotransmitters (and also free neurotransmitters and inhibitors) to the surface of a cell. The U-tube device, shown in the left, is made from stainless steel tubing with its hole of 150 μm facing towards right. The addition of the solution containing the ligand and the suction of the waste are controlled by two peristaltic pumps. A HEK-293 cell ($\sim 15 \mu\text{m}$ in diameter) is suspended from the recording electrode and placed $\sim 100 \mu\text{m}$ away from the hole. The linear flow rate of the solution is 1-4 cm/s. An optical fiber through which laser light for photolysis is delivered to the cell has a core diameter of 300 μm . The distance between the cell and the fiber is $\sim 400 \mu\text{m}$. The photolysis of caged glutamate liberates free glutamate, which activates the glutamate receptors, and the whole-cell response is recorded.

These two methods or techniques, described above, are the primary approaches we have used in the proposal research. Next I wish to describe the specific accomplishments, which I shall divide into five categories for the clarity of presentation: *aptamer selection and characterization*, *method development*, *AMPA and kainate receptor channel-opening mechanism*, *mechanism of action of GYKI inhibitors*, and *RNA structure and function*. The relationship of these results with the specific Tasks outlined in my original proposal will be also noted.

2.2. Aptamer Selection and Characterization

2.2.1. Summary

We have thus far selected two major classes of aptamers against the GluR2Q_{flip} AMPA receptor subunit, using SELEX (see Fig. 1). One class is competitive aptamers and the other is noncompetitive aptamers. In the second class, we have further selected two different types of noncompetitive aptamers: one is open-channel conformation specific, namely this type prefers to inhibit the open-channel conformation of the GluR2 receptor, whereas the other type prefers to inhibit the closed-channel receptor conformation. Thus we have successfully accomplished Task 1, as originally proposed. Our results of the selection and characterization of the competitive aptamers have been published. We are currently characterizing the structure and function of the other two types of noncompetitive aptamers. Below I wish to focus on our selection and characterization of the competitive aptamers using NBQX to illustrate our accomplishment.

2.2.2. Selection and Characterization of Competitive Aptamers Using NBQX

Using SELEX (in Fig. 1) and NBQX as the elution pressure, we have successfully identified a class of competitive aptamers. In this selection, we run a total of 14 rounds or cycles. Rounds 5, 10 and 14 were 3 negative selections. A negative selection was run using plain HEK-293 cell membrane in order to minimize the enrichment of nonspecific RNAs bound to membrane lipids. After 14 rounds, the DNA pools from round 11, 12 and 14 were cut by *EcoRI* and *HindIII* from the constant regions of the DNA template shown in Fig. 1b, and then ligated into vector pGEM3Z. Primer, M13F, was used for sequencing. Finally, 121 clones (41 from round 11, 40 from round 12, and 40 from round 14) were sequenced. Sequence alignment has allowed us to single out 3 types of sequences whose frequency of appearance in all rounds is different from each other. For example, the sequence represented by d14NB44 increased from 2.4% in round 11 to 27.5% in round 14, whereas the sequence represented by D14NB21 decreased from 26.8% to 2.5% at the end of the selection (yet both types of the sequences show inhibitory properties).

Using a radioligand binding assay or [³]AMPA with the S1-S2 protein (i.e., S1S2 protein is a partial GluR2 receptor containing only the soluble, extracellular binding domain), we have assayed the binding of these aptamers based on a competition between NBQX and AMPA, an agonist. We found, for instance, our aptamer – see Reprint 1 (7) – exhibited a K_d value of about 400 pM. Furthermore, to specifically characterize the biological activity of these RNAs, we carried out whole-cell recording to directly assay whether an evolved RNA was capable of inhibiting GluR2Q_{flip} expressed in HEK-293 cells. The synthetically prepared aptamer or synAN58 showed an IC_{50} value of 30 nM (see Fig. 3G in the reference of (7)). In addition, one of the aptamers can be reduced to a minimized length of 58 nucleotides (nt) from the original 99 nt (7) (please refer to the first reprint in Appendices or (7) for additional experimental details). AN58 showed a potency, rivaling any existing competitive antagonists for AMPA receptors, including NBQX, SPD 502, ZK200775 and YM872 (7).

We further determined the specificity of AN58 for all AMPA receptor subunits and a representative kainate subunit (i.e., GluR6) by testing its inhibition on each homomeric channel expressed in HEK-293 cells (Fig. 3D in the reference of (7)). AN58 inhibited all AMPA receptor subunits but not the GluR6 kainate receptor. This is desirable because kainate and AMPA receptors have different functionality *in vivo*. Moreover, AN58 exhibited a higher specificity for the GluR4 subunit, as compared to NBQX. AN58 was also tested with hippocampal neurons, because these cells contain various endogenous glutamate receptors and are considered a classical paradigm for testing excitatory neurotransmission. Using kainate as the nondesensitizing AMPA receptor agonist to evoke the whole-cell response, AN58 inhibited endogenous AMPA receptors, as expected (left panel of Fig. 3E in the reference of (7)). In contrast, AN58 was ineffective in inhibiting NMDA receptor response (right panel of Fig. 3E in the reference of (7)). AN58 was also found to retain the same inhibitory potency when the pH dropped from 7.4 to 6.4 (Fig. 3F in the reference of (7)). Under the same condition, NBQX loses its potency by >3-fold (8). This acidic pH is clinically linked to the infarcted brain regions (8), and thus the efficacy of inhibition by a potential drug at this acidic pH is a critical requirement for an effective stroke treatment. In addition, AN58 is stable in that it remains fully active even after ethanol precipitation, heating for >10 min at 70 °C, and/or storage in the frozen state for years. We further carried out the laser-pulse photolysis measurement of the channel opening rate process in the absence and presence of AN58. As shown, AN58 inhibited both the rate of the channel opening and the whole-cell current amplitude of GluR2 (fig. 3). In short, these are desired properties for this aptamer. I should also mention that these are experimental screens as proposed in Task 3, which we are using to assay a putative aptamer (see 2.2.4. *Selection and Characterization of Noncompetitive Aptamers Using GYKI Compounds*).

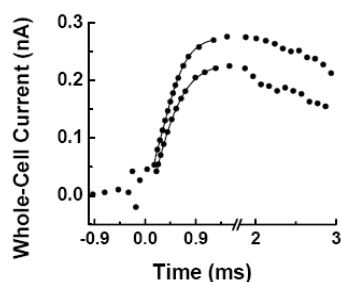


Fig. 3. Using the laser-pulse photolysis technique, AN58 was found to inhibit both the rate and the current amplitude of the opening of the GluR2Q_{flip} channel. The whole-cell current was evoked by ~100- μ M glutamate photolytically released from the caged glutamate, by a laser pulse fired at time zero, in the absence (upper trace) and presence (lower trace) of 75-nM AN58. The observed channel-opening rate constant is $2700 \pm 160 \text{ s}^{-1}$ (upper trace) and $2200 \pm 120 \text{ s}^{-1}$ (lower trace), respectively. For the simplicity of plotting, the data points were reduced by at least 10-fold.

2.2.3. The Choice of NBQX

In the first SELEX experiment, we decided to start with NBQX as the choice of the elution “pressure” so that aptamers bound to the agonist binding site or to a mutually exclusive site(s) on the receptor would be eluted. This is because NBQX is a classical competitive inhibitor for AMPA and kainate receptors and the selected aptamers would be predicted to be competitive inhibitors. NBQX was tested in clinical trials but failed with one of the main reasons being its poor water solubility. Furthermore the structure of the agonist-binding site with NBQX bound has been determined with the S1-S2 protein using both NMR (9) and X-ray crystallography (10). The S1-S2 protein is a partial receptor containing only the soluble, extracellular binding domain and thus lacking the ability of forming the channel. Thus we reasoned that once the aptamers selected, the putative nature of these competitive aptamers can be tested using this soluble protein in addition to the holo-receptor. For instance, whether an aptamer binds to the agonist site or not can be characterized using NMR (whereas it is not possible to do NMR using the holo-receptor). For this purpose, NBQX was a logical “control”

or starting point to work out a general experimental protocol for subsequent experiments using SELEX with noncompetitive inhibitors whose sites of action are unknown. Indeed, methods we have developed in applying SELEX to aptamer discovery using NBQX with a recombinant ion channel expressed in HEK-293 cells are the subject of one paper and one patent (see the next section, i.e., 2.3. *Method Development*).

Experimentally, we confirmed that AN58 was a competitive inhibitor. Specifically, the dose-response relationship of glutamate with the GluR2Q_{flip} channel was right-shifted in the presence of AN58 and eventually converged at saturating concentrations of glutamate, indicative of a competitive inhibition. In fact, the dose-response relationship of AN58 was similar to that of NBQX (7). Our preliminary study of AN58 with S1S2 using NMR also showed the chemical shifts upon binding of aptamers in reference to binding of glutamate.

2.2.4. Selection and Characterization of Noncompetitive Aptamers Using GYKI Compounds

GYKI compounds are 2,3-benzodiazepine derivatives and are one of the most popular inhibitors developed against AMPA receptors. I proposed to use these compounds to elute aptamers that are either bound to the same site(s) or a mutually exclusive site(s). Therefore the aptamers selected are putative noncompetitive inhibitors, the principle we have demonstrated using NBQX as described earlier in this report. The noncompetitive nature of these GYKI compounds was established based on radioligand binding studies previously (11) and our mechanistic investigation using the laser-pulse photolysis technique, which I shall describe later in this report (i.e., 2.5 *mechanism of action of GYKI inhibitors*).

Using the method we have worked out by the initial selection of competitive aptamers using NBQX, we further carried out SELEX procedures using two different GYKI compounds whose chemical structures are shown in Fig. 4. Specifically, Cf is a noncompetitive inhibitor, and its inhibition constant for the closed-channel form of the GluR2Q_{flip} receptor or a $K_I = 1 \mu\text{M}$ is six times smaller than for the open-channel form. In contrast, BDZ-2 is a noncompetitive inhibitor with a six-fold higher affinity or a $K_I = 6 \mu\text{M}$ for the open-channel conformation than for the closed-channel form. Again, the determination of these constants will be described in 2.4 *mechanism of action of GYKI inhibitors* later in this report. We have carried out preliminary characterization for the aptamers we selected using BDZ-2. Among those, one aptamer showed a preference of inhibiting the open-channel conformation, as expected (Fig. 5). Aptamers selected using Cf have also provided an expected trend in that they are closed-channel preferring. Furthermore, our preliminary studies of these aptamers with the GluR2Q_{flip} receptor channels expressed in HEK-293 cells show that both types of aptamers have apparent K_I values in 300-600 nM. Based on these values, these RNA inhibitors have higher affinity than their chemical counterparts used for elution and perhaps a group of noncompetitive inhibitors with the highest potency against AMPA receptors.

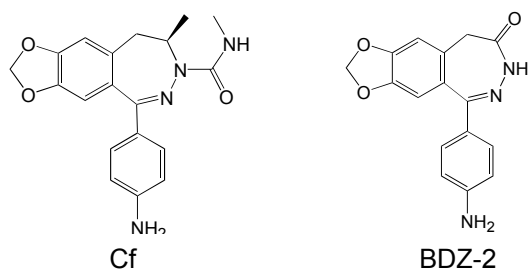


Fig. 4. Chemical structures of Cf (GYKI 53784) and BDZ-2. Both are the derivatives of the original compound GYKI 52466 [1-(4-aminophenyl)-4-methyl-7,8-methylenedioxy-5H-2,3-benzodiazepine] discovered in 1980s (1). For the simplicity of presentation, we named these compounds as Cf and BDZ-2.

The aptamers we have found represent a group of inhibitors developed to specifically recognize unique receptor conformation. We hypothesize that these conformation-specific aptamers or inhibitors shall have higher or exclusive selectivity towards either a unique AMPA receptor subunit or the AMPA receptor subtype than towards the kainate receptor subtype. At this moment, we are continuing on our studies of (a) finding out the minimized sequence length of an aptamer and (b) then testing it across all AMPA receptors and kainate receptor subunits as well as native NMDA receptors endogenously expressed in hippocampal neurons. This is the same procedure we used to characterize the competitive aptamers, as I described before; the details of the experimental screens can be found in reference (7). Finally, I should mention that the original proposal of selecting conformation-specific aptamers involved in the use of philanthotoxin-343. This chemical inhibitor was

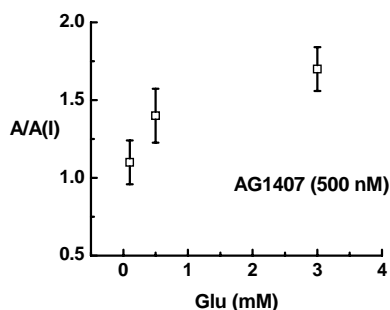


Fig. 5. The ratio of the current amplitude in the absence, A , and presence, A_i , of AG1407, an aptamer selected using BDZ-2 (see its chemical structure in Fig. 4 and the inhibitory properties of BDZ-2 in the text and also in 2.5 *mechanism of action of GYKI inhibitors*). The current was recorded at 0.1, 0.5 and 3 mM glutamate concentrations with the GluR2Q_{flip} receptor expressed in HEK-293 cells. The glutamate concentration at 0.1 mM and 3 mM correspond to the closed-channel and open-channel receptor forms. As seen, this aptamer is essentially an open-channel preferred inhibitor.

synthesized in Prof. Koji Nakanishi's laboratory in Columbia University and there is no any other commercial source available to obtain this compound. Prof. Nakanishi has graciously provided a small amount of this compound (about 2 mg). However, his lab is no longer making various derivatives of philanthotoxins. To our project, 2 mg was not a quantity that we could be certain for a successful SELEX run. Therefore, we decided to use two different GYKI compounds as shown in Fig. 4. Our effort turned out to be a success in two fronts. First, the aptamers we have selected are unique inhibitor templates for drug development. They are water soluble and highly potent, rivaling any existing small, organic compounds. Second, developing conformation-specific inhibitors has not been previously attempted. Here we show a promising method in discovering potential inhibitors with such properties.

2.3. Method Development

When we started the SELEX, we decided to use the holoprotein or the total GluR2Q_{flip} receptor rather than the S1S2 protein for selecting potential RNA inhibitors. This decision was based on the fact that the S1S2 lacks the ability to form a channel (it is a partial protein, containing only part of the extracellular domain of GluR2). It also turned out that when we used a GYKI inhibitor that was shown to be active as a noncompetitive inhibitor with the holo-receptor expressed in HEK-293 cells, mixing the same compound with S1S2 caused no chemical change in NMR, suggesting that S1S2 is an incomplete protein in forming noncompetitive sites. We have further excluded the possibility of using the GluR2Q_{flip} in detergent, because it was unclear whether a detergent could faithfully mimic the membrane environment so that the receptor in detergent could maintain the native function.

Using SELEX to evolve aptamers against a desired target generally requires target preparation. Various methods of target preparations have been developed (12), which has made SELEX increasingly routine especially for soluble targets (13). However, preparation of a transmembrane protein target is still challenging, and consequently the application of SELEX to aptamer selection against transmembrane proteins is limited. Membrane proteins often require lipid environment to maintain wild-type functionality and therefore, they may have to be prepared and presented for SELEX in a complex membrane background. As such, the evolution of aptamers can be dominated by an overwhelming amount of lipids (and other targets in the lipid environment), as compared to the amount of protein of interest in such a background. In the successful SELEX cases involving membrane proteins, native membrane tissues (i.e., *Torpedo californica* electroplax membrane and rat forebrain membrane) are used for RNA aptamer selection, because of the extremely rich quantity of protein targets (14, 15). Live cells are used for selection of ssDNA aptamers, including human red blood cell membrane (16) and hematopoietic tumor cells (17). In all cases described above, proteins used for SELEX are native to cell membrane. For recombinant membrane proteins not found in native tissues, either a cell line (18) or a partial, soluble portion of a membrane protein (19, 20) are constructed for SELEX. Specifically, to use the total GluR2Q_{flip} receptor, we needed therefore to express the receptor and use it in the membrane form, i.e., the GluR2 embedded in the HEK-293 cells (using a native cell source like motor neurons means a mixture of AMPA receptor subunits, rather than a pure GluR2Q_{flip} receptor). However, the drawback of this approach and potentially the failure of the experiment could be that during the SELEX, not only the receptor but also membrane lipids were equally accessible for RNAs. Thus, the receptor to lipid ratio was critical to the success of the selection. To maximize our chance of success, we explored the possibility of enhancing the receptor expression in single HEK-293 cells.

The method we successfully developed has enabled us to achieve a 7-fold increase of the GluR2Q_{flip} yield in single HEK-293S cells, as compared to a popular expression protocol using calcium phosphate, the gold standard of transient protein expression. The key to our method is to coexpress simian virus (SV) 40 large T antigen (TAg), a powerful oncoprotein, with the protein of interest. Specifically, the gene of the protein of interest is harbored in a plasmid containing the SV40 replication origin, and the TAg gene is encoded in a separate vector. Transient coexpression of TAg produces more proteins of interest per cell. This is because, among its functions, SV40 TAg disrupts the cell-cycle checkpoints by binding to and inactivating key tumor suppressors and cell-cycle regulatory proteins, such as p53 and pRB. Consequently, the cell turns into a growth-deregulated protein-making factory. Specifically, we characterized TAg enhancement of the single-cell expression of GluR2 to establish the optimal plasmid ratio and the most complementing cell line. We further characterized the function of the GluR2 receptor with intact cells, without removing TAg. In addition, using green fluorescence protein (GFP) as a reporter gene and fluorescence imaging of a population of HEK 293 cells as an independent detection method, we showed that the GFP expression in these cells increased similarly. Together, our results demonstrate that this method represents a significant improvement over conventional protein expression protocols. Furthermore, the method should be general for expressing both soluble and membrane proteins, and for characterizing the protein function directly in single cells. The work I described here has been published in the *Journal of Neuroscience Methods* and the reprint or Reprint 2 is attached. I should also mention that the method described and the aptamers presented are the subject of a patent application as well. Finally, the accomplishment described here is the direct result of our work related to Task 1.

In summary, the method we developed was a critical part of our successful selection of aptamers against the GluR receptor expressed in HEK-293 cells. In addition, our method has other significant benefits. For instance, as shown in our paper, coexpression of TAg is also beneficial to studying the AMPA receptors that are less efficiently expressed and/or when inhibitors are used, which causes the current amplitude to be smaller. Further discussion of the usefulness of this method can be found in the second reprint attached in the Appendices.

2.4. AMPA and Kainate Receptor Channel-Opening Mechanism

2.4.1. Channel Opening Rate Constants

AMPA-type ionotropic glutamate receptors mediate the majority of fast excitatory neurotransmission in the mammalian central nervous system, and are essential for the brain function such as memory and learning. Dysfunction of the receptors has been implicated in a variety of neurological diseases, including ALS. As an example, we used the laser-pulse photolysis technique and investigated the channel-opening mechanism for GluR4_{flip} or GluRD_{flip} (i.e., the flip isoform of GluRD), an AMPA receptor subunit. The minimal kinetic mechanism for the channel opening is consistent with binding of two glutamate molecules per receptor complex, and with the channel-opening probability being 0.95 ± 0.12 . The GluR4_{flip} channel opens with a rate constant of $(6.83 \pm 0.74) \times 10^4 \text{ s}^{-1}$ and closes with a rate constant of $(3.35 \pm 0.17) \times 10^3 \text{ s}^{-1}$ (see Fig. 6)

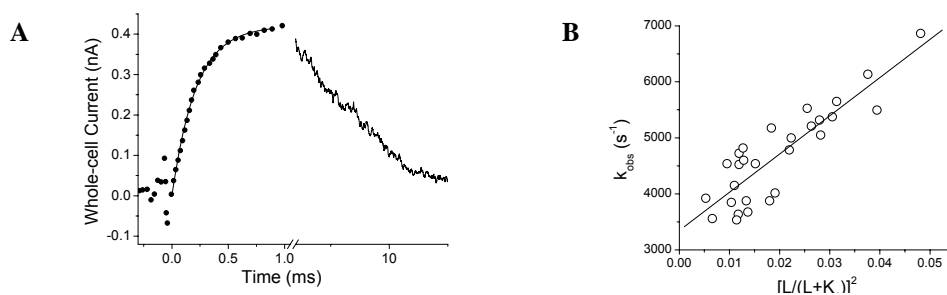


Fig. 6. Laser-pulse photolysis measurement of the channel-opening rate for GluR4_{flip}. A representative whole-cell current is shown in (A) for the channel opening initiated by the laser-pulse photolysis of caged glutamate at time zero. The fitting of the rising phase by a single exponential rate process, shown as the solid line, yielded the k_{obs} of $4,800 \pm 250 \text{ s}^{-1}$, corresponding to a $190 \mu\text{M}$ photolytically released glutamate. Note that the direction of the current response was plotted opposite to that recorded. For clarity, the number of the data points was reduced for plotting. The fall of the current in (A) was due to receptor desensitization. From the plot of k_{obs} versus glutamate concentration in (B) by equation, $k_{\text{obs}} = k_{\text{cl}} + k_{\text{op}} [L/(L + K_1)]^2$, the k_{cl} and k_{op} were determined to be $(3.35 \pm 0.17) \times 10^3 \text{ s}^{-1}$ and $(6.83 \pm 0.74) \times 10^4 \text{ s}^{-1}$, respectively. Each point represents a k_{obs} obtained at a particular concentration of photolytically released glutamate.

Therefore, the shortest rise time (20-80% of the receptor current response to glutamate) is predicted to be 20 μ s, which is about eight times shorter than previously estimated. These findings suggest that GluR4_{flip} is more kinetically GluR2Q_{flip}-like, another fast-activating AMPA receptor subunit. Throughout the grant funding period, we have systematically investigated, and published, the kinetic mechanism of channel opening for all AMPA receptor subunits, i.e. GluR1 (21, 22), GluR3 (6) and GluR4 (23). We have previously published the data with GluR2 AMPA receptor (24) and GluR6 kainate receptor (25). These are the proposed studies in Task 2. We are carrying out a kinetic investigation of GluR5 kainate receptor. Table 1 below is a summary all of the data we have thus far published. I should mention that (a) the table was from our paper by Pei *et al.* (6), and (b) the references listed in the table can be found in the same numbering as in the same article.

Table 3: k_{op} and k_{cl} values for Some Homomeric Ionotropic Glutamate Channels^a

Glutamate Receptors	k_{op} (s^{-1})	k_{cl} (s^{-1})	Technique	Reference	
NR1A/NR2A ^b	77	28	Single-channel recording	(68)	
GluR1Q _{flip} ^{c, d}	2.9×10^4	2.1×10^3	Laser-pulse photolysis	(31)	
		4.2×10^3 (73%)	Single-channel recording	(27)	
		4.2×10^2 (27%)			
GluR2Q _{flip}	8.0×10^4	2.6×10^3	Laser-pulse photolysis	(30)	
		3.1×10^3 (84%)	Single-channel recording	(28)	
		6.8×10^2 (16%)			
	1.6×10^4	5.0×10^3	Fitting	(43)	
GluR3 _{flip}	9.9×10^4	3.8×10^3	Laser-pulse photolysis	This study	
GluR3 _{flip}	9.6×10^4	1.1×10^3	Laser-pulse photolysis	This study	
GluR4 _{flip}	6.8×10^4	3.4×10^3	Laser-pulse photolysis	(32)	
		4.0×10^4	8.0×10^3	Fitting	(69)
			5.9×10^3	Single-channel recording	(26)
GluR6Q	1.1×10^4	4.2×10^2	Laser-pulse photolysis	(67)	
		1.0×10^4	4.4×10^2	Fitting	(52)
		1.0×10^4		Flow measurement	(46)

(a) In all data cited, glutamate is the agonist. (b) *Xenopus* oocytes are used for the study of NMDA channels, the rest of studies are with HEK-293 cell. (c) The k_{op} and k_{cl} values cited in the laser-pulse photolysis measurements are those at $n = 2$. (d) A channel-closing rate constant (k_{cl}) obtained from single-channel recording is converted from the mean lifetime of the open channel (τ) by $k_{cl} = 1/\tau$.

What is the significance of knowing the rate constants of the channel opening? The rate at which a ligand-gated ion channel opens is important to know, because it has major implications in signal transmission and regulation. First, knowing the constants of the channel-opening rate will allow us to predict more quantitatively the time course of the open-channel form of the receptor as a function of neurotransmitter or ligand concentration, which determines the transmembrane voltage change and in turn controls synaptic neurotransmission. Second, that knowledge will provide clues for mechanism-based design of compounds to regulate receptor function more effectively. This is the subject we are especially interested in for the proposed research because, as I shall demonstrate later in this proposal, understanding how an inhibitor, whether it is an aptamer or a GYKI compound, affects the channel-opening mechanism is essential in designing better inhibitors and using them more effectively as potential drugs. For instance, a competitive inhibitor will no longer be effective at a saturating concentration of an agonist. Third, characterizing the effect of structural variations on the rate constants of channel opening will offer a test of the function, which is relevant to the time scale on which the receptor is in the open-channel form, rather than in the inactive, desensitized form, i.e., ligand-bound, but channel-closed form. Examples of structural variations include those due to RNA editing and splicing, and site-specific mutations for investigating the structure-function relationship. Finally, knowing the channel-opening rate constants will be required to understand quantitatively the integration of nerve impulses that arrive

at a chemical synapse or that originate from the same synapse but from different receptors responding to the same chemical signals (neurotransmitters), such as glutamate.

I should mention that we have also characterized the flop version of all AMPA receptors. We found that the flop version of GluR2 responds differently to a GYKI compound as compared to the flip variant of GluR2Q. Therefore, we suspected that the flip/flop site (see Fig. 7) may be involved in formation of noncompetitive sites (we have also additional supportive evidence by NMR studies). This would be an important question to address for noncompetitive aptamers which we are developing. We have found, for instance, that the flop variant, except GluR1, has a roughly 3-fold larger k_{cl} than the flip counterpart (the GluR1 is an exception in that the flip and flop variants have identical k_{cl} , k_{op} and desensitization rate constants). Interestingly, in the spinal cord of ALS patients, the level of the GluR2 flip variant relative to that of the flop isoform is markedly elevated (26). Because the desensitization rate constant of the flip isoform at a given glutamate concentration is ~ 3 -5-fold slower than that of the flop isoform (27), the relative increase of the flip isoform consequently widens the time window for more Ca^{2+} insult (26). Thus our data suggest that the flip variants are a very important target of drug development. Today, we have published the GluR3 flop data, and the manuscript summarizing the rest of the data involving the flop variants, in the context of the flip counterparts, is being prepared.

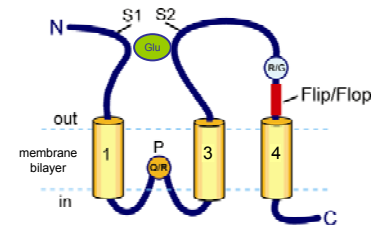


Fig. 7. Topology of an AMPA receptor subunit.

2.4.2. Receptor Occupancy and Channel Opening Rate Constants

An AMPA receptor is a tetrameric assembly and each subunit contains a glutamate binding site. The receptor can adopt multiple conductance levels, especially at high receptor occupancy, as observed in the single-channel recording of wildtype and mutant recombinant receptors (28, 29) as well as native AMPA receptors (30). However, it remains unclear whether receptor occupancy plays a significant role in determining the kinetic constants for an ensemble rate process of channel opening as a function of glutamate concentration. The ensemble rate process is manifested in a whole-cell current response to the binding of glutamate *in vitro* and best represents the glutamatergic synaptic activity *in vivo*, such as excitatory postsynaptic current (EPSC). Therefore, determining the number of glutamate molecules bound to a receptor or the percentage of the receptor occupancy pertinent to the rate of the channel opening is a basic question in understanding the function of AMPA receptors.

To address this question, we investigated the channel-opening kinetics for a GluR1 AMPA receptor channel carrying a substitution of leucine (L) to tyrosine (Y) or L497Y. The discovery of this point mutation by Stern-Bach *et al.* (28) is a significant event in understanding the structure and function relationship of AMPA receptors in that (a) phenomenologically, the single leucine-to-tyrosine substitution renders the homomeric receptor channels virtually non-desensitizing (28), and (b) the phenotypic effect of this mutation is conserved at equivalent positions in all AMPA receptor subunits, i.e. GluR1-4 (31-33). Furthermore, this mutation is thought to have no effect on either the main conductance level or the channel opening probability (28, 32, 34). From a crystallographic study, Sun *et al.* (31) revealed that this mutation resides in the receptor dimer interface of a tetrameric assembly and suggested that the rearrangement of the dimer interface is linked to receptor desensitization (31). Accordingly, the lack of desensitization for the mutant is ascribable to this mutation that prevents the dimer interface movement. We expressed GluR1Q_{flip} L497Y mutant in HEK-293 cells, and measured the channel-opening rate using a laser-pulse photolysis technique.

We found that the minimal number of glutamate molecules required to bind to the receptor and to open the channel is two (or $n = 2$), and that the entire channel-opening kinetics can be adequately described by just one channel-opening rate constant, k_{op} , that correlates to $n = 2$. This result suggests higher receptor occupancy ($n = 3$ and 4) does not give rise to different k_{op} values or, at least, not appreciably if the k_{op} values are different. Compared to the wildtype receptor (Li, G., and Niu, L. (2004) *J. Biol. Chem.* 279, 3990–3997), the channel-opening and channel-closing rate constants of the mutant are 1.5-fold and 13-fold smaller, respectively. Thus, the major effect of this mutation is to decrease the channel-closing rate constant by stabilizing the open-channel conformation. Finally, it is worth noting that because the mutant has an EC_{50} value of about 50 μM , as

compared with about 500 μM from the wild type, we were able to measure k_{obs} even at a saturating glutamate concentration. Thus we determined the k_{op} and k_{cl} from an entire range of glutamate concentration. We found the k_{op} value is similar with the value we measured for the wild type which we could only measure in a narrow range. More important, we also found that by using a limited range of data points for the mutant (i.e., the lower 20%), the k_{op} value obtained is identical, within the experimental error, with the k_{op} value obtained using the entire range of k_{obs} . Therefore, we believe that a k_{op} value we have carefully measured, even in a limited concentration range for some wild type receptors whose EC50 values often are in the mM range, should be valid. This is important because the experimental determination of k_{op} for any AMPA and kainate receptors has not been previously possible. For experimental details, please refer to this work which has been published in *J. Biol. Chem.* by Pei *et al.* (22).

2.5 Mechanism of Action of GYKI Inhibitors

Developing AMPA receptor inhibitors to control the excessive receptor activity has been a long pursued therapeutic approach for the treatment of various neurological disorders, including ALS (35). To make new inhibitors more potent and selective for AMPA receptors, the mechanism of action of existing inhibitors needs to be investigated, and the structure-reactivity relationship for those structurally related compounds needs to be characterized. This is especially meaningful for 2,3-benzodiazepine derivatives, also known as GYKI compounds, which represents one of the best classes of inhibitors in terms of their selectivity and affinity for AMPA receptors.

GYKI 52466 (1-(4-aminophenyl)-4-methyl-7,8-methylenedioxy-5H-2,3-benzodiazepine) is the first inhibitor in this class discovered in the 1980s (1) (see Fig. 8). Since then, hundreds of 2,3-benzodiazepine derivatives have been synthesized (36, 37). GYKI compounds are considered allosteric regulators or noncompetitive inhibitors, a conclusion drawn largely from binding studies using radioactive agonists (37). However, the detailed mechanism by which 2,3-benzodiazepines inhibit AMPA receptors is not well understood. This deficiency can be mainly ascribed to the fact that an AMPA receptor opens its channel in the μs time scale following glutamate binding (21, 23, 24), as I described earlier, but desensitizes or becomes inactivated while glutamate remains bound in the ms time region (38). As a result, agonist binding assay is most relevant to characterization of the inhibitory effect on desensitized receptors. We have shown that using the laser-pulse photolysis technique and the caged glutamate (4), we can measure the receptor channel opening separately from the receptor desensitization (6, 23-25).

We then investigated the mechanism of inhibition of the opening of the $\text{GluR2Q}_{\text{flip}}$ channel by two 2,3-benzodiazepine compounds, 1-(4-aminophenyl)-3,5-dihydro-7,8-methylenedioxy-4H-2,3-benzodiazepin-4-one (BDZ-2) and its 3-N-methylcarbamoyl derivative (BDZ-3) (11) (Fig. 8). BDZ-2 and BDZ-3 are structurally related to GYKI 52466, the original template (Fig. 8). Compared to GYKI 52466, the 4-methyl group of both BDZ-2 and BDZ-3 is replaced by a carbonyl group. I should mention that BDZ-2 is the compound we have used for the selection of open-channel conformation-specific aptamers. Therefore, we also wanted to understand how this compound acts with the $\text{GluR2Q}_{\text{flip}}$ receptor, and by what mechanism it operates as an inhibitor. We argue that the answer to this question is important in the future study of the mechanism of action of the aptamers displaced by the binding of BDZ-2.

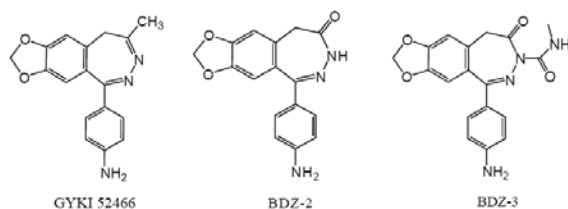


Fig. 8. Chemical structures of GYKI52466, BDZ-2 and BDZ-3.

Specifically, we measured the effects of BDZ-2 and BDZ-3 on both the channel-opening rate and the whole-cell current amplitude respectively. We found that both compounds preferably inhibit the open-channel state, meaning that both inhibitors have a higher affinity for the open-channel conformation than to the closed-channel conformation. Furthermore, BDZ-2 is a stronger noncompetitive inhibitor in that it inhibits the open-channel state with ~6-fold higher affinity than BDZ-3 does. We also found that both compounds bind to the same site. Binding of an inhibitor to the receptor involves in the formation of a loose, partially conducting channel intermediate, which rapidly isomerizes to a tighter, inhibitive complex. The isomerization reaction is

identified as the main step for the receptor to distinguish the structural difference between the two compounds. We conclude that addition of a bulky group at the N-3 position on the diazepine ring, as in BDZ-3 (Fig. 8), does not alter the mechanism of action, nor the site of binding, but does lower the inhibitory potency, possibly due to an unfavorable interaction of a bulky group at the N-3 position with the receptor site. The new mechanistic revelation on the structure-reactivity relationship is useful in designing conformation-specific, more potent inhibitors for the GluR2 AMPA receptor.

Using the rapid kinetic techniques, we have shown that the mechanism of action and the structure-reactivity relationship of the two 2,3-benzodiazepine derivatives can now be characterized in a more detailed fashion than previously possible. The new findings provide useful clues for future design and synthesis of 2,3-benzodiazepine inhibitors that are more potent and more specific towards a unique receptor conformation. Our finding that BDZ-3 acts mechanistically the same as BDZ-2, and binds to the same site as BDZ-2 does, but is a weaker inhibitor, indicates that addition of a substituent to the N-3 position on the diazepine ring of BDZ-2, resulting in an increase in size at this position, is expected to generate a weaker inhibitor. However, our finding also suggests a possibility that a photolabel, for instance, can be attached to the N-3 position, and the resulting compound can serve as a site-directed reagent for labeling and mapping of the inhibitory site on the receptor. The location of the site, inferred from the present study, is unknown. The location of this and any other regulatory site on any AMPA receptor subunit is in turn beneficial to the design and synthesis of newer 2,3-benzodiazepine derivatives.

Although the work I described was not explicitly described in my original proposal, I consider that the work on the rapid kinetic investigation as presented here is an integral part of aptamer discovery for two particular significances. First, understanding the mechanism of action of these compounds allows us to identify a chemical pressure for selecting mechanism-based aptamers using SELEX (see Fig. 1). In this case, choosing BDZ-2 has allowed us to select an open-channel conformation-specific aptamer. Furthermore, because BDZ-2 is a much stronger than BDZ-3, we have chosen BDZ-2 instead of BDZ-3 in SELEX. Second, the aptamers selected can be rigorously tested for its mechanism and site of interaction, as it was done for BDZ-2 and BDZ-3. For the detailed presentation of the results and the discussion of mechanism, please refer to the galley proof for this work, which will appear in *Biochemistry* in January, 2008.

2.6. RNA Structure and Function

Both theoretical (39) and experimental (40) work previously demonstrated the possibility that a single RNA sequence can assume multiple, distinctly folded structures with different functions. These structures or more precisely conformations are different structural folds of the same sequence generated through reversible thermodynamic pathways. For example, a selected RNA sequence can adopt a fold that catalyzes RNA cleavage or another fold that catalyzes RNA ligation (40). On binding of small metabolites, riboswitches can consequently switch their conformations and therefore functions (41). However, we describe that a single RNA sequence assumes two structures with different functions, both of which are required for inhibition of the GluR2 AMPA receptor. Yet, the two structures, once formed during transcription, are not interconvertible through unfolding and refolding (or denaturing and renaturing processes).

The sequence we present was evolved from SELEX against the GluR2 AMPA receptor (7) from a RNA library containing $>10^{15}$ sequences, which I described earlier in this report (i.e., 2.2.2. *Selection and Characterization of Competitive Aptamers Using NBQX*). The sequence, which we called AN58 (Fig. 9A), can be reduced from the original 99-nucleotide (nt) aptamer (i.e., aptGluR2-99) to a 58-nt RNA molecule without affecting its nanomolar potency (7), but a further reduction to a 53-nt or shorter RNA abolished activity (7). AN58 and its longer versions exhibited two or more than two bands in the native polyacrylamide gel electrophoresis (PAGE) (Fig. 9B). Surprisingly, however, the two bands of AN58, labeled as M1 and M2 (Fig. 9B), could not individually inhibit the GluR2 receptor, as characterized by whole-cell recording of the GluR2 channel expressed in HEK-293 cells (24) (Fig. 9C). Yet, when mixed with equal molar ratio, M1 and M2 inhibited the receptor as fully as they did before they were separated (Fig. 9D).

More surprisingly, M1 and M2 were found to have different functional roles in inhibiting the GluR2 receptor, a conclusion drawn from a series of whole-cell current recording experiments (Fig. 9E). First, an equal

molar mixture of the non-inhibitory 53-nt transcript with the purified M2 yielded no inhibition, but the mixture of the 53-nt transcript with the purified M1 produced an inhibition as strong as the mixture of purified M1 and M2 (Fig. 9E). As a control, RN87, another RNA whose sequence is unrelated to either AN58 or AN53, showed no inhibition itself or when mixed with either M1 or M2 (Fig. 9E). These results (Fig. 9, D and E) indicated that M1 and M2 functioned differently, probably by binding separately to two different sites, but M1 and M2 were required to act as a collaborating pair to inhibit GluR2 competitively (Fig. 9F). Given the mechanism of the collective action of M1 and M2 (Fig. 9F), the intrinsic inhibition constant or K_I for M1 and M2 was estimated to be 25 ± 4 and 27 ± 7 nM, respectively (data not shown). The experiment using different ratios of M1 and M2 further revealed that the stoichiometry of the inhibition was 1:1 (data not shown).

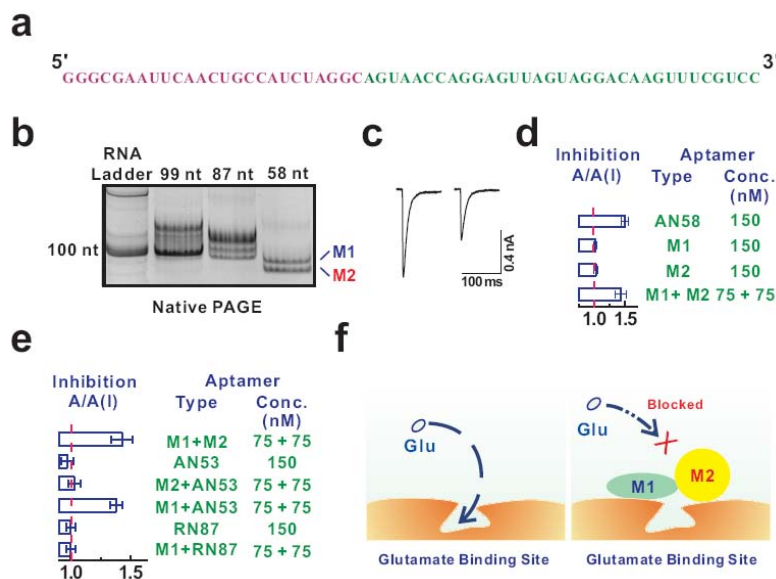


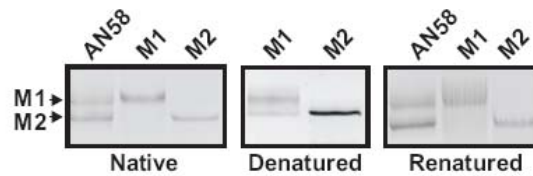
Fig. 9 (a) The sequence of aptamer AN58. Colored in purple is the 5' constant region, whereas the region colored in green is part of the selected sequence. (b) M1 and M2 derived from AN58 were visualized in a native PAGE (10%), together with their longer versions, i.e. 87-nt and 99-nt aptamers. (c) Representative whole-cell current response of GluR2Q_{flip} in HEK-293 cells to 500 μ M glutamate in the absence (left panel) and presence (right panel) of 30 nM AN58. (d) M1 or M2 alone caused no inhibition but an equal molar mixture of M1 and M2 restored the inhibition of GluR2 to the same level by the non-separated AN58 at identical concentrations. (e) Mixing of AN53 with M1, but not M2, yielded inhibition, but AN53 alone did not inhibit the receptor. As a control, the mixture of M1 and another non-functional sequence, RN87, caused no inhibition. (f) As a competitive inhibitory pair, M1 and M2 must bind to their corresponding sites simultaneously and in 1:1 stoichiometry ratio (see text) to block the glutamate binding.

Furthermore, we show that M1 and M2 can assume two distinct structural folds encoded by the same sequence. This conclusion was made based on evidence that includes (a) M1 and M2 both were of the same length by experiment using glyoxal, an RNA denaturing reagent, and (b) the sequence of M1 and M2 was the same by primer extension, using the synthetically made AN58 with the known sequence as the ladder (data not shown). However, both the primer extension reaction using the same 3'-end primer, which revealed a distinct difference in the reverse transcription (RT) pattern between M1 and M2, and the one-dimensional homonuclear NMR experiment, which probed the imino proton region, suggested that M1 and M2 have different structures.

Are M1 and M2 interconvertible folds? To answer this question, we attempted to unfold and refold M1 and M2. However, even after boiling or ethanol precipitation or freezing, M1 and M2 remained individual bands, as visualized on a native PAGE, and their biological activities also remained intact, as tested by whole-cell recording. After boiling in the presence of ~50% formamide for 15 min, M1 did partially unfold into a species that had mobility seemingly identical, on the denaturing PAGE, to that of M2 (Fig. 10, the middle panel; the lower band of the M1). However, the lower band originating from the M1 sample disappeared upon refolding, suggesting that M1, under such a harsh denaturing condition, could partially unfold to some other structure but not to M2. M2, on the other hand, appeared intact after such treatments as it remained a single band. Thus, M1 and M2, generated from the same sequence, were not different conformers or products of folding/refolding through a reversible pathway. Instead, M1 and M2 are different structural entities. Although they might be folded and refolded in their own repertoires of conformations or folding networks (at least this may be true for M1), there is not a thermodynamic pathway through which a conformation from one conformational repertoire can become the origin of the other conformational repertoire (i.e., the so-called conformational diffusion between the two networks) (39). Although we cannot rule out that there may be yet an unidentified denaturing condition under which M1 and M2 can both be denatured post-transcriptionally, the condition used in this study (see the legend of Fig. 10) is to our knowledge the strongest denaturing condition

known. Therefore, the structural differences between M1 and M2, in spite of a shared evolution origin and history, seem not to be a result of RNA-folding process or partitioning of conformations.

Fig. 10 Unfolding and refolding of M1 and M2. The left panel shows the different mobility of purified M1 and M2 in a native PAGE (10%), compared with the mixture of the original sample, AN58. When the purified M1 and M2 dissolved in the Loading Buffer II (Ambion) for denaturing PAGE, which contained 47.5% formamide, were boiled for 15 min and run in the denaturing PAGE (10%, 7 M urea), additional band appeared originating from the M1 sample (middle panel). The “denatured” M1 and M2 were then precipitated in ethanol and re-suspended in the external buffer; the refolded samples were visualized in another native PAGE (10%) (right panel). In the same native PAGE, the AN58 sample was treated by the same unfolding/refolding process. M1 and M2 used in the folding/refolding experiments were also purified to remove the contaminated polyacrylamide (7).



Our findings provide profound implications in the evolution and folding of RNA structure in nature. For instance, the transfer of *sequence information* between two different classes of nucleic acids is not generally considered difficult because such a process uses the one-to-one correspondence of Watson-Crick pairing. In contrast, the transfer of *function* is considered difficult because function is a property of a macromolecule that is inherently more complex than sequence. In a recent study, it was shown that the evolutionary conversion of a ribozyme (RNA) to a deoxyribozyme (DNA) of the same function can be accomplished but only with some critical sequence mutations (42). Our finding that the survival of one genotype ensures more than one phenotype through *in vitro* evolution demonstrates that the transfer of different functions through the same sequence in a sequential fashion from DNA to RNA as in our case is possible. Therefore RNA may be more phenotypically adaptable than proteins. Currently, no protein sequence is known to assume two different folds endowing two functions (40). Therefore our results suggest a possibility that in a real organism a single RNA sequence could evolve to “duplicate” RNA molecules with structure-dependent functional dissimilarities, which, in some cases, may precede gene duplication.

Furthermore, as is known conventionally, an RNA molecule can have different conformations with different functions but these conformations are reversibly interconvertible. For example, a selected RNA sequence can adopt a fold that catalyzes RNA cleavage or another fold that catalyzes RNA ligation, as shown from David Bartel’s lab at MIT. In this regard, our finding is novel in that there is not a precedent demonstrating that the two RNA structures assumed from the same sequence are not reversibly convertible by denaturing and refolding.

I should mention that the manuscript summarizing this work has been submitted to *Science*. Right before Christmas, I was notified that the manuscript has been sent for external review from the Editorial Office of *Science*. We would likely receive a decision after the mid January.

I should further emphasize that this work was completely a serendipitous discovery based on our work in the selection of aptamers against the GluR2 AMPA receptor using SELEX, as proposed in Task 1.

3. KEY RESEARCH ACCOMPLISHMENTS

- Successfully selected three different groups of aptamers, as proposed in Task 1. One group is competitive aptamers, whereas the other two groups show differential affinity towards different receptor conformations, one being the closed-channel and the other being the open-channel conformation.
- All of the three groups of aptamers inhibit the GluR2Q_{flip} receptor, a key AMPA receptor subunit to mediate glutamate-induced neurotoxicity linked to ALS, with apparent K_I values all in the nanomolar region. All of them are water soluble by nature but also are more potent than their chemical counterparts used in SELEX.
- Developed a method to enhance the single-cell receptor expression by 7-fold using a powerful oncoprotein, large T antigen (TAg). We show that the receptor function can be studied, as usual, in intact single cells without removing TAg. This method is of general application for expression of both membrane proteins and soluble proteins. The method is further applicable for a large culture production of protein of interest. Furthermore, our method expands SELEX to selection of aptamers against a recombinant, holo-membrane protein expressed in HEK-293 cells.
- Completed the systematic characterization of the kinetic mechanism of the channel opening for 9 receptor channels, and they are both the flip and flop variants of the GluR1, GluR2, GluR3 and GluR4 AMPA receptors, using the laser-pulse photolysis technique. Furthermore, we have also characterized the rapid kinetic investigation of the GluR6Q kainate receptor. These are the work in Task 2.
- We have further characterized the mechanism of action for one of the competitive aptamers, AN58, its specificity among all AMPA receptors, GluR6 kainate receptors and native NMDA receptors expressed in rat hippocampal neurons. All results show this aptamer exhibits the desired properties as a nanmolar affinity inhibitor. The other two groups of conformation-specific aptamers are being studied at this moment.
- We have also carried out rapid kinetic investigation on the mechanism of inhibition for a collection of 18 GYKI compounds. Our goal is to use the mechanistic information as a guide to evolve aptamers with known mechanism of action. Furthermore, our results shed light on further developing GYKI compounds with a better prediction of the structure-reactivity relationship.
- We have also determined the structure-function relationship for AN58, an aptamer which apparently can form two structures with the same sequence, rather than two different conformations, that cannot be denatured and refolded into other conformation.

I should mention that the last two projects are derived from the studies initially proposed. They all turned out to be interesting, and important questions. The answers to these questions bear important implications of the research projects we initially proposed.

4. REPORTABLE OUTCOMES

4. 1. One patent has been filed with USPTO:

Nucleic Acid Ligands Specific for Glutamate Receptors (2004) Li Niu, Zhen Huang, Hua Shi, John T. Lis

4. 2. Eight papers were published:

Li, G. & Niu, L. (2004) *J. Biol. Chem.* **279**, 3990–3997. How Fast Does the GluR1^{Qflip} AMPA Receptor Channel Open?

Huang, Z., Li, G., Pei, W.M., Sosa, L. A. & Niu, L. (2005) *J. Neurosci. Methods.* **142**, 159-166. Enhancing Protein Expression in Single HEK-293 Cells

Li, G., Sheng, Z. Y, Huang, Z. & Niu, L. (2005) *Biochemistry* **44**, 5835-41. Kinetic Mechanism of the Channel Opening of GluR^{Dflip} AMPA Receptor

Pei, W.M., Huang, Z., & Niu, L. (2007) *Biochemistry* **46**, 2027-2036. GluR3 Flip and Flop: Differences in Channel-Opening Kinetics

Kornreich, B. G., Niu, L., Roberson, M. S. & Oswald, R. E. (2007) *Neuroscience* **146**, 1158-1168. Epub 2007 Mar 26. Identification of C-terminal domain residues involved in protein kinase A-mediated potentiation of GluR6

Pei, W. M., Ritz, M., McCarthy, M., Huang, Z. & Niu, L. (2007) *J Biol Chem.* **282**, 22731-6. Epub 2007 June 1. Receptor Occupancy and Channel-Opening Kinetics: A Study of GluR1 L497Y AMPA Receptor

Huang, Z., Pei, W. M., Jayaseelan, S., Shi, H., Niu, L. (2007) *Biochemistry* **46**, 12648-55. Epub 2007 Oct 12. RNA Aptamers Selected against the GluR2 Glutamate Receptor Channel

Ritz, M., Micale, N., Grasso, S. and Niu, L. (2008) *Biochemistry*. In press. Mechanism of Inhibition of the GluR2 AMPA Receptor Channel Opening by 2,3-Benzodiazepine Derivatives

4. 3. One manuscript has been submitted and is being reviewed:

Huang, Z., Pei, W.M. Jayaseelan, S., Shekhtman, A. Shi, H., Lis, J. T. and Niu, L. (2007) submitted to *Science*. One RNA Aptamer Sequence, Two Structures: A Collaborating Pair that Inhibits Glutamate Receptors

4. 4. Four manuscripts are in preparation:

Pei, W. M. & Niu, L. (2008) Kinetic Mechanism of the Channel Opening for AMPA Receptor Flop Variants

Ritz, M., Micale, N., Grasso, S. and Niu, L. (2008) Mechanism of Inhibition of the GluR2 AMPA Receptor Channel Opening by GYKI 52466

Huang, Z. Han, Y and Niu, L. (2008) Selection of the Open-Channel Conformation-Specific Aptamers against the GluR2 AMPA Receptor

Park, J. S., Huang, Z. Han, Y, Wang, J. and Niu, L. (2008) Selection of the Closed-Channel Conformation-Specific Aptamers against the GluR2 AMPA Receptor

4. 5. Meeting presentation for the results obtained:

2004:

- Invited talk at International Conference on Nucleic Acids, Membrane and Signal Transduction, Okayama, Japan

2005:

- Invited talk at the 14th Summer Conversation in Progress of Nucleic Acids, and Proteins, Albany, NY
- Invited talk at the first meeting of American Academy of Nanomedicine, Baltimore, MD

2006:

- Poster presentation at the 50th Biophysical Society Meeting, Salt Lake City, UT (2 posters)
- 2006 DOD Meeting (Military Health Research Forum), San Jun, Puerto Rico
- Invited talk and chaired a session at the Ion Channel Retreat meeting, Vancouver, Canada

2007:

- Poster presentation at the 51st Biophysical Society Meeting, Baltimore, MD (2 posters)
- The Third International Meeting on Molecular Mechanism of Neurodegeneration, Milan, Italy

2008:

- Invited participation and presentation of our aptamer results in “Accelerating ALS Research: Translating basic discoveries into therapies for ALS”, a meeting sponsored by the ALS Association (Jan 13-16, 2008, Tampa, FL).

4. 6. Degree awarded that was supported by this award:

Dr. Weimin Pei, a graduate student in my lab who completed his Ph.D. thesis study in December 2006. He returned China early this year.

Mr. Mark Ritz, a graduate student who completed his MS degree and is now working in a chemical company in Albany, NY.

Mr. Leivi A. Sosa, an undergraduate who got his research training in my lab. He was awarded a BS and is now in Downstate Medical College in New York City. He has been enlisted as a navy officer subsequently.

Ms. Jamie Cohen, an undergraduate student who was a chemistry major, and got her research training in my lab. She is now a medical student in SUNY-Buffalo.

A complete list of research personnel who have received pay from this grant is attached at the end of the Appendices.

5. CONCLUSIONS

Making and using specific glutamate inhibitors to block excitotoxicity mediated by AMPA receptors currently suffers two major problems. First, the number of existing AMPA inhibitors is limited and so is their water solubility. Second, the inhibitors are generally characterized with the desensitized receptor form(s) because the commonly used methods are either equilibrium binding or conventional kinetic techniques, the latter of which has an insufficient time resolutions to assay the receptor that upon binding glutamate opens its channel in the microsecond time region and begins to desensitize even within a few milliseconds. As a result, the detailed mechanism of action and efficacy of these inhibitors/drugs are poorly understood. Together these problems have significantly hampered drug development for treatment of ALS including those veterans who have served in war and now suffer ALS.

We proposed to discover novel inhibitors in that they are RNA molecules and are water soluble by nature. So far, we have successfully accomplished that goal. Specifically, we have identified two classes of aptamers, both of which have apparent K_I in the nanomolar region for inhibiting the GluR2Q_{flip} receptor channel. These two classes are competitive and noncompetitive aptamers. In the noncompetitive category, we further identified two groups of aptamers specific towards unique receptor conformations. One group shows specificity towards the open-channel form whereas the other shows the higher affinity for the closed-channel

receptor conformation. I should emphasize that aptamers as high affinity, water soluble compounds have never been reported previously. Furthermore, there is no known inhibitor targeting specific AMPA receptor conformations. Therefore, our work not only represents a conceptual advance in development of inhibitors but also materialization of unique inhibitors or aptamers entirely different from traditional, small molecule inhibitors that are essentially organic compounds. The aptamers we have identified are ready to be further developed into potential therapeutics for not only ALS but also other neurological diseases involving the excessive glutamate receptor activity, such as stroke and epilepsy.

Currently, we are continuing on characterizing aptamers, especially the noncompetitive aptamers by using the same strategy I have described in this report and in the paper we have published. We have already begun to make chemical modification of the selected aptamers to change the biostability of these RNA inhibitors so that the neuroprotective properties of these aptamers can be tested *in vivo* (cellular based assays and then animal model studies in the future). We have made major breakthroughs thus far in our proposed work, and we are extremely excited to continue our work towards the goal of finding a new therapy for ALS.

Finally, I cannot express my gratitude enough for this funding. Without it, none of the accomplishments would have been possible.

6. REFERENCES

1. Tarnawa, I., Farkas, S., Berzsényi, P., Pataki, A., and Andrasi, F. (1989) Electrophysiological studies with a 2,3-benzodiazepine muscle relaxant: GYKI 52466. *Eur J Pharmacol.* 167, 193-199.
2. Ellington, A. D., and Szostak, J. W. (1990) In vitro selection of RNA molecules that bind specific ligands. *Nature* 346, 818-822
3. Tuerk, C., and Gold, L. (1990) Systematic evolution of ligands by exponential enrichment: RNA ligands to bacteriophage T4 DNA polymerase. *Science* 249, 505-510
4. Wieboldt, R., Gee, K. R., Niu, L., Ramesh, D., Carpenter, B. K., and Hess, G. P. (1994) Photolabile precursors of glutamate: synthesis, photochemical properties, and activation of glutamate receptors on a microsecond time scale. *Proc Natl Acad Sci U S A* 91, 8752-8756
5. Niu, L., and Hess, G. P. (1993) An acetylcholine receptor regulatory site in BC3H1 cells: characterized by laser-pulse photolysis in the microsecond-to-millisecond time region. *Biochemistry* 32, 3831-3835
6. Pei, W., Huang, Z., and Niu, L. (2007) GluR3 flip and flop: differences in channel opening kinetics. *Biochemistry* 46, 2027-2036
7. Huang, Z., Pei, W., Jayaseelan, S., Shi, H., and Niu, L. (2007) RNA Aptamers Selected against the GluR2 Glutamate Receptor Channel. *Biochemistry.* 46, 12648-12655. Epub 12007 Oct 12612.
8. Weiser, T. (2005) AMPA receptor antagonists for the treatment of stroke. *Curr Drug Targets CNS Neurol Disord* 4, 153-159.
9. McFeeters, R. L., and Oswald, R. E. (2002) Structural mobility of the extracellular ligand-binding core of an ionotropic glutamate receptor. Analysis of NMR relaxation dynamics. *Biochemistry* 41, 10472-10481.
10. Jin, R., Horning, M., Mayer, M. L., and Gouaux, E. (2002) Mechanism of activation and selectivity in a ligand-gated ion channel: structural and functional studies of GluR2 and quisqualate. *Biochemistry* 41, 15635-15643.
11. Grasso, S., Micale, N., Zappala, M., Galli, A., Costagli, C., Menniti, F. S., and De Micheli, C. (2003) Characterization of the mechanism of anticonvulsant activity for a selected set of putative AMPA receptor antagonists. *Bioorg Med Chem Lett.* 13, 443-446.
12. Gopinath, S. C. (2007) Methods developed for SELEX. *Anal Bioanal Chem* 387, 171-182
13. Breaker, R. R. (2004) Natural and engineered nucleic acids as tools to explore biology. *Nature* 432, 838-845.
14. Ulrich, H., Ippolito, J. E., Pagan, O. R., Eterovic, V. A., Hann, R. M., Shi, H., Lis, J. T., Eldefrawi, M. E., and Hess, G. P. (1998) In vitro selection of RNA molecules that displace cocaine from the

- membrane-bound nicotinic acetylcholine receptor. *Proc Natl Acad Sci U S A* 95, 14051-14056
15. Cui, Y., Rajasethupathy, P., and Hess, G. P. (2004) Selection of stable RNA molecules that can regulate the channel-opening equilibrium of the membrane-bound gamma-aminobutyric acid receptor. *Biochemistry* 43, 16442-16449.
 16. Morris, K. N., Jensen, K. B., Julin, C. M., Weil, M., and Gold, L. (1998) High affinity ligands from in vitro selection: complex targets. *Proc Natl Acad Sci U S A* 95, 2902-2907.
 17. Shangguan, D., Li, Y., Tang, Z., Cao, Z. C., Chen, H. W., Mallikaratchy, P., Sefah, K., Yang, C. J., and Tan, W. (2006) Aptamers evolved from live cells as effective molecular probes for cancer study. *Proc Natl Acad Sci U S A* 103, 11838-11843
 18. Pestourie, C., Cerchia, L., Gombert, K., Aissouni, Y., Boulay, J., De Franciscis, V., Libri, D., Tavitian, B., and Duconge, F. (2006) Comparison of different strategies to select aptamers against a transmembrane protein target. *Oligonucleotides* 16, 323-335
 19. Chen, C. H., Chernis, G. A., Hoang, V. Q., and Landgraf, R. (2003) Inhibition of heregulin signaling by an aptamer that preferentially binds to the oligomeric form of human epidermal growth factor receptor-3. *Proc Natl Acad Sci U S A* 100, 9226-9231. Epub 2003 Jul 9221.
 20. Mori, T., Oguro, A., Ohtsu, T., and Nakamura, Y. (2004) RNA aptamers selected against the receptor activator of NF-kappaB acquire general affinity to proteins of the tumor necrosis factor receptor family. *Nucleic Acids Res* 32, 6120-6128
 21. Li, G., and Niu, L. (2004) How fast does the GluR1Qflip channel open? *J Biol Chem* 279, 3990-3997. Epub 2003 Nov 3910.
 22. Pei, W., Ritz, M., McCarthy, M., Huang, Z., and Niu, L. (2007) Receptor occupancy and channel-opening kinetics: a study of GLUR1 L497Y AMPA receptor. *J Biol Chem* 282, 22731-22736. Epub 22007 Jun 22731.
 23. Li, G., Sheng, Z., Huang, Z., and Niu, L. (2005) Kinetic mechanism of channel opening of the GluRDflip AMPA receptor. *Biochemistry* 44, 5835-5841.
 24. Li, G., Pei, W., and Niu, L. (2003) Channel-opening kinetics of GluR2Q(flip) AMPA receptor: a laser-pulse photolysis study. *Biochemistry* 42, 12358-12366.
 25. Li, G., Oswald, R. E., and Niu, L. (2003) Channel-opening kinetics of GluR6 kainate receptor. *Biochemistry* 42, 12367-12375.
 26. Tomiyama, M., Rodriguez-Puertas, R., Cortes, R., Pazos, A., Palacios, J. M., and Mengod, G. (2002) Flip and flop splice variants of AMPA receptor subunits in the spinal cord of amyotrophic lateral sclerosis. *Synapse* 45, 245-249.
 27. Koike, M., Tsukada, S., Tsuzuki, K., Kijima, H., and Ozawa, S. (2000) Regulation of kinetic properties of GluR2 AMPA receptor channels by alternative splicing. *J Neurosci* 20, 2166-2174.
 28. Stern-Bach, Y., Russo, S., Neuman, M., and Rosenmund, C. (1998) A point mutation in the glutamate binding site blocks desensitization of AMPA receptors. *Neuron* 21, 907-918.
 29. Jin, R., Banke, T. G., Mayer, M. L., Traynelis, S. F., and Gouaux, E. (2003) Structural basis for partial agonist action at ionotropic glutamate receptors. *Nat Neurosci* 6, 803-810.
 30. Smith, T. C., and Howe, J. R. (2000) Concentration-dependent substate behavior of native AMPA receptors. *Nat Neurosci* 3, 992-997.
 31. Sun, Y., Olson, R., Horning, M., Armstrong, N., Mayer, M., and Gouaux, E. (2002) Mechanism of glutamate receptor desensitization. *Nature* 417, 245-253.
 32. Rosenmund, C., Stern-Bach, Y., and Stevens, C. F. (1998) The tetrameric structure of a glutamate receptor channel. *Science* 280, 1596-1599.
 33. Plested, A. J., Wildman, S. S., Lieb, W. R., and Franks, N. P. (2004) Determinants of the sensitivity of AMPA receptors to xenon. *Anesthesiology* 100, 347-358
 34. Robert, A., Irizarry, S. N., Hughes, T. E., and Howe, J. R. (2001) Subunit interactions and AMPA receptor desensitization. *J Neurosci* 21, 5574-5586.
 35. Brauner-Osborne, H., Egebjerg, J., Nielsen, E. O., Madsen, U., and Krogsgaard-Larsen, P. (2000) Ligands for glutamate receptors: design and therapeutic prospects. *J Med Chem* 43, 2609-2645.
 36. Zappala, M., Grasso, S., Micale, N., Polimeni, S., and De Micheli, C. (2001) Synthesis and structure-activity relationships of 2,3-benzodiazepines as AMPA receptor antagonists. *Mini Rev Med Chem* 1, 243-253

37. Solyom, S., and Tarnawa, I. (2002) Non-competitive AMPA antagonists of 2,3-benzodiazepine type. *Curr Pharm Des* 8, 913-939.
38. Trussell, L. O., and Fischbach, G. D. (1989) Glutamate receptor desensitization and its role in synaptic transmission. *Neuron* 3, 209-218.
39. Huynen, M. A., Stadler, P. F., and Fontana, W. (1996) Smoothness within ruggedness: the role of neutrality in adaptation. *Proc Natl Acad Sci U S A* 93, 397-401.
40. Schultes, E. A., and Bartel, D. P. (2000) One sequence, two ribozymes: implications for the emergence of new ribozyme folds. *Science* 289, 448-452.
41. Mandal, M., and Breaker, R. R. (2004) Gene regulation by riboswitches. *Nat Rev Mol Cell Biol.* 5, 451-463.
42. Paul, N., Springsteen, G., and Joyce, G. F. (2006) Conversion of a ribozyme to a deoxyribozyme through in vitro evolution. *Chem Biol.* 13, 329-338.

7. APPENDICES

The Appendices include three parts:

- (1) The PDF files of the eight papers published as listed in 4.2. are attached with this report;
- (2) Meeting abstracts;
- (3) A list of personnel who have been supported by this grant.

RNA Aptamers Selected against the GluR2 Glutamate Receptor Channel[†]Zhen Huang,[‡] Weimin Pei,[‡] Sabarinath Jayaseelan,[‡] Hua Shi,[§] and Li Niu^{*:‡}*Department of Chemistry, Center for Neuroscience Research, and Department of Biological Sciences, University at Albany, State University of New York, Albany, New York 12222**Received May 28, 2007; Revised Manuscript Received August 8, 2007*

ABSTRACT: The excessive activation of AMPA (α -amino-3-hydroxy-5-methyl-4-isoxazole propionic acid) receptors, a subtype of glutamate ion channels, has been implicated in various neurological diseases such as cerebral ischemia and amyotrophic lateral sclerosis. Inhibitors of AMPA receptors are drug candidates for potential treatment of these diseases. Using the systematic evolution of ligands by exponential enrichment (SELEX), we have selected a group of RNA aptamers against the recombinant GluR2Q_{flip} AMPA receptor transiently expressed in HEK-293 (human embryonic kidney) cells. One of the aptamers, AN58, is shown to competitively inhibit the receptor. The nanomolar affinity of AN58 rivals that of NBQX (6-nitro-7-sulfamoyl-benzof[*f*]quinoxaline-2,3-dione), one of the best competitive inhibitors. Like NBQX, AN58 has the highest affinity for GluR2, the selection target, among all AMPA receptor subunits. However, AN58 has a higher selectivity for the GluR4 AMPA receptor subunit and remains potent even at pH = 6.8 (i.e., a clinically relevant acidic pH), as compared with NBQX. Furthermore, this RNA molecule possesses stable physical properties. Therefore, AN58 serves as a unique lead compound for developing water-soluble inhibitors with a nanomolar affinity for GluR2 AMPA receptors.

α -Amino-3-hydroxy-5-methyl-4-isoxazole propionic acid (AMPA)¹ receptors of the glutamate ion channel family (1) are an important target of drug development, like the *N*-methyl-D-aspartate (NMDA) receptor of the same family, for the treatment of neurodegenerative diseases (2). At the receptor level, an AMPA receptor opens its channel in response to the binding of glutamate on the microsecond (μ s) time scale, much faster than NMDA receptor channels (3–6). The opening of the AMPA channel is thought to provide the initial membrane depolarization, thus enabling the NMDA channel to function by relieving the magnesium block (3, 7). AMPA receptors have four subunits: GluR1–4. The assembly of the same or different subunits, presumably in tetramers (8), produces functional ion channels (9, 10). The RNA editing at the Q/R (i.e., glutamine/arginine) site of GluR2 is an important mechanism of controlling calcium permeability of the receptor in that AMPA receptors with the unedited GluR2 (the Q form) are substantially calcium permeable, whereas those with the edited GluR2 (the R form) are not (10–14). Extra calcium entry into neurons through excessively activated AMPA receptors causes intracellular calcium overload, which in turn initiates cell death signaling pathways (15). Therefore, developing AMPA

receptor inhibitors to control excessive receptor activity has been a long-pursued therapeutic strategy.

Traditionally, synthetic chemistry has been the main approach in making small-molecule inhibitors. This strategy has yielded a large number of various types of AMPA receptor inhibitors, such as quinoxalines, dihydrophthalazine derivatives, and 2,3-benzodiazepine compounds. Although AMPA receptor inhibitors with nanomolar affinities have been synthesized, poor water solubility has been a serious problem that so often plagues the clinical usefulness of these compounds. 6-Nitro-7-sulfamoyl-benzof[*f*]quinoxaline-2,3-dione (NBQX), a classic competitive inhibitor of AMPA/kainate receptors (16), is an example of such a compound (17). To improve water solubility, a number of newer competitive antagonists were later synthesized (18–20). However, for 2,3-benzodiazepine derivatives, a class of noncompetitive AMPA receptor inhibitors developed with the most intense interest and effort to date (2), water solubility remains a major problem. Furthermore, to make new inhibitors by organic synthesis, slight chemical modifications of a previous template are often designed. The presumed effect of each modification must be tested before newer modifications can be introduced. Thus, the use of synthetic chemistry to prepare new inhibitors entails a template-based, stepwise process.

In the present study, we take a different approach in developing AMPA receptor inhibitors. The inhibitors we report here are aptamers, which are RNA molecules. Aptamers are selected from an RNA library using an *in vitro* iterative selection procedure known as systematic evolution of ligands by exponential enrichment (SELEX) (21, 22). RNA aptamers are water soluble by nature and can fold into specific tertiary structures that confer high affinity and specificity against biological targets that even do not exist

[†] This work was supported by Grants from the Department of Defense W81XWH-04-1-0106 (to L.N.), the ALS Association (to L.N.), and the Muscular Dystrophy Association (to L.N.), a postdoctoral fellowship from the Muscular Dystrophy Association (to Z.H.), and a SUNY FRAP A award (to H.S.).

^{*} To whom correspondence should be addressed. Phone: (518) 591-8819. Fax: (518) 442-3462. E-mail: lniu@albany.edu.

[‡] Department of Chemistry.

[§] Department of Biological Sciences.

¹ Abbreviations: AMPA, α -amino-3-hydroxy-5-methyl-4-isoxazole propionic acid; HEK-293 cells, human embryonic kidney cells; SELEX, systematic evolution of ligands by exponential enrichment; TAG, large T-antigen.

in nature (23, 24). Unlike conventional, template-based drug design, SELEX can produce lead compounds without templates. The lead compounds can be used to design newer, biostable RNA aptamers for both highly compartmentalized intracellular expression (25) and extracellular applications (23, 26, 27), such as the inhibition of AMPA receptors. Additionally, aptamers can be used as novel structural templates for the chemical synthesis of new inhibitors/drugs.

EXPERIMENTAL PROCEDURES

Receptor Preparation. Each of the AMPA receptor subunits, GluR1–4 (all flip variants), and the GluR6Q kainate receptor subunit was transiently expressed in the human embryonic kidney cells (HEK-293S) using a calcium phosphate protocol (3). The SV40 large T-antigen (TAG) gene was cotransfected to enhance single-cell receptor expression (28). The cells were maintained in Dulbecco's modified Eagle's medium supplemented with 10% fetal bovine serum in a 37 °C, 5% CO₂, humidified incubator. Forty-eight hours after transfection, the cells were either harvested for SELEX or directly used for patch clamp recording. To test selected aptamers on hippocampal neurons containing endogenous glutamate receptors, 1 day old, postnatal Sprague–Dawley rats were dissected and the hippocampal neurons were cultured as described (29).

SELEX. The RNA library for SELEX was prepared as described (30). The library was dissolved in the extracellular buffer (at a final concentration of 20 μM) containing (in mM) 150 NaCl, 3 KCl, 1 CaCl₂, 1 MgCl₂, 10 HEPES (pH 7.4). The fragmented HEK-293 cell membrane containing the GluR2Q_{flip} receptor was prepared by homogenizing the cells using a 50 mM Tris acetate buffer (pH = 7.4) containing 10 mM EDTA and 1 mM phenylmethanesulphonyl fluoride, followed by centrifugation to collect the membrane fragments. The membrane-bound receptor was adjusted to a final concentration of 50 nM as determined by [³H]AMPA binding. The reaction mixture was incubated at 22 °C for 40 min for RNA binding in the presence of 0.3 units/μL RNase inhibitor (Ambion). The desired RNAs were eluted using 1 mM NBQX and were then subject to reverse transcription and PCR.

Binding Assay. The binding affinity of putative RNA aptamers was measured by competition binding to the S1S2 soluble extracellular binding portion of the GluR2 receptor (31) in the presence and absence of NBQX. An RNA sample was internally labeled with [α-³²P]CTP (GE Health) and purified on a polyacrylamide gel electrophoresis (PAGE). The S1S2 protein was covalently linked to MagnaBind amine derivatized beads (Pierce). A binding reaction contained a mixture of 50 nM immobilized S1S2, 20 nM RNA, 6 ng/μL yeast tRNA (as a nonspecific competitor), and 10% DMSO in the extracellular buffer. [α-³²P]CTP-labeled RNA was mixed with ~40-fold excess amount of cold RNA sample. The background binding reaction contained additional 250 μM NBQX, since NBQX was used to evolve aptamers. All binding reactions were carried out at room temperature for 40 min. After binding, a sample mixture was loaded on to a dot-blot apparatus (Pierce) and washed using external buffer (3 × 200 μL/well). The radioactivity of the dot-blot binding was digitized in a phosphorimager (Typhoon Trio, GE Health), which was then quantified using ImageQuant TL (GE Health).

The K_d of an aptamer was estimated by nonlinear fitting of the binding data using eq 1

$$y = \frac{B_{\max} x}{K_d + x} \quad (1)$$

where y represents the total binding of the radioactive aptamer, B_{\max} is the maximum amount of bound radioactive aptamer, and x is the concentration of the free aptamer.

RNA Purification. RNA aptamers were purified for quantitative assay. The purification involved an initial run through PAGE to obtain the wanted RNA aptamers generated from in vitro transcription. The aptamer sample was passed through a Q anion exchange column integrated with a Bio-Rad DuoFlow system to remove polyacrylamide. The buffer containing 25 mM Tris–HCl and 200 mM NaCl was run at a flow rate of 1.0 mL/min to remove polyacrylamide. The aptamer was eluted by passing a solution of 25 mM Tris–HCl and 1.5 M NaCl at the same flow rate, and then dialyzed in the extracellular buffer for assays. The removal of polyacrylamide in the RNA sample was confirmed by the 1D NMR spectrum both before and after passage through the Q column on a Bruker spectrometer operating at a ¹H frequency of 400 MHz. The proton resonance lines characteristic of acrylamide oligomers (~1.4–2.4 ppm and 7–8 ppm) were used to monitor polyacrylamide in the RNA sample (32).

Whole-Cell Recording. The procedures for whole-cell current recording was previously described (3). The cells used for recording were prepared as previously described in the “Receptor Preparation” of the Experimental Procedures. Briefly, an Axopatch-200B amplifier (Axon Instrument) was used in whole-cell recording at a cutoff frequency of 2–20 kHz by a built-in, 8-pole Bessel filter and digitized at a 5–50 kHz sampling frequency by a Digidata 1322A (Axon Instruments). An electrode for whole-cell recording had a resistance of ~3 MΩ when filled with the electrode solution containing (in mM) 110 CsF, 30 CsCl, 4 NaCl, 0.5 CaCl₂, 5 EGTA, and 10 HEPES (pH 7.4 adjusted by CsOH). All reagents were dissolved in the extracellular buffer. When aptamers were included, the buffer further contained 0.05 units/μL RNase inhibitor (final concentration). A flow device (33) was used to apply glutamate in the absence and presence of aptamers to a cell expressing the receptor of interest. The same recording protocol was used for kainate with GluR6 and for NMDA with hippocampal neurons (29). Unless noted otherwise, each data point represented an average of at least three measurements collected from at least three cells. All whole-cell recordings were at –60 mV and 22 °C.

Origin 7 was used for data analysis and plotting. Uncertainties reported refer to standard deviation from the mean unless otherwise noted. Student's t tests were performed, as indicated in the corresponding data sets and figures. A P value less than or equal to 0.05 was considered significant.

RESULTS

Transiently Expressed GluR2Q_{flip} AMPA Receptor as the SELEX Target. For the target of aptamer selection, the GluR2 subunit we chose was the unedited, alternatively spliced “flip” isoform or GluR2Q_{flip}. The choice of this subunit and the specific receptor isoform was based on the finding that

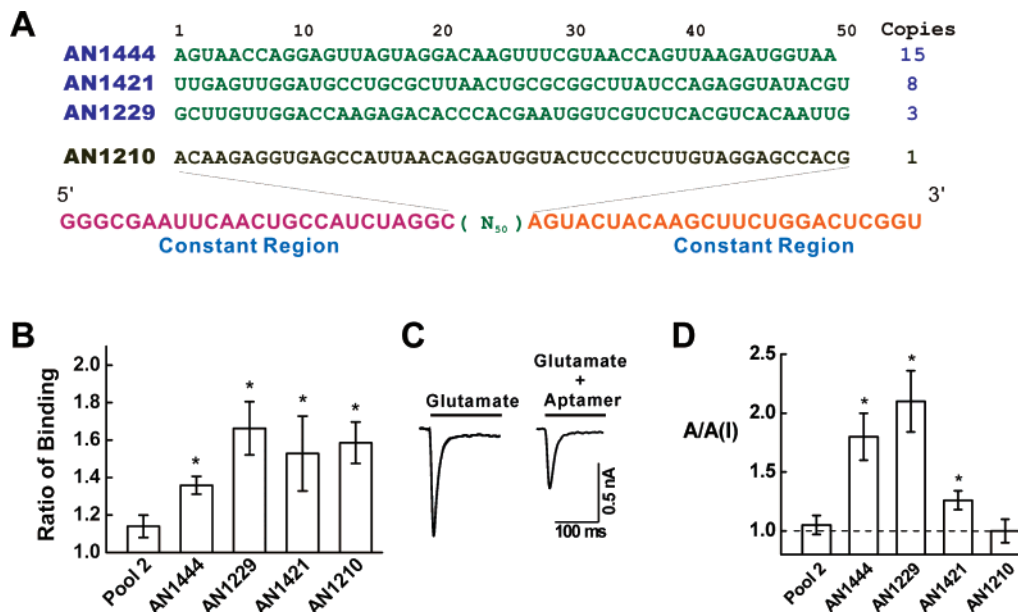


FIGURE 1: Three selected aptamers inhibit GluR2Q_{flip} AMPA receptors. (A) The three RNA sequences of the variable region (N50) were isolated from a total of 80 clones from rounds 12 and 14; overall, 14 rounds were carried out, including three negative selections (i.e., rounds 5, 10, and 13). The arbitrary standard of selecting a “hit” for binding and functional assays was that each sequence at least repeated its appearance three times among 80 clones. The name for each sequence is on the left, whereas on the right is the number of isolated individual sequences. The sequence of the constant region is displayed at the bottom. AN1210 whose sequence is listed as well is thought to bind to, but does not inhibit, the receptor. (B) The radioactivity was measured from the [α -³²P]CTP-labeled RNA binding to the S1S2 partial receptor (see text) in the absence and presence of NBQX, the selection pressure, and the ratio of the radioactivity was plotted (* indicates $P \leq 0.05$ from the two-tailed Student’s t test; $H_0: \mu = \mu_0 = 1$, 1 being the theoretical value of no binding here or no inhibition as in (D) below). For pool 2, $P = 0.0553$. (C) The whole-cell current response of GluR2Q_{flip} to 500 μ M glutamate was reduced in the presence of 150 nM AN1444. (D) The three aptamers selected inhibited GluR2Q_{flip}, shown as the ratio of the whole-cell current response in the absence and presence of 100 nM aptamer or $A/A(I)$. Unless otherwise noted, 500 μ M glutamate was used here and in all measurements in this study. The inhibition of these aptamers was verified by using a 300 nM control, i.e., either pool 2, the second-round library, or AN1210, a sequence different from any of the three sequences. For AN1210, no detectable inhibition was observed even at concentrations up to 700 nM.

GluR2Q_{flip} expression is aberrant in some neurological diseases. For example, in patients with amyotrophic lateral sclerosis (ALS), Q/R editing in the motor neurons is only 56% complete as compared to nearly 100% in the control (34). This significant, neuron-specific RNA editing defect is thought to be linked to selective motor neuron degeneration, a pathogenic hallmark in ALS (34). Similarly, the GluR2 Q/R editing defect is also found in pathological tissues of other neurodegenerative diseases, such as the prefrontal cortex of those with Alzheimer’s disease and the striatum of those with Huntington’s chorea (35). Furthermore, unlike the edited R form, the unedited Q form readily tetramerizes into functional AMPA receptors traffic to synapses (36). The expression of the alternatively spliced flip variant of GluR2, as compared to the flop, is also increased in the spinal motor neurons of ALS patients (37). The flip isoform of GluR2 is known to desensitize at least 3 times more slowly than the flop (38). Consequently, cells that contain more slowly desensitizing flip channels, such as motor neurons, are thought to be more vulnerable to excitotoxicity. These findings suggest that GluR2Q_{flip} is a key AMPA receptor subunit/isoform in mediating calcium-induced excitotoxicity.

For the target preparation, we expressed GluR2Q_{flip} transiently in HEK-293S cells, using a standard calcium phosphate protocol. To maximize the cell-surface receptor density by the transient transfection method, we coexpressed SV40 TAg with GluR2Q_{flip} in the same cell (28). Furthermore, we prepared the membrane fragments harboring intact GluR2Q_{flip} receptors for SELEX. In the successful selection

described below, the receptor density was ~ 0.61 pmol/mg of cell mass (i.e., fragmented membrane). To minimize the selection of unwanted “aptamers” toward other targets such as lipids and other proteins in the cell membrane, negative selection was included such that the HEK-293S cell membrane harboring no GluR2Q_{flip} (but with TAg) was used to filter off unwanted RNAs from enriched RNA libraries (see the legend of Figure 1).

Selection of Aptamers. A total of 14 rounds of SELEX cycles, including 3 rounds of negative selection, were carried out against GluR2Q_{flip} from a regular or unmodified RNA library containing $\sim 10^{15}$ RNAs (30). After cloning and sequencing, we identified three dominant sequences (Figure 1A). To determine whether these sequences corresponded to inhibitory RNA molecules, we first ran a radioactivity binding assay using the ³²P-labeled RNAs (see Experimental Procedures), including two additional controls, the RNA library from cycle 2 (pool 2) and AN1210 RNA, a single sequence identified from cycle 12 but without any sequence homology with the rest of the clones (Figure 1A). It appeared that even pool 2 showed some binding affinity (Figure 1B), albeit the lowest among the tested sequences. The presumed affinity exhibited in this radioligand-binding experiment could have originated from specific and/or nonspecific binding to the receptor. Specific binding refers to an aptamer bound to the agonist binding site because NBQX, a classic competitive inhibitor (see further description below), was used to evolve these aptamers. In addition, we used the S1S2 protein, an extracellular portion of GluR2, in the binding

assay, instead of the holo-receptor embedded in lipid membrane, for the purpose of reducing the nonspecific binding of RNA to lipid membrane.

To specifically characterize the biological activity of the selected RNA, we carried out whole-cell recording to directly assay whether an RNA was capable of inhibiting GluR2Q_{flip}. We reasoned that if an RNA was an inhibitor, as determined by the radioactivity assay (Figure 1B), it would be expected to inhibit the whole-cell current through the GluR2 channel, expressed in HEK-293S cells. Indeed, we found that all three sequences inhibited the activity of the GluR2Q_{flip} channel as evidenced by the reduction of the whole-cell current response to glutamate (Figure 1, parts C and D). In contrast, neither pool 2 nor AN1210 showed any inhibition (Figure 1D). In light of both binding (Figure 1B) and whole-cell recording data (Figure 1D), we also concluded that AN1210 (Figure 1A) could bind to the receptor but the binding did not cause inhibition.

Sequence Characterization. To begin to understand the structure–function relationship of these RNA aptamers, we first compared the three RNA sequences (Figure 1A). However, we found no apparent sequence similarity in the form of short-stretched “consensus sequences”, commonly observed as a SELEX outcome. A lack of short-stretched consensus sequences suggested that an aptamer may fold into a larger structural entity to act as an inhibitor. Other possibilities certainly exist, such as that an insufficient number of sequences were sampled for this comparison. In an attempt to address these possibilities, we focused on one individual aptamer, AN1444 (AN1444 was both more relatively abundant and potent) (Figure 1, parts A and D). We first explored whether the full sequence of AN1444 could be reduced into a shorter but fully functional sequence. Guided by the secondary structure prediction using the Mfold program (39), the full sequence of AN1444 was reduced to a 58 nucleotide (nt) long sequence with full activity (Figure 2A). One of the secondary structures predicted from the Mfold program is shown (Figure 2B). Removal of 26 nt from the 5′ direction (a constant region of the sequence template) from the original length resulted in a total loss of inhibitory function, suggesting that this segment played an essential role for the aptamer function. In contrast, progressive truncation of the sequence from the 3′ end showed that the 58 nt version or AN58 retained activity, whereas shorter versions, such as 53 nt, 49 nt, or 46 nt, did not (Figure 2A). The deletion of five or more nucleotides at the 3′ end of the 58 nt version presumably disrupted critical base pairing (Figure 2B) as predicted by Mfold (39). Interestingly, a lack of short-stretched consensus sequences was also reported in aptamers selected against human epidermal growth factor receptor 3 (40) and the TATA-binding protein (30). Thus, AN58 became our working template for the subsequent functional studies described below and the ongoing structural study.

Functional Characterization of Aptamer AN58. We have characterized the biological properties and activities of AN58 in ways described below (Figure 3) and compared them with NBQX. The comparison with NBQX is based on the fact that NBQX was used as the selection pressure to evolve the aptamers and NBQX is one of the most potent competitive inhibitors discovered to date (16). First, we performed the radioligand displacement binding experiment with AN58

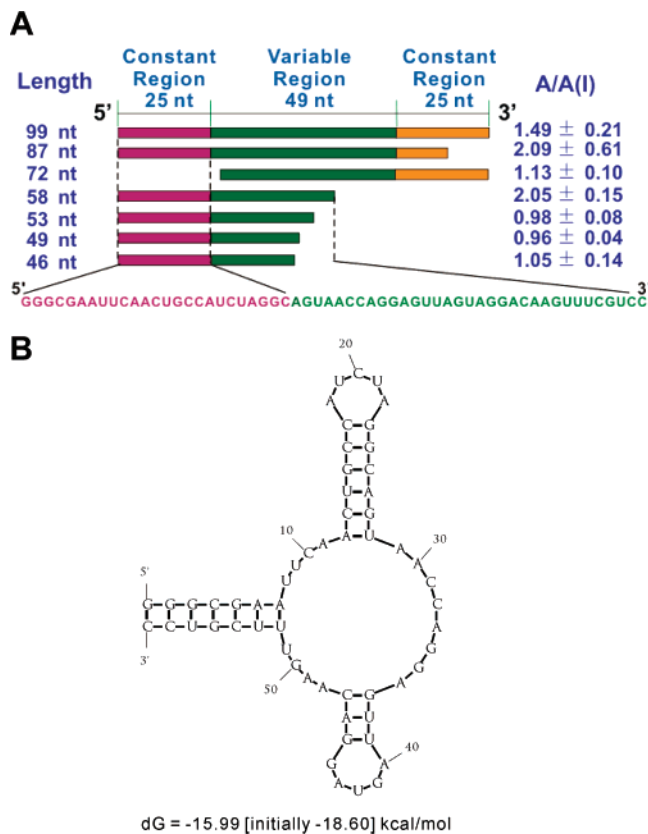


FIGURE 2: AN1444 was reduced to a 58 nt long, functional aptamer (AN58). (A) The original 99 nt AN1444 was truncated from both 5′ and 3′ directions. The corresponding shorter versions were tested using whole-cell recording with HEK-293S cells expressing the GluR2Q_{flip} receptor, and the results are reported as A/A(I). (B) A representative secondary structure of AN58 predicted by Mfold.

using the S1S2 ligand-binding core of GluR2 in the presence and absence of saturation of NBQX (Figure 3A). A K_d value of 0.419 ± 0.221 nM was estimated using eq 1 (Experimental Procedures). This value is more than 47-fold higher than the K_d of NBQX binding to the GluR2 S1S2 previously reported (41), suggesting that AN58 is a highly potent inhibitor. Second, we also measured the dose–response relationship of glutamate with the GluR2Q_{flip} channel expressed in HEK-293S cells in the absence and presence of AN58 (Figure 3B). The fact that the dose–response curve was right-shifted in the presence of AN58 and eventually converged at saturating concentrations of glutamate was also supportive of AN58 being a competitive inhibitor. This is plausible because NBQX-displaced RNA aptamers were supposedly bound to the agonist binding site or to a mutually exclusive site(s) on the receptor. In fact, the dose–response curve of AN58 was similar to that of NBQX (data not shown). Using whole-cell recording, we further determined that AN58 inhibited the GluR2Q_{flip} channel in a concentration-dependent manner, yielding an IC_{50} value of 121 ± 7 nM (Figure 3C).

Next we determined the specificity of AN58 for all AMPA receptor subunits and a representative kainate subunit (i.e., GluR6) by testing its inhibition on each homomeric channel expressed in HEK-293S cells (Figure 3D). AN58 inhibited all AMPA receptor subunits. The specificity of AN58 for these receptors was found to be comparable with NBQX, except for GluR4, where AN58 showed a higher affinity for reasons not yet known. In all AMPA receptor subtypes tested,

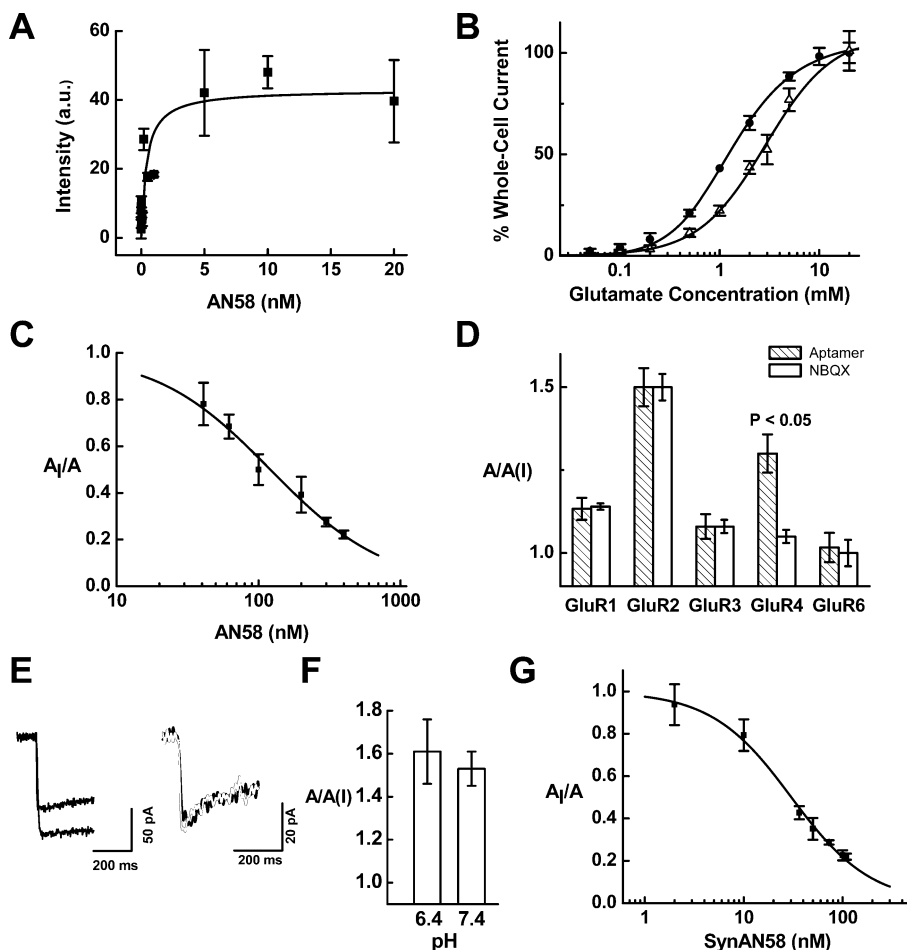


FIGURE 3: Comparison of inhibitory properties of aptamer AN58 with NBQX. (A) Radioligand displacement assay of AN58 with S1S2. Each point represents the average intensity in arbitrary units of three radioactivity measurements of specific binding. The K_d was determined to be 0.419 ± 0.221 nM by nonlinear fitting of the binding data using eq 1. (B) AN58 inhibited the GluR2Q_{flip} by a parallel shift of the dose–response curve in the presence of 150 nM AN58, consistent with a competitive mechanism. (C) The ratio of the whole-cell current recording in the presence and absence of AN58 with HEK-293S cells expressing the GluR2Q_{flip} channels. An IC_{50} value of 121 ± 7 nM was obtained by fitting the current amplitude as a function of the AN58 concentration to the Hill equation (55). (D) Specificity of AN58 to AMPA and GluR6 kainate receptors. Here, the specificity of both NBQX and AN58 was normalized against the GluR2Q response. To ensure the inhibition was comparable, the glutamate concentration was chosen to be equivalent to $\sim 25\%$ of the fraction of the open channel or roughly about half of the EC_{50} value for a particular channel. Specifically, the glutamate concentration was 100 μ M for GluR1 and GluR6 and 500 μ M for GluR2–4, whereas the aptamer concentration was kept at 150 nM (3, 4). AN58 showed higher affinity to GluR4 ($P \leq 0.05$ from a two-sample Student's t test, as compared with NBQX; $H_0: \mu_1 = \mu_2$). (E) AN58 inhibited endogenous AMPA receptors in rat hippocampal neurons, but was ineffective on NMDA receptors (right panel). The left panel shows the whole-cell current response, from the same neuron, induced by 300 μ M kainate in the absence (the lower trace) and presence of 150 nM AN58 (the upper trace). The right panel shows the whole-cell current response, induced by 1 mM NMDA and 100 μ M glycine in the absence (black) and presence of 150 nM AN58 (gray). (F) AN58 remained potent at pH = 6.4. All other conditions used for this experiment were the same as in (D) except that the GluR2Q_{flip} receptor was used exclusively for this assay and the extracellular buffer was adjusted to be the corresponding pH. The same buffer was used to dissolve AN58 for this assay. (G) The IC_{50} value for synthetically prepared AN58 or SynAN58 was determined to be 30 ± 1 nM from the fit of the whole-cell current amplitude to the Hill equation (55) as a function of the SynAN58 concentration.

AN58 exhibited the highest specificity to GluR2 subunit, presumably because GluR2 was the target of selection. However, neither AN58 nor NBQX inhibited the GluR6 kainate receptor at the concentration tested. This is desirable because kainate and AMPA receptors have different functions (42). Furthermore, AN58 was tested with hippocampal neurons, because these cells contained various endogenous glutamate receptors and are considered a classical paradigm for testing excitatory neurotransmission (43). With the use of kainate as the nondesensitizing AMPA receptor agonist (43) to evoke the whole-cell response, AN58 inhibited endogenous AMPA receptors, as expected (left panel in Figure 3E). In contrast, AN58 was ineffective in inhibiting NMDA receptor response (right panel in Figure 3E),

consistent with this “inherited property” from NBQX, a non-NMDA receptor inhibitor, and the fact that the full length predecessor of AN58 and all other discovered aptamers (Figure 1A) were not evolved against NMDA receptors.

AN58 further retained the inhibitory potency when the pH dropped from 7.4 to 6.4 (Figure 3F). Under the same pH condition, NBQX was reported to lose its potency by >3 -fold (17). This acidic pH is clinically linked to the infarcted brain regions (17), thus making the efficacy of inhibition by a potential drug at this acidic pH a critical requirement for effective stroke treatment. The full activity of AN58 may be attributed to the excellent stability of RNA under this slightly acidic condition (44). Furthermore, AN58 is stable in that it remains fully active even after ethanol precipitation,

heating for > 10 min at 70 °C, and/or storage in the frozen state for more than a year.

Although the IC₅₀ value of AN58 is in the nanomolar range, which is clearly desirable as compared with a large number of inhibitors prepared synthetically (2), the sequence identified from the RNA library may not confer the most optimized structure. To find a more optimal structure with a higher affinity, we tested chemically synthesized AN58. We reasoned that the synthetic AN58 might show a different conformation(s) and/or structure(s), because the synthetic RNA was made from the 3' to 5' direction, different from that of the enzymatic transcription. Indeed, by the whole-cell recording assay, the synthetic version of AN58 was found to have an IC₅₀ of ~30 nM (Figure 3G). This potency rivals existing competitive antagonists for AMPA receptors, including NBQX, SPD 502 (18), ZK200775 (19), and YM872 (20). Furthermore, this result suggests the possibility that the post-SELEX selection using doped library and other modifications may yield additional aptamer sequences/structures with even higher potency. The use of a doped library or a partially randomized library constructed based on the initially selected sequences provides a systematic search of structures with stronger activities (45).

DISCUSSION

As an initial proof of concept, we have used SELEX against the recombinant GluR2Q_{flip} receptor embedded in the membrane fragments of HEK-293S cells and successfully isolated a group of RNA aptamers. Our initial characterization of these aptamers focused on AN58. Its properties are compared favorably with those of NBQX. The nanomolar IC₅₀ value of AN58 assayed using whole-cell recording with the holo-GluR2Q_{flip} receptor in HEK-293S cells and the picomolar K_d value measured by radioligand displacement assay with the corresponding S1S2 ligand-binding core all suggest that AN58 rivals any existing AMPA receptor inhibitors currently known, including NBQX (2, 17). AN58 shows broad activity for all of AMPA receptor subunits, similar to NBQX, but has no activity for either GluR6 or NMDA receptors. As predicted, AN58 has the highest affinity for the GluR2 subunit, the target of selection.

The broad activity of AN58 toward AMPA receptors is likely attributed to the nature of AN58 being a competitive antagonist for the glutamate site, and glutamate is the common agonist or the common neurotransmitter. Furthermore, AMPA receptor genes share ~70% sequence homology (although the genes may undergo alternative splicing in both the C-terminus and the flip/flop region) (46). In the S1 extracellular binding domain, the sequence homology among AMPA receptors reaches more than 85%. However, AN58 does exhibit an improved affinity toward the GluR4 subunit, as compared to NBQX (Figure 3D). This result suggests that selection of aptamers that are more specific to an AMPA receptor subunit/conformation is possible, perhaps by using different types of compounds, such as noncompetitive inhibitors, as selection pressure.

One of the most important findings from this study is the demonstration of the possibility of developing an AMPA receptor inhibitor (i.e., AN58) that is equally potent, if not more potent than NBQX, and also water soluble. In addition, AN58 remains stable and potent even at a clinically relevant

acidic pH, whereas NBQX loses its potency by 3-fold. These characteristics, coupled with its physical stability, suggest that AN58 is a possible alternative to its chemical counterpart NBQX.

The determination of the binding site of AN58 on the receptor and the structure of AN58 using biochemical and structural means will be useful in the future. This work shall not only provide additional insights into the presumed mechanism of action of AN58 but also complementary information about the receptor site and the structure of AN58 for future development of inhibitors. Furthermore, the aptamer itself can be used as a new template and/or reagent targeting GluR2 and even other AMPA receptors as a whole. For this purpose, the aptamer needs to be chemically modified first, such as changing 2'-OH to 2'-F, to become nuclease-resistant (47). In addition, other types of chemical modifications are available, which can be used for enhancing pharmacokinetics, immobilization, or labeling of aptamers to make them useful as reagents and potential drugs (23, 27). For the latter, however, more work such as on the membrane permeability needs to be done.

The use of SELEX to evolve aptamers against a desired target generally requires target preparation. Various methods of target preparations have been developed (48), which have made SELEX increasingly routine, especially for soluble targets (23). However, preparation of a transmembrane protein target in both its entirety and functional form is still challenging. Consequently, the application of SELEX to aptamer selection against transmembrane proteins is limited as compared with SELEX with soluble targets. Membrane proteins often require a lipid environment to maintain wild-type functionality and may therefore have to be prepared and presented for SELEX in a complex background. As such, the evolution of aptamers can be dominated by an overwhelming amount of lipids and other targets in the lipid environment, as compared with the amount of target protein. In the successful SELEX cases involving membrane proteins, native membrane tissues (i.e., *Torpedo californica* electroplax membrane and rat forebrain membrane) have been used for RNA aptamer selection (49, 50). Live cells have been used for selection of ssDNA aptamers, including human red blood cell membrane (51) and hematopoietic tumor cells (52). In all the cases described above, proteins used for SELEX are native to cell membrane and these proteins are likely rich with respect to lipid quantity such that the SELEX are successful in these target-enriched environments. For recombinant membrane proteins not found in native tissues, a cell line (53) or a partial, soluble portion of a membrane protein (40, 54) has been constructed for SELEX.

Here we demonstrate that GluR2Q_{flip}, which may not be found in a pure isoform in a native tissue, can be transiently expressed in HEK-293S cells using a conventional transfection protocol and that the membrane fragments harboring the holo-receptor can be readily used as a SELEX target for the evolution of aptamers from a complex membrane background. It should be pointed out that the success of SELEX in our case correlated to the receptor density of ~0.61 pmol/mg of cell mass (i.e., in HEK-293S cells), which was achieved by coexpression of TAg (28). We did not, however, run the SELEX without TAg and therefore did not know whether a receptor density lower than what we used would have worked or not. Nevertheless, the use of HEK-

293S cells for transient expression of an ion channel, and other transmembrane proteins, is already a widely popular and routine method of receptor protein preparation for various assays. In comparison with the use of cell lines permanently expressing the protein of interest, transient expression is simpler and time saving. The use of membrane fragments harboring the protein of interest instead of live cells avoids the necessity of using chemically modified, nuclease-resistant RNA libraries. Therefore, our method entails minimal procedures to add to normal protocols for both membrane protein expression in cells and target preparation for SELEX.

ACKNOWLEDGMENT

We thank John T. Lis for his generous help and valuable advice, and David Shub, Caroline Koehrer, and Michael Zuker for helpful discussion. We thank Eric Gouaux for the S1S2 construct and Robert Oswald for the help with the S1S2 purification. We acknowledge Gang Li and Yan Han in our lab for collecting some data.

REFERENCES

- Dingledine, R., Borges, K., Bowie, D., and Traynelis, S. F. (1999) The glutamate receptor ion channels, *Pharmacol. Rev.* *51*, 7–61.
- Solyom, S., and Tarnawa, I. (2002) Non-competitive AMPA antagonists of 2,3-benzodiazepine type, *Curr. Pharm. Des.* *8*, 913–939.
- Li, G., Pei, W., and Niu, L. (2003) Channel-opening kinetics of GluR2Q(flip) AMPA receptor: a laser-pulse photolysis study, *Biochemistry* *42*, 12358–12366.
- Li, G., Sheng, Z., Huang, Z., and Niu, L. (2005) Kinetic mechanism of channel opening of the GluRDflip AMPA receptor, *Biochemistry* *44*, 5835–5841.
- Li, G., and Niu, L. (2004) How fast does the GluR1Qflip channel open? *J. Biol. Chem.* *279*, 3990–3997.
- Pei, W., Huang, Z., and Niu, L. (2007) GluR3 flip and flop: differences in channel opening kinetics, *Biochemistry* *46*, 2027–2036.
- Nowak, L., Bregestovski, P., Ascher, P., Herbet, A., and Prochiantz, A. (1984) Magnesium gates glutamate-activated channels in mouse central neurones, *Nature* *307*, 462–465.
- Rosenmund, C., Stern-Bach, Y., and Stevens, C. F. (1998) The tetrameric structure of a glutamate receptor channel, *Science* *280*, 1596–1599.
- Keinanen, K., Wisden, W., Sommer, B., Werner, P., Herb, A., Verdoorn, T. A., Sakmann, B., and Seeburg, P. H. (1990) A family of AMPA-selective glutamate receptors, *Science* *249*, 556–560.
- Hollmann, M., Hartley, M., and Heinemann, S. (1991) Ca²⁺ permeability of KA-AMPA-gated glutamate receptor channels depends on subunit composition, *Science* *252*, 851–853.
- Hume, R. I., Dingledine, R., and Heinemann, S. F. (1991) Identification of a site in glutamate receptor subunits that controls calcium permeability, *Science* *253*, 1028–1031.
- Burnashev, N., Monyer, H., Seeburg, P. H., and Sakmann, B. (1992) Divalent ion permeability of AMPA receptor channels is dominated by the edited form of a single subunit, *Neuron* *8*, 189–198.
- Jonas, P., and Spruston, N. (1994) Mechanisms shaping glutamate-mediated excitatory postsynaptic currents in the CNS, *Curr. Opin. Neurobiol.* *4*, 366–372.
- Geiger, J. R., Melcher, T., Koh, D. S., Sakmann, B., Seeburg, P. H., Jonas, P., and Monyer, H. (1995) Relative abundance of subunit mRNAs determines gating and Ca²⁺ permeability of AMPA receptors in principal neurons and interneurons in rat CNS, *Neuron* *15*, 193–204.
- Heath, P. R., and Shaw, P. J. (2002) Update on the glutamatergic neurotransmitter system and the role of excitotoxicity in amyotrophic lateral sclerosis, *Muscle Nerve* *26*, 438–458.
- Honore, T., Davies, S. N., Drejer, J., Fletcher, E. J., Jacobsen, P., Lodge, D., and Nielsen, F. E. (1988) Quinoxalinediones: potent competitive non-NMDA glutamate receptor antagonists, *Science* *241*, 701–703.
- Weiser, T. (2005) AMPA receptor antagonists for the treatment of stroke, *Curr. Drug Targets: CNS Neurol. Disord.* *4*, 153–159.
- Nielsen, E. O., Varming, T., Mathiesen, C., Jensen, L. H., Moller, A., Gouliaev, A. H., Watjen, F., and Drejer, J. (1999) SPD 502: a water-soluble and in vivo long-lasting AMPA antagonist with neuroprotective activity, *J. Pharmacol. Exp. Ther.* *289*, 1492–1501.
- Turski, L., Huth, A., Sheardown, M., McDonald, F., Neuhaus, R., Schneider, H. H., Dirnagl, U., Wiegand, F., Jacobsen, P., and Ottow, E. (1998) ZK200775: a phosphonate quinoxalinedione AMPA antagonist for neuroprotection in stroke and trauma, *Proc. Natl. Acad. Sci. U.S.A.* *95*, 10960–10965.
- Hara, H., Yamada, N., Kodama, M., Matsumoto, Y., Wake, Y., and Kuroda, S. (2006) Effect of YM872, a selective and highly water-soluble AMPA receptor antagonist, in the rat kindling and rekindling model of epilepsy, *Eur. J. Pharmacol.* *531*, 59–65.
- Tuerk, C., and Gold, L. (1990) Systematic evolution of ligands by exponential enrichment: RNA ligands to bacteriophage T4 DNA polymerase, *Science* *249*, 505–510.
- Ellington, A. D., and Szostak, J. W. (1990) In vitro selection of RNA molecules that bind specific ligands, *Nature* *346*, 818–822.
- Breaker, R. R. (2004) Natural and engineered nucleic acids as tools to explore biology, *Nature* *432*, 838–845.
- Lee, J. F., Stovall, G. M., and Ellington, A. D. (2006) Aptamer therapeutics advance, *Curr. Opin. Chem. Biol.* *10*, 282–289.
- Shi, H., Hoffman, B. E., and Lis, J. T. (1999) RNA aptamers as effective protein antagonists in a multicellular organism, *Proc. Natl. Acad. Sci. U.S.A.* *96*, 10033–10038.
- Ulrich, H. (2006) RNA aptamers: from basic science towards therapy, *Handb. Exp. Pharmacol.* *173*, 305–326.
- Blank, M., and Blind, M. (2005) Aptamers as tools for target validation, *Curr. Opin. Chem. Biol.* *9*, 336–342.
- Huang, Z., Li, G., Pei, W., Sosa, L. A., and Niu, L. (2005) Enhancing protein expression in single HEK 293 cells, *J. Neurosci. Methods* *142*, 159–166.
- Niu, L., Gee, K. R., Schaper, K., and Hess, G. P. (1996) Synthesis and photochemical properties of a kainate precursor and activation of kainate and AMPA receptor channels on a microsecond time scale, *Biochemistry* *35*, 2030–2036.
- Fan, X., Shi, H., Adelman, K., and Lis, J. T. (2004) Probing TBP interactions in transcription initiation and reinitiation with RNA aptamers that act in distinct modes, *Proc. Natl. Acad. Sci. U.S.A.* *101*, 6934–6939.
- Armstrong, N., and Gouaux, E. (2000) Mechanisms for activation and antagonism of an AMPA-sensitive glutamate receptor: crystal structures of the GluR2 ligand binding core, *Neuron* *28*, 165–181.
- Lukavsky, P. J., and Puglisi, J. D. (2004) Large-scale preparation and purification of polyacrylamide-free RNA oligonucleotides, *RNA* *10*, 889–893.
- Udgaonkar, J. B., and Hess, G. P. (1987) Chemical kinetic measurements of a mammalian acetylcholine receptor by a fast-reaction technique, *Proc. Natl. Acad. Sci. U.S.A.* *84*, 8758–8762.
- Kwak, S., and Kawahara, Y. (2005) Deficient RNA editing of GluR2 and neuronal death in amyotrophic lateral sclerosis, *J. Mol. Med.* *83*, 110–120.
- Akbarian, S., Smith, M. A., and Jones, E. G. (1995) Editing for an AMPA receptor subunit RNA in prefrontal cortex and striatum in Alzheimer's disease, Huntington's disease and schizophrenia, *Brain Res.* *699*, 297–304.
- Greger, I. H., Khatri, L., Kong, X., and Ziff, E. B. (2003) AMPA receptor tetramerization is mediated by Q/R editing, *Neuron* *40*, 763–774.
- Tomiyama, M., Rodriguez-Puertas, R., Cortes, R., Pazos, A., Palacios, J. M., and Mengod, G. (2002) Flip and flop splice variants of AMPA receptor subunits in the spinal cord of amyotrophic lateral sclerosis, *Synapse* *45*, 245–249.
- Koike, M., Tsukada, S., Tsuzuki, K., Kijima, H., and Ozawa, S. (2000) Regulation of kinetic properties of GluR2 AMPA receptor channels by alternative splicing, *J. Neurosci.* *20*, 2166–2174.
- Zuker, M. (2003) Mfold web server for nucleic acid folding and hybridization prediction, *Nucleic Acids Res.* *31*, 3406–3415.
- Chen, C. H., Chernis, G. A., Hoang, V. Q., and Landgraf, R. (2003) Inhibition of heregulin signaling by an aptamer that preferentially binds to the oligomeric form of human epidermal growth factor receptor-3, *Proc. Natl. Acad. Sci. U.S.A.* *100*, 9226–9231.
- Mayer, M. L., Ghosal, A., Dolman, N. P., and Jane, D. E. (2006) Crystal structures of the kainate receptor GluR5 ligand binding

- core dimer with novel GluR5-selective antagonists, *J. Neurosci.* 26, 2852–2861.
42. Lerma, J. (2006) Kainate receptor physiology, *Curr. Opin. Pharmacol.* 6, 89–97.
43. Patneau, D. K., Vyklicky, L., Jr., and Mayer, M. L. (1993) Hippocampal neurons exhibit cyclothiazide-sensitive rapidly desensitizing responses to kainate, *J. Neurosci.* 13, 3496–3509.
44. Oivanen, M., Kuusela, S., and Lonnberg, H. (1998) Kinetics and mechanisms for the cleavage and isomerization of the phosphodiester bonds of RNA by Bronsted acids and bases, *Chem. Rev.* 98, 961–990.
45. Knight, R., and Yarus, M. (2003) Analyzing partially randomized nucleic acid pools: straight dope on doping, *Nucleic Acids Res.* 31, e30.
46. Hollmann, M., and Heinemann, S. (1994) Cloned glutamate receptors, *Annu. Rev. Neurosci.* 17, 31–108.
47. Brody, E. N., and Gold, L. (2000) Aptamers as therapeutic and diagnostic agents, *J. Biotechnol.* 74, 5–13.
48. Gopinath, S. C. (2007) Methods developed for SELEX, *Anal. Bioanal. Chem.* 387, 171–182.
49. Ulrich, H., Ippolito, J. E., Pagan, O. R., Eterovic, V. A., Hann, R. M., Shi, H., Lis, J. T., Eldefrawi, M. E., and Hess, G. P. (1998) In vitro selection of RNA molecules that displace cocaine from the membrane-bound nicotinic acetylcholine receptor, *Proc. Natl. Acad. Sci. U.S.A.* 95, 14051–14056.
50. Cui, Y., Rajasethupathy, P., and Hess, G. P. (2004) Selection of stable RNA molecules that can regulate the channel-opening equilibrium of the membrane-bound γ -aminobutyric acid receptor, *Biochemistry* 43, 16442–16449.
51. Morris, K. N., Jensen, K. B., Julin, C. M., Weil, M., and Gold, L. (1998) High affinity ligands from in vitro selection: complex targets, *Proc. Natl. Acad. Sci. U.S.A.* 95, 2902–2907.
52. Shanguan, D., Li, Y., Tang, Z., Cao, Z. C., Chen, H. W., Mallikaratchy, P., Sefah, K., Yang, C. J., and Tan, W. (2006) Aptamers evolved from live cells as effective molecular probes for cancer study, *Proc. Natl. Acad. Sci. U.S.A.* 103, 11838–11843.
53. Pestourie, C., Cerchia, L., Gombert, K., Aissouni, Y., Boulay, J., De Franciscis, V., Libri, D., Tavitian, B., and Duconge, F. (2006) Comparison of different strategies to select aptamers against a transmembrane protein target, *Oligonucleotides* 16, 323–335.
54. Mori, T., Oguro, A., Ohtsu, T., and Nakamura, Y. (2004) RNA aptamers selected against the receptor activator of NF-kappaB acquire general affinity to proteins of the tumor necrosis factor receptor family, *Nucleic Acids Res.* 32, 6120–6128.
55. Blanpied, T. A., Clarke, R. J., and Johnson, J. W. (2005) Amantadine inhibits NMDA receptors by accelerating channel closure during channel block, *J. Neurosci.* 25, 3312–3322.

BI701036P

Enhancing protein expression in single HEK 293 cells

Zhen Huang, Gang Li, Weimin Pei, Leivi A. Sosa¹, Li Niu*

Department of Chemistry, Center for Neuroscience Research, University at Albany, SUNY, Albany, NY 12222, USA

Received 2 June 2004; received in revised form 7 September 2004; accepted 17 September 2004

Abstract

Recombinant proteins are routinely expressed in heterologous expression systems such as human embryonic kidney 293 (HEK 293) cells. The efficiency of the expression is critical when the expressed protein must be characterized at the single-cell level. Here we describe a simple method by which the protein expression efficiency in single HEK 293 cells is enhanced by coexpressing simian virus 40 large T antigen (TA_g), a powerful oncoprotein. Using the GluR2 ionotropic glutamate receptor as an example, we found that the receptor expression in single HEK 293S cells increased approximately seven-fold. The ratio of the plasmid amount of TA_g to that of the receptor was optimized at 1:10, while the receptor function was unaffected in the presence of TA_g. We further used fluorescence imaging from a population of cells as an independent detection method and found a similar increase in expression of green fluorescent protein (GFP) by TA_g coexpression. This method is thus applicable for enhancing the expression of both membrane and soluble proteins at the single-cell level. More importantly, the function of a protein can be studied directly in intact cells, a feature particularly useful for studying membrane proteins.
© 2004 Elsevier B.V. All rights reserved.

Keywords: Glutamate ion channels; Green fluorescent protein; Transient transfection; HEK 293 cells; Simian virus 40 large T antigen; Protein expression

1. Introduction

The use of human embryonic kidney 293 (HEK 293) cells has been one of the most popular ways for expression of recombinant proteins (Graham et al., 1977). There are a variety of transfection protocols to deliver a recombinant gene to those cells (Chen and Okayama, 1987; Corsaro and Pearson, 1981; Graham and van der Eb, 1973; Luthman and Magnusson, 1983; Washbourne and McAllister, 2002). Generally, those protocols provide a reasonable protein expression yield, especially when the culture volume is not restricted. In such a case, a larger volume of culture from which more cells can be harvested compensates for a low efficiency of protein expression at the single-cell level. However, a low efficiency of single-cell protein expression can be an insurmountable problem when the protein must be characterized by single-cell imaging and/or single-cell

recording. This is because the number of protein molecules expressed per cell is generally proportional to the signal strength. For instance, ion channel proteins are expressed routinely in HEK 293 cells and assayed directly using a single cell, either entirely (e.g., for whole-cell recording) or partially (e.g., for recording with membrane patches and for single-channel recording) (Hamill et al., 1981). As such, the number of ion channels expressed per cell is critical to their detection. Furthermore, in the presence of inhibitors, the protein signal is adversely reduced. Thus, these and many other types of studies will benefit from a method by which the efficiency of protein expression in single cells can be enhanced. Developing such a method was the goal of the present study.

The method we established originated from our interest of ionotropic glutamate receptors (Dingledine et al., 1999). These receptors are transmembrane channels that can open upon binding of glutamate, a neurotransmitter in the central nervous system (Dingledine et al., 1999). Glutamate receptors play special roles in brain activities, such as memory and learning, and have been implicated in a variety of neurological diseases, such as post-stroke cellular lesion and amyotrophic lateral sclerosis (Dingledine et al., 1999;

* Corresponding author. Tel.: +1 518 442 4447; fax: +1 518 442 3462.

E-mail address: lniu@albany.edu (L. Niu).

¹ Present address: SUNY Downstate Medical Center, 450 Clarkson Avenue, Brooklyn, NY 11203-2098, USA.

Heath and Shaw, 2002). To study the structure–function relationship, glutamate receptors are commonly expressed in HEK 293 cells and characterized directly in single cells. By our method, the receptor expression efficiency in single cells can be increased by about seven-fold, compared with a popular expression protocol using calcium phosphate in transfection (Chen and Okayama, 1987). The key to our method is to coexpress simian virus (SV) 40 large T antigen (TAg), a powerful oncoprotein (Ali and DeCaprio, 2001; Chen and Hahn, 2003; Simmons, 2000; Sullivan and Pipas, 2002), with the protein of interest. Specifically, the gene of the protein of interest is harbored in a plasmid containing the SV40 replication origin, and the TAg gene is encoded in a separate vector. Transient coexpression of TAg produces more proteins of interest per cell. This is because, among its functions, SV40 TAg disrupts the cell-cycle checkpoints by binding to and inactivating key tumor suppressors and cell-cycle regulatory proteins such as p53 and pRB (Ali and DeCaprio, 2001; Sullivan and Pipas, 2002). Consequently, the cell turns into a growth-deregulated protein-making factory. Specifically, we characterized TAg enhancement of the single-cell expression of GluR2, a key glutamate receptor subunit (Li et al., 2003b), to establish the optimal plasmid ratio and the most complementing cell line. We further characterized the function of the GluR2 receptor with intact cells, without removing TAg. In addition, using green fluorescence protein (GFP) (Chalfie et al., 1994) as a reporter gene and fluorescence imaging of a population of HEK 293 cells as an independent detection method, we showed that the GFP expression in these cells increased similarly. Together, our results demonstrate that this method represents a significant improvement over conventional protein expression protocols. Furthermore, the method should be general for expressing both soluble and membrane proteins, and for characterizing the protein function directly in single cells.

2. Materials and methods

2.1. Expression of plasmid DNAs and cell culture

The cDNA encoding GluR2 (unedited at the Q/R site, and flip isoform) in a pBlueScript vector (from Prof. Steve Heineemann at Salk Institute) was cloned into the pcDNA3.1 vector (Invitrogen, Carlsbad, CA) that contained the SV40 replication origin (8.6 kb). To identify cells that might express the GluR2 receptor for recording, the GluR2 plasmid was cotransfected with a GFP plasmid lacking the SV40 replication origin (from Prof. Ben Szaro at SUNY-Albany). As a result, the GFP expression in cells or the resulting green color intensity was not affected by coexpression of TAg (see the text). However, a different GFP construct (pEGFP-C3, 4.7 kb) (Clontech, Palo Alto, CA) that did contain the SV40 replication origin was used in the enhancement of GFP expression by TAg (the TAg plasmid, 6.0 kb, from Prof. Jeremy Nathans at Johns Hopkins University). All the plasmids were

propagated in an *Escherichia coli* host (DH5 α) and purified using a kit from QIAGEN (Valencia, CA).

The cell lines used in this study were regular HEK 293 cells (from Prof. Robert Oswald at Cornell University), 293S cells (from Prof. Gobind Khorana at MIT) and 293T cells (American Tissue Culture Collection, Cat. No. CRL-11268, Manassas, VA). All cell lines were maintained in Dulbecco's modified Eagle's medium supplemented with 10% fetal bovine serum, 100 U/ml penicillin and 100 μ g/ml streptomycin in a 37 °C, 10% CO₂, humidified incubator.

A standard calcium phosphate method (Chen and Okayama, 1987) was used in most of transient transfections for gene delivery, although lipofectamine (Invitrogen, Cat. No. 18324-111, Carlsbad, CA) was used in some transfections (see text). The GluR2 plasmid used was \sim 3–6 μ g (the plasmid amount used here and below was for a culture in the 35 mm dish). As a cell marker, the GFP plasmid that lacked the SV40 replication origin was cotransfected with the GluR2 with the ratio of the plasmid of GFP to that of GluR2 by weight being 1:10 (Li et al., 2003b). The amount of the TAg plasmid varied in experiments (see Section 3). The amount of pEGFP plasmid was 1–3 μ g whereas the weight ratio of pEGFP plasmid to TAg plasmid varied from 2:1 to 15:1. All the cells used for recording or imaging were those that grew in between 48 and 58 h after transfection.

2.2. Whole-cell current recording

Because the expression of the GluR2 gene leads to the formation of functional channels (Boulter et al., 1990), both the expression and the functional properties of this receptor are testable by measuring the magnitude and the time course of the glutamate-induced whole-cell current from an entire cell. The ratio of the current amplitude in the absence and presence of TAg, but at a constant glutamate concentration, was therefore used to represent the effect of TAg in enhancing the receptor expression.

The procedure for recording the GluR2 channel activity was previously described (Li et al., 2003b). Briefly, the recording electrodes were pulled from glass capillaries (World Precision Instruments, Sarasota, FL). The electrode resistance was \sim 3 M Ω when filled with the electrode solution. The electrode solution contained (in mM) 110 CsF, 30 CsCl, 4 NaCl, 0.5 CaCl₂, 5 EGTA, and 10 HEPES (pH 7.4 adjusted by CsOH). The external bath solution contained (in mM) 150 NaCl, 3 KCl, 1 CaCl₂, 1 MgCl₂, 10 HEPES (pH 7.4 adjusted by HCl). Whole-cell recordings were done at -60 mV, and 22 °C. Specifically, a cell that expressed the GluR2 receptor was bathed in the external solution. Glutamate was applied from a cell-flow device (Udgaonkar and Hess, 1987) to the cell, and the resulting whole-cell current was recorded using an Axopatch-200B amplifier at cutoff frequency of 2 kHz by a built-in, 8-pole Bessel filter, and digitized at 5 kHz sampling frequency using a Digidata 1322A from Axon Instruments (Union City, CA). The data were acquired using pCLAMP 8 (also from Axon). The rise time of

the glutamate-induced whole-cell current response (10–90%) was 2.3 ± 0.1 ms, an average of the measurement from >100 cells. Each data point was an average of at least three measurements collected from at least three cells unless otherwise noted. Origin 7 (Origin Lab, Northampton, MA) was used for plotting. Uncertainties refer to standard error of the fits unless noted otherwise.

2.3. Fluorescence imaging and quantification

The GFP fluorescence in cells was imaged using a confocal laser scanning microscope (ZEISS LSM510 META, Carl Zeiss, Thornwood, NY), and recorded using a RETIGA Ex digital camera (Qimaging, Burnaby, BC, Canada) with the QCapture software (Suite 2.66 from Qimaging, Burnaby, BC, Canada). For bright-field images, 1 ms exposure time was used at gain 3000 and offset 0. For fluorescence images, 15 ms exposure time was used at gain 3500 and offset 2000. Images were digitized using Image J software (version 1.30 from <http://rsb.info.nih.gov/ij/>).

The fluorescence intensity in a single cell was assumed to be linearly proportional to the amount of the GFP expressed in the cell. Likewise, the accumulated fluorescence intensity per image that included many cells was assumed to be the averaged measure of the GFP expression in those cells. For each 35 mm Petri dish used to express GFP, three bright-field images were taken from three randomly chosen locations, and each image contained about 2000 cells. For the corresponding area, three fluorescence images were also recorded. Each fluorescence image contained 1360×1036 pixels, and each pixel was scored to a value possibly ranging from 7 to 220 (on 8-bit digital scale using Image J). The background value was set to be 35 on this scale; below this value, no cell could be visually recognized. This value was then deducted from the value of each pixel in calculating the fluorescence intensity of a green cell. On average, a green cell was represented by >1000 pixels. The accumulated fluorescence intensity per image was tabulated into a histogram with the bin width of 10. The fluorescence intensity from 85 to 15% range in the histogram was chosen for comparison of the TAG enhancement in 293S cells, excluding those that were too bright and too dim. This was the same practice used qualitatively in choosing green cells for whole-cell recording. The corresponding range of the fluorescence intensity of the cells cotransfected with the TAG gene was compared to that of the control. The ratio of these values was used as the measure of the TAG enhancement of the GFP expression in HEK 293S cells.

3. Results

3.1. TAG enhancement of glutamate receptor expression in single HEK 293 cells assayed by whole-cell recording

The whole-cell current response of the GluR2 receptor to $200 \mu\text{M}$ glutamate was higher from single HEK 293 cells

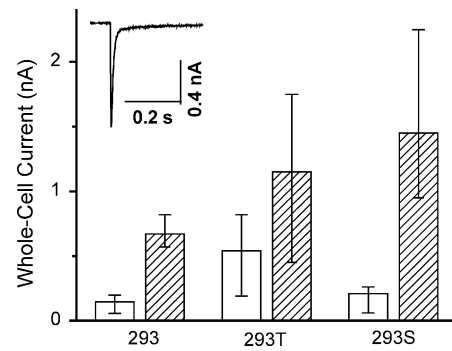


Fig. 1. TAG enhances the GluR2 receptor expression in different HEK 293 cell lines, detected by whole-cell recording. The whole-cell current response to $200 \mu\text{M}$ glutamate with (dashed column) and without (open column) the coexpression of TAG (the inset is a representative current response) is shown. The height of each column represents the average of the current amplitudes from >40 cells, and the bar represents the range of the current observed for 10–90% of the cells. As compared to the control (open column), the receptor current response, enhanced by TAG coexpression, was increased by 4.5-fold in the regular 293 cell line, 2.1-fold in the 293T cell line and 6.9-fold in the 293S cell line. In these experiments, the amount of TAG, GFP and GluR2 plasmids used for transfection was 0.4, 0.4 and $4 \mu\text{g}$, respectively.

cotransfected with TAG than the control or the cell transfected with only GluR2 (Fig. 1). This result suggested that the GluR2 expression in single cells was higher when the cells coexpressed TAG. Moreover, we identified 293S cells (Stillman and Gluzman, 1985) as the most complementing cell type among all three HEK 293 cell lines tested. This was evidenced by a seven-fold increase in glutamate-induced current response in 293S cells (Stillman and Gluzman, 1985), compared with a two- and five-fold increase in 293T cells (Sena-Esteves et al., 1999) and regular 293 cells (Graham et al., 1977), respectively (Fig. 1).

The 293S cell line is a suspension-adapted cell type (Stillman and Gluzman, 1985), whereas the regular 293 and 293T cell lines are known to be suitable for static culture. The 293S cell line, like the regular 293 cell line but unlike the 293T cell line, does not constitutively express TAG (Stillman and Gluzman, 1985). Thus, without introduction by transfection of the TAG gene to these cells, it would be expected and indeed was found (see control values: open columns in Fig. 1) that the efficiency of the receptor expression was higher in the 293T cell. This observation was consistent with the presumed function of TAG, which is to increase the protein expression in that same cell. When TAG was cotransfected with all these cell types, the receptor expression was higher than the corresponding control, as expected, but was the highest in the 293S cell (Fig. 1) for reasons yet not clear. The 293S cells used in our experiments were grown in static culture like other 293 cell lines, rather than in suspension. We found that the 293S cells in static culture were suitable for electrophysiological recording where only the dish-attached cells were picked to make gigaohm seals. In static culture, the majority of 293S cells were indeed attached to Petri dishes, albeit more loosely than regular 293 or 293T cells. Based on these results (Fig. 1), we decided to use 293S cells for the rest of the experiments.

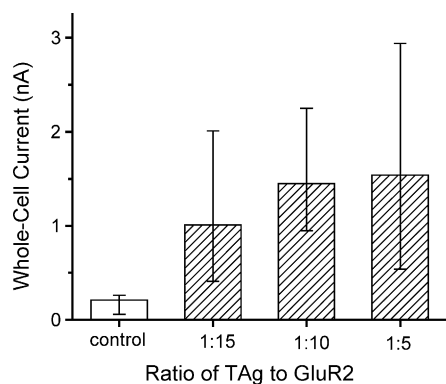


Fig. 2. Enhancement of the GluR2 expression by TAg in HEK 293S cells reaches seven-fold at the 10:1 ratio for the amount of the TAg DNA plasmid used compared to the GluR2 plasmid in transient transfection. Different receptor expression in 293S cells was observed, as shown by the receptor current response to 200 μ M glutamate, at different ratios of TAg plasmid amount used for transient transfection, compared to the GluR2 plasmid amount. The GluR2 DNA plasmid was kept to be 4 μ g per 35 mm dish. The control was from cells expressing GluR2 only, shown as open column. The height of each column represents the average of the current amplitudes from >40 cells, and the bar represents the range of the current observed for 10–90% of the cells.

3.2. Optimal ratio of TAg plasmid used for transient transfection

Next, we varied the amount of the TAg plasmid relative to that of GluR2 to determine the optimal ratio of TAg for transient expression with HEK 293S cells. This ratio would correspond to a minimal amount of the TAg plasmid that must be used to reach the maximal enhancement of the protein expression. The result of this experiment (Fig. 2) showed that, to reach the seven-fold increase in the receptor expression, the optimal ratio of the amount of the TAg plasmid to the amount of the GluR2 plasmid used in transfection was 1:10.

Notice that we used the amount of the TAg plasmid in microgram (μ g) for transient transfection, rather than the amount of the TAg protein actually expressed in the cell, to represent the magnitude of the enhancement of the receptor expression per cell. This is because both the exact amount of TAg sufficient to influence the protein expression in cells and the time it took for the cell to synthesize that amount of TAg after the transient transfection are difficult to assess. After the TAg plasmid was co-introduced into the cell by transfection, the expression of both GluR2 and TAg would presumably occur concomitantly. Given that the presence of TAg led to enhancing the receptor expression in the same cell, we assumed that the expression of TAg must have reached a level sufficient to deregulate the cell-cycle control prior to a significant production of the GluR2 receptor. This assumption was supported by the observation that without TAg, receptor expression was lower at the single-cell level (in both regular 293 cells and 293S cells), compared with the yield in the presence of TAg (either in 293T cells that constitutively expressed TAg or in all three cell types, i.e., regular 293, 293T and 293S cells, but with TAg coexpression) (Figs. 1 and 2). When the plasmid amount of TAg in cotransfection was increased, a

higher expression of the receptor in the cells was observed, compared to the control. Thus, it was assumed that a greater quantity of plasmid proportionally increased the amount of the TAg protein expressed in cells. As an empirical method, using the exact amount of the TAg plasmid for transfection seemed to enable us to control the level of the enhancement of the receptor expression by TAg. Finally, the amount of TAg required to effectively deregulate the cell-cycle control, although unknown, may be low. Such a minimal amount of TAg synthesized in the cell presumably at the early stage of gene expression should be sufficient for the cell to be in a growth-deregulated state, before the expression of the protein of interest is peaked.

3.3. Whole-cell recording assay of the functional properties of glutamate receptors

A method to improve single-cell protein expression should be ideally amenable to the condition where the function of the protein can be assayed in a single cell *directly* or without removing TAg. This is particularly advantageous for studying glutamate ion channels because glutamate channels, like many other membrane proteins, are routinely characterized using electrophysiological recordings in the cell where they are expressed. To test whether our method offered this additional benefit, we measured the properties of the GluR2 channel in the absence and presence of TAg. Our results showed that the coexpression of TAg did not affect GluR2 function, as evidenced by identical desensitization rate constants (Fig. 3A) and current–voltage relationships (Fig. 3B). This finding was also consistent with the identical glutamate dose–response relationship we reported earlier (Li et al., 2003b) for this receptor. Separately, we further tested the desensitization rate constant and the dose–response relationship for other glutamate receptors, such as GluR1 and GluR4 receptors (data not shown). All the results showed that the presence of TAg in the cell expressing the corresponding glutamate receptor did not affect the kinetic properties of the receptor.

3.4. TAg enhancement of GFP expression visualized by fluorescence imaging

We demonstrated, using the GluR2 receptor, that protein expression efficiency was increased at the single-cell level. By inference, protein production efficiency should likewise improve in a population of cells. Therefore, testing the enhancement of protein expression from a large population would serve as a control to validate the conclusions of the single-cell study (Figs. 1 and 2). For this purpose, we examined the TAg enhancement of GFP expression in HEK 293S cells by fluorescence imaging (Fig. 4). There were two notable features in the design of this control experiment using GFP. First, unlike the GluR2 receptor, GFP is a soluble protein and is widely used as a gene expression marker (Chalfie et al., 1994). Second, the use of fluorescence imaging to quan-

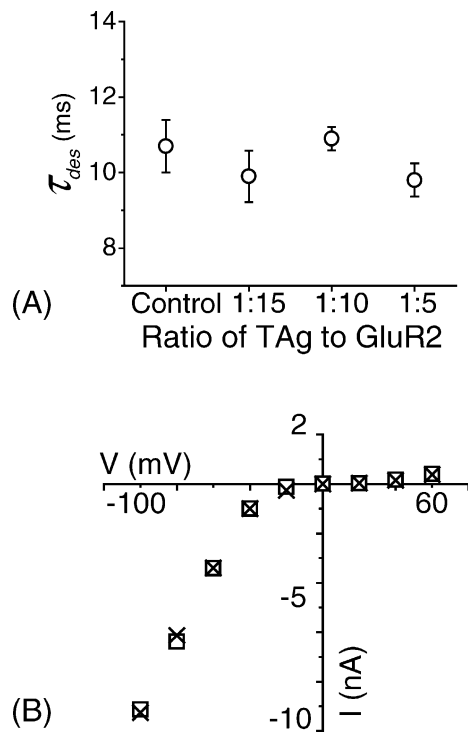


Fig. 3. Coexpression of TAg does not affect the functional properties of the GluR2 receptor expressed in HEK 293S cells. (A) Using whole-cell recording, the desensitization time constant (τ_{des}) was measured at different ratios of the amount of the TAg plasmid used in transient transfection, compared to the amount of the GluR2 plasmid. The desensitization of the GluR2 channel induced by the continuous binding of glutamate at 200 μ M was fitted by a single-exponential rate (an example of the receptor desensitization, seen as the fall of the current, is shown in the inset of Fig. 1). (B) Current–voltage relationship, as determined using 200 μ M glutamate and whole-cell recording. Each symbol reflects an average of at least three measurements from at least three cells expressing the GluR2 receptor with (\square) and without (\times) the coexpression of TAg. The ratio of the amount of TAg plasmid (0.4 μ g) to that of GluR2 plasmid was 1:10.

tify the GFP expression in a large number of cells was a different detection method, compared to the use of whole-cell recording to assay the GluR2 activity from single cells. Analysis of the fluorescence intensity of GFP expressed in 293S cells with and without TAg showed that TAg enhanced GFP expression (Fig. 4A), as expected, to the maximum of about seven-fold (Fig. 4B), although at the 1:10 plasmid ratio, the enhancement was slightly less than that obtained by single-cell recording (Fig. 1).

It should be noted that GFP was also used as a *cell marker* in the whole-cell recording experiments (Figs. 1–3) because a green-colored cell was easily identifiable, and such a cell would likely express the GluR2 receptor (the ratio of the plasmid used for GFP to GluR2 was 1:10). The plasmid that harbored the GFP gene used in those experiments did not contain the SV40 replication origin, unlike the GFP construct used for the GFP enhancement experiment (Fig. 4). Consequently, the GFP intensity was about the same in the absence and presence of TAg (the fluorescence images are not shown). The use of the GFP plasmid lacking the SV40

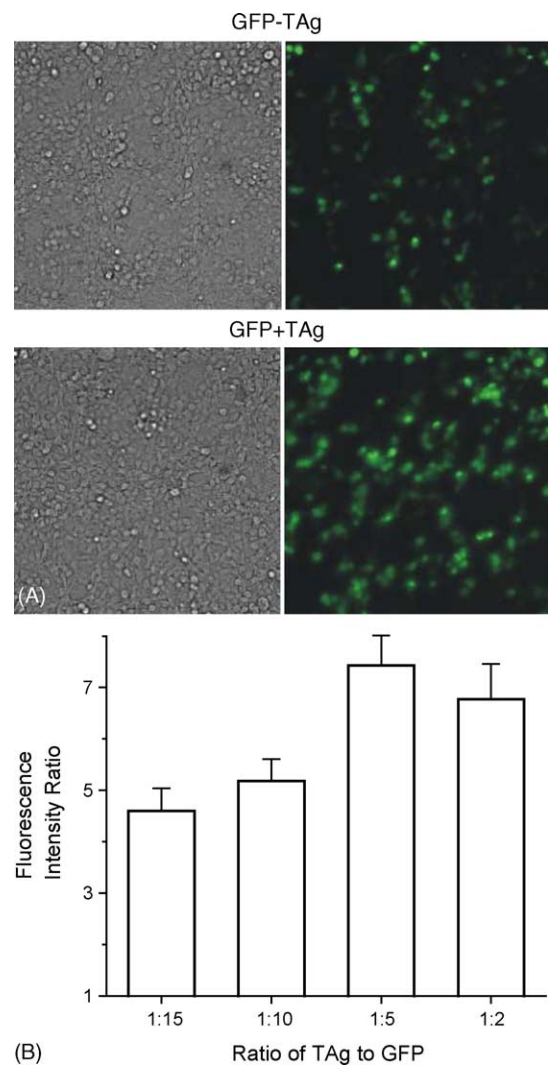


Fig. 4. Coexpression of TAg enhances GFP expression in HEK 293S cells determined by fluorescence imaging and quantification. (A) Comparison of the bright-field (left panel) and green fluorescence images (right panel) for the same number of cells expressing GFP with (lower pair, GFP + TAg) and without (upper pair, GFP – TAg) TAg coexpression. The image acquisition and quantification were described in detail in Section 2. Specifically, the images shown here were from cells transfected with 1 μ g GFP and 0.1 μ g TAg plasmid. (B) The ratio of the fluorescence intensity, as compared to the control (without TAg coexpression), at different ratios of the amount of TAg used to that of the GFP plasmid. The GFP plasmid used for transfection (i.e., pEGFP-C3) was kept to be 1 μ g per 35 mm dish. The absolute fluorescence intensity was determined from the accumulation of about 2000 cells counted from the bright-field image. Three images were taken from each dish, and a total of three dishes were used for image analysis as shown for each column. The fluorescence intensity was averaged and plotted as a ratio to the control, i.e., the fluorescence intensity from the cells expressing GFP without TAg.

replication origin in the single-cell experiments (Figs. 1–3) ensured that only the expression of the GluR2 gene, rather than the expression of both the GluR2 and GFP genes, was affected by the coexpression of TAg. Thus, this experimental design permitted a quantitative comparison of the results of fluorescence imaging of GFP with that of whole-cell recording of GluR2. The lack of the SV40 replication origin in the

GFP plasmid construct used in recordings (Figs. 1–3) and consequently the invariant fluorescent intensity of the cells in the absence and presence of TAg confirmed the function of TAg in deregulating cell growth through the SV40-controlled pathway (Ali and DeCaprio, 2001).

In designing the GFP enhancement experiment by TAg, we considered the difference in assaying protein expression by different techniques. This was because in the whole-cell recording assay, only the GluR2 receptor molecules embedded on the surface of the cellular membrane were detectable. In contrast, the GFP expressed was detectable by fluorescence imaging regardless of its location because GFP is a soluble protein. Fleck et al. (2003) studied glutamate receptor expression/trafficking and reported that only ~40% of the glutamate receptors (e.g., GluR6 kainate receptor subunit) are on the surface of the membrane of HEK 293 cells, whereas 60% of the receptors, once made, are sequestered in the endoplasmic reticulum (ER). For the same receptor, we found previously that the green fluorescence intensity is linearly proportional to the amplitude of the receptor current (Li et al., 2003a). This means that the greener the cell, the larger the current is at a given glutamate concentration. Based on those results, we used 3–6 μg of plasmid encoding the GluR2 gene for transfection in the single-cell experiments (Figs. 1–3). We assumed that 40% of the plasmid amount, or 1–3 μg , would be responsible for producing surface-embedded GluR2 receptors (since glutamate was applied extracellularly and the glutamate-binding site was located in the extracellular face of the receptor) (Armstrong and Gouaux, 2000). In the GFP-enhancement experiment, we used 1–3 μg of the GFP plasmid (Fig. 4). Although a smaller amount of GFP plasmid was used, compared to the total amount of the GluR2 plasmid used for transfection, the entire amount of GFP expressed was detectable by fluorescence imaging. As observed (Fig. 4A), GFP lit up an entire cell with its characteristic green fluorescence color.

3.5. Effect of TAg coexpression on cell growth

The imaging of the GFP fluorescence from a population of cells enabled us to acquire additional information about the effect of TAg coexpression by transient transfection on cellular morphology, viability and growth. First, the cell morphology (Fig. 4A) was unaffected in the presence of TAg. This was true for all 293 cell lines tested. Second, the green fluorescence intensity peaked on day 2 after transfection, although on day 1 the fluorescence intensity of the cell culture subject to the TAg coexpression was visibly higher than controls. After cotransfection of the TAg gene, the doubling time and the cell viability of the culture were no different from controls. These results are consistent with the conclusion that additional amount of protein was made at the single-cell level per unit time in the presence of TAg. Third, the transfection efficiency was slightly higher than control (13% versus ~20% based on 15 transfections and 100% cell count). The transfection efficiency was determined by the percentage of green

cells observed by fluorescence imaging in the total number of cells observed by bright-field microscopy for the same sample (see the comparison of these images in Fig. 4A). One explanation for these results might be that the GFP level in some cells became high enough to be detected but only in the presence of TAg. Together, these results (Fig. 4) indicate that the major TAg enhancement can be accounted for by the increase in protein production at the single-cell level, and such a conclusion agrees with the one previously described for the single-cell assay of the GluR2 receptor expression (Figs. 1 and 2).

4. Discussion

We described a method for improving the single-cell expression efficiency of recombinant proteins by about seven-fold, compared to the efficiency from a popular transfection protocol (Chen and Okayama, 1987). To achieve this enhancement, a powerful oncoprotein, SV40 TAg, was co-expressed with the gene of interest in HEK 293S cells at the optimal ratio of 1:10 in weight for the plasmid amount of TAg used to that of the protein of interest. We demonstrated this method by using two proteins and two detection techniques: a membrane-bound glutamate receptor whose expression level was assayed by electrophysiological recording with single 293S cells, and soluble GFP whose expression was visualized by fluorescence imaging of a population of cells. We further demonstrated that the function of the protein of interest can be assayed directly, if desired, by using an intact cell without removing TAg. Therefore, this method is expected to be useful for single-cell characterization of the protein signal by recordings and/or imaging, because the level of protein expression by a single cell may become high enough to be detected or augmented to achieve a stronger signal. Finally, this method is simple to implement.

The transient transfection method using calcium phosphate precipitation is a very popular method to deliver gene to cells, such as HEK 293 cells. This method is considered a benchmark, compared with many other alternatives, non-viral transfection protocols, because of its relative high transfection efficiency (Chen and Okayama, 1987). The method we described takes advantage of the high transfection efficiency by using the calcium phosphate precipitation for gene delivery, but further improves the yield of protein expression by increasing the expression efficiency per transfected cell. In the presence of TAg, the transfected cell makes more proteins because TAg deregulates the control of the cell growth cycle. Therefore, our method is expected to work in other permissive cell lines, provided that the gene of interest, together with the TAg gene, is first delivered to the host cell. We postulate how the genes are delivered to the host cell may have little influence on the ratio of the enhancement when the TAg is coexpressed. As a test, we alternatively used the lipofection method (Washbourne and McAllister, 2002) to transfect HEK 293S cells with the GluR2 and TAg genes.

We found that the ratio of enhancement of the GluR2 receptor expression was identical to that of the calcium phosphate precipitation method (data not shown). This result suggests that the method we presented may be equally effective for other gene delivery approaches.

The HEK 293 cell is a widely used cell line for mammalian gene expression for both soluble and membrane proteins. The method we described should therefore be generally applicable. Among three different HEK 293 cell lines tested in the present study, namely regular 293, 293T and 293S cells, we found empirically that the suspension-adapted 293S cell line was most complementary to the use of TAG. However, we do not yet know why the 293S cell line is superior. Nevertheless, the advantage of using the suspension-adapted 293S cells further suggests that our method is fully adaptable for suspension culture in shake flasks and bioreactors for a larger scale of production of more proteins per unit volume of culture medium. This may be particularly useful when expensive reagents are needed and when the culture is scaled up. Furthermore, the use of 293S cells may be especially advantageous for preparing membrane proteins, because this cell line is known to express proteins whose activities are modulated by complex post-translation, a feature often observed for membrane proteins (Berg et al., 1993).

How can our method be used to specifically improve studies of ion channel receptors? Membrane proteins such as channels and transporters are routinely expressed in HEK 293 cells and directly assayed in single cells. Thus, our method should be beneficial in general and may be most beneficial in particular for studying proteins whose expression is not efficient or whose signal must be studied at very low concentrations of ligands. For instance, the expression of the GluR2 receptor channel, as used in the present study, is not as efficient as that of GluR6. In some reports, a saturating concentration of glutamate must be used to detect the receptor response (Grosskreutz et al., 2003). In such cases, enhancing the receptor yield in single cells will surely permit a larger current response at the same concentration of glutamate. Furthermore, this method will be useful in inhibitor–receptor studies, because in the presence of inhibitors, the receptor response is less than in their absence. Finally, the use of outside-out patches to achieve a faster receptor response, compared with the use of a whole cell, is a popular method in electrophysiological recording (Hamill et al., 1981). This recording configuration can minimize the distortion of the receptor response due to rapid channel desensitization. However, when outside-out patches are used, only a fraction of the receptor molecules expressed from an entire cell can be sampled because the area of the membrane from an outside-out patch is several hundred times smaller than that of an entire cell. Consequently, greater efficiency of the receptor expression in a single cell from which an outside-out membrane patch is excised is required. The use of TAG to increase the number of receptor molecules expressed in single cells is therefore expected to be helpful for such studies.

Acknowledgements

We thank David Tieman for assistance in imaging and Lisa Maroski for manuscript editing. This work was supported in part by grants from Department of Defense (W81XWH-04-1-0106), American Heart Association (0130513T), the ALS Association, and Muscular Dystrophy Association.

References

- Ali SH, DeCaprio JA. Cellular transformation by SV40 large T antigen: interaction with host proteins. *Semin Cancer Biol* 2001;11(1):15–23.
- Armstrong N, Gouaux E. Mechanisms for activation and antagonism of an AMPA-sensitive glutamate receptor: crystal structures of the GluR2 ligand binding core. *Neuron* 2000;28(1):165–81.
- Berg DT, McClure DB, Grinnell BW. High-level expression of secreted proteins from cells adapted to serum-free suspension culture. *Biotechniques* 1993;14(6):972–8.
- Boulter J, Hollmann M, O’Shea-Greenfield A, Hartley M, Deneris E, Maron C, et al. Molecular cloning and functional expression of glutamate receptor subunit genes. *Science* 1990;249(4972):1033–7.
- Chalfie M, Tu Y, Euskirchen G, Ward WW, Prasher DC. Green fluorescent protein as a marker for gene expression. *Science* 1994;263(5148):802–5.
- Chen W, Hahn WC. SV40 early region oncoproteins and human cell transformation. *Histol Histopathol* 2003;18(2):541–50.
- Chen C, Okayama H. High-efficiency transformation of mammalian cells by plasmid DNA. *Mol Cell Biol* 1987;7(8):2745–52.
- Corsaro CM, Pearson ML. Competence for DNA transfer of ouabain resistance and thymidine kinase: clonal variation in mouse L-cell recipients. *Somatic Cell Genet* 1981;7(5):617–30.
- Dingledine R, Borges K, Bowie D, Traynelis SF. The glutamate receptor ion channels. *Pharmacol Rev* 1999;51(1):7–61.
- Fleck MW, Cornell E, Mah SJ. Amino-acid residues involved in glutamate receptor 6 kainate receptor gating and desensitization. *J Neurosci* 2003;23(4):1219–27.
- Graham FL, Smiley J, Russell WC, Nairn R. Characteristics of a human cell line transformed by DNA from human adenovirus type 5. *J Gen Virol* 1977;36(1):59–74.
- Graham FL, van der Eb AJ. Transformation of rat cells by DNA of human adenovirus 5. *Virology* 1973;54(2):536–9.
- Grosskreutz J, Zoerner A, Schlesinger F, Krampfl K, Dengler R, Bülfer J. Kinetic properties of human AMPA-type glutamate receptors expressed in HEK293 cells. *Eur J Neurosci* 2003;17(6):1173–8.
- Hamill OP, Marty A, Neher E, Sakmann B, Sigworth FJ. Improved patch-clamp techniques for high-resolution current recording from cells and cell-free membrane patches. *Pflugers Arch* 1981;391(2):85–100.
- Heath PR, Shaw PJ. Update on the glutamatergic neurotransmitter system and the role of excitotoxicity in amyotrophic lateral sclerosis. *Muscle Nerve* 2002;26(4):438–58.
- Li G, Oswald RE, Niu L. Channel-opening kinetics of GluR6 kainate receptor. *Biochemistry* 2003a;42(42):12367–75.
- Li G, Pei W, Niu L. Channel-opening kinetics of GluR2Q(flip) AMPA receptor: a laser-pulse photolysis study. *Biochemistry* 2003b;42(42):12358–66.
- Luthman H, Magnusson G. High efficiency polyoma DNA transfection of chloroquine treated cells. *Nucl Acids Res* 1983;11(5):1295–308.
- Sena-Esteves M, Saeki Y, Camp SM, Chiocca EA, Breakefield XO. Single-step conversion of cells to retrovirus vector producers with herpes simplex virus-Epstein-Barr virus hybrid amplicons. *J Virol* 1999;73(12):10426–39.
- Simmons DT. SV40 large T antigen functions in DNA replication and transformation. *Adv Virus Res* 2000;55:75–134.

- Stillman BW, Gluzman Y. Replication and supercoiling of simian virus 40 DNA in cell extracts from human cells. *Mol Cell Biol* 1985;5(8):2051–60.
- Sullivan CS, Pipas JM. T antigens of simian virus 40: molecular chaperones for viral replication and tumorigenesis. *Microbiol Mol Biol Rev* 2002;66(2):179–202.
- Udgaonkar JB, Hess GP. Chemical kinetic measurements of a mammalian acetylcholine receptor by a fast-reaction technique. *Proc Natl Acad Sci USA* 1987;84(24):8758–62.
- Washbourne P, McAllister AK. Techniques for gene transfer into neurons. *Curr Opin Neurobiol* 2002;12(5):566–73.

GluR3 Flip and Flop: Differences in Channel Opening Kinetics[†]

Weimin Pei, Zhen Huang, and Li Niu*

Department of Chemistry and Center for Neuroscience Research, University at Albany, SUNY, Albany, New York 12222

Received October 25, 2006; Revised Manuscript Received November 27, 2006

ABSTRACT: Ample evidence from earlier studies of α -amino-3-hydroxy-5-methyl-4-isoxazolepropionic acid (AMPA) receptors, GluR3 included, suggests that alternative splicing not only enriches AMPA receptor diversity but also, more importantly, creates receptor variants that are functionally different. However, it is not known whether alternative splicing affects the receptor channel opening that occurs in the microsecond time domain. Using a laser-pulse photolysis technique combined with whole-cell recording, we characterized the channel opening rate process for two alternatively spliced variants of GluR3, i.e., GluR3_{flip} and GluR3_{flop}. We show that the alternative splicing that generates flip and flop variants of GluR3 receptors regulates the channel opening process by controlling the rate of channel closing but not the rate of channel opening or the glutamate binding affinity. Specifically, the flop variant closes its channel almost 4-fold faster than the flip variant. We therefore propose that the function of the flip–flop sequence module in the channel opening process of AMPA receptors is to stabilize the open channel conformation, presumably by its pivotal structural location. Furthermore, a comparison of the flip isoform among all AMPA receptor subunits, based on the magnitude of the channel opening rate constant, suggests that GluR3 is kinetically more similar to GluR2 and GluR4 than to GluR1.

As a post-transcriptional regulatory mechanism (1), alternative splicing generates two molecular entities known as “flip” and “flop” in each of the four AMPA¹ receptor subunits, i.e., GluR1–4 or GluRA–D (2). The alternative splicing correlates to a 38-amino acid sequence in the extracellular binding domain between the M3 and M4 transmembrane segments but results in a difference of only 9–11 amino acids between the flip and flop isoforms (2). Since its discovery in AMPA receptors (2), the alternative splicing has been recognized as a unique molecular determinant giving rise to both structural and functional diversities in AMPA receptors (3–6). For example, flop variants desensitize (i.e., become inactivated when glutamate remains bound to the receptor) at least 3 times faster than the flip counterparts for GluR2–4 (7). Flip and flop variants have different sensitivity to allosteric modulators, such as cyclothiazide (CTZ) (8–10) and metal ions (11, 12). In the brain, the expression of alternatively spliced variants is tissue-, cell type-, and age-dependent (2, 7, 13, 14). In some neurological disorders, the relative level of expression of the flip to the flop isoforms is aberrant (15–18). For instance, in the spinal motor neurons of patients with amyotrophic lateral sclerosis (ALS), the level of the AMPA receptor flip

variants is significantly elevated relative to that of the flop variants (18). Such an increase in the level of flip isoform expression is thought to make those neurons especially vulnerable to glutamate insult (18, 19).

Despite a wealth of knowledge about alternative splicing, whether it affects the channel opening process of AMPA receptors is currently unknown. To address this question, we focus our initial attention on characterizing the channel opening kinetics for the two alternatively spliced variants of the GluR3 AMPA receptor, i.e., GluR3_{flip} and GluR3_{flop}.

GluR3 plays a specific functional role in the central nervous system. For instance, GluR3 assembled with GluR2, one of the two major AMPA receptor populations in adult hippocampus, strengthens the synapses and stabilizes long-term changes in synaptic efficacy (20). The level of expression of GluR3 in the hippocampus, together with GluR1 and GluR2 but not with GluR4, increases with development (21). GluR3 is also involved in neurological diseases. For instance, the production of autoantibodies against GluR3 contributes to the etiology of several types of human epilepsies (22, 23). Interestingly, GluR3 is expressed on the surface of most normal, cancerous, and autoimmune-associated T cells (24). Furthermore, GluR3 is upregulated in the spinal cord of transgenic mice with the copper zinc superoxide dismutase (SOD1) mutation (G93A), a familial ALS mouse model (25). At the molecular level, GluR3 is less well understood than other AMPA receptor subunits. For instance, the mean lifetime of the GluR3 open channel, determined traditionally using single-channel recording, is lacking, unlike other AMPA receptor subunits (26–28). Thus far, there is no systematic study of the phosphorylation of GluR3 (6), yet such studies have revealed how phosphorylation can modu-

[†] This work was supported by grants from the Department of Defense (W81XWH-04-1-0106), the ALS Association, and the Muscular Dystrophy Association (to L.N.). Z.H. is supported by a postdoctoral fellowship from the Muscular Dystrophy Association.

* To whom correspondence should be addressed. Telephone: (518) 591-8819. Fax: (518) 442-3462. E-mail: lniu@albany.edu.

¹ Abbreviations: AMPA, α -amino-3-hydroxy-5-methyl-4-isoxazolepropionic acid; ALS, amyotrophic lateral sclerosis; CTZ, cyclothiazide; GFP, green fluorescent protein; HEK-293 cells, human embryonic kidney cells; TAG, large T-antigen.

late the receptor properties in trafficking, surface expression, and synaptic plasticity in other AMPA receptor subunits (6).

Here we report the kinetic characterization of the channel opening rate constants for GluR3_{flip} and GluR3_{flop} variants using a laser-pulse photolysis technique, together with a photolabile precursor of glutamate [γ -*O*-(α -carboxy-2-nitrobenzyl)glutamate] or caged glutamate. Photolysis of the caged glutamate rapidly liberates free glutamate with a $t_{1/2}$ of $\sim 30 \mu\text{s}$ (29). Using this technique, we previously characterized the channel opening kinetic mechanism for the flip variants of GluR1, GluR2, and GluR4 AMPA receptor channels (30–32). Thus, this work also completed a systematic study of all flip AMPA receptor variants. We found that the alternative splicing affects the channel opening process by controlling the rate of channel closing but not the rate of channel opening. Specifically, the flop variant shuts the channel almost 4-fold faster than the flip variant. Furthermore, both the flip and flop channels of GluR3, like GluR2 and GluR4, but unlike GluR1, are among some of the fastest channels known to date.

EXPERIMENTAL PROCEDURES

cDNA Expression and Cell Culture. The cDNAs encoding rat GluR3_{flip} and GluR3_{flop} separately in the pBluescript vector were provided by S. Heinemann and were individually cloned into pcDNA3.1 (Invitrogen, Carlsbad, CA). The GluR3_{flip} or GluR3_{flop} homomeric channels were transiently expressed in human embryonic kidney (HEK) 293S cells. HEK-293S cells were cultured in Dulbecco's modified Eagle's medium supplemented with 10% fetal bovine serum in a 37 °C, 5% CO₂, humidified incubator. Unless otherwise noted, HEK-293S cells were also cotransfected with a plasmid encoding green fluorescent protein (GFP) and another plasmid encoding simian virus 40 large T-antigen (TAg) (33). GFP was used as a transfection marker for cell recording; TAg was used to potentiate the GluR3 expression (see the text). The weight ratio of the plasmid for GFP and TAg to that of GluR3 was 1:3:30, and the GluR3 cDNA used for transfection was $\sim 15\text{--}20 \mu\text{g}/35 \text{ mm}$ dish. Cells were used 48 h after transfection.

Whole-Cell Recording. All experiments were performed with HEK-293S cells voltage-clamped at -60 mV and 22 °C. The recording of glutamate-induced whole-cell current was described previously (30). In brief, an Axopatch-200B amplifier (Axon Instruments, Union City, CA) was used in whole-cell recording at a cutoff frequency of 2–20 kHz by a built-in, eight-pole Bessel filter and digitized at a 5–50 kHz sampling frequency with a Digidata 1322A device (Axon Instruments). The resistance of recording electrodes was $\sim 3 \text{ M}\Omega$ when filled with the electrode solution containing 110 mM CsF, 30 mM CsCl, 4 mM NaCl, 0.5 mM CaCl₂, 5 mM EGTA, and 10 mM HEPES (pH 7.4 adjusted with CsOH). The external bath solution contained 150 mM NaCl, 3 mM KCl, 1 mM CaCl₂, 1 mM MgCl₂, and 10 mM HEPES (pH 7.4 adjusted with NaOH). The GFP fluorescence in transfected cells was visualized using a Zeiss (Thornwood, NY) Axiovert S100 microscope with a fluorescence detection system. To initiate whole-cell current response, solutions containing free glutamate were applied using a flow device (30, 34), and the rise time was typically

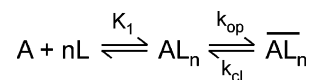


FIGURE 1: General mechanism of channel opening for GluR3. Here, A represents the active, unliganded form of the receptor, L the ligand or glutamate, AL_n the closed channel states with n ligand molecules bound, and \overline{AL}_n the open channel states. The number of glutamate molecules to bind to the receptor and to open its channel, n , can be from 1 to 4, assuming that a recombinant GluR3 receptor channel is a tetrameric complex, and each subunit has one glutamate binding site. It is further assumed that a ligand does not dissociate from the open channel state. k_{op} and k_{cl} are the channel opening and channel closing rate constants, respectively. For simplicity and without contrary evidence, it is assumed that glutamate binds with equal affinity or K_1 , the intrinsic equilibrium dissociation constant, at all binding steps.

$\sim 1\text{--}2 \text{ ms}$ (10–90%). When free glutamate was used, the whole-cell current was corrected for desensitization during the rise time by a previously described method (34).

Laser-Pulse Photolysis. The use of the laser-pulse photolysis technique and the caged glutamate (29) (Invitrogen, Carlsbad, CA) to measure the rate of an AMPA receptor channel opening with a time resolution of $\sim 60 \mu\text{s}$ were described previously (30). Briefly, a Minilite II pulsed Q-switched Nd:YAG laser (Continuum, Santa Clara, CA) delivered single pulses at 355 nm, tuned by a third harmonic generator, with a pulse length of 8 ns. The laser light was coupled to a fiber optic, and the energy was adjusted to 200–800 μJ . To determine the concentration of glutamate photolytically released from the caged glutamate, at least two solutions with known concentrations of free glutamate were used to calibrate the current amplitude from the same cell before and after a laser pulse. The current amplitudes obtained from the flow measurements were compared with the amplitude from the laser measurement with reference to the dose–response relation. In addition, the concentration of photolytically released glutamate was considered constant during the rise time in which the observed rate constant was measured (see Figure 4A; the k_{obs} was determined from the rise time of $<1 \text{ ms}$). In 1 ms, for instance, a glutamate molecule could have only diffused a root-mean-square distance of $\sim 1.2 \mu\text{m}$, estimated by Fick's second law, yet the laser irradiation area around a HEK-293 cell of $\sim 10 \mu\text{m}$ in diameter was 400–500 μm . Thus, the diffusion of glutamate after photolysis, but within the time frame of our measurement of channel opening rate constants, was inconspicuous. It should be noted that in this estimate, we assumed the diffusion coefficient of glutamate was $7.5 \times 10^{-6} \text{ cm}^2/\text{s}$, based on the measured value for glutamine at room temperature (35).

Data Analysis. On the basis of the kinetic mechanism of channel opening in Figure 1, the observed rate constant, k_{obs} , for the whole-cell current rise in response to glutamate is given by eq 1

$$k_{obs} = k_{cl} + k_{op} \left(\frac{L}{L + K_1} \right)^n \quad (1)$$

All of the terms are defined in the legend of Figure 1. In the derivation of eq 1, the ligand binding rate was assumed to be fast relative to the channel opening rate. This assumption was supported by the consistent observation of

a single first-order rate process for the whole-cell current rise (see the results and discussion in the text), given by eq 2

$$I_t = I_{\max}(1 - e^{-k_{\text{obs}}t}) \quad (2)$$

where I_t represents the whole-cell current amplitude at time t and I_{\max} represents the maximum current amplitude. Using eq 2, the k_{obs} at a given glutamate concentration was calculated. A set of k_{cl} and k_{op} values corresponding to a particular number of ligand(s) required to bind and open the channel, i.e., $n = 1-4$, was obtained using eq 1. Furthermore, K_1 was separately estimated from the dose-response relationship, using eq 3; the derivation of eq 3 was based on the general mechanism of channel opening in Figure 1.

$$I_A = I_M R_M \frac{L^n}{L^n + \Phi(L + K_1)^n} \quad (3)$$

where I_A represents the current amplitude, I_M the current per mole of receptor, R_M the number of moles of receptors on the cell surface, and Φ^{-1} the channel opening equilibrium constant. Other terms have already been defined. The corrected current amplitude (31, 34) was used to construct the dose-response relationship. Unless otherwise noted, triplicate data from three cells were collected in all measurements. Linear regression and nonlinear fitting were performed using Origin version 7 (Origin Lab, Northampton, MA).

RESULTS

Expression of GluR3 in HEK-293 Cells and Whole-Cell Current Recording. We first established a condition under which the GluR3 receptor could be sufficiently expressed in HEK-293 cells for whole-cell recording even at low glutamate concentrations. Earlier studies of GluR3 are primarily involved in the use of *Xenopus* oocytes (36, 37), where the expression of the receptor is more readily detectable but typically at the cost of obscuring the rapid channel desensitization and thus an accurate measurement of the receptor response; this is apparently due to the sheer size of an oocyte. Although using smaller HEK-293 cells achieves a better solution exchange rate, thus permitting a more accurate study of the kinetic properties of GluR3, a lower level of expression in single HEK-293 cells is entailed. Perhaps it is not coincidental that very few studies of GluR3 have used HEK-293 cells for expression, and when those studies were actually performed, often a high glutamate concentration was required to elicit a detectable response. In fact, we observed the average response at saturating concentrations of glutamate was ~ 130 pA for GluR3_{flip}-expressing HEK-293 cells, similar to literature values (38). A small magnitude of whole-cell current response presented a challenge in measuring the GluR3 channel activity at low agonist concentrations, which was required in our experiment to measure the channel closing rate constant (the rationale is presented below).

To improve the receptor expression in single HEK-293 cells and consequently augment the average magnitude of a whole-cell response, we coexpressed TAG with the GluR3 receptor (Figure 2A). TAG is a powerful oncoprotein capable of disrupting cell cycle control (39). Coexpression of TAG

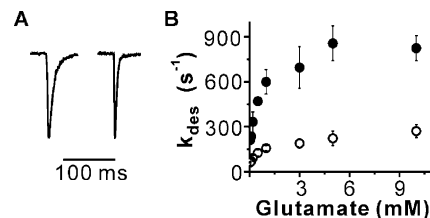


FIGURE 2: Glutamate-induced whole-cell response of GluR3_{flip} and GluR3_{flop} expressed in HEK-293 cells. (A) Representative whole-cell current responses via GluR3_{flip} channels (left) and GluR3_{flop} channels (right) to application of 500 μM glutamate. The amplitude of the current response is 520 and 370 pA for the flip and flop channels, respectively, but the two traces are scaled vertically for comparison of the desensitization rate profile. The GluR3_{flop} channel was desensitized with a rate constant of 470 s^{-1} at this glutamate concentration, whereas the GluR3_{flip} channel was desensitized with a rate constant of only 130 s^{-1} . Note that a first-order rate was adequate for describing the desensitization for both isoforms of GluR3. (B) Dependence of the desensitization rate constant (k_{des}) on glutamate concentration for GluR3_{flip} (○) and GluR3_{flop} (●) channels. Each data point is an average of at least three measurements from at least three cells. An error bar represents the standard error of the mean.

increased the average whole-cell response of GluR3_{flip} to glutamate at saturating concentrations to ~ 650 pA (the number of cells tested was 20 or $n = 20$), compared to ~ 130 pA without TAG ($n = 3$). For GluR3_{flop}, which was usually expressed less robustly, the average current amplitude was ~ 250 pA ($n = 5$) when TAG was coexpressed. The largest current amplitudes observed for GluR3_{flip} and GluR3_{flop} were 1.9 and 1.7 nA, respectively. As controls, expressing either TAG alone, GFP alone, or the two together in HEK-293S cells, did not lead to current response (33). Coexpressing TAG and GFP with GluR3 did not affect the GluR3 activity either, as evidenced by an identical desensitization rate at a given glutamate concentration from cells transfected with GluR3 only and cells additionally transfected with TAG and GFP. These results are therefore consistent with our earlier report of using TAG to successfully potentiate GluR2Q_{flip} expression in HEK-293S cells (33). Furthermore, the method we described, i.e., coexpressing TAG in the same cell, made it possible to assay the GluR3 activity at low concentrations of glutamate.

Inspection of the rate of desensitization with different concentrations of glutamate showed that the flop isoform always desensitized more than 3 times faster than the flip isoform (Figure 2A, B). For instance, the largest rate constant we observed for GluR3_{flip} and GluR3_{flop} were 230 and 820 s^{-1} , respectively. These values agree with those obtained using outside-out patches excised from either HEK-293 cells (38) or *Xenopus* oocytes (7). That the desensitization rate constants we determined are identical to those published previously is further consistent with the fact that coexpressing TAG in the same cells did not affect the GluR3 channel activity.

Characterization of Caged Glutamate with GluR3 Expressed in HEK-293 Cells. To characterize the channel opening rate constants of the GluR3 receptors, we used a laser-pulse photolysis technique, together with the caged glutamate (Figure 3A), which releases free glutamate upon photolysis with a $t_{1/2}$ of ~ 30 μs (29). To ensure that the receptor kinetics can be measured, the caged glutamate must be biologically inert on the receptor. In a series of experi-

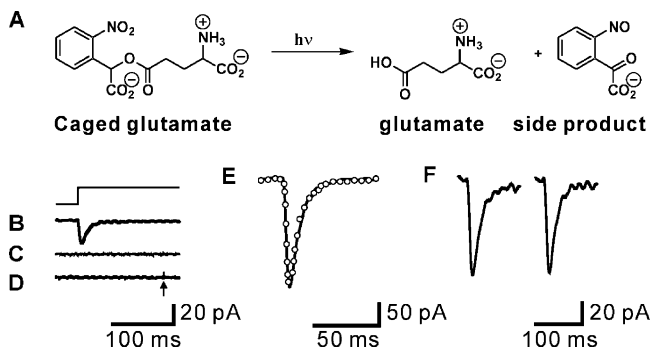


FIGURE 3: Caged glutamate is biologically inert as characterized with GluR3_{flip} expressed in HEK-293 cells voltage-clamped at -60 mV. (A) Photolysis of the caged glutamate releases free glutamate and the side product as shown. (B) Displayed is the whole-cell current response from a cell expressing GluR3_{flip} to $100 \mu\text{M}$ glutamate. Glutamate (and any other compound or compounds) was applied to the cell using a solution flow device (see Experimental Procedures). The flow-pulse protocol is shown above the current response. (C) The caged glutamate at a concentration of 2 mM (i.e., the highest concentration used in this study), dissolved in the external buffer and applied to the same cell as in panel B, did not induce any detectable whole-cell current response in the absence of laser light. (D) Firing of a laser at a cell exposed to external buffer which contained no caged glutamate did not induce any current response from the cell. The arrow indicates the timing of the laser pulse. (E) Superimposed are the whole-cell current responses to $500 \mu\text{M}$ free glutamate in the absence (—) and presence (○) of 2 mM caged glutamate from the same cell. The number of the data point for the current trace containing the caged glutamate was reduced for the clarity of presentation. (F) Whole-cell responses to $350 \mu\text{M}$ free glutamate in the absence (left) and presence (right) of $350 \mu\text{M}$ side product from photolysis.

ments (Figure 3B–F) designed to test the biological properties of the caged glutamate, we found, on the same cell that expressed the GluR3 channel (as seen by a current response to free glutamate, Figure 3B), the caged glutamate did not activate the GluR3 channel without the laser flash (Figure 3C). Firing the laser in the absence of the caged glutamate did not induce current response from cells that expressed GluR3 (Figure 3D). The caged glutamate did not inhibit or potentiate the GluR3 response when the receptor was activated by free glutamate, as evidenced by identical current amplitudes in the presence and absence of caged glutamate (Figure 3E). Furthermore, the side product(s) generated from photolyzing the caged glutamate (Figure 3A) did not affect the glutamate-induced receptor response (Figure 3F). Together, these results show that the caged glutamate was biologically inert and thus suitable for studying the GluR3 channels. This conclusion is consistent with the initial finding with rat hippocampal neurons that expressed endogenous AMPA receptors (29) and our previous studies of other AMPA receptors (30–32).

Rate of Channel Opening. Using the laser-pulse photolysis technique with the caged glutamate, we determined the rate constants for the opening of the GluR3_{flip} and GluR3_{flipop} channels. Upon laser photolysis, free glutamate was liberated, leading to a rapid increase in the whole-cell current representing the opening of the receptor channel (Figure 4A). The rising phase of the current obeyed a single-exponential rate throughout the entire concentration range of glutamate (i.e., 80 – $260 \mu\text{M}$), which supported the assumption that the rate of channel opening was slow compared to the rate of glutamate binding. Thus, the observed rate reflected channel

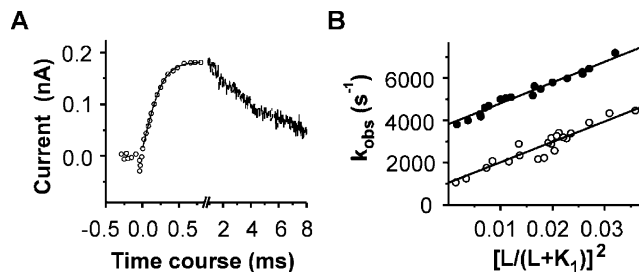


FIGURE 4: Laser-pulse photolysis measurement of the channel opening kinetics for GluR3_{flip} and GluR3_{flipop}. (A) Representative whole-cell current from the opening of the GluR3_{flip} channel initiated by the laser-pulse photolysis of caged glutamate at time zero. The fitting of the current rise using eq 2 (in Experimental Procedures) is shown as the solid line superimposed with the experimental data points. For clarity, the number of data points was reduced in the rising phase of the current. The observed rate constant (k_{obs}) of 2400 s^{-1} obtained from this trace corresponds to a glutamate concentration of $170 \mu\text{M}$. Note that the direction of the current response was plotted as the opposite of that recorded. (B) Plot of k_{obs} vs glutamate concentration by eq 1 in the linear form. The empty circles represent k_{obs} values for GluR3_{flip} and filled circles represent those for GluR3_{flipop}. Each data point represents one k_{obs} obtained at a particular concentration of photolytically released glutamate. The k_{cl} and k_{op} values were determined by linear fit to be $(1.1 \pm 0.2) \times 10^3$ and $(9.6 \pm 1.1) \times 10^4 \text{ s}^{-1}$ for GluR3_{flip} and $(3.8 \pm 0.1) \times 10^3$ and $(9.9 \pm 0.5) \times 10^4 \text{ s}^{-1}$ for GluR3_{flipop}, respectively. In the linear fitting, we chose an n of 2; $K_1 = 1.0 \text{ mM}$ for GluR3_{flip} and 0.95 mM for GluR3_{flipop}.

opening. The result was inconsistent with the assumption that the channel opening rate was either comparable to or faster than the ligand binding rate (note that all of these kinetic scenarios have been discussed in detail in our previous studies; see ref 31). Accordingly, a general kinetic rate expression, i.e., eq 1 (in Experimental Procedures), was derived for the observed rate constant, k_{obs} , with n ligand molecules bound to open the channel, AL_n , as a function of ligand concentration.

Using eq 1, we estimated the channel opening rate constant, k_{op} , and the channel closing rate constant, k_{cl} , together with the corresponding K_1 value, from the plot of k_{obs} versus the concentration of glutamate for GluR3_{flip} and GluR3_{flipop} (Figure 4B). Table 1 lists four sets of k_{op} , k_{cl} , and K_1 values, corresponding to an n of 1–4. The n of 1–4 was based on the assumption that a recombinant GluR3 receptor is a tetramer (40, 41), and each subunit contains one glutamate binding site. From our results, the following conclusions can be drawn. First, the fitting was satisfactory when n equaled 2–4, but not when n equaled 1 (see R^2 values in Table 1). Second, the fitting results are statistically identical when $n = 2$ –4. For instance, when n increased from 2 to 4, the fitted k_{op} changed little (see Table 1). Third, the conclusions described above applied to the kinetic results of both GluR3_{flip} and GluR3_{flipop}. As an independent estimate of K_1 with respect to different numbers of ligands bound to a receptor complex, we determined the dose–response relationship for both GluR3_{flip} and GluR3_{flipop} (Figure 5). Using eq 3, we found that the dose–response relationship of both variants showed a similar pattern in that the fitting was satisfactory when n equaled 2–4 but poor when n equaled 1 (Table 2). Furthermore, a K_1 value obtained from the dose–response curve (Figure 5) agreed with that obtained from kinetic measurement (Figure 4B) at a given n , with

Table 1: k_{op} and k_{cl} Values for GluR3_{flip} and GluR3_{flop} When $n = 1-4^a$

n	GluR3 _{flip}				GluR3 _{flop}			
	k_{op} ($\times 10^{-5}$ s $^{-1}$)	k_{cl} ($\times 10^{-3}$ s $^{-1}$)	K_1 (mM)	R^2	k_{op} ($\times 10^{-5}$ s $^{-1}$)	k_{cl} ($\times 10^{-3}$ s $^{-1}$)	K_1 (mM)	R^2
1	0.20 \pm 1.6	1.2 \pm 2.0	1.6 \pm 16	0.679	0.15 \pm 0.10	1.1 \pm 1.0	0.34 \pm 0.49	0.890
2	0.97 \pm 1.2	1.0 \pm 0.5	1.0 \pm 0.90	0.908	0.99 \pm 1.1	3.8 \pm 0.3	0.97 \pm 0.76	0.970
3	1.1 \pm 2.0	1.4 \pm 0.9	0.50 \pm 0.50	0.901	1.1 \pm 1.6	4.1 \pm 0.6	0.50 \pm 0.50	0.960
4	1.2 \pm 1.9	1.7 \pm 0.9	0.35 \pm 0.25	0.895	1.3 \pm 1.9	4.3 \pm 0.9	0.33 \pm 0.20	0.952

^a n is the number of glutamate molecules required to bind and open the channel.

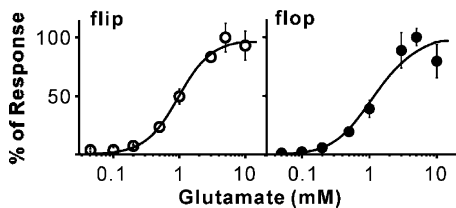


FIGURE 5: Dose–response relationship of the GluR3_{flip} (O) and GluR3_{flop} (●) channels with glutamate. The whole-cell currents from different cells were normalized to the current obtained at 0.5 mM glutamate, and the current amplitude at 5 mM was set to 100%. The solid lines represent the fits when $n = 2$ by eq 3, and the K_1 , Φ , and I_{MRM} values are listed in Table 2.

the exception, in both isoforms, of an n of 1 (see Tables 1 and 2).

Difference in the Channel Opening Properties of GluR3_{flip} and GluR3_{flop}. Comparison of the corresponding set of rate constants, excluding $n = 1$, shows that GluR3_{flop} closes its channel more than 3-fold faster than GluR3_{flip}, yet both open their respective channels with an identical rate constant. Therefore, the flip–flop module of GluR3 regulates the channel opening process by controlling how fast the open channel closes. It should be especially emphasized that the same conclusion could be made empirically from k_{obs} without even knowing the values of k_{op} and k_{cl} . If $L \ll K_1$ or at low agonist concentrations, $k_{obs} \approx k_{cl}$ (see eq 1), suggesting that the evaluation of k_{cl} was independent of whatever the n value was (in fact, estimating k_{cl} was independent of the k_{op} term altogether; see eq 1). Thus, that the k_{obs} value of GluR3_{flip} at the low glutamate concentration was 3-fold smaller than that of GluR3_{flop} (in Figure 4B) led naturally to the same conclusion.

Furthermore, both the rate and the dose–response data suggest that K_1 is the same for both GluR3 variants (Tables 1 and 2). For instance, when $n = 2$, K_1 is 1.0 ± 0.70 mM for GluR3_{flip} and 0.95 ± 0.65 mM for GluR3_{flop}, suggesting that the flip–flop module does not affect the binding affinity of glutamate. The same conclusion can be qualitatively made from the analysis of the dose–response relationships using the Hill equation (42). The EC_{50} value or the ligand concentration that corresponds to 50% of the maximum response is 1.0 ± 0.20 mM for GluR3_{flip} and 1.1 ± 0.30 mM for GluR3_{flop} with Hill coefficients of 1.8 and 1.7, respectively. Again, the EC_{50} values for GluR3_{flip} and GluR3_{flop} are identical. In fact, EC_{50} is similar to K_1 numerically (note that the Hill equation does not specify the number of bound ligand molecules). Interestingly, the flip and flop isoforms of GluR2, another AMPA receptor subunit, also have identical EC_{50} values: 1.39 mM for GluR2Q_{flip} and 1.38 mM for GluR2Q_{flop} (43).

The Channel Opening Rate Was Measured Separately from Channel Desensitization. Our analysis of the channel opening

kinetics was based on the mechanism for channel opening (Figure 1), which did not involve channel desensitization. We reasoned that the desensitization reaction could not have proceeded appreciably during the current rise, assuming that the desensitization had occurred simultaneously upon binding of glutamate (44, 45). As shown in Figure 4A, the k_{obs} of 2400 s $^{-1}$, calculated from the current rise for the GluR3_{flip} channel opening, was ~ 30 times larger than the desensitization rate of 80 s $^{-1}$ in Figure 2B at the same glutamate concentration, i.e., 170 μ M. As such, when the current increased to 95%, during which the k_{obs} of 2400 s $^{-1}$ was calculated, the desensitization reaction with a rate constant of 80 s $^{-1}$ proceeded only $\sim 4\%$. Thus, the kinetic process occurring within the current rising phase was dominated by the channel opening reaction, and its rate constant could be calculated using a simple kinetic rate expression (eq 2). It should be noted that the estimate of the “contamination” of the desensitization reaction within the rise time was reasonably accurate because the receptor was exposed to glutamate in a microsecond “concentration jump” triggered by laser photolysis, and consequently, the start of the glutamate-induced reactions was virtually synchronized. In addition, a simultaneous fit of both the rising and falling phases (in Figure 4A) by two first-order rate equations, one representing channel opening and the other representing desensitization, yielded a k_{obs} value identical ($\pm 5\%$ error range) to that obtained using a single-exponential fit of the rising phase only (using eq 2). Together, the whole-cell current rise representing the channel opening reaction can be treated as a kinetically distinct process in our measurement. Indeed, it has been proposed previously that the channel opening reaction or the gating pathway can be considered a kinetic process separate from desensitization (44, 46), and the open channel state is thought to preferentially return to the closed state and can open again, without entering the desensitization state (47).

DISCUSSION

We have investigated the kinetic mechanism of channel opening for the two alternatively spliced variants of GluR3. We find the alternative splicing that generates flip and flop variants of GluR3 AMPA receptors controls the channel opening process by regulating the rate of channel closing but not the rate of channel opening. Below, we discuss the use of the channel opening and channel closing rate constants in an effort to understand the receptor properties and offer implications of alternative splicing in regulating the channel function.

Channel Opening Rate Constants and Receptor Occupancy. The results from our study of GluR3 are consistent with the minimal number of glutamate molecules required to bind to and to open the channel being 2 (30–32). This is

Table 2: K_1 Values Estimated from Dose–Response Curve for GluR3_{flip} and GluR3_{flop}

<i>n</i>	GluR3 _{flip}				GluR3 _{flop}			
	K_1 (mM)	Φ	$I_m R_m$ (nA)	R^2	K_1 (mM)	Φ	$I_m R_m$ (nA)	R^2
1	2.6 ± 751	0.14 ± 45	88 ± 3479	0.780	7.0 ± 1252	0.12 ± 24	108 ± 2359	0.738
2	1.0 ± 0.70	0.55 ± 0.89	166 ± 90	0.997	0.95 ± 0.65	0.79 ± 0.40	190 ± 130	0.956
3	0.70 ± 0.50	0.35 ± 0.64	141 ± 80	0.990	0.62 ± 1.0	0.68 ± 3.2	177 ± 355	0.955
4	0.36 ± 0.30	0.75 ± 1.5	184 ± 169	0.989	0.43 ± 0.59	0.81 ± 3.6	188 ± 400	0.955

true for both the flip and flop variants (see Table 1). For either of the isoforms, our results show that k_{op} remains essentially invariant when $n = 2–4$ (Table 1). If receptor complexes bound with more than two glutamate molecules have higher conductance levels, then the higher conductance levels associated with higher agonist occupancy do not give rise to different channel opening rate constants. Alternatively, the receptor complexes with higher occupancy have different rate constants of channel opening, but the fraction of these complexes in the overall receptor population all bound with glutamate is not high enough to significantly alter k_{obs} values. It is also possible that the concentration range of glutamate released by photolysis may not be wide enough for our data analysis (in Figure 4B). However, regardless of how k_{obs} is used to calculate k_{op} and k_{cl} with respect to a specific n value, the set of k_{op} and k_{cl} values when $n = 2$ is phenomenologically representative of the channel opening kinetics for both GluR3_{flip} and GluR3_{flop}. We thus favor an interpretation of k_{op} and k_{cl} with an n of 2 being the minimal values of the channel opening and channel closing rate constants.

From the elegant study of the single-channel records of both the wild-type and mutant GluR3 receptors, Rosenmund and co-workers (40) suggested that binding of two agonist molecules per tetrameric receptor complex is necessary to open the channel, and binding of more than two agonist molecules leads to the open channels with higher mean single-channel conductance. Evidence that supports this conclusion includes the single-channel study of native AMPA receptors at varying glutamate concentrations (48) and the single-channel/crystallographic studies of GluR2 with different agonists (28). Given that an AMPA receptor may be a dimer of “dimers” (49), binding of one glutamate molecule per dimer or two per tetramer as a minimal stoichiometry is plausible (32). Furthermore, despite the fact that channel conductance of AMPA receptors depends on agonist occupancy, it is unclear how a change in conductance affects synaptic response seen as macroscopic current. It has been suggested that glutamate at the synapse may not be able to visit multiple conductance levels of synaptic AMPA receptors (48), because glutamate cannot be present in the synaptic cleft at concentrations of >1 mM for more than 100–200 μ s or because the channels desensitize rapidly (50, 51).

Alternative Splicing Regulates the GluR3 Channel Opening Process. The channel opening rate constant defines how fast a channel opens following the binding of glutamate. The channel closing rate constant represents how fast an open channel closes and thus is a measure of the lifetime of an open channel with the relationship $k_{cl} = 1/\tau$, where τ is the lifetime expressed as a time constant (31). In this study, we determined k_{op} to be 97 000 s^{-1} for GluR3_{flip} and 99 000 s^{-1} for GluR3_{flop} and k_{cl} to be 1000 s^{-1} for GluR3_{flip} and 3800 s^{-1} for GluR3_{flop}. On the basis of these results, we conclude that alternative splicing does not affect the channel opening

rate reaction but does affect the channel closing rate process of GluR3 in that the flop variant has a markedly faster channel closing rate than the flip counterpart. Furthermore, on the basis that the flip and flop variants have identical K_1 values or EC_{50} values, the alternative splicing may not affect the rate of binding of glutamate to the receptor.

Our findings also reveal how the alternative splicing regulates the channel function. First, at high concentrations of glutamate, the time course is unaffected by alternative splicing, because for GluR3, $k_{op} \gg k_{cl}$, and the time constant of the current rise, i.e., $1/(k_{op} + k_{cl})$, is mainly determined by k_{op} . Second, because alternative splicing mainly affects k_{cl} , it will influence more effectively the channel activity of GluR3 at lower glutamate concentrations. Third, alternative splicing has little influence on the channel opening probability, P_{op} , or the probability that a channel can open once it is bound with ligand(s) (31, 52, 53). This is because $P_{op} = k_{op}/(k_{op} + k_{cl})$, and again, $k_{op} \gg k_{cl}$. Specifically, the P_{op} values for GluR3_{flip} and GluR3_{flop} are estimated to be 0.99 ± 0.12 and 0.96 ± 0.10 , respectively, consistent with a high P_{op} value in general for AMPA receptors (32). In fact, because $k_{op} \gg k_{cl}$, P_{op} naturally approaches unity; see $P_{op} = k_{op}/(k_{op} + k_{cl})$, regardless of the n value or agonist occupancy. Physiologically, the synaptic concentration of glutamate can be as high as 1 mM (50, 54). Therefore, it is unlikely that alternative splicing plays a significant role in shaping the initial events of synaptic activity when the glutamate concentration is that high.

Given the prediction that the flip–flop module affects channel activity, it is plausible that alternative splicing has a major impact on excitatory postsynaptic current (EPSC) at low glutamate concentrations, such as in the slow-rising component of the AMPA receptor-mediated conductance at the cerebellar mossy fiber-granule cell synapse (55). Such a slow synaptic current is mediated possibly by two mechanisms, a prolonged local release of glutamate via a narrow fusion pore and a spillover or the diffusion of glutamate from distant sites (55). Both mechanisms may involve a low synaptic glutamate concentration. For example, in the cerebellar mossy fiber-granule cell synapse, a glutamate concentration of $\sim 130 \mu$ M through a spillover mechanism is thought to be responsible for the slow-rising EPSC (55). Moreover, both spillover and narrow fusion pore release are believed to play important roles in developmental strengthening of central glutamatergic synaptic connections (55, 56). Under such a condition where low glutamate concentrations are prevalent, the kinetically distinct flip and flop variants may be relevant for synaptic transmission. Furthermore, because the flip isoform dwells on the open channel state longer, more calcium can enter the cell that harbors the flip isoform per unit time. This prediction is consistent with the pathogenic hypothesis by which an elevated level of expres-

sion of the flip isoforms of AMPA receptors in the spinal motor neurons of ALS patients shall render those cells more vulnerable to excitotoxicity (18).

The Flip–Flop Alternative Splicing Sequence Is a Structure-Stabilizing Module. Armstrong and Gouaux (41, 57) first proposed that opening of an AMPA channel is initiated by the closure of receptor domains or lobes 1 and 2, after agonist binding, from their X-ray crystallographic study of the S1S2 extracellular binding domains of AMPA receptors. The trapping of agonist bound to the extracellular domains causes a conformational strain in the extracellular portion of the receptor, leading to the opening of the gate in the transmembrane segment (41, 58). Using these structural concepts, the k_{op} obtained for the GluR3 channel may represent the rate of domain closure induced by glutamate binding, and the k_{cl} should then correspond to the rate of re-opening of the bilobe structure to return to its original active conformation. It should be noted that the magnitude of the channel closing rate constant, k_{cl} , or the mean lifetime of the open channel, τ ($k_{cl} = 1/\tau$), reflects the stability of the open channel state of the receptor. Therefore, the flip sequence in the flip–flop alternative splicing module promotes a more stable open channel conformation than does the flop sequence, simply because the k_{cl} of GluR3_{flip} is smaller than that of GluR3_{flop}. Consequently, the flip–flop module is hypothesized to operate to “tune” the channel opening equilibrium. It should be pointed out that generally for proteins, substrate-induced conformational changes correlate to rate constants in the range of $10\text{--}10^4\text{ s}^{-1}$ (59). Therefore, on the basis of the values of k_{op} and k_{cl} for the GluR3 receptors, the link of k_{op} to the rate of bilobe closure and the link of k_{cl} to the rate of re-opening of the closed bilobe as major conformational changes are plausible.

It is worth noting that the alternatively spliced region of AMPA receptors is located in the S2 extracellular domain or right above the fourth transmembrane domain. Unless its location is accidental, we hypothesize that the alternatively spliced region in AMPA receptors is situated in a pivotal position in that it serves as a structural “lamppost” involved in stabilizing the extracellular binding domain when this domain transiently changes its conformation upon binding to glutamate or when the gate in the transmembrane domain is open. Specifically, if the flip sequence is used as the benchmark, the flop sequence corresponds to a structurally weakened lamppost such that the closed bilobe structure is less stable or the re-opening of this structure is kinetically more favorable as it has a larger k_{cl} . Obviously, further studies are needed to test this hypothesis. If true, the alternative splicing has a structural meaning: it regulates the stability of the open channel conformation.

Time Course for GluR3_{flip} and GluR3_{flop}. The time course of channel opening describes the speed by which channels open, defined by k_{op} , and the duration of the open channels, defined by k_{cl} , at a given concentration of ligand for the ensemble rate process (31). Consequently, the time course for the opening of GluR3_{flip} and GluR3_{flop} channels can be constructed using k_{cl} and k_{op} values as a function of glutamate concentration, according to eq 1 (in Figure 6). Specifically, the time course was calculated to be the rise time of the whole-cell current increase from 20 to 80%. As expected, when the glutamate concentration increases, the time course decreases and the difference in the time course between the

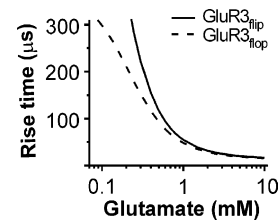


FIGURE 6: Time course for GluR3_{flip} and GluR3_{flop} as a function of glutamate concentration. The time course is expressed as the rise time of the whole-cell current. The rise time is defined as the time for the receptor current response to rise from 20 to 80% and is obtained by converting a k_{obs} value by eq 1, using experimentally determined k_{op} and k_{cl} values at $n = 2$ for a corresponding glutamate concentration.

flip and flop variants narrows (Figure 6). This is because at high ligand concentrations, the magnitude of k_{op} dominates the kinetic behavior of the channel, and the k_{op} values for GluR3_{flip} and GluR3_{flop} are identical (regardless of the number of ligand molecules bound to a receptor to open its channel). Consequently, the shortest rise time, which is achieved at a saturating glutamate concentration, is ~ 14 and $\sim 13\ \mu\text{s}$ for the flip and flop isoforms, respectively.

In the description of the time course, the desensitization was assumed not to occur appreciably in the same period of time, and such an assumption was reasonable as discussed earlier. However, the inclusion of the desensitization rate is needed to define the total time duration (50, 60), which further includes the current falling to the baseline, similar to defining the size and duration of EPSP. Furthermore, to define rigorously an *in vivo* time course, additional factors must be considered, such as the time of glutamate uptake from the synaptic cleft and the relative location of receptors in the postsynaptic density. Other factors that complicate the measurement of an *in vivo* time course include a prolonged local release of glutamate and a slow rise time due to a low synaptic concentration of glutamate. A prolonged local release could occur because the neurotransmitter is released through a narrow fusion pore or because the neurotransmitter is diffused from distant sites, i.e., “spillover” (55). A slow rise time has been recorded from AMPA synapses (56, 61–63). Therefore, the time course we constructed (Figure 6) only sets the upper limit for the early part of the channel activity, assuming synchronized activation of the receptors at the same location.

When the glutamate concentration is sufficiently low, the rate of glutamate binding becomes rate-limiting because ligand binding is a bimolecular process (Figure 1). Consequently, an observed rate of current rise will no longer reflect the channel opening (32). To ensure that the ligand binding rate was fast enough during our laser-pulse photolysis measurement so that the relatively slow channel opening process was always observed, we only used those k_{obs} values that corresponded to glutamate concentrations of $\geq 80\ \mu\text{M}$ for data analysis (in Figure 4B). The glutamate concentration of $80\ \mu\text{M}$ is equivalent to evoking $\sim 4\%$ of the channels (i.e., the fraction of the open channel state in all channel populations, which is defined by eq 3 and shown in Figure 5 for both GluR3 isoforms). This kinetic rationale and the resulting practice have been thoroughly discussed in our previous studies of other AMPA receptor channels (31).

Knowing the time course of synaptic conductance is necessary for investigation of information processing in the

Table 3: k_{op} and k_{cl} Values for Some Homomeric Ionotropic Glutamate Channels^a

glutamate receptor	k_{op} (s ⁻¹)	k_{cl} (s ⁻¹)	technique	ref
NR1A/NR2A ^b	77	28	single-channel recording	68
GluR1Q _{flip} ^{c,d}	2.9×10^4	2.1×10^3	laser-pulse photolysis	31
		4.2×10^3 (73%)	single-channel recording	27
		4.2×10^2 (27%)		
GluR2Q _{flip}	8.0×10^4	2.6×10^3	laser-pulse photolysis	30
		3.1×10^3 (84%)	single-channel recording	28
		6.8×10^2 (16%)		
	1.6×10^4	5.0×10^3	fitting	43
GluR3 _{flop}	9.9×10^4	3.8×10^3	laser-pulse photolysis	this study
GluR3 _{flip}	9.6×10^4	1.1×10^3	laser-pulse photolysis	this study
GluR4 _{flip}	6.8×10^4	3.4×10^3	laser-pulse photolysis	32
	4.0×10^4	8.0×10^3	fitting	69
		5.9×10^3	single-channel recording	26
GluR6Q	1.1×10^4	4.2×10^2	laser-pulse photolysis	67
	1.0×10^4	4.4×10^2	fitting	52
	1.0×10^4		flow measurement	46

^a In all data cited, glutamate is the agonist. ^b *Xenopus* oocytes were used for the study of NMDA channels; the rest of the studies were with HEK-293 cells. ^c The k_{op} and k_{cl} values cited in the laser-pulse photolysis measurements are those at $n = 2$. ^d A channel closing rate constant (k_{cl}) obtained from single-channel recording is converted from the mean lifetime of the open channel (τ) via the relationship $k_{cl} = 1/\tau$.

brain, as it determines such basic properties as temporal precision and reliability (64, 65) and the gain of rate-encoded signals (66). It is also required to characterize the integration of nerve impulses that arrive at a chemical synapse or that originate from the same synapse but from different receptors or even from different isoforms of the same receptor responding to the same chemical signals, like glutamate. Such a study is especially meaningful for ionotropic glutamate receptors, because all three channel subtypes, namely, NMDA, AMPA, and kainate channels, are known to have different channel opening rate constants in response to the same agonist, glutamate.

Comparison of the Channel Opening Rate Constants of GluR3 with Those of Other Glutamate Receptors. Our study of GluR3 channel opening kinetics also constitutes a complete characterization of the channel opening rate constants for the flip variants of all AMPA receptor channels (Table 3). The comparison of the channel opening kinetics among these receptor subunits reveals clear differences in the channel opening and channel closing rate constants. Most strikingly, the magnitude of the k_{op} values for both GluR3_{flip} and GluR3_{flop} channels suggests that both variants are fast-activating channels, similar to GluR2 and GluR4 but different from GluR1 (see Table 3). Any of the k_{op} values in GluR2–4 are at least 3-fold larger than the k_{op} of GluR1. In terms of K_1 and EC_{50} values, GluR3 is also more similar to GluR2 and GluR4, i.e., ~ 1 mM (30, 32, 43), than to GluR1, i.e., ~ 0.5 mM (31). Interestingly, only the flip and flop variants of GluR1 do not exhibit different rates of desensitization (7). Our preliminary study of the channel opening kinetics of GluR1Q_{flop} (unpublished data) shows that its k_{cl} and k_{op} values are identical to those of the GluR1Q_{flip} channels (31). Together, these results suggest that GluR2, GluR3, and GluR4 are kinetically similar to each other, but different from GluR1.

Because of a relatively low K_1 or EC_{50} for GluR1 compared to other AMPA channels, a greater proportion of the GluR1 channel can open at a given concentration of glutamate, such as 1 mM, albeit with a relatively slower rate, compared with other AMPA channels. This difference is particularly significant when the glutamate concentration is

low but disappears when the glutamate concentration reaches saturation with respect to all AMPA channels. However, when k_{cl} is used as a unifying standard for comparison, it is apparent that GluR3_{flip} has the smallest k_{cl} , whereas GluR4_{flip} has the largest k_{cl} ; GluR1Q_{flip} and GluR2Q_{flip}, on the other hand, seem to have similar k_{cl} values. What this difference means physiologically is not yet known. It is clear, however, that functional differences among these channels should manifest more pronouncedly at lower glutamate concentrations. Finally, with limited information available, all AMPA channels have nevertheless larger channel opening rate constants, compared with the GluR6 kainate receptor channel (67) (Table 3). Whether this difference represents general kinetic properties between kainate and AMPA receptors also merits future studies.

ACKNOWLEDGMENT

We are grateful to Steve Heinemann for the GluR3 clones and to anonymous reviewers for insightful comments. We thank Lisa Maroski for editing.

REFERENCES

- Gallo, J. M., Jin, P., Thornton, C. A., Lin, H., Robertson, J., D'Souza, I., and Schlaepfer, W. W. (2005) The role of RNA and RNA processing in neurodegeneration, *J. Neurosci.* 25, 10372–10375.
- Sommer, B., Keinänen, K., Verdoorn, T. A., Wisden, W., Burnashev, N., Herb, A., Kohler, M., Takagi, T., Sakmann, B., and Seeburg, P. H. (1990) Flip and flop: A cell-specific functional switch in glutamate-operated channels of the CNS, *Science* 249, 1580–1585.
- Hollmann, M., and Heinemann, S. (1994) Cloned glutamate receptors, *Annu. Rev. Neurosci.* 17, 31–108.
- Dingledine, R., Borges, K., Bowie, D., and Traynelis, S. F. (1999) The glutamate receptor ion channels, *Pharmacol. Rev.* 51, 7–61.
- Erreger, K., Chen, P. E., Wyllie, D. J., and Traynelis, S. F. (2004) Glutamate receptor gating, *Crit. Rev. Neurobiol.* 16, 187–224.
- Palmer, C. L., Cotton, L., and Henley, J. M. (2005) The molecular pharmacology and cell biology of α -amino-3-hydroxy-5-methyl-4-isoxazolepropionic acid receptors, *Pharmacol. Rev.* 57, 253–277.
- Mosbacher, J., Schoepfer, R., Monyer, H., Burnashev, N., Seeburg, P. H., and Ruppersberg, J. P. (1994) A molecular determinant for submillisecond desensitization in glutamate receptors, *Science* 266, 1059–1062.

8. Partin, K. M., Patneau, D. K., and Mayer, M. L. (1994) Cyclothiazide differentially modulates desensitization of α -amino-3-hydroxy-5-methyl-4-isoxazolepropionic acid receptor splice variants, *Mol. Pharmacol.* **46**, 129–138.
9. Partin, K. M., Fleck, M. W., and Mayer, M. L. (1996) AMPA receptor flip/flop mutants affecting deactivation, desensitization, and modulation by cyclothiazide, aniracetam, and thiocyanate, *J. Neurosci.* **16**, 6634–6647.
10. Kessler, M., Rogers, G., and Arai, A. (2000) The norbornenyl moiety of cyclothiazide determines the preference for flip-flop variants of AMPA receptor subunits, *Neurosci. Lett.* **287**, 161–165.
11. Shen, Y., and Yang, X. L. (1999) Zinc modulation of AMPA receptors may be relevant to splice variants in carp retina, *Neurosci. Lett.* **259**, 177–180.
12. Karkanas, N. B., and Papke, R. L. (1999) Lithium modulates desensitization of the glutamate receptor subtype *gluR3* in *Xenopus* oocytes, *Neurosci. Lett.* **277**, 153–156.
13. Fleck, M. W., Bähring, R., Patneau, D. K., and Mayer, M. L. (1996) AMPA receptor heterogeneity in rat hippocampal neurons revealed by differential sensitivity to cyclothiazide, *J. Neurophysiol.* **75**, 2322–2333.
14. Lambolez, B., Ropert, N., Perrais, D., Rossier, J., and Hestrin, S. (1996) Correlation between kinetics and RNA splicing of α -amino-3-hydroxy-5-methylisoxazole-4-propionic acid receptors in neocortical neurons, *Proc. Natl. Acad. Sci. U.S.A.* **93**, 1797–1802.
15. Eastwood, S. L., Burnet, P. W., and Harrison, P. J. (1997) *GluR2* glutamate receptor subunit flip and flop isoforms are decreased in the hippocampal formation in schizophrenia: A reverse transcriptase-polymerase chain reaction (RT-PCR) study, *Brain Res. Mol. Brain Res.* **44**, 92–98.
16. Stine, C. D., Lu, W., and Wolf, M. E. (2001) Expression of AMPA receptor flip and flop mRNAs in the nucleus accumbens and prefrontal cortex after neonatal ventral hippocampal lesions, *Neuropsychopharmacology* **24**, 253–266.
17. Seifert, G., Schroder, W., Hinterkeuser, S., Schumacher, T., Schramm, J., and Steinhauser, C. (2002) Changes in flip/flop splicing of astroglial AMPA receptors in human temporal lobe epilepsy, *Epilepsia* **43**, 162–167.
18. Tomiyama, M., Rodriguez-Puertas, R., Cortes, R., Pazos, A., Palacios, J. M., and Mengod, G. (2002) Flip and flop splice variants of AMPA receptor subunits in the spinal cord of amyotrophic lateral sclerosis, *Synapse* **45**, 245–249.
19. Kawahara, Y., Ito, K., Sun, H., Aizawa, H., Kanazawa, I., and Kwak, S. (2004) Glutamate receptors: RNA editing and death of motor neurons, *Nature* **427**, 801.
20. Shi, S., Hayashi, Y., Esteban, J. A., and Malinow, R. (2001) Subunit-specific rules governing AMPA receptor trafficking to synapses in hippocampal pyramidal neurons, *Cell* **105**, 331–343.
21. Zhu, J. J., Esteban, J. A., Hayashi, Y., and Malinow, R. (2000) Postnatal synaptic potentiation: Delivery of *GluR4*-containing AMPA receptors by spontaneous activity, *Nat. Neurosci.* **3**, 1098–1106.
22. Rogers, S. W., Andrews, P. I., Gähring, L. C., Whisenand, T., Cauley, K., Crain, B., Hughes, T. E., Heinemann, S. F., and McNamara, J. O. (1994) Autoantibodies to glutamate receptor *GluR3* in Rasmussen's encephalitis, *Science* **265**, 648–651.
23. Mantegazza, R., Bernasconi, P., Baggi, F., Spreafico, R., Ragona, F., Antozzi, C., Bernardi, G., and Granata, T. (2002) Antibodies against *GluR3* peptides are not specific for Rasmussen's encephalitis but are also present in epilepsy patients with severe, early onset disease and intractable seizures, *J. Neuroimmunol.* **131**, 179–185.
24. Ganor, Y., Besser, M., Ben-Zakay, N., Unger, T., and Levite, M. (2003) Human T cells express a functional ionotropic glutamate receptor *GluR3*, and glutamate by itself triggers integrin-mediated adhesion to laminin and fibronectin and chemotactic migration, *J. Immunol.* **170**, 4362–4372.
25. Rembach, A., Turner, B. J., Bruce, S., Cheah, I. K., Scott, R. L., Lopes, E. C., Zagami, C. J., Beart, P. M., Cheung, N. S., Langford, S. J., and Cheema, S. S. (2004) Antisense peptide nucleic acid targeting *GluR3* delays disease onset and progression in the SOD1 G93A mouse model of familial ALS, *J. Neurosci. Res.* **77**, 573–582.
26. Swanson, G. T., Kamboj, S. K., and Cull-Candy, S. G. (1997) Single-channel properties of recombinant AMPA receptors depend on RNA editing, splice variation, and subunit composition, *J. Neurosci.* **17**, 58–69.
27. Derkach, V., Barria, A., and Soderling, T. R. (1999) Ca^{2+} /calmodulin-kinase II enhances channel conductance of α -amino-3-hydroxy-5-methyl-4-isoxazolepropionate type glutamate receptors, *Proc. Natl. Acad. Sci. U.S.A.* **96**, 3269–3274.
28. Jin, R., Banke, T. G., Mayer, M. L., Traynelis, S. F., and Gouaux, E. (2003) Structural basis for partial agonist action at ionotropic glutamate receptors, *Nat. Neurosci.* **6**, 803–810.
29. Wieboldt, R., Gee, K. R., Niu, L., Ramesh, D., Carpenter, B. K., and Hess, G. P. (1994) Photolabile precursors of glutamate: Synthesis, photochemical properties, and activation of glutamate receptors on a microsecond time scale, *Proc. Natl. Acad. Sci. U.S.A.* **91**, 8752–8756.
30. Li, G., Pei, W., and Niu, L. (2003) Channel-opening kinetics of *GluR2*_{flip} AMPA receptor: A laser-pulse photolysis study, *Biochemistry* **42**, 12358–12366.
31. Li, G., and Niu, L. (2004) How fast does the *GluR1Q* flip channel open? *J. Biol. Chem.* **279**, 3990–3997.
32. Li, G., Sheng, Z., Huang, Z., and Niu, L. (2005) Kinetic mechanism of channel opening of the *GluR1Q* flip AMPA receptor, *Biochemistry* **44**, 5835–5841.
33. Huang, Z., Li, G., Pei, W., Sosa, L. A., and Niu, L. (2005) Enhancing protein expression in single HEK 293 cells, *J. Neurosci. Methods* **142**, 159–166.
34. Udgaonkar, J. B., and Hess, G. P. (1987) Chemical kinetic measurements of a mammalian acetylcholine receptor by a fast-reaction technique, *Proc. Natl. Acad. Sci. U.S.A.* **84**, 8758–8762.
35. Longworth, L. G. (1953) Diffusion measurements at 25° of aqueous solutions of amino acids, peptides and sugars, *J. Am. Chem. Soc.* **75**, 5705–5709.
36. Watase, K., Sekiguchi, M., Matsui, T. A., Tagawa, Y., and Wada, K. (1997) Dominant negative mutant of ionotropic glutamate receptor subunit *GluR3*: Implications for the role of a cysteine residue for its channel activity and pharmacological properties, *Biochem. J.* **322**, 385–391.
37. Quirk, J. C., and Nisenbaum, E. S. (2003) Multiple molecular determinants for allosteric modulation of alternatively spliced AMPA receptors, *J. Neurosci.* **23**, 10953–10962.
38. Stern-Bach, Y., Russo, S., Neuman, M., and Rosenmund, C. (1998) A point mutation in the glutamate binding site blocks desensitization of AMPA receptors, *Neuron* **21**, 907–918.
39. Chen, W., and Hahn, W. C. (2003) SV40 early region oncoproteins and human cell transformation, *Histol. Histopathol.* **18**, 541–550.
40. Rosenmund, C., Stern-Bach, Y., and Stevens, C. F. (1998) The tetrameric structure of a glutamate receptor channel, *Science* **280**, 1596–1599.
41. Armstrong, N., and Gouaux, E. (2000) Mechanisms for activation and antagonism of an AMPA-sensitive glutamate receptor: Crystal structures of the *GluR2* ligand binding core, *Neuron* **28**, 165–181.
42. Lofffield, R. B., and Eigner, E. A. (1969) Molecular order of participation of inhibitors (or activators) in biological systems, *Science* **164**, 305–308.
43. Koike, M., Tsukada, S., Tsuzuki, K., Kijima, H., and Ozawa, S. (2000) Regulation of kinetic properties of *GluR2* AMPA receptor channels by alternative splicing, *J. Neurosci.* **20**, 2166–2174.
44. Raman, I. M., and Trussell, L. O. (1995) The mechanism of α -amino-3-hydroxy-5-methyl-4-isoxazolepropionate receptor desensitization after removal of glutamate, *Biophys. J.* **68**, 137–146.
45. Vyklicky, L., Jr., Patneau, D. K., and Mayer, M. L. (1991) Modulation of excitatory synaptic transmission by drugs that reduce desensitization at AMPA/kainate receptors, *Neuron* **7**, 971–984.
46. Heckmann, M., Bufler, J., Franke, C., and Dudel, J. (1996) Kinetics of homomeric *GluR6* glutamate receptor channels, *Biophys. J.* **71**, 1743–1750.
47. Jin, R., Horning, M., Mayer, M. L., and Gouaux, E. (2002) Mechanism of activation and selectivity in a ligand-gated ion channel: Structural and functional studies of *GluR2* and quisqualate, *Biochemistry* **41**, 15635–15643.
48. Smith, T. C., and Howe, J. R. (2000) Concentration-dependent substate behavior of native AMPA receptors, *Nat. Neurosci.* **3**, 992–997.
49. Mayer, M. L., and Armstrong, N. (2004) Structure and function of glutamate receptor ion channels, *Annu. Rev. Physiol.* **66**, 161–181.
50. Clements, J. D., Lester, R. A., Tong, G., Jahr, C. E., and Westbrook, G. L. (1992) The time course of glutamate in the synaptic cleft, *Science* **258**, 1498–1501.

51. Diamond, J. S., and Jahr, C. E. (1997) Transporters buffer synaptically released glutamate on a submillisecond time scale, *J. Neurosci.* *17*, 4672–4687.
52. Traynelis, S. F., and Wahl, P. (1997) Control of rat GluR6 glutamate receptor open probability by protein kinase A and calcineurin, *J. Physiol.* *503*, 513–531.
53. Matsubara, N., Billington, A. P., and Hess, G. P. (1992) How fast does an acetylcholine receptor channel open? Laser-pulse photolysis of an inactive precursor of carbamoylcholine in the microsecond time region with BC3H1 cells, *Biochemistry* *31*, 5507–5514.
54. Colquhoun, D., Jonas, P., and Sakmann, B. (1992) Action of brief pulses of glutamate on AMPA/kainate receptors in patches from different neurones of rat hippocampal slices, *J. Physiol.* *458*, 261–287.
55. Nielsen, T. A., DiGregorio, D. A., and Silver, R. A. (2004) Modulation of glutamate mobility reveals the mechanism underlying slow-rising AMPAR EPSCs and the diffusion coefficient in the synaptic cleft, *Neuron* *42*, 757–771.
56. Renger, J. J., Egles, C., and Liu, G. (2001) A developmental switch in neurotransmitter flux enhances synaptic efficacy by affecting AMPA receptor activation, *Neuron* *29*, 469–484.
57. Armstrong, N., Mayer, M., and Gouaux, E. (2003) Tuning activation of the AMPA-sensitive GluR2 ion channel by genetic adjustment of agonist-induced conformational changes, *Proc. Natl. Acad. Sci. U.S.A.* *100*, 5736–5741.
58. Sun, Y., Olson, R., Horning, M., Armstrong, N., Mayer, M., and Gouaux, E. (2002) Mechanism of glutamate receptor desensitization, *Nature* *417*, 245–253.
59. Fersht, A. (1999) *Structure and Mechanism in Protein Science*, W. H. Freeman, New York.
60. Trussell, L. O., and Fischbach, G. D. (1989) Glutamate receptor desensitization and its role in synaptic transmission, *Neuron* *3*, 209–218.
61. Choi, S., Klingauf, J., and Tsien, R. W. (2000) Postfusional regulation of cleft glutamate concentration during LTP at ‘silent synapses’, *Nat. Neurosci.* *3*, 330–336.
62. Carter, A. G., and Regehr, W. G. (2000) Prolonged synaptic currents and glutamate spillover at the parallel fiber to stellate cell synapse, *J. Neurosci.* *20*, 4423–4434.
63. Schoppa, N. E., and Westbrook, G. L. (2001) Glomerulus-specific synchronization of mitral cells in the olfactory bulb, *Neuron* *31*, 639–651.
64. Galarreta, M., and Hestrin, S. (2001) Spike transmission and synchrony detection in networks of GABAergic interneurons, *Science* *292*, 2295–2299.
65. Cathala, L., Brickley, S., Cull-Candy, S., and Farrant, M. (2003) Maturation of EPSCs and intrinsic membrane properties enhances precision at a cerebellar synapse, *J. Neurosci.* *23*, 6074–6085.
66. Mitchell, S. J., and Silver, R. A. (2003) Shunting inhibition modulates neuronal gain during synaptic excitation, *Neuron* *38*, 433–445.
67. Li, G., Oswald, R. E., and Niu, L. (2003) Channel-opening kinetics of GluR6 kainate receptor, *Biochemistry* *42*, 12367–12375.
68. Wyllie, D. J., Behe, P., and Colquhoun, D. (1998) Single-channel activations and concentration jumps: Comparison of recombinant NR1a/NR2A and NR1a/NR2D NMDA receptors, *J. Physiol.* *510*, 1–18.
69. Robert, A., and Howe, J. R. (2003) How AMPA receptor desensitization depends on receptor occupancy, *J. Neurosci.* *23*, 847–858.

BI062213S

How Fast Does the GluR1Q_{flip} Channel Open?*

Received for publication, September 22, 2003, and in revised form, November 5, 2003
Published, JBC Papers in Press, November 10, 2003, DOI 10.1074/jbc.M310410200

Gang Li‡ and Li Niu§

From the Department of Chemistry and the Center for Neuroscience Research, State University of New York,
Albany, New York 12222

Opening of a ligand-gated ion channel is the step at which the binding of a neurotransmitter is transduced into the electrical signal by allowing ions to flow through the transmembrane channel, thereby altering the postsynaptic membrane potential. We report the kinetics for the opening of the GluR1Q_{flip} channel, an α -amino-3-hydroxy-5-methyl-4-isoxazolepropionic acid receptor subunit of the ionotropic glutamate receptors. Using a laser-pulse photolysis technique that permits glutamate to be liberated photolytically from γ -O-(α -carboxy-2-nitrobenzyl)glutamate (caged glutamate) with a time constant of ~ 30 μ s, we show that, after the binding of glutamate, the channel opened with a rate constant of $(2.9 \pm 0.2) \times 10^4$ s⁻¹ and closed with a rate constant of $(2.1 \pm 0.1) \times 10^3$ s⁻¹. The observed shortest rise time (20–80% of the receptor current response), *i.e.* the fastest time by which the GluR1Q_{flip} channel can open, was predicted to be 35 μ s. This value is three times shorter than those previously reported. The minimal kinetic mechanism for channel opening consists of binding of two glutamate molecules, with the channel-opening probability being 0.93 ± 0.10 . These findings identify GluR1Q_{flip} as one of the temporally efficient receptors that transduce the binding of chemical signals (*i.e.* glutamate) into an electrical impulse.

The rate at which a ligand-gated ion channel opens is important to know because it has major implications in signal transmission and regulation. First, knowing the constants for the channel-opening rate will allow one to predict more quantitatively the time course of the open channel form of the receptor as a function of neurotransmitter or ligand concentration, which determines the transmembrane voltage change and in turn controls synaptic neurotransmission. Second, that knowledge will provide clues for mechanism-based design of compounds to regulate receptor function more effectively. Third, characterizing the effect of structural variations on the rate constants for channel opening will offer a test of the function, which is relevant to the time scale on which the receptor is in the open channel form, rather than in the desensitized form, *i.e.* ligand-bound, but closed channel form. Examples of structural variations include those due to RNA editing, RNA splic-

ing, and site-specific mutations for investigating the structure-function relationship. Finally, knowing the channel-opening rate constants will be required to understand quantitatively the integration of nerve impulses that arrive at a chemical synapse or that originate from the same synapse, but from different receptors responding to the same chemical signals (neurotransmitters) such as glutamate.

We report here the kinetics for the opening of the GluR1Q_{flip} receptor channel. GluR1 is one of the four subunits of the α -amino-3-hydroxy-5-methyl-4-isoxazolepropionic acid (AMPA)¹ receptor (1, 2). As a subtype of ionotropic glutamate receptors, AMPA receptors mediate fast synaptic neurotransmission in the mammalian central nervous system (1, 2). The GluR1 subunit plays a specific role in a wide range of biological functions such as the expression of synaptic plasticity (3–6), the formation of memory (7–9), the development of the dendritic architecture of motor neurons (10), the excitotoxic necrosis induced via acid sphingomyelinase-mediated and NF- κ B-mediated signal transduction pathways (11), and the generation of sensitization by drugs of abuse (12–14).

The kinetic properties of the GluR1 receptor related to desensitization have been well characterized. For example, GluR1 desensitizes rapidly with a maximal time constant of 4 ms, achieved at saturating glutamate concentration (15–18). Amino acid residue 750 (*i.e.* serine at GluR1_{flip}) has been identified as sensitive to allosteric modulators of AMPA receptors such as cyclothiazide (16). Furthermore, the single channel recording of GluR1 revealed that the major component (73%) has a lifetime of 0.24 ms (6). However, the kinetic mechanism of channel opening is not known. The rate of channel opening appears to be too fast to be resolved by commonly used kinetic approaches such as solution exchange techniques. Consequently, the kinetic constants pertaining to the channel-opening process have been estimated only by fitting the rate parameters associated with the deactivation and desensitization processes that occur relatively slowly compared with channel opening (17, 19). By no means, however, is this “slow” time scale actually slow: even early studies of the native AMPA receptors show that, within a few milliseconds, the receptors desensitize (20, 21). By inference, the channel must open faster.

In this study, we used a laser-pulse photolysis technique to release biologically active glutamate from biologically inert caged glutamate or γ -O-(α -carboxy-2-nitrobenzyl)glutamate with a time constant of ~ 30 μ s (Fig. 1) (22) and characterized the kinetic mechanism of glutamate-induced channel opening prior to channel desensitization. We found that the GluR1Q_{flip} channel opens in response to the binding of the natural neurotransmitter glutamate with a rate constant of 29,000 s⁻¹ and closes with a constant of 2100 s⁻¹. Once bound to glutamate,

* This work was supported in part by American Heart Association Grant 0130513T and by grants from the Amyotrophic Lateral Sclerosis Association and the Muscular Dystrophy Association (to L. N.). The costs of publication of this article were defrayed in part by the payment of page charges. This article must therefore be hereby marked “advertisement” in accordance with 18 U.S.C. Section 1734 solely to indicate this fact.

‡ Supported by a postdoctoral fellowship from the Muscular Dystrophy Association.

§ To whom correspondence should be addressed: Dept. of Chemistry, SUNY, 1400 Washington Ave., Albany, NY 12222. Tel.: 518-442-4447; Fax: 518-442-3462; E-mail: lniu@albany.edu.

¹ The abbreviations used are: AMPA, α -amino-3-hydroxy-5-methyl-4-isoxazolepropionic acid; GFP, green fluorescent protein.

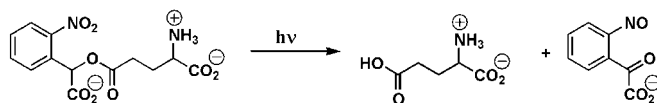


FIG. 1. Photolysis of caged glutamate.

the receptor has a 0.93 probability to open. We offer possible interpretations for the biological significance of these results in the context of other glutamate receptors.

MATERIALS AND METHODS

Expression of cDNA and Cell Culture—The original cDNA encoding GluR1Q_{flip} in a pBluescript vector was provided by Prof. Steve Heinemann (Salk Institute) and cloned into the pcDNA3.1 vector (Invitrogen). The plasmid was propagated in an *Escherichia coli* host (DH5 α) and purified using a kit from QIAGEN Inc. (Valencia, CA). HEK-293 cells were cultured in Dulbecco's modified Eagle's medium supplemented with 10% fetal bovine serum in a 5% CO₂ humidified incubator at 37 °C. GluR1Q_{flip} was transiently expressed in these cells using a calcium phosphate method (23). Unless otherwise noted, HEK-293 cells were also cotransfected with a plasmid encoding green fluorescent protein (GFP; a generous gift from Prof. Ben Szaro, State University of New York at Albany). GFP was used as an intracellular marker, and green cells were selected for recordings. The weight ratio of the plasmid for GFP to that for GluR1 was 1:10, and the GluR1 plasmid was used for transfection at ~3–5 μ g/35-mm dish. Transfected cells were allowed to grow for >48 h before use.

Whole-cell Current Recording—Recording electrodes were pulled from glass capillaries (World Precision Instruments, Inc., Sarasota, FL) and fire-polished. The electrode resistance was ~3 megaohms when filled with the electrode solution. The electrode solution contained 110 mM CsF, 30 mM CsCl, 4 mM NaCl, 0.5 mM CaCl₂, 5 mM EGTA, and 10 mM HEPES (pH 7.4 adjusted with CsOH). The external bath solution contained 150 mM NaCl, 3 mM KCl, 1 mM CaCl₂, 1 mM MgCl₂, and 10 mM HEPES (pH 7.4 adjusted with NaOH). All chemicals were from commercial sources. The GFP fluorescence in cells was visualized using an Axiovert S100 microscope with a fluorescent detection system (Carl Zeiss, Inc., Thornwood, NY). The whole-cell current was recorded using an Axopatch 200B amplifier at a cutoff frequency of 2–20 kHz with a built-in, 4-pole Bessel filter and digitized at sampling frequency of 5–50 kHz using a Digidata 1322A apparatus (Axon Instruments, Inc., Union City, CA). The data acquisition software used was pCLAMP8 (Axon Instruments, Inc.).

Laser-pulse Photolysis—The setup for the laser-pulse photolysis experiment has been described previously (24, 25). γ -O-(α -Carboxy-2-nitrobenzyl)glutamate (Molecular Probes, Inc., Eugene, OR) (22) was dissolved in the external bath buffer and applied to a cell using a cell-flow device (see below). Once a HEK-293 cell was in the whole-cell mode, it was lifted from the bottom of the dish and suspended in the external bath solution. After the cell was equilibrated with caged glutamate for 250 ms, the laser was fired to liberate the free glutamate. A single laser pulse at 355 nm with a pulse length of 8 ns was generated from a Minilite II pulsed Q-switched Nd:YAG laser (Continuum, Santa Clara, CA) tuned by a third harmonic generator. The laser light was coupled to a fiber optic (FiberGuide Industries, Stirling, NJ), and the power was adjusted to 200–800 μ J, as detected by a joulemeter (Gentec, Quebec, Canada).

To vary the concentration of the photolytically released glutamate in kinetic measurements, the power of the laser was adjusted, and/or the concentration of the caged glutamate was varied. To determine the concentration of the photolytically released glutamate, at least two glutamate solutions with known concentrations were used to measure the current amplitudes from the same cell before and after a laser pulse. The free glutamate solution was applied to the cell using the cell-flow device (see below). The current amplitudes obtained from the cell-flow measurements were compared with the amplitude from the laser measurement, with reference to the dose-response relationship. These measurements also permitted us to monitor any damage to the receptors and/or the cell for successive laser experiments with the same cell.

Cell-flow Measurements—The cell-flow device (26) was used to deliver either caged glutamate for laser-pulse photolysis or free glutamate to monitor the cell damage and to calibrate the concentration of photolytically released glutamate. The cell-flow device consisted of a U-tube with an aperture of ~150 μ m. The linear flow rate, controlled by two peristaltic pumps, was 4 cm/s. A HEK-293 cell was placed 50–100 μ m away from the U-tube aperture. The rise time of the glutamate-induced

whole-cell current response (10–90%) was 2.3 ± 0.1 ms, an average of the measurement from >100 cells expressing the receptor. When free glutamate was used, the amplitude of the whole-cell current was corrected for receptor desensitization during the rise time by a method described previously (26). This correction is necessary because the observed current amplitude depends on the rise time of the amplitude, the fraction of the open channel (*i.e.* the percentage of the channel that is open), and the desensitization rate constant. The reduction in the current amplitude due to desensitization is particularly significant when the receptor of interest desensitizes rapidly, as does the GluR1 receptor (6, 16, 17). The method used to correct the receptor desensitization during the rise time is based on hydrodynamic theories that describe fluid flowing over a spherical object, such as, by approximation, a HEK-293 cell suspended in the external bath solution. When a solution flows over a cell, the time that the ligand molecules in the solution mix with receptors on the cell surface varies because of uneven flow rates of the ligands over the spherical surface of a cell. This asynchronization in mixing distorts both the rate and amplitude of the current rise. By the correction method, the time course of the current is first divided into a constant time interval, and then the observed current (I_{obs}) is corrected for the desensitization that occurs during each time interval (Δt). After the current is determined for each of n constant time intervals ($n\Delta t = t_n$, where t_n is equal to or greater than the current rise time), the corrected total current (I_A) is given by Equation 1,

$$I_A = (e^{\alpha\Delta t} - 1) \sum_{i=1}^n (I_{\text{obs}})_i \Delta t_i + (I_{\text{obs}})_n \Delta t_n \quad (\text{Eq. 1})$$

where α represents the rate constant for receptor desensitization, and $(I_{\text{obs}})_i \Delta t_i$ represents the observed current during the i th time interval. I_A obtained from this correction method is independent of the flow speed of the solution. The validity of this method was demonstrated using several independent approaches (26). (The current correction program was kindly provided by Prof. George P. Hess, Cornell University.)

All recordings were made with cells that were voltage-clamped at –60 mV, pH 7.4, and 22 °C. Each data point is an average of at least three measurements collected from at least three cells unless otherwise noted. Linear regression and nonlinear fitting (Levenberg-Marquardt and simplex algorithms) were performed using Origin Version 7 software (Origin Lab, Northampton, MA). Uncertainties are reported as S.E. of the fits unless noted otherwise.

RESULTS

Glutamate-induced GluR1Q_{flip} Response—A typical glutamate-induced whole-cell response is illustrated in Fig. 2A. The current through the GluR1Q_{flip} homomeric channel expressed in HEK-293 cells increased rapidly, indicating channel opening, and then returned toward the base line, indicating desensitization. As a control, both non-transfected cells and cells expressing only GFP gave no response even at 10 mM glutamate, a concentration that otherwise would have evoked a maximal current response for the transfected cells expressing GluR1Q_{flip} (see the dose-response curve in Fig. 3A). The receptor desensitization was rapid (Fig. 2B) and essentially complete (Fig. 2A), which is consistent with previous observations (6, 15–17). A first-order rate was adequate to describe >95% of the progression of the desensitization reaction at all concentrations of glutamate. This analysis agreed with those previously reported (6, 15, 16), although Robert *et al.* (17) described an additional but minor (0.5–2%) desensitization process with a much slower rate. The desensitization rate constant increased with increasing glutamate concentration, but eventually became invariant (Fig. 2B). The mean value of the maximal rate constant, independent of ligand concentration, was 230 s^{-1} or a time constant of ~4 ms.

Based on the magnitude and profile of the desensitization rate, we evaluated whether the presence of GFP affected the kinetic properties of GluR1Q_{flip} expressed in the green fluorescent HEK-293 cells (the green color was due to the expression of GFP) because the green cells were selected for measurements. We found that the desensitization rate constant obtained from green cells expressing both GFP and GluR1Q_{flip} at

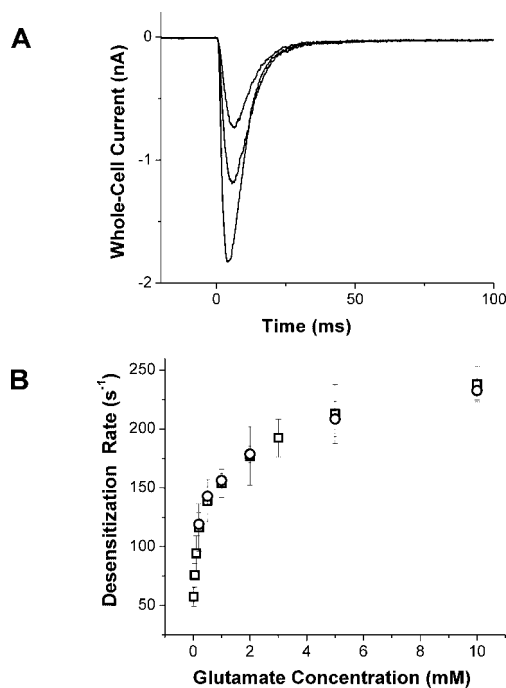


FIG. 2. Coexpression of GFP does not affect the kinetic properties of GluR1Q_{nip} in HEK-293 cells. *A*, whole-cell current response to glutamate at concentrations of 2000 (lower trace), 500 (middle trace), and 200 (upper trace) μM . *B*, comparison of the desensitization rate constants obtained from cells with and without coexpression of GFP. The desensitization rate was characterized by a first-order rate constant and is shown with the S.E. \circ , measurements for HEK-293 cells expressing only GluR1Q_{nip}; \square , measurements for HEK-293 cells expressing both GluR1Q_{nip} and GFP. Each data point is an average of at least three measurements from three cells.

a given glutamate concentration was statistically no different from the rate constant obtained from non-green cells expressing only GluR1Q_{nip} (Fig. 2*B*). Furthermore, the relative current amplitude determined under the same conditions was comparable (Fig. 3*A*). Therefore, we concluded that the presence of GFP in the same cell did not affect the kinetic property of GluR1Q_{nip}, and GFP was thus used for convenient identification of cells expressing GluR1Q_{nip}. In addition, a nearly linear correlation was observed between the intensity of the green fluorescence and the amplitude of the receptor response from the same cell.

It has been documented that the desensitization rate observed using whole cells is slower than that using outside-out patches for the same receptor (6, 16, 17). The largest difference reported is 2.9-fold (16). The reason for this discrepancy in rate is not known, although several explanations have been proposed (6, 16, 17), including the slower solution exchange rate with a whole cell because of its geometry and/or the faster desensitization rate constant observed with outside-out patches because of the altered kinetic properties of the receptor in such a membrane configuration (27). Nevertheless, our purpose for measuring desensitization (shown in Fig. 2*B*) was to use the desensitization rate constant as a relative measure to test whether the presence of GFP in the same cell affected the desensitization rate of the receptor. Furthermore, the magnitude of the desensitization rate we observed using the whole-cell recording was consistent with values reported by others. For instance, at 1 mM glutamate, the desensitization time constant we obtained was 6 ms (or a rate constant of 160 s⁻¹). This value was identical, within experimental error, to the value observed in the whole-cell recording of the same receptor by both Partin *et al.* (16) and Derkach *et al.* (6).

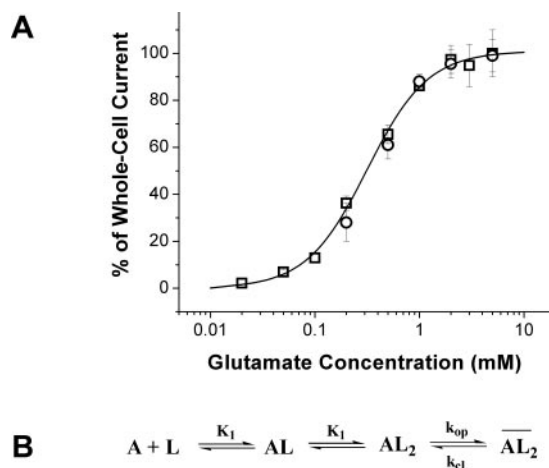


FIG. 3. Whole-cell current amplitude as a function of glutamate concentration or dose-response relationship. *A*, the whole-cell currents from different cells were normalized to the current obtained at 1 mM glutamate, and the current amplitude at 10 mM was set to 100%. The best fit parameters using Equation 2 (solid line) were as follows: $K_1 = 0.53 \pm 0.06$ mM, $\Phi = 0.19 \pm 0.04$, and $I_M R_M = 123 \pm 5$. \circ , measurements for HEK-293 cells expressing only GluR1Q_{nip}; \square , measurements for HEK-293 cells expressing both GluR1Q_{nip} and GFP. The observed whole-cell current was corrected for desensitization (see “Materials and Methods”). *B*, shown is a minimal kinetic mechanism for the channel opening of GluR1Q_{nip}. The mechanism involves two ligand-binding steps. *A*, the active unliganded form of the receptor; *L*, the ligand (glutamate); *AL* and *AL₂*, ligand-bound closed channel forms; *AL₂^o*, the open channel form of the receptor. For simplicity, it is assumed that glutamate binds to the two sites with equal affinity (designated by K_1).

Minimal Kinetic Mechanism for Channel Opening—Fig. 3*A* shows the dose-response relationship, established with the current amplitude corrected for receptor desensitization (see “Materials and Methods”), as a function of glutamate concentration. The relationship is described by Equation 2,

$$I_A = I_M R_M \frac{L^2}{L^2 + \Phi(L + K_1)^2} \quad (\text{Eq. 2})$$

where I_A represents the current amplitude, L is the molar concentration of the ligand, I_M is the current/mole of receptor, and R_M is the moles of receptor in the cell. Φ is the reciprocal of the channel-opening equilibrium constant, and K_1 is the intrinsic dissociation constant for the ligand. The derivation of Equation 2 was based on a minimal kinetic mechanism for channel opening, shown in Fig. 3*B*. This mechanism is a general one for ligand-gated ion channels (28), including glutamate receptors (20, 29–33), in which the binding of two glutamate molecules is sufficient to open the channel (29, 34, 35). For simplicity, it was assumed that the intrinsic equilibrium dissociation constant (K_1) for both ligand-binding steps was the same (see below for additional discussion of this mechanism). Accordingly, the best fit of the dose-response curve yielded $K_1 = 0.53 \pm 0.06$ mM using Equation 2. The K_1 value from this study is comparable with the reported values of EC_{50} (the ligand concentration that corresponds to 50% of the maximal response), ranging from ~ 0.5 to 0.7 mM (6, 16, 36).

Characterization of Caged Glutamate with GluR1Q_{nip} in HEK-293 Cells—In this study, we used a laser-pulse photolysis technique to characterize the channel-opening kinetics for the GluR1Q_{nip} homomeric receptor. This technique permits rapid photolytic release of free glutamate, with $t_{1/2} \sim 30$ μs , from its photolabile precursor or caged glutamate (Fig. 1) (22). To use this technique, the caged glutamate must be biologically inert with respect to the GluR1Q_{nip} receptor expressed in HEK-293 cells. As shown in Fig. 4, the glutamate-elicited receptor re-

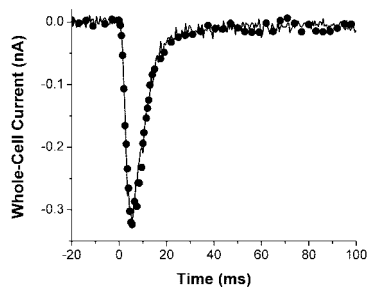


FIG. 4. **Caged glutamate is biologically inert with respect to GluR1Q_{flip} expressed in HEK-293 cells.** Superimposed are the whole-cell currents induced by 200 μM glutamate in the absence (*solid line*) and presence (*closed circles*) of 2 mM caged glutamate. The sampling frequency was 5 kHz. For clarity, however, the number of points shown in the *closed circle* trace was reduced in various regions of the current trace.

sponses in the presence and absence of caged glutamate had identical current amplitudes and desensitization rates. In this test, the concentration of caged glutamate was 2 mM, the highest used in the laser experiments. Therefore, this result (Fig. 4) demonstrated that the caged glutamate did not activate the GluR1Q_{flip} channel, nor did it inhibit or potentiate the glutamate response. This conclusion is consistent with the earlier characterization of the caged glutamate using endogenous glutamate receptors in rat hippocampal neurons (22).

Channel-opening Kinetics Characterized by the Laser-pulse Photolysis Technique—Using the laser-pulse photolysis technique with caged glutamate, we determined the rate constants for the opening of the GluR1Q_{flip} channel. A representative whole-cell current response obtained in these experiments is illustrated in Fig. 5A. The current increased as a result of the opening of the receptor channel and then decreased because of channel desensitization. A single exponential rate law (given in Equation 3) accounted for $\sim 95\%$ of the increase in current.

$$I_t = I_A(1 - e^{-k_{\text{obs}}t}) \quad (\text{Eq. 3})$$

I_t represents the current amplitude at time t , and I_A represents the maximal current amplitude. (An example of the fit using Equation 3 is indicated by the *solid line* in Fig. 5A.) Moreover, the rising phase of the current remained monophasic over the entire range of concentrations of photolytically released glutamate (*i.e.* between 50 and 250 μM). This result was consistent with the assumption that the ligand-binding rate was fast relative to the channel-opening rate (see the mechanism in Fig. 3B and the discussion below). The observed first-order rate process, as shown in Fig. 5A, therefore represented the channel-opening rate step. Accordingly, Equation 4 was derived, which enabled us to determine the channel-opening (k_{op}) and channel-closing (k_{cl}) rate constants.

$$k_{\text{obs}} = k_{\text{cl}} + k_{\text{op}} \left(\frac{L}{L + K_1} \right)^2 \quad (\text{Eq. 4})$$

Shown in Fig. 5B is the best fit of the observed first-order rate constant (k_{obs}) as a function of glutamate concentration by Equation 4, yielding $k_{\text{cl}} = (2.1 \pm 0.1) \times 10^3 \text{ s}^{-1}$ and $k_{\text{op}} = (2.9 \pm 0.2) \times 10^4 \text{ s}^{-1}$.

In kinetic analysis of the channel-opening rate using Equation 4, we assumed that the rate of channel opening is slow relative to the rate of ligand binding in both the first and second steps (Fig. 3B). Consequently, the observed rate process reflects the transition from the doubly liganded, closed channel form to the open channel form. Kinetically, then, the rising phase of the receptor response is expected to be a single expo-

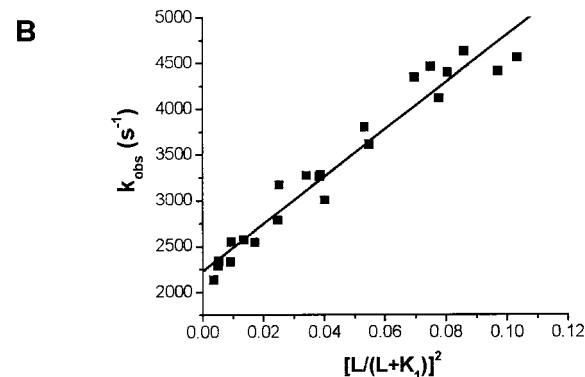
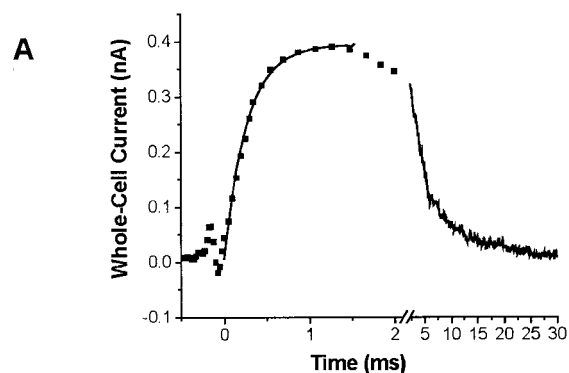


FIG. 5. **Laser-pulse photolysis measurements of the channel-opening kinetics for GluR1Q_{flip}.** *A*, a representative whole-cell current from the opening of the GluR1Q_{flip} channel initiated by the laser-pulse photolysis of caged glutamate at time 0. The fitting of the rise in current (using Equation 3) is shown as a *solid line* superimposed with the data points. The k_{obs} was $3800 \pm 150 \text{ s}^{-1}$, corresponding to a 160 μM concentration of photolytically released glutamate. Note that the direction of the current response is plotted opposite to that recorded. For clarity, the number of data points was reduced for plotting. *B*, plot of k_{obs} versus glutamate concentration using Equation 4. Each point represents a k_{obs} obtained at a particular concentration of photolytically released glutamate. The k_{cl} and k_{op} were determined to be $(2.1 \pm 0.1) \times 10^3$ and $(2.9 \pm 0.2) \times 10^4 \text{ s}^{-1}$, respectively.

ponential rate process and to remain so even when the concentration of ligand is varied. In our experiments, at all concentrations of photolytically liberated glutamate, the rising phase was accounted for adequately by a single first-order rate constant. Thus, this result is consistent with the assumption that the channel-opening rate is slower than the ligand-binding rate. Conversely, if the ligand-binding rate were similar to the channel-opening rate, there would be a biphasic rate process in the rising phase as the concentration of ligand is varied. In that case, one rate would represent ligand binding, whereas the other would reflect channel opening. If the ligand-binding rate were slow compared with the rate of channel opening, the concentration dependence of k_{obs} would not be adequately described by Equation 4. For instance, the rate will be linearly dependent on the concentration of glutamate if the binding rate for the first and second steps is assumed to be the same (37).

Because ligand binding is a bimolecular process, at sufficiently low concentrations of ligand, the rate of ligand binding will eventually become rate-limiting for the kinetic mechanism shown in Fig. 3B. To ensure that ligand binding was always fast so that the relatively slow channel-opening rate process could be observed, the lowest concentration of glutamate at

which we measured k_{obs} was chosen as 40 μM (Fig. 5B). The 40 μM ligand concentration corresponded to the fraction of the channel in the open form being $\sim 4\%$ (the fraction of the open channel is defined by Equation 2 and is shown in Fig. 2B). This was the same fraction at which the k_{obs} was comparable with the k_{cl} for the nicotinic acetylcholine receptor (38). (Using the fraction of the open channel, rather than the absolute concentration, takes into account the different K_1 values for different receptors.) Furthermore, the k_{cl} for the nicotinic acetylcholine receptor was in agreement with the lifetime of the open channel, which was characterized independently using single channel recording (38). Likewise, the k_{cl} of 2100 s^{-1} obtained in this study for the GluR1Q_{flip} receptor is close to the value of the lifetime (of the major component), ~ 0.3 ms or a rate constant of 3100 s^{-1} , for the same receptor, but obtained from single channel recording (see details under "Discussion") (6). Therefore, the fraction of the open channel at $\sim 4\%$, which corresponded to the 40 μM glutamate concentration for the GluR1Q_{flip} receptor, should be high enough such that the rate constant we measured should pertain to the channel-opening process rather than to ligand binding.

Presently, the rate of glutamate binding to the receptor, which leads to the opening of the channel, is not known. However, Madden and co-workers (39) reported that the rate constant for glutamate binding to the extracellular portion of the GluR4 receptor, known as S1S2, is indeed large. The association rate constant at 5 °C is $1.6 \times 10^7 \text{ M}^{-1} \text{ s}^{-1}$ (39). At room temperature, this rate constant is expected to become even larger provided that ligand binding behaves linearly according to the Arrhenius equation (40). However, that rate constant, as the authors pointed out, should be taken in the context that S1S2 is only a partial protein and lacks the ability to form the channel.

The Channel-opening Rate Can Be Separated from the Channel Desensitization Rate in the Laser-pulse Photolysis Measurements—As shown in Fig. 5B, the observed channel-opening rate became faster as the glutamate concentration increased (by the relationship given in Equation 4). Concurrently, the observed desensitization rate also became faster (Fig. 2B). However, the rate of channel opening, seen as the rise in the whole-cell current, was always faster than the rate of desensitization, seen as the fall in current (Fig. 5A). This was observed in all the current recordings of the laser-pulse photolysis measurements. Consequently, simultaneous fitting of both the rising and falling phases by two first-order rate equations yielded a k_{obs} value that was identical ($\pm 5\%$ error range) to the k_{obs} value obtained in the single exponential fit using Equation 3. Thus, k_{obs} was treated as an elementary rate process, using Equation 4, without the complication of the desensitization reaction.

Unlike ours, earlier mechanisms proposed for the channel opening of various glutamate receptors, including GluR1, all involved the desensitization reaction, and such reaction was assumed to occur once glutamate was bound (33, 35, 41). The omission of desensitization in our kinetic analysis of channel opening was based on our experimental evidence that the desensitization reaction did not proceed appreciably during the current rise, had the desensitization reaction occurred. This evidence is apparent in Figs. 2B and 5A. The observed first-order rate constant for the channel opening is 3800 s^{-1} (Fig. 5A), whereas the rate of channel desensitization is 120 s^{-1} at the same glutamate concentration, *i.e.* 160 μM (Fig. 2B). Therefore, when the current increased to 95%, where the first-order rate constant was estimated for channel opening, the desensitization reaction proceeded to only $\sim 7\%$. This estimate is plausible because it is based on a virtually synchronized activation

of all channels on the cell surface triggered by the laser-pulse photolysis of caged glutamate. We therefore conclude that the channel-opening rate process can be measured effectively as a rate process that is kinetically distinct and separable from the slower desensitization process, which becomes appreciable only on a longer time scale.

The comparison of the rate of glutamate-induced channel opening with the rate of channel desensitization, as described above, further demonstrates that the rate of channel opening for GluR1Q_{flip} far exceeds the rate of desensitization. This should be especially the case at high concentrations of glutamate. Physiologically, the synaptic concentration of glutamate can be as high as 1 mM (42, 43). However, when its concentration is very low, glutamate might desensitize AMPA receptors without ever opening the channel, as previously suggested (20, 30, 42, 44). In our experiments, we were not able to determine whether there were receptors that never opened the channel because (a) these receptors were pre-desensitized through closed states, and/or (b) they were trapped in the ligand-bound closed states following the binding of glutamate. All these receptor states would be electrically "silent." As in any other electrophysiological recording methods, these electrically silent states are not observable (at least not directly). Thus, it was implicit that these receptor states were not included in the minimal mechanism in Fig. 3B.

The activation of the glutamate channel as a kinetic process separate from desensitization was proposed (33, 35) and demonstrated explicitly in several early studies. For example, binding of cyclothiazide to glutamate receptors has been shown to prevent desensitization (45). A single leucine-to-tyrosine substitution (L497Y in GluR1Q_{flip} or L507Y in GluR3) also abolishes desensitization for the corresponding homomeric channels (46). By measuring the rate of GluR2 channel closure after ligand removal (k_{off}) versus the rate of receptor desensitization (k_{des}), the $k_{\text{off}}/k_{\text{des}}$ ratio was 15 for glutamate, compared with 2.2 for quisqualate, another agonist (47). Therefore, the high ratio indicates that the GluR2Q channel, once opened after glutamate binding, preferentially returns to the closed states without entering the desensitization state (47). Here we have demonstrated that, using the laser-pulse photolysis technique, the rate of channel opening can be indeed measured uniquely and prior to channel desensitization.

DISCUSSION

The kinetic process of GluR1Q_{flip} receptor activation to form the transmembrane ion channel is thought to proceed rapidly after the binding of the natural neurotransmitter glutamate. However, little is known about the kinetic mechanism of channel opening. Some critical kinetic information was obtained previously by fitting the slower deactivation/desensitization rate constants. In this study, we applied the laser-pulse photolysis technique with caged glutamate, which provided ~ 60 - μs time resolution. This technique enabled us to measure directly the kinetic constants that govern the transition between the doubly liganded, closed state and the open state.

Channel-opening (k_{op}) and Channel-closing (k_{cl}) Rate Constants—The channel-opening rate constant ($k_{\text{op}} = 29,000 \text{ s}^{-1}$) defines the time scale by which the GluR1Q_{flip} channel opens after the binding of glutamate. It therefore reflects the rate of the conformational change from the doubly liganded, closed form of the receptor to the open channel form. Armstrong and Gouaux (48) and Armstrong *et al.* (49) suggested that the opening of the channel is triggered by the closure of receptor domains or lobes 1 and 2 after the binding of agonist. The "trapping" of agonists such as glutamate by domain closure causes a conformational strain in the extracellular portion of the receptor. Such strain is translated into the gate, presum-

ably in the transmembrane region, thereby opening the channel (48, 50). By this notion, k_{op} likely represents the rate of this domain closure induced by the binding of glutamate. Furthermore, the magnitude of k_{op} indicates that the $t_{1/2}$ of channel opening is 24 μ s. This value is consistent with the microsecond time scale by which the amino acid residues in the ligand-binding pockets can undergo motions, as observed by NMR spectroscopy (51).

The channel-closing rate constant ($k_{cl} = 2100 \text{ s}^{-1}$) is a measure of how fast an open channel returns to the doubly liganded, closed state (Fig. 3B). Thus, it reflects the lifetime of the open channel for the GluR1Q_{flipp} receptor ($k_{cl} = 1/\tau$, where τ is the lifetime expressed as a time constant). The lifetime of the GluR1 channel has been determined using single channel recording (6). The distribution of the open times was described by two time constants of $\sim 0.3 \text{ ms}$ (73%) and 2 ms (27%) (6). The major component has an equivalent rate constant of $\sim 3000 \text{ s}^{-1}$, which is slightly higher than the k_{cl} of 2100 s^{-1} obtained in this study. One possible reason for the disparity in the rate constant is that our value reflects the rate constant for the ensemble rate process originating from the macroscopic receptor response, rather than individual channel events observed at the single channel level. Nevertheless, the two values may be roughly comparable, reflecting in general a short duration of the open channel for the majority of the receptors.

The channel-opening probability (P_{op}) reflects the probability that a channel will open once it is bound with ligand(s) (38). Based on the experimentally determined k_{op} and k_{cl} values, P_{op} for the GluR1Q_{flipp} channel was estimated to be 0.93 ± 0.10 , given by the ratio $k_{op}/(k_{op} + k_{cl})$ (52). This value is comparable with those previously reported (ranging from 0.8 to 0.9) by non-stationary variance analysis of glutamate-induced macroscopic currents (6, 17, 19). Quantitatively, the P_{op} of 0.93 indicates that the rate of the forward reaction (*i.e.* the reaction of channel opening) is ~ 14 times faster than the rate of the backward reaction (*i.e.* the reaction of channel closing). Thus, the presumed conformational change from the doubly liganded, closed channel form to the open channel form is relatively favorable. A high value of P_{op} , like the one obtained here, further implies that the open channel form of the receptor is relatively stable because $k_{cl} \ll k_{op}$.

Time Course of Channel Opening—The time course of the opening of a channel describes the duration of the open channel for the ensemble rate process and takes into account how fast the channel opens, defined by k_{op} , and how long the channel remains open (*i.e.* the lifetime of the channel), defined by k_{cl} . The time course of channel opening is influenced by the synaptic concentration of ligand because the rate of channel opening is ligand-dependent (see Equation 4). With the k_{cl} and k_{op} values known, the time course for the opening of the GluR1Q_{flipp} channel at any given concentration of glutamate can be established quantitatively using Equation 4 (Fig. 6). To represent the time course, we used the rise time of the current response, defined by an increase in receptor current of 20–80% in response to glutamate. As shown in Fig. 6, the rise time became shorter with increasing concentrations of ligand. When the ligand concentration reached 5 mM, the rise time became virtually invariant. Under this condition, the shortest rise time was calculated to be $\sim 35 \mu$ s. This value sets the lower limit for the duration of the open channel.

Several attempts (all of which used fast solution exchange techniques) have been made previously to estimate the shortest current rise time. These values range from 180 to $>400 \mu$ s, reported as a 10–90% rise time (17, 19). These rise times are at least 3-fold longer than the value obtained in this study (35 μ s). In a recent report by Grosskreutz *et al.* (53), a piezoelectrically

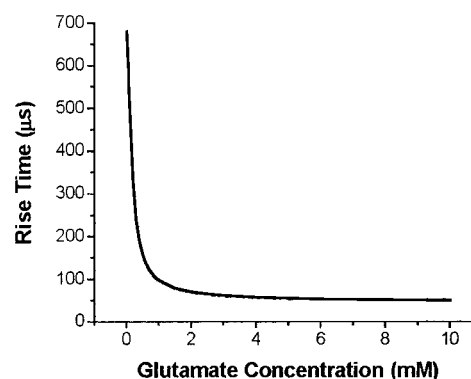


FIG. 6. Rise time for the opening of the GluR1Q_{flipp} channel as a function of glutamate concentration. The rise time is defined as the time it takes for the receptor current response to rise from the 20% level to the 80% level (Fig. 5A) and is obtained by converting a k_{obs} value by Equation 4 using the experimentally determined k_{op} and k_{cl} values.

driven solution exchange technique was used to measure the activation kinetics for human GluR1Q_{flipp}, for which a minimal solution exchange time of $\sim 50 \mu$ s was claimed. However, at the saturating concentration of glutamate, a time constant of 120 μ s was obtained by directly fitting the rising phase of the current. In comparison, we found that the time constant for the channel-opening process under the saturation condition was 32 μ s (*i.e.* $1/(k_{op} + k_{cl})$). Our value is more than three times shorter than the value reported by Grosskreutz *et al.* (53). The comparison, as such, should be valid because those authors further reported that the human AMPA receptors have kinetic properties that are similar to those of the rodent AMPA receptors (53), like the one used in our study. Conceivably, the longer rise time observed in all previous measurements for the same channel could be attributed to a slower solution exchange time or the time resolution, which limited the measurement of the faster receptor kinetics. Generally, the time resolution of these solution exchange techniques is $\sim 200 \mu$ s (1, 6, 17, 19).

When the glutamate concentration decreases to the extent that ligand binding becomes rate-limiting, the rise time as a function of glutamate concentration (Fig. 6) will be no longer tenable. When that happens, the k_{obs} value will reflect the rate of ligand binding, the slowest step, rather than channel opening. The rise time may be less sensitive, accordingly, to the change in ligand concentration rather than as predicted by Equation 4. This phenomenon has been observed experimentally in the muscle nicotinic acetylcholine receptor (54). Furthermore, neither the relationship as predicted in Fig. 6 nor the minimal mechanism as presented in Fig. 3B takes into account the possible difference in the properties of the receptors that exhibit different subconductance levels, as observed in single channel recording (6, 19). Rather, the prediction of the rise time (Fig. 6) represents the ensemble kinetic properties of this channel based on the measurement of macroscopic current.

Comparison of the Channel-opening Rate Constants for GluR1Q_{flipp} and Other Receptor Channels—The k_{op} of $29,000 \text{ s}^{-1}$ for the GluR1Q_{flipp} homomeric receptor channel suggests that this is a fast activating channel compared with other ligand-gated cation-conducting channels. For instance, the muscle-type nicotinic acetylcholine receptor has a k_{op} of 9400 s^{-1} (38), and the GluR6Q kainate receptor channel has a k_{op} of $11,000 \text{ s}^{-1}$ (55). The k_{cl} of 2100 s^{-1} for the GluR1Q_{flipp} homomeric channel suggests that it also closes more rapidly than most channels. For instance, the channel-closing rate constant for both the muscle-type nicotinic acetylcholine receptor (38) and the GluR6Q kainate receptor (55) is nearly 4-fold smaller than the channel-closing rate constant for GluR1. Compared with native heteromeric AMPA receptors in hippocampal neu-

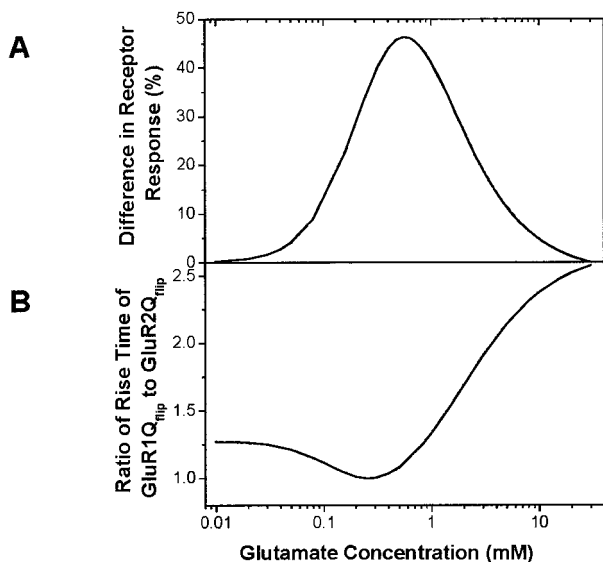


FIG. 7. Comparison of the channel-opening properties of GluR1Q_{flip} and GluR2Q_{flip}. *A*, difference between the dose-response relationships of GluR1Q_{flip} and GluR2Q_{flip}. In both cases, the relative whole-cell response was set to 100%. Therefore, the difference shown represents a maximum of 100%. The K_1 value used for GluR2Q_{flip} was 1.27 mM (56). *B*, ratio of the rise time of GluR1Q_{flip} (Fig. 6) to that of GluR2Q_{flip} (56). Note that the time course of channel opening does not include the contribution from desensitization because the desensitization that eventually leads to the closure of the channel does not contribute appreciably during the rise time.

rons (31), the k_{cl} and k_{op} for GluR1Q_{flip} are ~3- and 2-fold higher, respectively.

It is especially useful to compare the channel-opening rate constants for GluR1Q_{flip} and GluR2Q_{flip} (56) because both are AMPA receptor subunits, and both share considerable sequence homology, including identical RNA splicing status (*i.e.* flip variant). Yet, the magnitude of k_{op} for GluR1Q_{flip} is nearly 3-fold smaller, suggesting that GluR1Q_{flip} opens its channel in response to the binding of the same neurotransmitter, *i.e.* glutamate, three times slower than GluR2Q_{flip}. Conversely, both channels close roughly on the same time scale based on the k_{cl} values for GluR1Q_{flip} and GluR2Q_{flip} of 2100 and 2600 s⁻¹, respectively (56).

The comparison of the channel-opening rate constants for these two closely related AMPA receptor subunits suggests a unique pattern of neuronal integration if it is assumed that both GluR1 and GluR2 co-localize at the same postsynapse and can be activated simultaneously in response to the same chemical signal, *i.e.* glutamate. In fact, it is known that GluR1 and GluR2 are the predominant subunits in the composition of AMPA receptors in the CA1 region of the hippocampus (57). Furthermore, individual AMPA receptor subunits such as GluR1 may function independently (17). To highlight the implications of neuronal integration, Fig. 7 (*A* and *B*) shows the difference of the receptor response as a function of glutamate concentration and the ratio of the rise time between the two receptor types. The difference between the receptor responses to glutamate is a result of a >2-fold difference in the K_1 value (or roughly the EC₅₀ value). At a glutamate concentration of 0.6 mM and below, a higher fraction of the GluR1Q_{flip} receptor channel could open compared with the GluR2Q_{flip} channel. When the glutamate concentration was lowered (see the left-hand side of Fig. 7*B*), the rise time became increasingly monophasic due to the opening of the GluR1Q_{flip} channel. If these results are indicative of how the GluR1Q_{flip} and GluR2Q_{flip} receptors function at the same postsynapse, then at lower glutamate concentrations, it is expected that the inte-

grated neuronal signal will be slow and mostly GluR1Q_{flip}-like. However, as the glutamate concentration increases, a biphasic rate process will appear in the overall rise, with the fast component contributed by the GluR2Q_{flip} channel opening.

What is the origin of this large disparity in the k_{op} value for these two closely related receptor subunits? The answer is presently unknown. Armstrong and Gouaux (48) proposed that the closure of the two extracellular domains or lobes that comprise the glutamate-binding site induces channel opening. Furthermore, the degree of lobe closure can be induced by full agonists such as glutamate and AMPA, an intermediate degree induced by partial agonist, and the smallest degree induced by antagonists (48, 58). Therefore, assuming that k_{op} is linked to the dynamic movement of the lobe closure, the disparity in k_{op} between the two receptor channels could be due to the difference in the degree of glutamate-induced bilobe closure in these two receptors. Then, by analogy, the bilobe closure induced by binding of glutamate to GluR2Q_{flip} is more complete than that induced by binding of glutamate to GluR1Q_{flip}. This implies that some structural differences exist in the glutamate-binding pocket between the two receptors because the ligand that binds and opens the two channels in this case is the same. The structural difference may arise from several possible sources such as a difference in lobe 1, to which glutamate binds first, or lobe 2, whose closure is translated into the dynamic movement of the receptor channel (48). Evidently, to test this hypothesis, more study is needed.

Characterization of the Channel-opening Kinetics by Macroscopic Receptor Current—The laser-pulse photolysis technique enabled us to measure the GluR1Q_{flip} channel-opening kinetics based on the glutamate-induced macroscopic current. Photolytic release of free glutamate has a time resolution of ~60 μs. Such high resolution is required to resolve the kinetic process of channel opening from the ensuing rapid desensitization reaction. Piezoelectric perfusion devices, which have been considered the most rapid, direct ligand application method, have time resolutions in the range of 200–400 μs for solution exchange (1, 6, 17, 19). The laser-pulse photolysis technique therefore offers a better time resolution. This technique is particularly useful for determining the channel-opening kinetic constants for both kainate and AMPA receptors because these receptors have been more difficult to study using the single channel recording technique with glutamate compared with the muscle nicotinic acetylcholine receptor, which has been classically characterized by single channel recording (59–62). Specifically, a much briefer opening duration (*i.e.* a faster channel-closing rate) of a kainate or an AMPA channel compared with the muscle nicotinic acetylcholine receptor is often observed. Moreover, the brief opening duration of such a channel makes it even more difficult to analyze the “flickering” in open channel bursts to investigate the mechanism of inhibition (63, 64).

Since the first demonstration of its use in the kinetic investigation of the channel-opening mechanism for the muscle-type nicotinic acetylcholine receptor (38), the laser-pulse photolysis technique has been applied to several other receptor types (31, 32, 65), including the GluR6Q kainate receptor (55) and the GluR2Q_{flip} AMPA receptor (56). It has further enabled kinetic investigations of the mechanism of drug-receptor interactions in the microsecond-to-millisecond time domain where the receptors were in their functional forms before receptor desensitization (66–69). It is now possible to explore, with a time resolution of ~60 μs, the structural and functional relationships of receptor subunits, the role of an individual subunit in heteromeric receptor complexes, and the mechanism by which this homomeric receptor channel is regulated.

Acknowledgment—We thank Weimin Pei for cloning the gene to the pcDNA3.1 vector.

REFERENCES

- Dingledine, R., Borges, K., Bowie, D., and Traynelis, S. F. (1999) *Pharmacol. Rev.* **51**, 7–61
- Hollmann, M., and Heinemann, S. (1994) *Annu. Rev. Neurosci.* **17**, 31–108
- Petralia, R. S., Esteban, J. A., Wang, Y. X., Partridge, J. G., Zhao, H. M., Wenthold, R. J., and Malinow, R. (1999) *Nat. Neurosci.* **2**, 31–36
- Liao, D., Zhang, X., O'Brien, R., Ehlers, M. D., and Haganir, R. L. (1999) *Nat. Neurosci.* **2**, 37–43
- Takahashi, T., Svoboda, K., and Malinow, R. (2003) *Science* **299**, 1585–1588
- Derkach, V., Barria, A., and Soderling, T. R. (1999) *Proc. Natl. Acad. Sci. U. S. A.* **96**, 3269–3274
- Reisel, D., Bannerman, D. M., Schmitt, W. B., Deacon, R. M., Flint, J., Borhardt, T., Seeburg, P. H., and Rawlins, J. N. (2002) *Nat. Neurosci.* **5**, 868–873
- Bliss, T. V., and Collingridge, G. L. (1993) *Nature* **361**, 31–39
- Lee, H. K., Takamiya, K., Han, J. S., Man, H., Kim, C. H., Rumbaugh, G., Yu, S., Ding, L., He, C., Petralia, R. S., Wenthold, R. J., Gallagher, M., and Haganir, R. L. (2003) *Cell* **112**, 631–643
- Inglis, F. M., Crockett, R., Korada, S., Abraham, W. C., Hollmann, M., and Kalb, R. G. (2002) *J. Neurosci.* **22**, 8042–8051
- Yu, Z., Cheng, G., Wen, X., Wu, G. D., Lee, W. T., and Pleasure, D. (2002) *Neurobiol. Dis.* **11**, 199–213
- Fitzgerald, L. W., Ortiz, J., Hamedani, A. G., and Nestler, E. J. (1996) *J. Neurosci.* **16**, 274–282
- Sutton, M. A., Schmidt, E. F., Choi, K. H., Schad, C. A., Whisler, K., Simmons, D., Karanian, D. A., Monteggia, L. M., Neve, R. L., and Self, D. W. (2003) *Nature* **421**, 70–75
- Carlezon, W. A., Jr., Todtenkopf, M. S., McPhie, D. L., Pimentel, P., Pliakas, A. M., Stellar, J. R., and Trzciniska, M. (2001) *Neuropsychopharmacology* **25**, 234–241
- Mosbacher, J., Schoepfer, R., Monyer, H., Burnashev, N., Seeburg, P. H., and Ruppersberg, J. P. (1994) *Science* **266**, 1059–1062
- Partin, K. M., Fleck, M. W., and Mayer, M. L. (1996) *J. Neurosci.* **16**, 6634–6647
- Robert, A., Irizarry, S. N., Hughes, T. E., and Howe, J. R. (2001) *J. Neurosci.* **21**, 5574–5586
- Banke, T. G., Greenwood, J. R., Christensen, J. K., Liljefors, T., Traynelis, S. F., Schousboe, A., and Pickering, D. S. (2001) *J. Neurosci.* **21**, 3052–3062
- Banke, T. G., Bowie, D., Lee, H., Haganir, R. L., Schousboe, A., and Traynelis, S. F. (2000) *J. Neurosci.* **20**, 89–102
- Raman, I. M., and Trussell, L. O. (1992) *Neuron* **9**, 173–186
- Fleck, M. W., Bähring, R., Patneau, D. K., and Mayer, M. L. (1996) *J. Neurophysiol.* **75**, 2322–2333
- Wieboldt, R., Gee, K. R., Niu, L., Ramesh, D., Carpenter, B. K., and Hess, G. P. (1994) *Proc. Natl. Acad. Sci. U. S. A.* **91**, 8752–8756
- Chen, C., and Okayama, H. (1987) *Mol. Cell. Biol.* **7**, 2745–2752
- Hess, G. P., and Grewer, C. (1998) *Methods Enzymol.* **291**, 443–473
- Niu, L., Grewer, C., and Hess, G. P. (1996) *Techniques in Protein Chemistry*, Vol. VII, pp. 139–149, Academic Press, Inc., New York
- Udgaonkar, J. B., and Hess, G. P. (1987) *Proc. Natl. Acad. Sci. U. S. A.* **84**, 8758–8762
- Tong, G., and Jahr, C. E. (1994) *J. Neurophysiol.* **72**, 754–761
- Katz, B., and Thesleff, S. (1957) *J. Physiol. (Lond.)* **138**, 63–80
- Jonas, P., Major, G., and Sakmann, B. (1993) *J. Physiol. (Lond.)* **472**, 615–663
- Patneau, D. K., and Mayer, M. L. (1991) *Neuron* **6**, 785–798
- Li, H., Nowak, L. M., Gee, K. R., and Hess, G. P. (2002) *Biochemistry* **41**, 4753–4759
- Jayaraman, V. (1998) *Biochemistry* **37**, 16735–16740
- Heckmann, M., Bufler, J., Franke, C., and Dudel, J. (1996) *Biophys. J.* **71**, 1743–1750
- Clements, J. D., Feltz, A., Sahara, Y., and Westbrook, G. L. (1998) *J. Neurosci.* **18**, 119–127
- Raman, I. M., and Trussell, L. O. (1995) *Biophys. J.* **68**, 137–146
- Wahl, P., Anker, C., Traynelis, S. F., Egebjerg, J., Rasmussen, J. S., Krosgaard-Larsen, P., and Madsen, U. (1998) *Mol. Pharmacol.* **53**, 590–596
- Udgaonkar, J. B., and Hess, G. P. (1986) *J. Membr. Biol.* **93**, 93–109
- Matsubara, N., Billington, A. P., and Hess, G. P. (1992) *Biochemistry* **31**, 5507–5514
- Abele, R., Keinänen, K., and Madden, D. R. (2000) *J. Biol. Chem.* **275**, 21355–21363
- Connors, K. A. (1990) *Chemical Kinetics: The Study of Reaction Rates in Solution*, pp. 245–253, VCH Publishers, Inc., New York
- Koike, M., Tsukada, S., Tsuzuki, K., Kijima, H., and Ozawa, S. (2000) *J. Neurosci.* **20**, 2166–2174
- Colquhoun, D., Jonas, P., and Sakmann, B. (1992) *J. Physiol. (Lond.)* **458**, 261–287
- Clements, J. D., Lester, R. A., Tong, G., Jahr, C. E., and Westbrook, G. L. (1992) *Science* **258**, 1498–1501
- Trussell, L. O., and Fischbach, G. D. (1989) *Neuron* **3**, 209–218
- Patneau, D. K., Vyklicky, L., Jr., and Mayer, M. L. (1993) *J. Neurosci.* **13**, 3496–3509
- Stern-Bach, Y., Russo, S., Neuman, M., and Rosenmund, C. (1998) *Neuron* **21**, 907–918
- Jin, R., Horning, M., Mayer, M. L., and Gouaux, E. (2002) *Biochemistry* **41**, 15635–15643
- Armstrong, N., and Gouaux, E. (2000) *Neuron* **28**, 165–181
- Armstrong, N., Mayer, M., and Gouaux, E. (2003) *Proc. Natl. Acad. Sci. U. S. A.* **100**, 5736–5741
- Sun, Y., Olson, R., Horning, M., Armstrong, N., Mayer, M., and Gouaux, E. (2002) *Nature* **417**, 245–253
- McFeeters, R. L., and Oswald, R. E. (2002) *Biochemistry* **41**, 10472–10481
- Traynelis, S. F., and Wahl, P. (1997) *J. Physiol. (Lond.)* **503**, 513–531
- Grosskreutz, J., Zoerner, A., Schlesinger, F., Krampfl, K., Dengler, R., and Bufler, J. (2003) *Eur. J. Neurosci.* **17**, 1173–1178
- Franke, C., Hatt, H., Parnas, H., and Dudel, J. (1991) *Biophys. J.* **60**, 1008–1016
- Li, G., Oswald, R. E., and Niu, L. (2003) *Biochemistry* **42**, 12367–12375
- Li, G., Pei, W. M., and Niu, L. (2003) *Biochemistry* **42**, 12358–12366
- Petralia, R. S., and Wenthold, R. J. (1992) *J. Comp. Neurol.* **318**, 329–354
- Armstrong, N., Sun, Y., Chen, G. Q., and Gouaux, E. (1998) *Nature* **395**, 913–917
- Neher, E., and Sakmann, B. (1976) *Nature* **260**, 799–802
- Colquhoun, D., and Sakmann, B. (1985) *J. Physiol. (Lond.)* **369**, 501–557
- Auerbach, A., and Sachs, F. (1984) *Biophys. J.* **45**, 187–198
- Sine, S. M., and Steinbach, J. H. (1986) *J. Physiol. (Lond.)* **373**, 129–162
- Neher, E., and Steinbach, J. H. (1978) *J. Physiol. (Lond.)* **277**, 153–176
- Neher, E. (1983) *J. Physiol. (Lond.)* **339**, 663–678
- Jayaraman, V., Thiran, S., and Hess, G. P. (1999) *Biochemistry* **38**, 11372–11378
- Niu, L., and Hess, G. P. (1993) *Biochemistry* **32**, 3831–3835
- Niu, L., Abood, L. G., and Hess, G. P. (1995) *Proc. Natl. Acad. Sci. U. S. A.* **92**, 12008–12012
- Grewer, C., and Hess, G. P. (1999) *Biochemistry* **38**, 7837–7846
- Jayaraman, V., Usherwood, P. N., and Hess, G. P. (1999) *Biochemistry* **38**, 11406–11414

Receptor Occupancy and Channel-opening Kinetics

A STUDY OF *GLUR1 L497Y* AMPA RECEPTOR*[§]

Received for publication, December 26, 2006, and in revised form, May 14, 2007 Published, JBC Papers in Press, June 1, 2007, DOI 10.1074/jbc.M611821200

Weimin Pei, Mark Ritz, Michael McCarthy, Zhen Huang¹, and Li Niu²

From the Department of Chemistry and Center for Neuroscience Research, University at Albany, State University of New York, New York 12222

AMPA glutamate ion channels are tetrameric receptors in which activation to form the open channel depends on the binding of possibly multiple glutamate molecules. However, it is unclear whether AMPA receptors bound with a different number of glutamate molecules (*i.e.* one being the minimal and four being the maximal number of glutamate molecules) open the channels with different kinetic constants. Using a laser pulse photolysis technique that provides microsecond time resolution, we investigated the channel-opening kinetic mechanism of a nondesensitizing AMPA receptor, *i.e.* GluR1Q_{flip} L497Y or a leucine-to-tyrosine substitution mutant, in the entire range of glutamate concentrations to ensure receptor saturation. We found that the minimal number of glutamate molecules required to bind to the receptor and to open the channel is two (or $n = 2$), and that the entire channel-opening kinetics can be adequately described by just one channel-opening rate constant, k_{op} , which correlates to $n = 2$. This result suggests that higher receptor occupancy ($n = 3$ and 4) does not give rise to different k_{op} values or, at least, not appreciably if the k_{op} values are different. Furthermore, compared with the wild-type receptor (Li, G., and Niu, L. (2004) *J. Biol. Chem.* 279, 3990–3997), the channel-opening and channel-closing rate constants of the mutant are 1.5- and 13-fold smaller, respectively. Thus, the major effect of this mutation is to decrease the channel-closing rate constant by stabilizing the open channel conformation.

The α -amino-3-hydroxy-5-methyl-4-isoxazole-propionic acid (AMPA)³ glutamate receptors are ligand-gated ion channels that are activated by binding of neurotransmitter glutamate (1, 2). An AMPA receptor is a tetrameric assembly with each subunit containing a glutamate binding site. The receptor can adopt multiple conductance levels, especially at high receptor occupancy, as observed in the single-channel records of

wild-type and mutant recombinant receptors (3, 4) as well as native AMPA receptors (5). However, it remains unclear whether receptor occupancy plays a significant role in determining the kinetic constants for an ensemble rate process of channel opening as a function of glutamate concentration. The ensemble rate process is manifested in a whole-cell current response to the binding of glutamate *in vitro* and best represents the glutamatergic synaptic activity *in vivo*, such as excitatory postsynaptic current. Therefore, determining the number of glutamate molecules bound to a receptor or the percentage of the receptor occupancy pertinent to the rate of the channel opening is a basic question to be answered for understanding the function of AMPA receptors.

To address this question, we investigated the channel-opening kinetics for a GluR1 AMPA receptor channel carrying a substitution of leucine (L) to tyrosine (Y) or L497Y. The discovery of this point mutation by Stern-Bach *et al.* (3) was a significant event in understanding the structure and function relationship of AMPA receptors in that (*a*) phenomenologically, the single leucine-to-tyrosine substitution renders the homomeric receptor channels virtually non-desensitizing (3), and (*b*) the phenotypic effect of this mutation is conserved at equivalent positions in all AMPA receptor subunits, *i.e.* GluR1–4 (6–8). Furthermore, this mutation is thought to have no effect on either the main conductance level or the channel opening probability (3, 7, 9). From a crystallographic study, Sun *et al.* (6) revealed that this mutation resides in the receptor dimer interface of a tetrameric assembly and suggested that the rearrangement of the dimer interface is linked to receptor desensitization (6). Accordingly, the lack of desensitization for the mutant is ascribable to this mutation that prevents the dimer interface movement. In the present study, we expressed GluR1Q_{flip} L497Y mutant in HEK-293 cells and measured the channel-opening rate using a laser pulse photolysis technique and a photolabile precursor of glutamate or caged glutamate (γ -O-(α -carboxy-2-nitrobenzyl)glutamate). Photolysis of the caged glutamate liberates free glutamate with a $t_{1/2}$ of $\sim 30 \mu\text{s}$ (10). Using this technique we previously determined the rate constants of the channel opening for the wild-type GluR1Q_{flip} receptor (11). Therefore, comparison of the rate constants of the mutant with the wild-type receptor may reveal the effect of this mutation on the channel-opening process.

What were the advantages in choosing this mutant for this study? First, because the mutant receptor was non-desensitizing, we could determine the concentration of photolytically released glutamate for kinetic analysis by directly calibrating the peak current amplitude observed in the laser pulse photol-

* This work was supported in part by Grant W81XWH-04-1-0106 from the U. S. Department of Defense and by grants from the ALS Association and the Muscular Dystrophy Association. The costs of publication of this article were defrayed in part by the payment of page charges. This article must therefore be hereby marked "advertisement" in accordance with 18 U.S.C. Section 1734 solely to indicate this fact.

[§] The on-line version of this article (available at <http://www.jbc.org>) contains supplemental Fig. 1.

¹ Supported by a postdoctoral fellowship from the Muscular Dystrophy Association.

² To whom correspondence should be addressed. Tel.: 518-591-8819; Fax: 518-442-3462; E-mail: lniu@albany.edu.

³ The abbreviations used are: AMPA, α -amino-3-hydroxy-5-methyl-4-isoxazolepropionic acid; caged glutamate, γ -O-(α -carboxy-2-nitrobenzyl)glutamate; HEK-293 cells, human embryonic kidney cells.

Receptor Occupancy and Channel-opening Kinetics

ysis with the peak current amplitude observed in solution flow measurement with known glutamate concentrations. This direct calibration would not be possible in studying the wild-type receptor because of its rapid desensitization. Second, because the mutant channel had a higher affinity to glutamate or a lowered EC_{50} value (9, 12), we were able to measure the observed channel-opening rate in the entire range of glutamate concentrations and thus determine the putative effect of different receptor occupancy on the channel-opening rate constant. Again, this was not possible in the study of the wild-type receptor (11).

EXPERIMENTAL PROCEDURES

Cell Culture—The cDNA encoding the GluR1Q_{flip} L497Y mutant receptor was kindly provided by Dr. Mark Fleck. The homomeric GluR1Q_{flip} L497Y mutant was expressed in HEK-293 cells by transient transfection as described (11), except that Lipofectamine (Invitrogen) was used. The weight ratio of the plasmid of GluR1Q_{flip} L497Y to that of green fluorescent protein was 10:1, and 3–5 μ g of GluR1Q_{flip} L497Y cDNA was used in transfection. Green fluorescent protein was used as a transfection marker for recording. The cells were maintained in Dulbecco's modified Eagle's medium at 37 °C and 5% CO₂. The cells were used for recording from 48 h after transfection.

Whole-cell Recording and Laser Pulse Photolysis—The whole-cell recordings and the laser pulse photolysis measurements were at –60 mV and 22 °C, and the procedures were described previously (11). Briefly, the electrode had a resistance of ~3 megohms when filled with electrode solution, which contained (in mM) 110 CsF, 30 CsCl, 4 NaCl, 0.5 CaCl₂, 5 EGTA, and 10 HEPES (pH 7.4 adjusted by CsOH). The external solution contained (in mM) 150 NaCl, 3 KCl, 1 CaCl₂, 1 MgCl₂, 10 HEPES (pH 7.4). A U-tube device (11) was used to apply glutamate to a cell, and the resulting rise time of the glutamate-induced whole-cell current response (10–90%) observed was ~2 ms. The current traces were sampled at 5–50 kHz frequency and filtered at 2–20 kHz by an 8-pole Bessel filter. The data were acquired using pCLAMP 8 (Axon Instruments). In the laser pulse photolysis measurements, the caged glutamate (Invitrogen) was photolyzed using a 355 nm laser pulse from a Minilite II pulsed Q-switched Nd:YAG laser (Continuum). To determine the concentration of photolytically released glutamate, at least two free glutamate solutions with known concentrations were applied to a cell to calibrate the current amplitudes from the same cell before and after a laser photolysis. The current amplitudes obtained from known glutamate concentrations were compared with the amplitude evoked by photolytically released glutamate (11, 13, 14).

Data Analysis—Based on the kinetic mechanism of channel opening (Fig. 1), the observed rate constant, k_{obs} , of the whole-cell current rise in response to glutamate is given by Equation 1.

$$k_{obs} = k_{cl} + k_{op} \left(\frac{L}{L + K_1} \right)^n \quad (\text{Eq. 1})$$

All other terms are defined in the Fig. 1 legend. In deriving Equation 1, the rate of ligand binding was assumed to be fast relative to the rate of channel opening. This assumption was



FIGURE 1. A general mechanism of channel opening for AMPA receptors. Here, *A* represents the active, unliganded form of the receptor, *L* the ligand or glutamate, *AL_n* the closed channel state with *n* ligand molecules bound, and \overline{AL}_n the open channel state. The number of glutamate molecules to bind to the receptor and to open its channel, *n*, can be from 1 to 4, assuming that a receptor is a tetrameric complex and each subunit has one glutamate binding site. It is further assumed that a ligand does not dissociate from the open channel state. The k_{op} and k_{cl} are the channel-opening and channel-closing rate constants, respectively. For simplicity and without contrary evidence, it is assumed that glutamate binds with equal affinity or K_1 , the intrinsic equilibrium dissociation constant, at all binding steps.

supported by the consistent observation of a single first-order rate, in Equation 2, for the whole-cell current rise in the entire range of glutamate concentrations (see Fig. 2 results),

$$I_t = I_A(1 - e^{-k_{obs}t}) \quad (\text{Eq. 2})$$

where I_t and I_A represent the whole-cell current amplitude at time *t* and the maximum current amplitude. Using Equation 2, the k_{obs} at a given glutamate concentration was calculated. A set of k_{cl} and k_{op} as well as K_1 corresponding to a particular number of ligand(s) bound, *i.e.* $n = 1-4$ (see Fig. 1 legend), was obtained using Equation 1. As an independent measure, K_1 was estimated from the dose-response relationship, shown in Equation 3, based on the general mechanism of channel opening (Fig. 1).

$$I_A = I_M R_M \frac{L^n}{L^n + \Phi(L + K_1)^n} \quad (\text{Eq. 3})$$

In Equation 3, I_M is the current per mole of receptor, R_M the number of moles of receptors on the cell surface, and Φ^{-1} the channel-opening equilibrium constant. Unless otherwise noted, at least triplicate sets of data from three cells were collected in all measurements. Linear regression and nonlinear fitting were performed using Origin 7 software (Origin Lab, Northampton, MA).

Using the Φ value analysis based on the transition state theory (15–17), we calculated the change of the free energy of the transition state for the mutant and the wild-type receptor using Equation 4.

$$\Phi = \frac{\Delta\Delta G_{TS-C}}{\Delta\Delta G_{O-C}} \quad (\text{Eq. 4})$$

Here Φ is the ratio of change of free energy of activation for opening of the channel, $\Delta\Delta G_{TS-C}$, to the equilibrium free energy of channel opening, $\Delta\Delta G_{O-C}$. The $\Delta\Delta G$ values were calculated by Equation 5 using k_{op} and k_{cl} values for both the mutant and the wild-type receptors.

$$\Delta G = RT \ln \left(\frac{\kappa T}{hk} \right) \quad (\text{Eq. 5})$$

In Equation 5, R is the gas constant, T the temperature in Kelvin scale, h the Planck's constant, κ the Boltzmann constant, and k the rate constant.

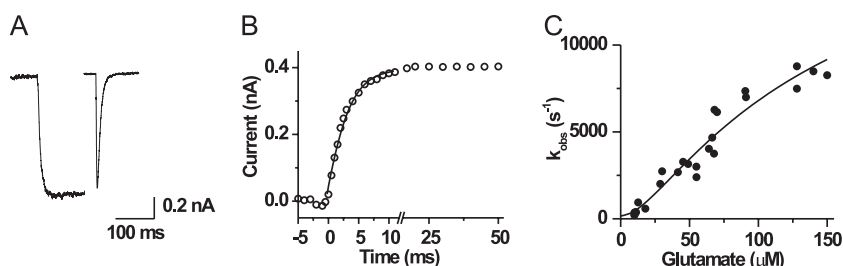


FIGURE 2. Laser pulse photolysis measurements of the channel-opening kinetics for GluR1Q_{flip} L497Y mutant. *A*, representative whole-cell current response via the GluR1Q_{flip} L497Y channel (left) to application of 200 μM glutamate as compared with the GluR1Q_{flip} wild-type channel response (right). *B*, representative whole-cell current from the opening of the GluR1Q_{flip} L497Y channel initiated by the laser pulse photolysis of caged glutamate. The laser was triggered at time zero. The fitting of the current rise to obtain the k_{obs} using Equation 2 is shown as a solid line. For clarity of the presentation, the number of data points was reduced in the rising phase of the current. The k_{obs} of 658 s⁻¹ obtained from this trace corresponded to a glutamate concentration of 12 μM. The direction of the current response was plotted opposite to that recorded. *C*, nonlinear regression of k_{obs} versus glutamate concentration relationship (solid line) according to Equation 1. The best nonlinear fitted parameters are: $k_{\text{op}} = (2.0 \pm 1.0) \times 10^4 \text{ s}^{-1}$, $k_{\text{cl}} = 160 \pm 91 \text{ s}^{-1}$, $K_1 = 70 \pm 41 \text{ μM}$, and $n = 2.0 \pm 2.1$ (R^2 value of 0.951). If the n value was fixed at 2 and the K_1 value at 70 μM, obtained from the rate measurement and the dose-response curve (see Fig. 3), the linear fit of the k_{obs} versus glutamate concentration using Equation 1 yielded $k_{\text{op}} = (1.9 \pm 0.1) \times 10^4 \text{ s}^{-1}$ and $k_{\text{cl}} = 140 \pm 160 \text{ s}^{-1}$.

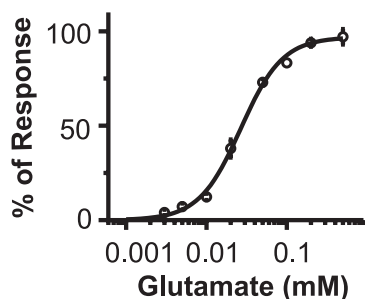


FIGURE 3. Dose-response relationship of the GluR1Q_{flip} L497Y mutant receptor. The glutamate-induced whole-cell current from different cells was normalized to the current obtained at 50 μM glutamate, and the current amplitude at 0.5 mM was set to be 100%. Each point represents the mean of the relative amplitude of glutamate response obtained from at least three cells. The best fit parameters using Equation 3 (solid line) are: $I_M R_M$ of 110 ± 8 , K_1 of $68 \pm 38 \text{ μM}$, Φ of 0.096 ± 0.067 , and n of 2.0 ± 0.19 with an R^2 value of 0.994.

TABLE 1
Summary of nonlinear fit

k_{cl}^a	n	k_{op}	K_1	R^2
s ⁻¹		s ⁻¹	μM	
50	2.1 ± 0.1	(2.0 ± 0.1) × 10 ⁴	67.4 ± 3.1	0.960
100	2.1 ± 0.1	(1.9 ± 0.1) × 10 ⁴	68.6 ± 3.2	0.956
150	2.2 ± 0.1	(2.0 ± 0.1) × 10 ⁴	69.4 ± 3.4	0.948
200	2.1 ± 0.1	(2.1 ± 0.1) × 10 ⁴	72.8 ± 3.5	0.933
250	2.2 ± 0.1	(2.1 ± 0.1) × 10 ⁴	69.6 ± 3.4	0.918

^a k_{cl} is fixed.

RESULTS

Channel-opening Kinetics for GluR1Q_{flip} L497Y—A glutamate-induced, whole-cell current from the mutant channel exhibited a sustained current response, whereas the wild-type response showed rapid desensitization (Fig. 2A). This is consistent with the original observation by Stern-Bach *et al.* (3). Only when the glutamate concentration approached saturation did the mutant channel desensitize. For instance, at 0.5 mM glutamate, a saturating concentration for the mutant, the desensitization rate constant was 25 s⁻¹. In contrast, the wild-

type GluR1Q_{flip} homomeric receptor channel desensitizes rapidly, with a maximum rate constant of ~300 s⁻¹ (11, 18, 19).

Using the laser pulse photolysis technique, we measured the channel-opening rate for the GluR1Q_{flip} L497Y channel as a function of glutamate concentration. Photolysis of the caged glutamate led to a whole-cell current rise (Fig. 2B). At least 95% of the whole-cell current rise followed a single exponential rate process (*i.e.* Equation 2 under “Experimental Procedures”) and remained so in the entire range of glutamate concentrations, *i.e.* from 10 to 140 μM. The range of the glutamate concentration corresponded to 14–92% of the fraction of the open channel (see the dose-response curve in Fig. 3). That a monoexponential rate for channel opening was persistently observed throughout the entire range of glutamate concentrations supported the assumption that the rate of ligand binding was fast relative to the rate of channel

opening. Therefore, the current rise reflected the channel opening (Fig. 2B). Based on this assumption and a general mechanism of channel opening (in Fig. 1), Equation 1 was derived in which k_{obs} represented the rate of transition from the AL_n state to its corresponding open state, \overline{AL}_n . Note that Equation 1 represents a general formulation of the rate law, taking into account all of the possible number of ligands that can bind to and open the channel, namely $n = 1-4$. The permitted values of n in integer are based on the notion that an AMPA receptor is a tetramer and each subunit contains one ligand binding site (7, 20).

The Minimal Number of Glutamate Molecules Bound to the Receptor to Open the Channel Is Two—The rate of channel opening as a function of glutamate concentration (Fig. 2C) was analyzed as described below. First, using Equation 1, we found that the best nonlinear fit returned the value of n , the number of glutamate molecules bound to open the channel, to be close to 2 (see the legend for Fig. 2C). Along with this analysis, we obtained a set of k_{cl} , k_{op} , and K_1 as the best fit values for the channel-opening kinetic mechanism.

From the same analysis, a k_{cl} value of $160 \pm 91 \text{ s}^{-1}$ was obtained (Fig. 2 legend). This value agreed with the rate constant we observed at the lower end of the glutamate concentration range, namely $k_{\text{obs}} \approx 200 \text{ s}^{-1}$ (Fig. 2C). This was expected because, when $L \ll K_1$, Equation 1 was reduced to $k_{\text{obs}} \approx k_{\text{cl}}$ suggesting that (*a*) the rate constant at a low glutamate concentration would reflect k_{cl} , and (*b*) the value of k_{cl} was independent of whatever might be the n value. Based on this reasoning, we further examined our regression analysis by fixing k_{cl} (Table 1). In so doing, we reduced one variable, which enabled us to improve the regression analysis. Using various k_{cl} values close to 160 s⁻¹, we found that the fitted values of n continued to be tightly close to 2 (Table 1). These results were consistent with $n = 2$ being the best fit to our data in the entire range of glutamate concentrations.

The analysis described above also yielded a K_1 of $70 \pm 41 \text{ μM}$ (see Fig. 2 legend). To independently verify this value, we deter-

TABLE 2
Summary of nonlinear fit

See supplemental Fig. 1 for the fitting.

n^a	k_{cl} s^{-1}	k_{op} s^{-1}	K_1 μM	R^2
1	-780 ± 455	$(2.5 \pm 0.8) \times 10^4$	238 ± 124	0.937
2	159 ± 343	$(2.0 \pm 0.3) \times 10^4$	71 ± 17	0.939
3	554 ± 320	$(2.0 \pm 0.3) \times 10^4$	48 ± 10	0.929
4	543 ± 310	$(2.0 \pm 0.3) \times 10^4$	33 ± 6.0	0.929

^a The value of n is fixed.

mined the dose-response curve using the amplitude of the whole-cell current (Fig. 3). The regression analysis of the dose-response relationship using Equation 3 yielded the best fit of K_1 to be $68 \pm 38 \mu M$ (Fig. 3 legend), consistent with the value obtained from the rate measurement (Fig. 2C).

We also noted that the value of k_{op} was unchanged even when different k_{cl} values were used in data analysis (Table 1); the same was true for K_1 . We then asked whether k_{op} would change with different n values. The results show that k_{op} remained invariant when n increased (Table 2 and supplemental Fig. 1), presumably with a concomitant increase of glutamate concentration and receptor occupancy (5, 7). Taken together, our results (from Fig. 1C and Tables 1 and 2) suggest that it is sufficient to use k_{op} and k_{cl} at $n = 2$ to represent the channel-opening kinetics of the mutant channel in the entire range of glutamate concentrations. We thus favor an interpretation of $k_{op} = (1.9 \pm 0.1) \times 10^4 s^{-1}$ and $k_{cl} = 140 \pm 160 s^{-1}$ at $n = 2$ as the representative values of the channel-opening and channel-closing rate constants (see Fig. 2 legend). We emphasize that statistical F-criteria could not completely deny other n , although our analysis did yield $n = 2$ as the best fit for the channel-opening kinetics (Table 2). However, $n = 1$ was rejected because a negative k_{cl} value was returned from the data analysis (Table 2 and supplemental Fig. 1).

It should be noted that the data analysis described above did not assume a biased number of glutamate molecule(s) bound to the receptor in order to open its channel. Furthermore, the experimental basis for these conclusions was from the study of the L497Y GluR1 mutant rather than the wild-type receptor, although the major conclusions from the study of the mutant described here and the wild-type receptor we reported earlier (11) are the same.

DISCUSSION

The Channel-opening Rate Is Dominated by the Receptor Bound with Two Glutamate Molecules—Evidence from all of our experiments and data analysis was well corroborated and supported the argument that binding of two or more glutamate molecules per receptor, *i.e.* $n = 2-4$ but not $n = 1$, was all sufficient to open the channel, and k_{op} remained essentially invariant among $n = 2-4$. If receptor complexes bound with more than two glutamate molecules have higher conductance levels, higher conductance levels associated with higher agonist occupancy do not give rise to different channel-opening rate constants as compared with k_{op} at $n = 2$. One possible explanation is that open channel conformations in different receptor occupancy, or $n = 2-4$, are similar. In this case, once the receptor accepts the minimal number of agonist molecules (*i.e.* $n = 2$)

so that a sufficient amount of energy can be harnessed from agonist binding to open the channel, a higher receptor occupancy may simply stabilize the open channel conformation to different extents (21). Alternatively, the receptor complexes with higher occupancy could have k_{op} values different from the value at $n = 2$. However, the fractions of these complexes in the overall receptor population that undergo the channel-opening reaction could not have been significant enough to alter k_{obs} , despite the fact that we did not know at what concentration(s) higher receptor occupancy or higher conductance levels began to contribute to the whole-cell current. Previously, it has been proposed that AMPA receptors with two to four glutamate molecules bound enter desensitization at similar rates and recover from the desensitization with similar rates as well (22).

Even though an AMPA receptor can adopt higher conductance levels observed in single-channel recording when glutamate concentration increases (4, 5, 7), it has been hypothesized that glutamate may not be able to populate higher conductance levels of synaptic AMPA receptors *in vivo* (5). Furthermore, the glutamate concentration in the synaptic cleft is estimated to be no higher than 1 mM for more than a few hundred μs (23, 24). Therefore, it is reasonable that AMPA channels actually function as a receptor complex activated predominantly by the binding of two glutamate molecules. Obviously, it should be noted that the conclusion drawn from our study was based on a homomeric mutant channel rather than heteromeric native AMPA receptors *in vivo*.

The binding of two glutamate molecules per receptor to open the channel is a plausible stoichiometry (11), if an AMPA receptor is considered a dimer of “dimers” (25). As such, binding of one glutamate molecule per dimer or two per dimer of dimers is possible. Interestingly, two subunits acting as a dimer in a tetrameric receptor composition, undergoing a concerted transition between inactive and active states, was also proposed for intracellular cyclic GMP-gated channels (26), where the opening of the channels also depends on the receptor occupancy (26, 27).

The Major Effect of the L497Y Mutation on GluR1 is to Stabilize the Open Channel Conformation—Comparison of the channel-opening kinetic constants of the mutant with those of the wild-type GluR1_{flip} receptor, which we characterized previously (11), shows that the k_{op} and k_{cl} for the mutant at $n = 2$ are ~ 1.5 - and ~ 13 -fold smaller than those for the wild-type receptor, respectively. Thus, the major effect of this point mutation is to decrease the channel-closing rate or to prolong the lifetime of the open channel ($k_{cl} = 1/\tau$, where τ is the lifetime expressed in time constant). As a result, the open channel state is stabilized. To better understand the effect of this mutation on stabilizing the open channel state, we applied the Φ value analysis to infer transition state structures from changes in kinetics on mutation, a procedure used in protein folding, catalysis, and conformational transitions (15–17). The value of Φ indicates the extent to which a mutated residue is involved in the formation of the transition state on a scale of 0 to 1 (*i.e.* 0 and 1 represent that the influence of the side chain is either absent or fully present in the transition state because of that mutation). Using Equation 4, we estimated $\Phi = 0.16$ (Fig. 4). A fractional value of Φ suggests that upon mutation, the site near L497Y was

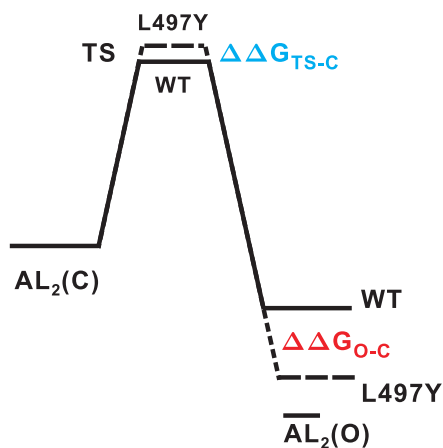


FIGURE 4. The free energy diagram for the transition from the closed channel state (C) to the open channel state (O) for the GluR1Q_{flip} wild type and L497Y mutant. Individual free energy change was calculated by Equation 5 using corresponding rate constants (*i.e.* k_{op} and k_{cl} values), and the diagram was constructed using Equation 4, based on $\Delta\Delta G_{TS-C} = 0.21$ kcal/mol (note that the subscript "TS" stands for transition state) and $\Delta\Delta G_{O-C} = 1.3$ kcal/mol. The Φ value was calculated to be 0.16.

not entirely wild type-like. Instead, the local environment near tyrosine 497 has changed somewhat due to the mutation, as compared with the leucine residue at the same position in the wild-type receptor. This single amino acid substitution further affected the transition state (*i.e.* $\Delta\Delta G_{TS-C} = 0.21$ kcal/mol; see the legend for Fig. 4). Thus, this analysis suggests that the major effect of the L497Y mutation in GluR1 is to stabilize the channel-opening state (by an amount of $\Delta\Delta G = 1.3$ kcal/mol; see Fig. 4). This is consistent with the structural revelation by which the same mutation stabilizes the dimer interface of the S1S2 mutant receptor (6). However, the L497Y mutation further causes a non-native, structural change near the mutation site in the closed channel state, inferred from the non-zero Φ value. This change may be linked to a reduction of the K_1 or EC_{50} value for glutamate in the mutant (9, 11, 28), although how the structural change due to this point mutation affects glutamate binding affinity is not clear.

Implications Based on the Kinetic Constants and Free Energy Diagram—Based on the results of this study, including the free energy diagram (Fig. 4), we predict that a change of the free energy of the open channel state compared with that of the wild-type receptor, the benchmark, affects the stability of the open channel state and thus alters the channel-closing rate constant and vice versa. For instance, the k_{cl} of the L497Y mutant is smaller than that of the wild type, suggesting that this structural modification lowers the energy level of the open channel state by stabilizing it. In contrast, our study of the alternatively spliced variants of GluR3 or GluR3 flip and GluR3 flop shows that the flop isoform has a larger k_{cl} than the flip isoform, presumably reflecting that the flop isoform destabilizes the channel-open state (29). By the same prediction, any mutation or change of structure (whether it is located in the dimer interface, such as the mutation in GluR2, but is equivalent to the L497Y in GluR1 (6), or elsewhere but nevertheless stabilizes the open channel state) would slow the rate of channel closing. If a mutation does not affect the stability of the open channel conformation, that mutation is expected not to affect

the channel-closing rate constant and vice versa. Therefore, the assessment of the effect of a mutation on k_{cl} provides a measure of whether the mutation exerts any structural impact on stability of the open channel conformation.

Relationship between Channel Closing and Desensitization—As compared with the GluR1Q_{flip} wild-type receptor (11), both the channel-closing rate and the desensitization rate of the L497Y mutant are decreased. These results are consistent with the hypothesis that desensitization begins from the closed channel state, as proposed previously (30, 31), but not from the open channel state. Furthermore, the channel-closing rate process kinetically controls the channel desensitization, provided that both reactions occur, such as when $n = 2-4$. By this notion, desensitization begins in parallel to the channel-opening reaction once glutamate is bound but proceeds from the closed channel state and with a slower rate. In fact, in this and all other studies of AMPA receptor channels, we have found that the rate of channel closing is markedly faster than the rate of the channel desensitization (11, 13, 14, 29). The common "species" that links the two reactions is the closed channel state, although it is unclear which closed channel form(s) enters the desensitization pathway. As shown in this study, a higher concentration of the open channel state for the L497Y mutant, which correlates to a longer lifetime or more stable open channel conformation, actually "inhibited" a speedy return of the channel to the closed channel state and thus a speedy entry to the desensitization state (see Fig. 1A) compared with the wild type. If the desensitization could have started from the open channel state, a higher concentration of the open channel state would have resulted in a faster desensitization rate than the wild type. Indeed, this hypothesis is consistent with previous observations that desensitization is agonist-promoted (32) and that the L497Y mutant channels can desensitize, albeit very slowly and only at very high concentrations of ligand, as observed by us and others (6, 9). Moreover, that the rate of the channel closing controls the rate of desensitization is supported by our results with the GluR3 receptors in that the k_{cl} of the GluR3 flop variant is ~ 4 -fold larger than that of the flip isoform, and the flop isoform desensitizes ~ 4 -fold faster than the flip isoform (29). On the other hand, for the flip and flop isoforms of GluR1, the k_{cl} of both isoforms is identical, within experimental errors, and as expected, the channel desensitization rate constant is also no different.⁴ Further studies are obviously needed to test our predictions and hypothesis.

It should be noted that the underlying assumption in our hypothesis described above is that the control of the desensitization through the channel-closing rate step requires the channel to open in the first place. An exception to our hypothesis is that at a glutamate concentration much lower than required for activation, so that a channel cannot open, desensitization can still occur (22, 33, 34). In this case, the kinetic control mechanism using the rapid channel-opening reaction to regulate the concentration of the ligand-bound, closed channel state through which the channel desensitizes simply does not exist.

⁴ W. Pei and L. Niu, unpublished data.

Receptor Occupancy and Channel-opening Kinetics

Acknowledgments—We thank Drs. Mark Fleck for the GluR1 L497Y construct, Igor Zurbenko for helpful discussions, and Richard Givens for allowing us to test his version of the caged glutamate.

REFERENCES

1. Chen, P. E., and Wyllie, D. J. (2006) *Br. J. Pharmacol.* **147**, 839–853
2. Dingledine, R., Borges, K., Bowie, D., and Traynelis, S. F. (1999) *Pharmacol. Rev.* **51**, 7–61
3. Stern-Bach, Y., Russo, S., Neuman, M., and Rosenmund, C. (1998) *Neuron* **21**, 907–918
4. Jin, R., Banke, T. G., Mayer, M. L., Traynelis, S. F., and Gouaux, E. (2003) *Nat. Neurosci.* **6**, 803–810
5. Smith, T. C., and Howe, J. R. (2000) *Nat. Neurosci.* **3**, 992–997
6. Sun, Y., Olson, R., Horning, M., Armstrong, N., Mayer, M., and Gouaux, E. (2002) *Nature* **417**, 245–253
7. Rosenmund, C., Stern-Bach, Y., and Stevens, C. F. (1998) *Science* **280**, 1596–1599
8. Plested, A. J., Wildman, S. S., Lieb, W. R., and Franks, N. P. (2004) *Anesthesiology* **100**, 347–358
9. Robert, A., Irizarry, S. N., Hughes, T. E., and Howe, J. R. (2001) *J. Neurosci.* **21**, 5574–5586
10. Wieboldt, R., Gee, K. R., Niu, L., Ramesh, D., Carpenter, B. K., and Hess, G. P. (1994) *Proc. Natl. Acad. Sci. U. S. A.* **91**, 8752–8756
11. Li, G., and Niu, L. (2004) *J. Biol. Chem.* **279**, 3990–3997
12. Jin, R., Horning, M., Mayer, M. L., and Gouaux, E. (2002) *Biochemistry* **41**, 15635–15643
13. Li, G., Pei, W., and Niu, L. (2003) *Biochemistry* **42**, 12358–12366
14. Li, G., Sheng, Z., Huang, Z., and Niu, L. (2005) *Biochemistry* **44**, 5835–5841
15. Pandit, A. D., Krantz, B. A., Dothager, R. S., and Sosnick, T. R. (2007) *Methods Mol. Biol.* **350**, 83–104
16. Fersht, A. R. (2004) *Proc. Natl. Acad. Sci. U. S. A.* **101**, 17327–17328
17. Fersht, A. R., and Sato, S. (2004) *Proc. Natl. Acad. Sci. U. S. A.* **101**, 7976–7981
18. Mosbacher, J., Schoepfer, R., Monyer, H., Burnashev, N., Seeburg, P. H., and Ruppertsberg, J. P. (1994) *Science* **266**, 1059–1062
19. Derkach, V., Barria, A., and Soderling, T. R. (1999) *Proc. Natl. Acad. Sci. U. S. A.* **96**, 3269–3274
20. Armstrong, N., and Gouaux, E. (2000) *Neuron* **28**, 165–181
21. Colquhoun, D. (1998) *Br. J. Pharmacol.* **125**, 924–947
22. Robert, A., and Howe, J. R. (2003) *J. Neurosci.* **23**, 847–858
23. Clements, J. D., Feltz, A., Sahara, Y., and Westbrook, G. L. (1998) *J. Neurosci.* **18**, 119–127
24. Diamond, J. S., and Jahr, C. E. (1997) *J. Neurosci.* **17**, 4672–4687
25. Mayer, M. L., and Armstrong, N. (2004) *Annu. Rev. Physiol.* **66**, 161–181
26. Liu, D. T., Tibbs, G. R., Paoletti, P., and Siegelbaum, S. A. (1998) *Neuron* **21**, 235–248
27. Ruiz, M. L., and Karpen, J. W. (1997) *Nature* **389**, 389–392
28. Partin, K. M., Fleck, M. W., and Mayer, M. L. (1996) *J. Neurosci.* **16**, 6634–6647
29. Pei, W., Huang, Z., and Niu, L. (2007) *Biochemistry* **46**, 2027–2036
30. Clements, J. D., Lester, R. A., Tong, G., Jahr, C. E., and Westbrook, G. L. (1992) *Science* **258**, 1498–1501
31. Raman, I. M., and Trussell, L. O. (1995) *Biophys. J.* **68**, 137–146
32. Tang, C. M., Dichter, M., and Morad, M. (1989) *Science* **243**, 1474–1477
33. Trussell, L. O., Thio, L. L., Zorumski, C. F., and Fischbach, G. D. (1988) *Proc. Natl. Acad. Sci. U. S. A.* **85**, 4562–4566
34. Colquhoun, D., Jonas, P., and Sakmann, B. (1992) *J. Physiol. (Lond.)* **458**, 261–287

Kinetic Mechanism of Channel Opening of the GluRD_{flip} AMPA Receptor[†]

Gang Li, Zhenyu Sheng, Zhen Huang, and Li Niu*

Department of Chemistry, Center of Biochemistry and Biophysics, and Center for Neuroscience Research, State University of New York, Albany, New York 12222

Received December 9, 2004; Revised Manuscript Received February 7, 2005

ABSTRACT: AMPA-type ionotropic glutamate receptors mediate the majority of fast excitatory neurotransmission in the mammalian central nervous system and are essential for brain functions, such as memory and learning. Dysfunction of these receptors has been implicated in a variety of neurological diseases. Using a laser-pulse photolysis technique, we investigated the channel opening mechanism for GluRD_{flip} or GluR4_{flip} (i.e., the flip isoform of GluRD), an AMPA receptor subunit. The minimal kinetic mechanism for channel opening is consistent with binding of two glutamate molecules per receptor complex. The GluRD_{flip} channel opens with a rate constant of $(6.83 \pm 0.74) \times 10^4 \text{ s}^{-1}$ and closes with a rate constant of $(3.35 \pm 0.17) \times 10^3 \text{ s}^{-1}$. On the basis of these rate constants, the channel opening probability is calculated to be 0.95 ± 0.12 . Furthermore, the shortest rise time (20–80% of the receptor current response to glutamate) is predicted to be 20 μs , which is ~ 8 times shorter than the previous estimate. These findings suggest that the kinetic property of GluRD_{flip} is similar to that of GluR2Q_{flip}, another fast-activating AMPA receptor subunit.

Individual AMPA¹ receptor subunits, i.e., GluR1–4 or GluRA–D, can form homomeric functional channels in heterologous expression systems, such as human embryonic kidney (HEK) 293 cells (*1*). Recent studies using individual receptor subunits have yielded much information about the structure and function of this important subtype of ionotropic glutamate receptor (*1, 2*). However, the kinetic mechanism of receptor channel opening is not well understood. In the microsecond time region, an AMPA receptor can open its channel upon binding of glutamate to transmit a nerve impulse, whereas within 1–10 ms, the same receptor desensitizes to an inactive, channel-closed form with glutamate still bound (*3*). The mechanism of desensitization is relatively well understood (*3–7*), largely because the time resolution of various fast solution exchange techniques is generally in the range of a few hundred microseconds, and is therefore sufficient for the assessment of the desensitization reaction. However, the solution exchange techniques have not been successful in measuring the channel opening process of AMPA receptors, which occurs in the microsecond time domain.

Determining the kinetic mechanism of receptor channel opening is useful. Knowing the rate constant will enable a more quantitative prediction of the time course of the open channel as a function of neurotransmitter concentration, which determines the change in transmembrane voltage and

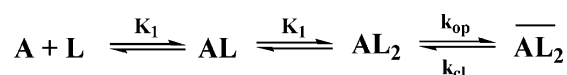


FIGURE 1: Minimal kinetic mechanism of channel opening. A represents the active, unliganded form of the receptor and L the ligand (glutamate). AL and AL₂ represent the ligand-bound closed channel forms, and $\overline{AL_2}$ represents the open channel form of the receptor. For simplicity, it is assumed that glutamate binds at both steps with equal affinity, designated by K_1 . Other symbols are defined in the text, along with a more full discussion of the mechanism. This mechanism is used to describe the channel opening kinetics for GluRD_{flip}.

in turn controls synaptic neurotransmission. Furthermore, knowing the kinetic mechanism will provide clues for mechanism-based design of therapeutic compounds for treating neurological diseases involving AMPA receptors, such as post-stroke cellular lesion and amyotrophic lateral sclerosis (*8*). In addition, a systematic characterization of all AMPA receptors will be necessary to determine their functional differences. Knowledge of these functional traits will aid both the understanding of the properties of possible subunit combinations forming heteromeric AMPA receptors and the development of subunit-specific inhibitors and drugs.

We recently characterized the kinetic mechanism of glutamate-induced channel opening (Figure 1) for GluR1 (*9*) and GluR2 (*10*), two of the four homomeric AMPA receptor channels. In the study presented here, we investigated the channel opening mechanism for the GluRD or GluR4 receptor. As in our previous studies, we used a laser-pulse photolysis technique, which permits free glutamate to be photolytically liberated from caged glutamate [i.e., γ -O-(α -carboxy-2-nitrobenzyl)glutamate] with a $t_{1/2}$ of $\sim 30 \mu\text{s}$ (*11*). The laser-pulse photolysis approach enabled us to measure the channel opening rate process, which occurs on the microsecond time scale, without the complication of channel desensitization.

[†] This work was supported by grants from the American Heart Association (0130513T), the Amyotrophic Lateral Sclerosis Association, the Muscular Dystrophy Association, and the Department of Defense (W81XWH-04-1-0106) (to L.N.). G.L. was supported by a postdoctoral fellowship from the Muscular Dystrophy Association.

* To whom correspondence should be addressed. Telephone: (518) 591-8819. Fax: (518) 442-3462. E-mail: lniu@albany.edu.

¹ Abbreviations: AMPA, α -amino-3-hydroxy-5-methyl-4-isoxazole-propionic acid; GFP, green fluorescence protein; HEK-293 cells, human embryonic kidney (293) cells.

MATERIALS AND METHODS

Expression of cDNA and Cell Culture. The plasmid encoding the full-length GluRD_{flip} subunit was propagated in *Escherichia coli* DH5 α cells and purified using a QIAGEN (Valencia, CA) kit. GluRD_{flip} was transiently expressed in HEK-293S cells using a procedure previously described (9). Unless otherwise noted, HEK-293S cells were also cotransfected with a plasmid encoding green fluorescence protein (GFP), and the green fluorescent cells were selected for patch clamping 48 h after transfection. The weight ratio of the plasmid for GFP to that for GluRD_{flip} used in transfection was 1:10, and the amount of GluRD_{flip} plasmid was \sim 3–5 μ g/35 mm Petri dish.

Whole-Cell Current Recording. The procedure for whole-cell current recording was previously described (9). Briefly, the electrode had a resistance of \sim 3 M Ω after it was filled with the electrode solution: 110 mM CsF, 30 mM CsCl, 4 mM NaCl, 0.5 mM CaCl₂, 5 mM EGTA, and 10 mM HEPES (pH 7.4 adjusted by CsOH). The external bath solution contained 150 mM NaCl, 3 mM KCl, 1 mM CaCl₂, 1 mM MgCl₂, and 10 mM HEPES (pH 7.4). All chemicals were from commercial sources. A U-tube flow device was used to apply glutamate to a cell, and the resulting rise time of the glutamate-induced whole-cell current response (10–90%) observed was \sim 2 ms (9). The current traces were sampled at 5–50 kHz and filtered at 2–20 kHz by an eight-pole Bessel filter. The data were acquired using pCLAMP 8 (Axon Instruments, Union City, CA). All whole-cell recordings were at -60 mV and 22 $^{\circ}$ C.

Dose-Response Relationship. On the basis of the channel opening mechanism in Figure 1, eq 1 was derived to describe the dose-response relationship

$$I_A = I_M R_M \frac{L^2}{L^2 + \Phi(L + K_1)^2} \quad (1)$$

where I_A represents the current amplitude, L the molar concentration of the ligand, I_M the current per mole of receptor, and R_M the number of moles of receptor in the cell. Φ^{-1} is the channel opening equilibrium constant, and K_1 is the intrinsic dissociation constant for the ligand. For simplicity and with no experimental evidence to the contrary, the affinity of glutamate, K_1 , was assumed to be the same for both the first and second glutamate binding steps (see further discussion of this mechanism in the text). All current traces were corrected for desensitization by a method previously described (12). The corrected current amplitude was used to construct the dose-response relationship.

Laser-Pulse Photolysis. The procedure for the laser-pulse photolysis experiment has been described previously (9). In brief, caged glutamate (Molecular Probes, Eugene, OR) was dissolved in the external bath buffer and applied to a cell in the whole-cell mode using the U-tube flow device. A laser pulse from the third harmonic output (355 nm, 8 ns pulse length) of a Minilite II pulsed Q-switched Nd:YAG laser (Continuum, Santa Clara, CA) was used to photolyze the caged glutamate after it was equilibrated with a cell for 250 ms. The laser energy was adjusted to 200–800 μ J at the end face of the fiber through which the laser light was introduced to that cell. To determine the concentration of photolytically released glutamate, at least two free glutamate

solutions with known concentrations were used to calibrate the current amplitudes from the same cell. The current amplitudes obtained from known glutamate concentrations were compared with the amplitude evoked by glutamate photolytically released from a photolysis measurement, with reference to the dose-response relationship.

Using the laser-pulse photolysis technique, we measured the rate constant for the rising phase of the whole-cell current generated by glutamate that was released photolytically. The rising phase was found to be monoexponential at all concentrations of glutamate, and the observed first-order rate constant (k_{obs}) was thus determined using eq 2. This observation was consistent with the assumption that the channel opening rate was slow compared with the ligand binding rate (see further discussion in the text). Accordingly, the channel opening (k_{op}) and channel closing (k_{cl}) rate constants were calculated by fitting the k_{obs} versus the ligand concentration according to eq 3, together with the use of K_1 obtained from the dose-response relationship described above. In eq 2, I_t represents the current amplitude at time t and I_A the maximum current amplitude.

$$I_t = I_A (1 - e^{-k_{\text{obs}} t}) \quad (2)$$

$$k_{\text{obs}} = k_{\text{cl}} + k_{\text{op}} \left(\frac{L}{L + K_1} \right)^2 \quad (3)$$

Channel Opening Probability (P_{op}). The P_{op} or the probability by which the GluRD_{flip} channel opens once it is bound with ligand(s) was calculated using eq 4 (9) in which k_{op} and k_{cl} were determined experimentally.

$$P_{\text{op}} = \frac{k_{\text{op}}}{k_{\text{op}} + k_{\text{cl}}} \quad (4)$$

Time Course of the Opening of the GluRD_{flip} Channel. The time course of the opening of a receptor channel reflects the observed rate by which the open channel is formed at a given concentration of ligand. The rate at which a channel is open at a given concentration of ligand is characteristic of k_{op} and k_{cl} . Specifically, to represent the time course, we used the rise time of the current response, defined by the increase in receptor current from 20 to 80% (9). The rise time was obtained first by using eq 3 to obtain k_{obs} based on the experimentally determined k_{cl} and k_{op} for GluRD_{flip} as a function of glutamate concentration and then by using eq 2 to obtain the time corresponding to the current rise from 20 to 80%.

Unless noted otherwise, each data point was an average of at least three measurements collected from at least three cells. Origin 7 (Origin Lab, Northampton, MA) was used for both linear and nonlinear regression. Uncertainties are reported as the standard error of the mean.

RESULTS

Dose-Response Relationship and Minimal Kinetic Mechanism of Channel Opening. Glutamate-induced whole-cell current was observed from the HEK-293 cells that expressed GluRD_{flip} (Figure 2A, inset). To demonstrate that the current response was from the opening of the GluRD_{flip} channel, we tested the cells that had current response to glutamate yet found no current response to the external buffer. We had

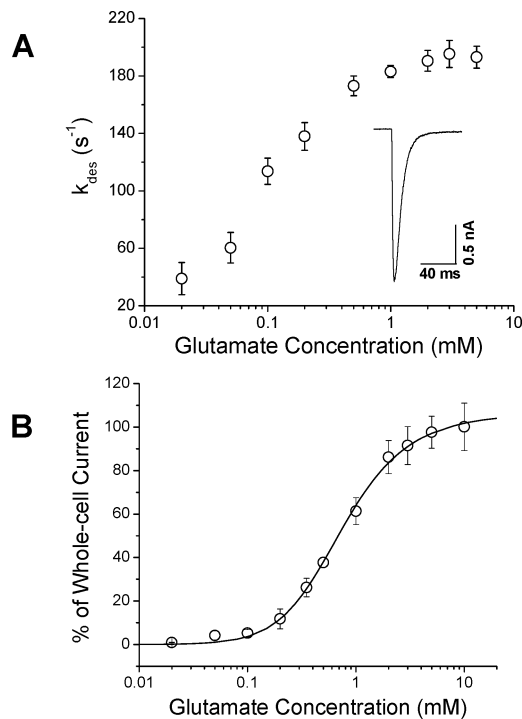


FIGURE 2: (A) Dependence of the desensitization rate constant, k_{des} , of GluRD_{flip} on glutamate concentration. The inset is a representative whole-cell current response of GluRD_{flip} expressed in an HEK-293S cell to 2 mM glutamate, by using flow measurement. The desensitization rate was characterized by a first-order rate constant and is shown with the standard error of the mean. Each data point is an average of at least three measurements from three cells. (B) Dose-response relationship. The whole-cell currents from different cells were normalized to the current obtained at 0.5 mM glutamate, and the current amplitude at 5 mM was set to 100%. Best-fit parameters using eq 1 (—) were as follows: $K_1 = 1.11 \pm 0.40$ mM, $\Phi = 0.24 \pm 0.16$, and $I_M R_M = 131 \pm 20$.

previously observed that both nontransfected cells and transfected cells expressing only GFP, a cell marker, gave no response even at 10 mM glutamate (10), a concentration that evoked a maximum current response for the transfected cells expressing GluRD_{flip} (see the dose-response curve in Figure 2B). Furthermore, coexpression of GFP in the same cell that expressed GluRD_{flip} did not affect the kinetic properties of the receptor as evidenced by the desensitization rate constant being identical to those of cells transfected with only GluRD_{flip} (data not shown). In Figure 2A, the desensitization rate constant is shown as a function of glutamate concentration. A first-order rate law was sufficient to characterize more than 95% of the current response at all concentrations of glutamate, consistent with previous reports (3, 13). The average value of the maximum desensitization rate constant is ~ 190 s⁻¹, which is seen at a glutamate concentration of greater than 3 mM (Figure 2A).

The desensitization rate constant obtained using whole cells in this study is smaller than the value previously reported using outside-out patches at a given glutamate concentration (3). An example can be seen in Figure 2A, in which the desensitization rate constant at 3 mM glutamate was 196 s⁻¹, but was 260 s⁻¹ when outside-out patches were used (3). This phenomenon has been thoroughly investigated for the GluR1Q_{flip} receptor expressed in HEK-293 cells (14, 15), and the largest reported difference is 2.9-fold; i.e., the rate constant obtained from whole cells is 2.9-fold smaller

than the value obtained from outside-out patches (15). The discrepancy in rate constant at an identical glutamate concentration but seemingly different membrane configurations could be attributed to a slower solution exchange rate with a whole cell, because of its geometry (14–16). Alternatively, this discrepancy could arise from a faster desensitization rate constant observed with outside-out patches because of altered kinetic properties of the receptor in such a membrane configuration (14–16). Nevertheless, the mean conductance of the GluRD_{flip} channel observed using whole-cell recording was similar to that using outside-out patches (17). These results indicate that the whole-cell current recording was suitable for studying the GluRD_{flip} channel.

Next, we determined the dose-response relationship for the GluRD_{flip} channel, which describes the dependence of the current amplitude as a function of glutamate concentration. The best fit by eq 1 yielded an intrinsic dissociation constant of glutamate, K_1 , of 1.11 ± 0.40 mM (Figure 2B). The K_1 value is qualitatively comparable with the reported values of EC_{50} (the ligand concentration that corresponds to 50% of the maximum response), which range from 0.5 to 1.8 mM (1, 13).

Characterization of the Channel Opening Kinetics of GluRD_{flip}. Before using the laser-pulse photolysis technique to characterize the channel opening rate constant, we tested the biological properties of caged glutamate with the GluRD_{flip} receptor. We found that the whole-cell current was identical (data not shown) in the absence and presence of 2 mM caged glutamate, the highest concentration of caged glutamate used in this study, suggesting that caged glutamate is biologically inert. This finding is consistent with the conclusion from both the initial report (11) and our recent studies of other AMPA receptor channels using the caged glutamate (9, 10).

Using the laser-pulse photolysis technique and the caged glutamate, we measured the channel opening rate constant for GluRD_{flip}. Figure 3A shows a representative whole-cell response to photolytically released glutamate. The current increased initially as a result of the channel opening and then decreased because of channel desensitization. In analyzing the rising phase of the whole-cell current induced by photolysis, we observed that $\sim 95\%$ of the current rise was adequately ascribed to a single-exponential rate process (see the solid line in Figure 3A). Equation 2 was thus used to calculate the first-order rate constant, k_{obs} , which corresponded to a particular glutamate concentration. From the plot of k_{obs} versus glutamate concentration according to eq 3 (in Figure 3B), a k_{cl} of $(3.35 \pm 0.17) \times 10^3$ s⁻¹ and a k_{op} of $(6.83 \pm 0.74) \times 10^4$ s⁻¹ were thus obtained.

As seen in Figure 3A, the rising phase of the current followed a single-exponential rate process for the entire glutamate concentration range from 80 to 310 μ M (the latter was the highest concentration of glutamate collected in photolysis). This kinetic feature is consistent with the assumption that the rate of channel opening is slow relative to the rate of ligand binding. On the basis of this assumption, the rising phase of the receptor response is expected not only to follow a single-exponential rate process, reflecting the channel opening rate step, but also to remain single-exponential even when the concentration of ligand is varied (9). Accordingly, eq 3 was derived and used for calculating

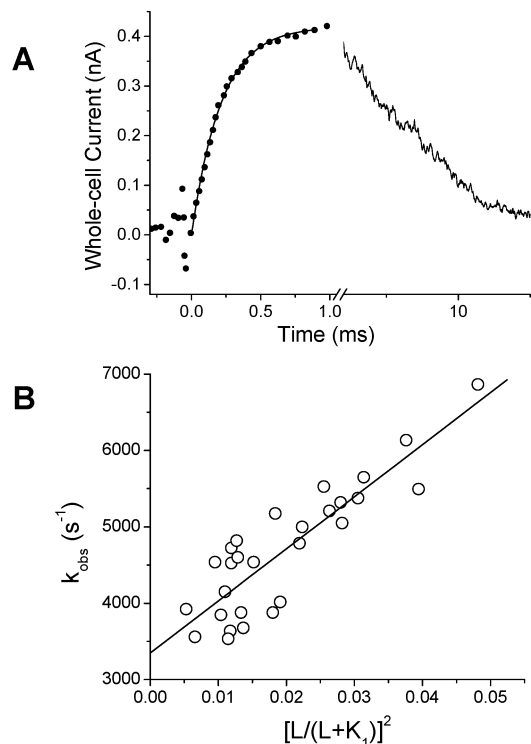


FIGURE 3: Laser-pulse photolysis measurement of the channel opening rate for GluRD_{flip}. **A** representative whole-cell current is shown in panel A for the opening of the GluRD_{flip} channel initiated by the laser-pulse photolysis of caged glutamate at time zero. The fitting of the rising phase by eq 2, shown as the solid line, yielded a k_{obs} of $4800 \pm 250 \text{ s}^{-1}$, corresponding to $190 \mu\text{M}$ photolytically released glutamate. Note that the direction of the current response was plotted opposite to that recorded. For clarity, the number of the data points was reduced for plotting. From the plot of k_{obs} vs glutamate concentration by eq 3 in panel B, k_{cl} and k_{op} were determined to be $(3.35 \pm 0.17) \times 10^3$ and $(6.83 \pm 0.74) \times 10^4 \text{ s}^{-1}$, respectively. Each point represents a k_{obs} obtained at a particular concentration of photolytically released glutamate.

k_{op} and k_{cl} . It should be pointed out that deviation would be observed from this monophasic kinetic feature in the rising phase of the current if the bimolecular ligand binding step were either rate-determining or comparable to the rate of channel opening (9).

Lower Limit of Ligand Concentration for Determining the Channel Opening Rate Constants. As shown in Figure 1, ligand binding is a bimolecular process, and it precedes channel opening. The ligand concentration thus affects the kinetic observation. When the ligand concentration is sufficiently high, it is always valid to assume that the rate of channel opening is slow compared to the rate of ligand binding. Consequently, the rising phase reflects the channel opening, and eq 3 is valid. When the ligand concentration is low enough, however, the ligand binding will become rate-limiting. As a result, eq 3 will no longer be valid. Therefore, we established the following criterion to set the lower limit of ligand concentration to ensure that the channel opening reaction was measurable.

Specifically, the lowest concentration of glutamate which we used for the calculation of k_{op} and k_{cl} by eq 3 (in Figure 3B) was chosen to be $80 \mu\text{M}$. The glutamate concentration of $80 \mu\text{M}$ corresponded to the fraction of the channel in the open form being $\sim 4\%$ (the fraction of the open channel can be determined by eq 1; see Figure 2B). At the 4% fraction of the open channel form, the k_{obs} obtained by the laser-

pulse photolysis technique was found to be comparable to the numerical value of k_{cl} (this is true when $L \ll K_1$, then $k_{\text{obs}} \approx k_{\text{cl}}$; see eq 3). Moreover, the k_{cl} can be compared to the lifetime of the open channel, which may be measured independently using single-channel recording (18–21). Indeed, we found that the k_{cl} value we determined using the laser-pulse photolysis technique was well corroborated with the value obtained from single-channel studies (9, 10, 22). For instance, the k_{cl} of 2600 s^{-1} obtained from the laser-pulse photolysis measurement of the GluR2Q_{flip} AMPA receptor (10) is comparable to the lifetime of the open channel ($\sim 0.32 \text{ ms}$ in time constant or 3100 s^{-1} in rate constant) obtained from single-channel recording (23). We therefore concluded that the ligand concentration that correlates to the 4% fraction of the open channel form is sufficiently high not to limit the rate of ligand binding. Consequently, ligand concentrations that correspond to 4% or more of the fraction of the open channel form can be used to calculate the rate constants of channel opening.

DISCUSSION

In this study, we characterized the kinetic mechanism of glutamate-induced opening of the GluRD_{flip} homomeric channel by using a laser-pulse photolysis technique with a time resolution of $\sim 60 \mu\text{s}$. Our results provide new insights into the function of this subunit.

Kinetic Mechanism of Channel Opening. The opening of the GluRD_{flip} homomeric channel upon glutamate binding is illustrated by the minimal kinetic mechanism in Figure 1, in which k_{op} and k_{cl} as well as K_1 have been determined. The magnitude of k_{op} ($6.83 \times 10^4 \text{ s}^{-1}$) defines how fast the conformation of the doubly liganded, closed form of the receptor changes to the open channel conformation. On the basis of the structural events proposed by Armstrong and Gouaux (24, 25), the k_{op} may be correlated to the rate process of the glutamate-induced bilobe closure seen in the S1S2 extracellular binding domain, which presumably leads to the channel opening. Then, the $t_{1/2}$ of the bilobe closure can be calculated to be $10 \mu\text{s}$ from k_{op} . The magnitude of this value is comparable with the one observed by NMR in a study of the motion of amino acid residues in ligand-binding pockets (26). Conversely, the magnitude of k_{cl} (3400 s^{-1}) defines the rate at which an open channel returns to the doubly liganded closed state. Thus, it represents the lifetime of the open channel or a τ of 0.30 ms (i.e., $\tau = 1/k_{\text{cl}}$).

By the mechanism in Figure 1 and consistent with our data, the opening of the GluRD_{flip} channel requires a minimal binding of two glutamate molecules per receptor complex. This mechanism is general for other AMPA receptors (22, 27–30), including the GluR1Q_{flip} and GluR2Q_{flip} channels we characterized using the same kinetic technique (9, 10). Binding of two glutamate molecules per receptor complex with a tetrameric composition, one for each dimer rather than to each subunit, is a plausible stoichiometry for opening the channel considering that the receptor complex is a dimer-of-dimers assembly (2). The stoichiometry issue was also investigated by analyzing the conductance states at the single-channel level. It was found that both native and recombinant AMPA receptors exhibit multiple conductance levels and the receptor channel dwells on larger conductance levels as the agonist concentration is increased (17, 31). Using single-

channel recording, Rosenmund et al. (32) carried out an elegant study and concluded that binding of two agonist molecules per tetrameric receptor complex is necessary to open the channel. Binding of up to four agonist molecules increases mean single-channel conductance as compared with binding of two agonist molecules.

To determine k_{op} and k_{cl} , the rate of glutamate binding to the receptor was assumed to be fast compared with the rate of channel opening, consistent with the kinetic behavior of the rising phase of the whole-cell current. At present, however, the association rate constant of glutamate with the whole receptor is unknown. Pioneering studies by Madden and co-workers (33) on the kinetics of glutamate binding to the GluRD-derived S1S2 extracellular binding domain provide some clues about how fast glutamate may bind to the whole receptor. The rate constant of association of glutamate with the S1S2 partial receptor was $\sim 10^7$ – 10^8 $M^{-1} s^{-1}$ at 5 °C (33). Because the rate of association of glutamate with wild-type S1S2 was too fast, it was not possible to further separate the microscopic rate constants for step 1, the agonist docking step, from step 2, the subsequent locking process (33). Nevertheless, the association rate constant determined at 5 °C is expected to become even larger at room temperature, assuming that the association rate constant behaves according to the Arrhenius equation (34). The rate of glutamate binding to its site on the S1S2 receptor may be even faster because of a favorable electrostatic interaction between the receptor and glutamate, which steers glutamate to its site when a glutamate molecule approaches by free diffusion (35). Such a favorable electrostatic interaction to steer ligand or substrate binding to its target protein, thus accelerating the basal association rate constant, was observed in other association processes, such as the binding of acetylcholine, a neurotransmitter, to acetylcholinesterase (36).

The Channel Opening Rate Can Be Uniquely Measured Using the Laser-Pulse Photolysis Technique. The use of the laser-pulse photolysis technique made it possible to resolve the channel opening process in the microsecond time domain from the ensuing desensitization reaction in the millisecond time region. The separation of the two rate processes is apparent via examination of the following experimental evidence. As seen in Figure 3A, the k_{obs} for the rising phase is 4800 s^{-1} . However, at the same glutamate concentration, 190 μM , the observed desensitization rate constant is 130 s^{-1} as seen in Figure 2B. Using these rate constants, we can estimate the percentage of desensitization that occurred within the rising phase of the current from which the channel opening rate constant was measured. If glutamate binding had initiated the desensitization at time zero, as it initiated the channel opening, in 0.6 ms the desensitization reaction would have proceeded $\sim 8\%$. However, the channel opening reaction would progress to 95% of completion, the extent to which the k_{obs} was measured in our experiment as shown in Figure 3A. Therefore, the desensitization did not interfere appreciably with the measurement of the channel opening rate of GluRD_{flip}. Furthermore, because the k_{obs} and the time interval for the current rise used for this estimation were based on a virtually synchronized release of free glutamate triggered by the laser-pulse photolysis, this estimate was thus reasonable. Consistent with this conclusion, we found that simultaneous fitting of the current rise and fall yielded a k_{obs} value similar to the value obtained by a single-exponential

Table 1: Channel Opening and Channel Closing Rate Constants for Glutamate Receptors^a

glutamate receptor type	k_{op} (s^{-1})	k_{cl} (s^{-1})	technique	ref
GluR1Q _{flip}	2.9×10^4	2.1×10^3	laser-pulse photolysis	9
	—	$\sim 3.3 \times 10^3$	single-channel recording ^b	14
GluR2Q _{flip}	8.0×10^4	2.6×10^3	laser-pulse photolysis	10
	—	3.1×10^3	single-channel recording ^b	23
GluR4 _{flip}	6.8×10^4	3.4×10^3	laser-pulse photolysis	this work
	4.0×10^4	8.0×10^3	fitting	13
	—	5.9×10^3	single-channel recording	17
GluR6Q	1.1×10^4	4.2×10^2	laser-pulse photolysis	22
	1.0×10^4	4.4×10^2	fitting	41
	1.0×10^4	—	flow measurement	40

^a In all data cited, glutamate is the agonist. ^b The lifetime refers to the major component.

fit of the current rise using eq 2. Together, these results show that the channel opening rate constant can be measured from the rising phase of the macroscopic receptor current, and this measurement is free from the complication of the desensitization reaction. Hence, the formulation of the kinetic scheme for channel opening in Figure 1 does not involve the reaction pathway(s) for channel desensitization and in turn gives rise to a simple kinetic equation, i.e., eq 3, for determining k_{op} and k_{cl} .

Earlier studies suggested that when the glutamate concentration is very low, glutamate binding may desensitize AMPA receptors without ever opening the channel (4, 37–39). Furthermore, binding of even one glutamate molecule per receptor complex is thought to be sufficient to desensitize the channel (13). Under any of these circumstances, the receptor would be pre-desensitized through the closed states and would be thus electrically silent. Such a process would not be detected, at least not directly, by any electrophysiological methods. These receptor states were thus not included in the minimal mechanism in Figure 1.

Comparison of the k_{op} and k_{cl} Values with Reported Ones for GluRD_{flip} and Other Glutamate Receptors. Previously, k_{op} has not been experimentally determined for GluRD_{flip}. On the basis of a limited number of kinetic parameters, Robert and Howe (13) estimated the rate constant of k_{op} to be $4.0 \times 10^4 s^{-1}$ (assuming a 2β value or the channel opening is initiated after binding of two glutamate molecules from their fitting). That estimated value is 1.7-fold smaller than our value of k_{op} ($6.83 \times 10^4 s^{-1}$). However, the lifetime of the open channel for GluRD_{flip} was determined using single-channel recording (17). A single time constant of 0.17 ms or an equivalent rate constant of $\sim 6000 s^{-1}$ was calculated from the histogram of the open times, which was compiled from all conductance states (17). The mean lifetime of the open channel in this case was close to the resolution of openings in the single-channel recording, which was 0.15–0.2 ms (17). Although not large, we do not yet know the reason for this 1.7-fold discrepancy in the value of k_{cl} between our study (i.e., $k_{cl} = 3400 s^{-1}$) and the single-channel approach. Qualitatively, however, the two values do suggest that the channel closing process is rapid.

Comparison of the k_{op} and k_{cl} values of GluRD_{flip} with those of other AMPA and kainate homomeric channels (Table 1) shows two notable features. First, all AMPA channels have rate constants for channel opening and closing larger than the corresponding values of the GluR6Q kainate

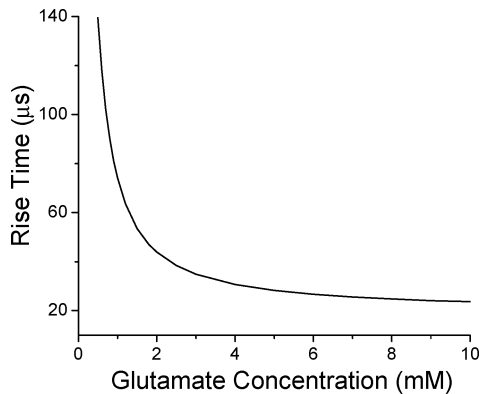


FIGURE 4: Dependence of the rise time on glutamate concentration for the opening of the GluRD_{flip} channel. The rise time is defined as the time for the receptor current to rise from the 20% to the 80% level. The rise time is calculated as described in Materials and Methods. The fastest rise time is predicted to be $\sim 20 \mu\text{s}$.

receptor (22, 40, 41). Second, comparison of GluRD_{flip} with other AMPA receptor subunits (Table 1) shows that the kinetic properties of GluRD_{flip} are more similar to those of GluR2Q_{flip} than to those of GluR1Q_{flip}. However, the GluRD_{flip} channel closes slightly faster than does the GluR2Q_{flip} channel, whereas the channel opening rate constant is roughly identical. Interestingly, the intrinsic dissociation constant for glutamate or the K_1 value for GluRD_{flip} (1.1 mM) is also similar to that of GluR2Q_{flip} (1.3 mM) (10), compared with that of GluR1Q_{flip} (0.53 mM) (9).

Channel Opening Probability (P_{op}). On the basis of the experimentally determined k_{op} and k_{cl} values, the P_{op} for the GluRD_{flip} channel was calculated to be 0.95 ± 0.12 by eq 4. This value is comparable to those previously reported for two other homomeric AMPA receptor channels, all of which are above 0.90 (9, 10). Quantitatively, the P_{op} of 0.95 indicates that the rate of the forward reaction (i.e., the channel opening) is ~ 20 times faster than the rate of the backward reaction (i.e., channel closing). Thus, the presumed conformational change from the doubly liganded, closed channel state to the open channel state is relatively favorable. A large P_{op} value, like the one obtained here, further suggests that the open channel state of the receptor is relatively stable, because $k_{cl} \ll k_{op}$.

Time Course of the Opening of the GluRD_{flip} Channel. The time course of the opening of the GluRD_{flip} channel was determined as described in Materials and Methods. As seen in Figure 4, the rise time can be predicted at any given concentration of glutamate. The rise time decreases with increasing concentrations of ligand and becomes the shortest, $\sim 20 \mu\text{s}$, when glutamate binding is saturated. Thus, $20 \mu\text{s}$ sets the fastest observed time scale for this channel to open. It should be pointed out the contribution of desensitization to the time course of channel opening or to the rise time is negligible and thus not included, for reasons described in the Results.

Solution exchange techniques were previously used to estimate the fastest rise time of the macroscopic current for several AMPA receptor channels (5, 42, 43). In particular, a recent study by Grosskreutz et al. (43) reported a $120 \mu\text{s}$ time constant as the fastest current rise for the opening of AMPA receptor homomeric channels, including GluRD. In contrast, the time constant of the channel-opening process for the saturation condition in this study is $14 \mu\text{s}$ [see eq 3;

when $L \gg K_1$, $\tau = 1/(k_{op} + k_{cl})$]. Thus, the previous estimate by Grosskreutz et al. (43) is 8 times slower than our value. In fact, the time constant measured by Grosskreutz et al. for the channel opening at the ligand saturation condition, $120 \mu\text{s}$, is not much larger than the lifetime of the open channel or the equivalent k_{cl} from either the value reported in this study or the value previously measured by Swanson et al. using single-channel recording (17). The slower channel opening rate or an equivalent longer rise time, estimated by using various solution exchange techniques, may be attributed to a slower solution exchange time of $\sim 200 \mu\text{s}$ in general (1, 13, 14, 42).

ACKNOWLEDGMENT

We thank Weimin Pei in the lab for the initial help with this work and Drs. Peter H. Seeburg for the GluRD_{flip} construct and Vasanthi Jayaraman for providing it. We also thank Drs. Dean Madden, Geoffrey Swanson, and Vasanthi Jayaraman for helpful discussion.

REFERENCES

- Dingledine, R., Borges, K., Bowie, D., and Traynelis, S. F. (1999) The glutamate receptor ion channels, *Pharmacol. Rev.* 51, 7–61.
- Mayer, M. L., and Armstrong, N. (2004) Structure and function of glutamate receptor ion channels, *Annu. Rev. Physiol.* 66, 161–181.
- Mosbacher, J., Schoepfer, R., Monyer, H., Burnashev, N., Seeburg, P. H., and Ruppertsberg, J. P. (1994) A molecular determinant for submillisecond desensitization in glutamate receptors, *Science* 266, 1059–1062.
- Trussell, L. O., and Fischbach, G. D. (1989) Glutamate receptor desensitization and its role in synaptic transmission, *Neuron* 3, 209–218.
- Robert, A., Irizarry, S. N., Hughes, T. E., and Howe, J. R. (2001) Subunit interactions and AMPA receptor desensitization, *J. Neurosci.* 21, 5574–5586.
- Vyklicky, L., Jr., Patneau, D. K., and Mayer, M. L. (1991) Modulation of excitatory synaptic transmission by drugs that reduce desensitization at AMPA/kainate receptors, *Neuron* 7, 971–984.
- Sun, Y., Olson, R., Horning, M., Armstrong, N., Mayer, M., and Gouaux, E. (2002) Mechanism of glutamate receptor desensitization, *Nature* 417, 245–253.
- Heath, P. R., and Shaw, P. J. (2002) Update on the glutamatergic neurotransmitter system and the role of excitotoxicity in amyotrophic lateral sclerosis, *Muscle Nerve* 26, 438–458.
- Li, G., and Niu, L. (2004) How fast does the GluR1Q_{flip} channel open? *J. Biol. Chem.* 279, 3990–3997.
- Li, G., Pei, W., and Niu, L. (2003) Channel-opening kinetics of GluR2Q_{flip} AMPA receptor: A laser-pulse photolysis study, *Biochemistry* 42, 12358–12366.
- Wieboldt, R., Gee, K. R., Niu, L., Ramesh, D., Carpenter, B. K., and Hess, G. P. (1994) Photolabile precursors of glutamate: Synthesis, photochemical properties, and activation of glutamate receptors on a microsecond time scale, *Proc. Natl. Acad. Sci. U.S.A.* 91, 8752–8756.
- Udgaonkar, J. B., and Hess, G. P. (1987) Chemical kinetic measurements of a mammalian acetylcholine receptor by a fast-reaction technique, *Proc. Natl. Acad. Sci. U.S.A.* 84, 8758–8762.
- Robert, A., and Howe, J. R. (2003) How AMPA receptor desensitization depends on receptor occupancy, *J. Neurosci.* 23, 847–858.
- Derkach, V., Barria, A., and Soderling, T. R. (1999) Ca^{2+} /calmodulin-kinase II enhances channel conductance of α -amino-3-hydroxy-5-methyl-4-isoxazolepropionate type glutamate receptors, *Proc. Natl. Acad. Sci. U.S.A.* 96, 3269–3274.
- Partin, K. M., Fleck, M. W., and Mayer, M. L. (1996) AMPA receptor flip/flop mutants affecting deactivation, desensitization, and modulation by cyclothiazide, aniracetam, and thiocyanate, *J. Neurosci.* 16, 6634–6647.

16. Tong, G., and Jahr, C. E. (1994) Regulation of glycine-insensitive desensitization of the NMDA receptor in outside-out patches, *J. Neurophysiol.* **72**, 754–761.
17. Swanson, G. T., Kamboj, S. K., and Cull-Candy, S. G. (1997) Single-channel properties of recombinant AMPA receptors depend on RNA editing, splice variation, and subunit composition, *J. Neurosci.* **17**, 58–69.
18. Neher, E., and Sakmann, B. (1976) Single-channel currents recorded from membrane of denervated frog muscle fibres, *Nature* **260**, 799–802.
19. Colquhoun, D., and Sakmann, B. (1985) Fast events in single-channel currents activated by acetylcholine and its analogues at the frog muscle end-plate, *J. Physiol.* **369**, 501–557.
20. Auerbach, A., and Sachs, F. (1984) Single-channel currents from acetylcholine receptors in embryonic chick muscle. Kinetic and conductance properties of gaps within bursts, *Biophys. J.* **45**, 187–198.
21. Sine, S. M., and Steinbach, J. H. (1986) Activation of acetylcholine receptors on clonal mammalian BC3H-1 cells by low concentrations of agonist, *J. Physiol.* **373**, 129–162.
22. Li, G., Oswald, R. E., and Niu, L. (2003) Channel-opening kinetics of GluR6 kainate receptor, *Biochemistry* **42**, 12367–12375.
23. Jin, R., Banke, T. G., Mayer, M. L., Traynelis, S. F., and Gouaux, E. (2003) Structural basis for partial agonist action at ionotropic glutamate receptors, *Nat. Neurosci.* **6**, 803–810.
24. Armstrong, N., and Gouaux, E. (2000) Mechanisms for activation and antagonism of an AMPA-sensitive glutamate receptor: Crystal structures of the GluR2 ligand binding core, *Neuron* **28**, 165–181.
25. Armstrong, N., Mayer, M., and Gouaux, E. (2003) Tuning activation of the AMPA-sensitive GluR2 ion channel by genetic adjustment of agonist-induced conformational changes, *Proc. Natl. Acad. Sci. U.S.A.* **100**, 5736–5741.
26. McFeeters, R. L., and Oswald, R. E. (2002) Structural mobility of the extracellular ligand-binding core of an ionotropic glutamate receptor. Analysis of NMR relaxation dynamics, *Biochemistry* **41**, 10472–10481.
27. Clements, J. D., Feltz, A., Sahara, Y., and Westbrook, G. L. (1998) Activation kinetics of AMPA receptor channels reveal the number of functional agonist binding sites, *J. Neurosci.* **18**, 119–127.
28. Jonas, P., Major, G., and Sakmann, B. (1993) Quantal components of unitary EPSCs at the mossy fibre synapse on CA3 pyramidal cells of rat hippocampus, *J. Physiol.* **472**, 615–663.
29. Jayaraman, V. (1998) Channel-opening mechanism of a kainate-activated glutamate receptor: Kinetic investigations using a laser-pulse photolysis technique, *Biochemistry* **37**, 16735–16740.
30. Li, H., Nowak, L. M., Gee, K. R., and Hess, G. P. (2002) Mechanism of glutamate receptor-channel function in rat hippocampal neurons investigated using the laser-pulse photolysis (LaPP) technique, *Biochemistry* **41**, 4753–4759.
31. Smith, T. C., and Howe, J. R. (2000) Concentration-dependent substate behavior of native AMPA receptors, *Nat. Neurosci.* **3**, 992–997.
32. Rosenmund, C., Stern-Bach, Y., and Stevens, C. F. (1998) The tetrameric structure of a glutamate receptor channel, *Science* **280**, 1596–1599.
33. Abele, R., Keinänen, K., and Madden, D. R. (2000) Agonist-induced isomerization in a glutamate receptor ligand-binding domain. A kinetic and mutagenetic analysis, *J. Biol. Chem.* **275**, 21355–21363.
34. Connors, K. A. (1990) *Chemical Kinetics. The Study of Reaction Rates in Solution*, VCH Publishers, New York.
35. Kubo, M., and Ito, E. (2004) Structural dynamics of an ionotropic glutamate receptor, *Proteins* **56**, 411–419.
36. Radic, Z., Kirchoff, P. D., Quinn, D. M., McCammon, J. A., and Taylor, P. (1997) Electrostatic influence on the kinetics of ligand binding to acetylcholinesterase. Distinctions between active center ligands and fasciculin, *J. Biol. Chem.* **272**, 23265–23277.
37. Raman, I. M., and Trussell, L. O. (1992) The kinetics of the response to glutamate and kainate in neurons of the avian cochlear nucleus, *Neuron* **9**, 173–186.
38. Patneau, D. K., and Mayer, M. L. (1991) Kinetic analysis of interactions between kainate and AMPA: Evidence for activation of a single receptor in mouse hippocampal neurons, *Neuron* **6**, 785–798.
39. Colquhoun, D., Jonas, P., and Sakmann, B. (1992) Action of brief pulses of glutamate on AMPA/kainate receptors in patches from different neurones of rat hippocampal slices, *J. Physiol.* **458**, 261–287.
40. Heckmann, M., Bufler, J., Franke, C., and Dudel, J. (1996) Kinetics of homomeric GluR6 glutamate receptor channels, *Biophys. J.* **71**, 1743–1750.
41. Traynelis, S. F., and Wahl, P. (1997) Control of rat GluR6 glutamate receptor open probability by protein kinase A and calcineurin, *J. Physiol.* **503**, 513–531.
42. Banke, T. G., Bowie, D., Lee, H., Huganir, R. L., Schousboe, A., and Traynelis, S. F. (2000) Control of GluR1 AMPA receptor function by cAMP-dependent protein kinase, *J. Neurosci.* **20**, 89–102.
43. Grosskreutz, J., Zoerner, A., Schlesinger, F., Krampfl, K., Dengler, R., and Bufler, J. (2003) Kinetic properties of human AMPA-type glutamate receptors expressed in HEK293 cells, *Eur. J. Neurosci.* **17**, 1173–1178.

BI047413N

IDENTIFICATION OF C-TERMINAL DOMAIN RESIDUES INVOLVED IN PROTEIN KINASE A-MEDIATED POTENTIATION OF KAINATE RECEPTOR SUBTYPE 6

B. G. KORNREICH,^a L. NIU,^{a,c} M. S. ROBERSON^b
AND R. E. OSWALD^{a*}

^aDepartment of Molecular Medicine, Cornell University, Ithaca, NY 14853, USA

^bDepartment of Biomedical Sciences, Cornell University, Ithaca, NY 14853, USA

^cDepartment of Chemistry, Center for Biochemistry and Biophysics, The State University of New York at Albany, Albany, NY 12222, USA

Abstract—Glutamate receptors are the major excitatory receptors in the vertebrate CNS and have been implicated in a number of physiological and pathological processes. Previous work has shown that glutamate receptor function may be modulated by protein kinase A (PKA)–mediated phosphorylation, although the molecular mechanism of this potentiation has remained unclear. We have investigated the phosphorylation of specific amino acid residues in the C-terminal cytoplasmic domain of the rat kainate receptor subtype 6 (GluR6) as a possible mechanism for regulation of receptor function. The C-terminal tail of rat GluR6 can be phosphorylated by PKA on serine residues as demonstrated using [γ -³²P]ATP kinase assays. Whole cell recordings of transiently transfected human embryonic kidney (HEK) 293 cells showed that phosphorylation by PKA potentiates whole cell currents in wildtype GluR6 and that removal of the cytoplasmic C-terminal domain abolishes this potentiation. This suggested that the C-terminal domain may contain residue(s) involved in the PKA-mediated potentiation. Single mutations of each serine residue in the C-terminal domain (S815A, S825A, S828A, and S837A) and a truncation after position 855, which removes all threonines (T856, T864, and T875) from the domain, do not abolish PKA potentiation. However, the S825A/S837A mutation, but no other double mutation, abolishes potentiation. These results demonstrate that phosphorylation of the C-terminal tail of GluR6 by PKA leads to potentiation of whole cell response, and the combination of S825 and S837 in the C-terminal domain is a vital component of the mechanism of GluR6 potentiation by PKA. © 2007 IBRO. Published by Elsevier Ltd. All rights reserved.

Key words: glutamate receptor, kainate receptor, phosphorylation, receptor regulation.

*Corresponding author. Tel: +1-607-253-3877; fax: +1-607-253-3659. E-mail address: reo1@cornell.edu (R. E. Oswald).

Abbreviations: CaM kinase II, Ca²⁺/calmodulin-dependent protein kinase II; GFP, green fluorescent protein; GluR, glutamate receptor; GluR6, kainate receptor subtype 6; GluR6 Δ C-term, GluR6 truncated before S815; GluR6 Δ 855, GluR6 truncated before T856; GST, glutathione S-transferase; HEK, human embryonic kidney; iGluR, ionotropic glutamate receptor; LTD, long-term depression; LTP, long-term potentiation; NMDA, *N*-methyl-D-aspartate; PKA, protein kinase A; PKA_{cat}, protein kinase A catalytic subunit; PKC, protein kinase C; WT, wildtype.

0306-4522/07/\$30.00+0.00 © 2007 IBRO. Published by Elsevier Ltd. All rights reserved.
doi:10.1016/j.neuroscience.2007.02.012

Glutamate receptors (GluRs) are the major excitatory receptors in the vertebrate CNS and have been implicated in a number of normal CNS functions including synaptic plasticity, and pathological processes such as epilepsy, Parkinson's disease, schizophrenia, and ischemic cell death (Dingledine et al., 1999). GluRs are ligand-activated membrane receptors and consist of two large families: metabotropic (linked through G proteins to downstream second messengers) receptors termed mGluRs and ionotropic (current passing) receptors referred to as iGluRs (Dingledine et al., 1999). iGluRs have been subdivided based upon their agonist specificities and sequence homology into *N*-methyl-D-aspartate (NMDA), AMPA, and kainate receptors (Lerma, 2006). Each receptor is believed to be composed of a tetramer of subunits that oligomerize to form functional channels in the cell membrane (Dingledine et al., 1999). To date, five mammalian kainate receptor subunits (GluR5-7, KA1-2) have been identified based upon their high affinity for this compound (Bettler et al., 1990, 1992; Egebjerg et al., 1991; Werner et al., 1991; Herb et al., 1992).

Previous studies suggest that iGluR function may be modulated by protein phosphorylation (Raymond et al., 1993; Wang et al., 1993, 1994; Roche et al., 1996; Lee et al., 1998). Basal and induced phosphorylation of AMPA and kainate GluRs by protein kinase A (PKA), protein kinase C (PKC), and Ca²⁺/calmodulin-dependent protein kinase II (CaM kinase II) has been demonstrated (McGlade-McCulloh et al., 1993; Moss et al., 1993; Raymond et al., 1993). Phosphorylation of NMDA receptors has similarly been reported (Chen and Huang, 1992; Tingley et al., 1993; Lieberman and Mody, 1994). Mutational studies, immunochemical assays, phosphoamino acid analysis and phosphopeptide mapping suggest that basal and kinase-dependent phosphorylation of GluRs occurs primarily on serine and threonine residues (Blackstone et al., 1994; Omkumar et al., 1996; Roche et al., 1996; Barria et al., 1997; Leonard and Hell, 1997; Mammen et al., 1997; Tingley et al., 1997; Lee et al., 1998). PKA-mediated potentiation of whole cell currents has been demonstrated in human embryonic kidney (HEK293) cells transiently transfected with rat GluR6 cDNA (Raymond et al., 1993; Wang et al., 1993). Raymond et al. (1993) demonstrated that intracellularly applied protein kinase A catalytic subunit (PKA_{cat}) increased the amplitude of glutamate-induced whole cell current. Although the specific site(s) of phosphorylation was (were) not identified, potentiation was abolished by a S684A point mutation and by inclusion of an inhibitor of PKA (PKI) in the pipette solution. Wang et al.

(1993) observed potentiation of kainate-induced currents in GluR6-transfected HEK293 cells when PKA_{cat} was directly perfused into individual cells. A S684A point mutation decreased PKA_{cat}-induced current potentiation while a S666A mutation had no effect. The double mutation S684A/S666A abolished PKA_{cat}-induced potentiation. These experiments were reported at a time when the assumed transmembrane topology of the glutamate receptor placed the N- and C-termini and the S1 region in an extracellular location and S2 intracellularly (Hollmann et al., 1989; Keinänen et al., 1990). This topology assumed that the sites of interest in these studies (i.e. S684 and S666) were intracellular and were therefore exposed to PKA_{cat} and PKI. Subsequent immunocytochemical, phos-

phorylation, and N-glycosylation studies (Hollmann et al., 1994; Wo and Oswald, 1994, 1995a,b; Bennett and Dingledine, 1995) indicate an extracellular location for S2, thereby placing positions 684 and 666 in an extracellular location (Fig. 1). Reconciliation of the findings of Raymond et al. (1993) and Wang et al. (1993) with the corrected transmembrane topology (Hollmann et al., 1994; Wo and Oswald, 1994, 1995a) of the GluR6 subunit requires one or a combination of the following possibilities: (1) extracellular phosphorylation of sites 684 and 666 by kinases in the extracellular milieu (or by PKA released from lysed cells in the Raymond et al. (1993) paper), (2) intracellular phosphorylation of GluR6 en route from the endoplasmic reticulum (ER) to the cell membrane, or (3) the presence of one

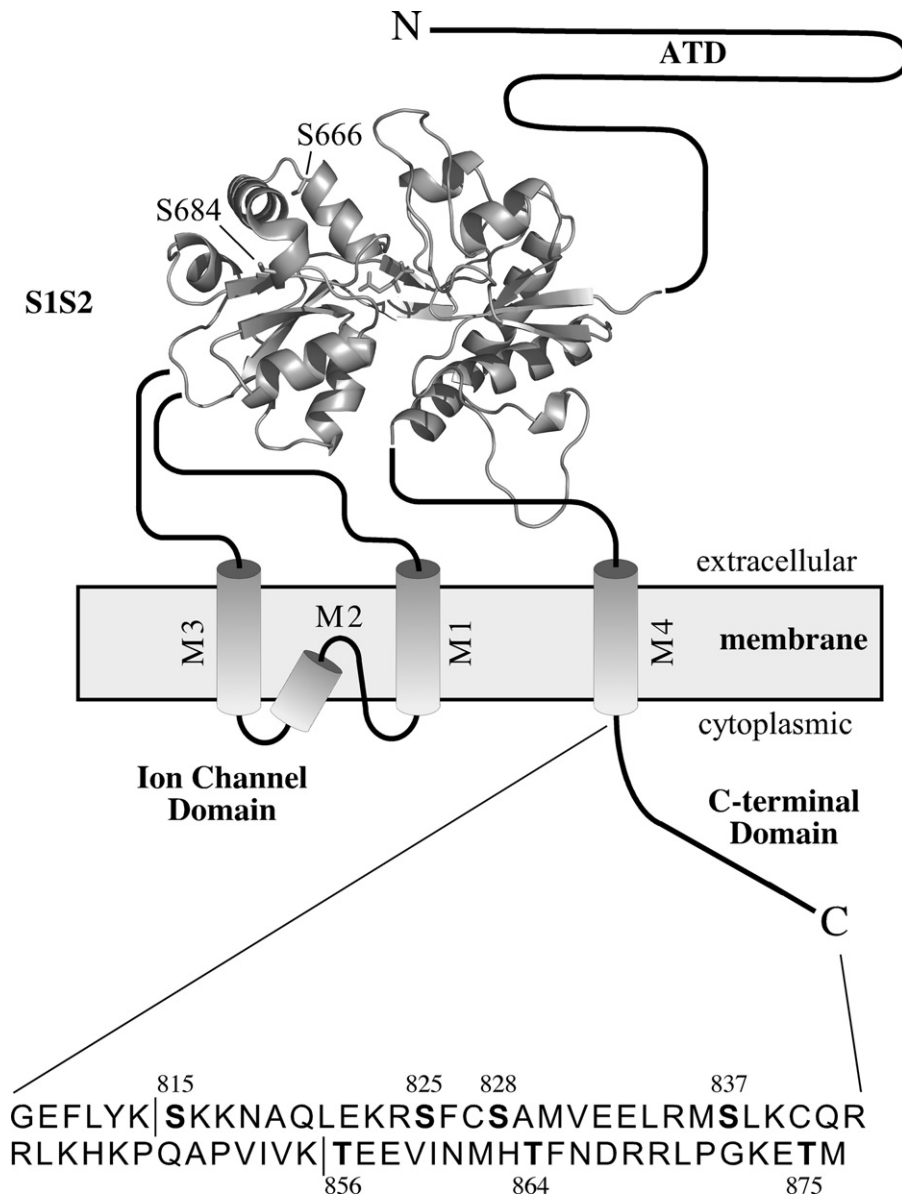


Fig. 1. Schematic of the domains of the GluR6 receptor. ATD refers to the amino terminal domain and M1 through M4 refer to membrane-associated regions of the protein. The structure shown is the S1S2 (extracellular ligand-binding domain of a GluR) of GluR6 (1S7Y; Mayer, 2005). The vertical lines in the sequence illustrate where the truncations were made for Fig. 3 (line before S815; GluR6 Δ C-term) and Figs. 2, 4, and 5 (line before T856; GluR6 Δ 855).

or more additional intracellular sites for PKA-mediated phosphorylation of GluR6. The goal of the present study was to identify putative site(s) in the cytoplasmic C-terminal domain involved in mediating PKA phosphorylation.

While the C-terminal tail of rat GluR6 does not contain a primary PKA consensus site (R-R-X-S/T, where X is any amino acid; Zetterqvist et al., 1976; Kennelly and Krebs, 1991), it does contain a number of sites that could interact with PKA based upon similarity of neighboring residues to the classic recognition motif (Fig. 1; 1S7Y; Mayer, 2005). Although the PKA consensus sequence is relatively well defined, previous work has shown that PKA can phosphorylate target peptides whose amino acid sequence differs somewhat from this sequence (Kemp et al., 1975; Smith et al., 1999). Our experimental approach was to determine whether the isolated C-terminal tail of GluR6 is phosphorylated by PKA, and if so, whether serine or threonine residues in the C-terminus were phosphorylated. Mutant receptors carrying the specific serine/threonine residues were expressed in HEK293 cells and the effects of altering specific residues on PKA-mediated potentiation of whole cell currents were determined. By this approach, we have identified two serine residues in the C-terminal tail of GluR6; together these two serine residues mediate fully the potentiation of the whole cell current response, once they are phosphorylated by PKA.

EXPERIMENTAL PROCEDURES

Molecular biology

Mutations were introduced into wildtype (WT) rat GluR6 (Q form; kindly provided by Dr. Steve Heinemann, Salk Institute, La Jolla, CA, USA) using the QuikChange[®] XL Site-Directed Mutagenesis Kit (Stratagene, La Jolla, CA, USA). Oligonucleotides were synthesized and verified by the Bioresource Center, Cornell University.

Bacterial expression of GluR6 C-terminal tail-glutathione S-transferase (GST) fusion protein

cDNA encoding the WT C-terminal tail of rat GluR6 (G809-A877) was generated by PCR (Saiki et al., 1988). PCR fragments were subcloned into EcoR1 and BamH1 sites of the PGEX-2T plasmid vector (Amersham Biosciences, Piscataway, NJ, USA) predigested with the same restriction enzymes, and the resultant constructs were sequenced. This construct was used as a template for site directed mutagenesis. WT and mutant constructs were then transformed into *E. coli* BL21 (Cohen et al., 1972), cultured at 37 °C in LB broth (Fisher Scientific, Fair Lawn, NJ, USA) supplemented with 100 $\mu\text{g ml}^{-1}$ ampicillin to an OD_{560} of 0.7 and induced with 250 μM isopropyl-1-thio- β -D-galactopyranoside for 4 h at 37 °C. Bacteria were harvested and lysed in ice cold PBS by three freeze-thaw cycles followed by sonication. The lysed bacterial extract was centrifuged at 12,000 $\times g$ for 20 min and the supernatant was incubated with glutathione-sepharose 4B (Amersham Biosciences) for 1 h. Sepharose beads with bound GluR6 tail-GST fusion protein were then washed and incubated with thrombin (Amersham Biosciences; 1 unit/sample) at 4 °C for 16 h where necessary to cleave GST from GluR6 tail peptide. Samples were subjected to SDS-PAGE to verify presence of GluR6 tail-GST fusion protein and successful thrombin cleavage. Thrombin-treated and untreated protein samples were then used as substrates in parallel for [γ -³²P]ATP/kinase assays.

[γ -³²P]ATP/PKA assay

PKA phosphorylation reactions were carried out for 30 min at 37 °C using 1 μl PKA_{cat} (100 U ml⁻¹), 25 μl GluR6 tail-GST fusion protein preparation, kinase buffer (40 mM Hepes, 40 mM MgCl₂, 50 mM β -glycerophosphate, 4 mM Na₃VO₄, 4 mM dithiothreitol, 2 mM phenylmethylsulfonyl fluoride, 2 mM benzamidine, adjusted to achieve the same total volume for all tubes), 5 μM nonradioactive ATP and 9 μM [γ -³²P]ATP (20 $\mu\text{Ci/tube}$; New England Nuclear, Boston, MA, USA). Following the kinase reaction, the mixture was diluted 1:1 in 2 \times SDS loading buffer (100 mM Tris, pH 6.8, 4% SDS, 20% glycerol, 0.25% Bromophenol Blue) and resolved by SDS-PAGE. The degree of phosphorylation was evaluated by autoradiography.

Cell culture and transfection

HEK293 cells were maintained in Dulbecco's Modified Eagle Medium (DMEM; Life Technologies, Gaithersburg, MD, USA) supplemented with 10% (v/v) fetal bovine serum (FBS; Life Technologies), 100 U ml⁻¹ sodium penicillin G, and 100 $\mu\text{g ml}^{-1}$ streptomycin sulfate in a humidified 5% CO₂ incubator at 37 °C. When 60% confluent, cells were cotransfected with either WT or mutant rat GluR6 cDNA in pcDNA1/Amp expression vector (Invitrogen, Carlsbad, CA, USA) and green fluorescent protein (GFP) cDNA in the pEGFP-N1 plasmid (Clontech Laboratories, Palo Alto, CA, USA) using the calcium phosphate method (Chen and Okayama, 1987). One microgram of GluR6 DNA was used for each 35 mm dish. GFP was used as a marker of gene expression in transiently transfected cells (Plautz et al., 1996; Subramanian and Srienc, 1996). GFP cDNA concentration was maintained at 50% that of GluR6 concentration to increase the positive predictive value of GFP. Transfection efficiency of GFP-cotransfected cells was evaluated after 36 h by visual inspection of GFP fluorescence. For use in experiments, cells were collected, resuspended in growth medium, and replated at lower density 30 min prior to study to facilitate lifting cells off of the dish. Immediately prior to study, the replated cells were washed twice with Dulbecco's phosphate buffered saline (PBS; Life Technologies) and were bathed in the extracellular solution (145 mM NaCl, 3 mM KCl, 1 mM CaCl₂, 2 mM MgCl₂, 10 mM Hepes, and 5 mM glucose buffered to pH 7.4) for our study.

Electrophysiological recording

The whole cell current recording configuration of the patch clamp technique was used (Hamill et al., 1981). Pipettes were pulled from borosilicate glass capillary tubes to a tip diameter of 2–3 μm and a resistance of 2–3 M Ω when filled with the pipette solution (140 mM KCl, 10 mM Hepes, 11 mM EGTA, 1 mM CaCl₂, 2 mM MgCl₂, 2 mM tetraethylammonium, and 4 mM ATP, buffered to pH 7.3). PKA_{cat} (100 U ml⁻¹; Sigma Chemical Company, St. Louis, MO, USA) was added to the pipette solution when potentiation by phosphorylation was tested. Recordings were obtained using an Axopatch 200B amplifier (Molecular Devices Corporation, Sunnyvale, CA, USA) and passed through an internal low pass filter with a cutoff frequency of 5 kHz before being digitized at a sampling frequency of 20 kHz and analyzed using PClamp 6 or 8 (Molecular Devices Corporation). All recordings were obtained at a holding potential of -60 mV at 21 °C using the cells between 36 and 96 h after transfection. After achieving the whole cell patch clamp configuration, the cells was lifted off the dish and placed within 50 μm of the 150 μm diameter outflow of a U-tube application device (Udgaonkar and Hess, 1987). The solution exchange time for this device, determined by using open pipette tip measurements of voltage changes in response to 500 mM CsCl, was approximately 0.9 ms. Given unstirred layers and the shape of the cell, the 10–90% solution exchange time was 1–3 ms (Francis et al., 2001). The first agonist application (1 mM glutamate) was

achieved within 2 min of obtaining whole cell configuration. Subsequent agonist applications were delivered at 4 min intervals.

Data analysis

The PKA-mediated potentiation was typically maximal or near maximal at 6 min, so the ratio of the 6 min to 2 min current amplitude was used as a measure of the effect of PKA. This accounted for the effects of variable GluR6 expression. The Wilcoxon rank sum test was used to determine statistical significance of differences in normalized current amplitudes among GluR6 constructs. The two-tailed Fisher exact test was used to determine the statistical significance of differences in percentages of cells demonstrating potentiation among GluR6 constructs.

RESULTS

[γ - 32 P]ATP/PKA assay

Previous work suggests that kinase-mediated modulation of ionotropic glutamate receptor function may involve direct phosphorylation of residues within the C-terminal domain (Kohr and Seeburg, 1996; Roche et al., 1996; Lee et al., 1998; Zheng et al., 1998; Banke et al., 2000). PKA, a kinase that has been implicated in the modulation of glutamate receptor function and more specifically in the potentiation of agonist-induced currents in GluR6 (Raymond et al., 1993; Wang et al., 1993; Banke et al., 2000), phos-

phorylates peptides primarily on serine and threonine residues (Kennelly and Krebs, 1991; Songyang et al., 1994). The C-terminal domain of rat GluR6 contains four serine residues (S815, S825, S828, and S837) and three threonine residues (T856, T864, and T875; Fig. 1). Although the C-terminal tail of rat GluR6 does not contain a primary PKA consensus site (R-R-X-S/T, where X is any amino acid; Zetterqvist et al., 1976; Kennelly and Krebs, 1991; Songyang et al., 1994), it does contain a number of sites that could interact with PKA based upon charge distribution and similarity of neighboring residues to the established recognition motif. To test whether PKA can phosphorylate the C-terminal domain of GluR6, and, if so, to determine whether phosphorylation occurs on serine or threonine residues, [γ - 32 P]ATP/PKA assays using bacterially expressed WT and mutant C-terminal domain GST-fusion proteins as substrate were performed. As shown in Fig. 2A, the WT C-terminal tail of GluR6 was phosphorylated by PKA. The S815A/S825A/S828A/S837A quadruple mutation abolished phosphorylation of bacterially expressed GST-fusion protein (Fig. 2A and C). However, truncation of the C-terminal segment immediately C-terminal to K855 (removing T856, T864, and T875; GluR6 Δ 855), did not abolish phosphorylation. These findings suggest that one or more of the serine residues in the WT construct were

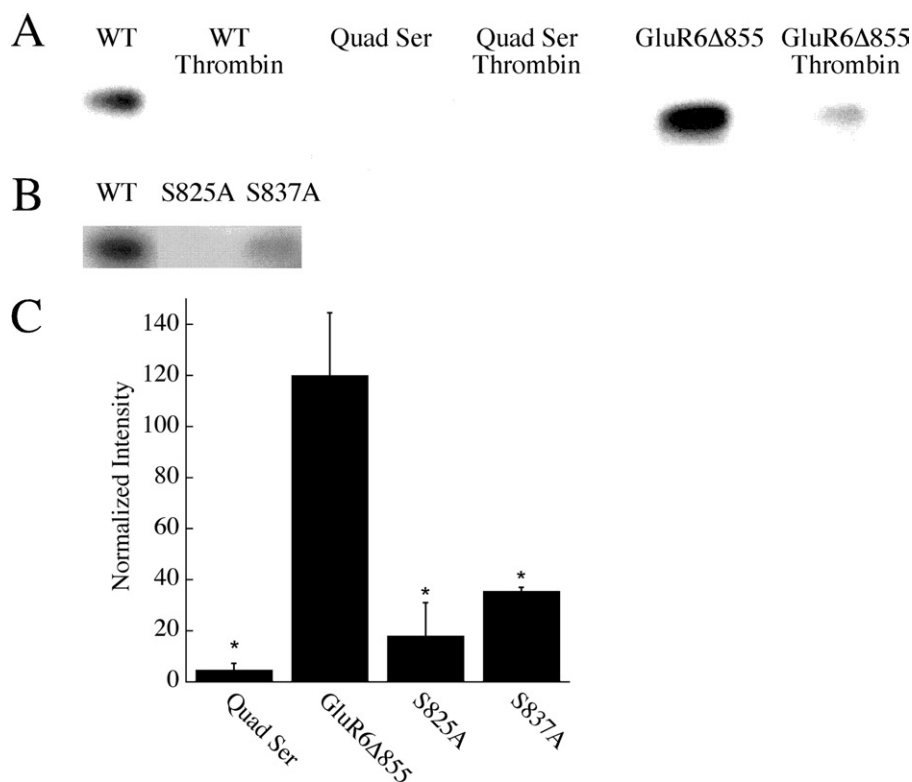


Fig. 2. Phosphorylation of the GST-C terminal peptide of GluR6. (A) The first lane is the WT peptide conjugated to GST. In the second lane, the GST has been cleaved from the peptide and the peptide runs at the tracking dye (not shown). The third lane shows the peptide for which all four serines were mutated to alanine (GST conjugate) and the fourth lane is the same construct treated with thrombin. The fifth lane is the peptide truncated before T856 (GST conjugate; GluR6 Δ 855) and the sixth lane is the same construct treated with thrombin to cleave the GST. (B) The first lane is the WT conjugated to GST, the second lane is a similar construct with the S825A mutation, and the third lane is the S837A mutation. (C) Quantitation of the autoradiograms. To control for variability between replicates, values were normalized to the intensity for WT. Significance was tested with a one-sample *t*-test. Significant differences ($P < 0.05$) are indicated with an asterisk.

likely phosphorylated. Thrombin cleavage of GST from phosphorylated WT and GluR6 Δ 855 fusion protein complexes resulted in a loss of signal intensity when compared with uncleaved peptides. This suggests that the 8 kD phosphorylated C-terminal portion of the GST fusion peptide migrates to the nonresolvable dye front once cleaved by thrombin and demonstrates that phosphorylation occurs on the C-terminal segment peptide. As a control, GST alone was not phosphorylated by PKA (data not shown). Taken together, these results indicated that the peptide mimicking the C-terminal tail of GluR6 can be phosphorylated by PKA on one or more of its serine residues. We then constructed a series of mutant receptors based on these results, expressed these holoreceptors in HEK293 cells and determined if specific serine residues in the C-terminal region of GluR6 were required for PKA phosphorylation, using whole cell recording.

Whole cell recording

C-terminal tail truncation. To test whether the C-terminal domain of GluR6 was required for PKA-mediated potentiation of GluR6, we compared whole cell current responses in HEK293 cells transiently transfected with WT rat GluR6 cDNA with those obtained in cells transfected with a mutant GluR6 cDNA construct in which the entire cytoplasmic C-terminal domain was deleted. WT GluR6 showed a time-dependent potentiation of whole cell current upon serial application of 1 mM glutamate when PKA was included in the intracellular pipette buffer (Fig. 3A). However, truncation of the total C-terminal domain (GluR6 Δ C-term) rendered the mutant insensitive to the intracellular presence of PKA (Fig. 3B) and led to a rundown in current, suggesting that the C-terminal domain is

essential to the mechanism of PKA-mediated potentiation of GluR6.

Selective serine and threonine mutagenesis. The functional role of specific C-terminal serine and threonine residues in PKA-mediated potentiation of GluR6 was investigated using site-directed mutagenesis. Whole cell currents elicited by application of 1 mM glutamate 6 min after attaining whole cell configuration were normalized to those obtained upon initial (2 min) agonist application. The ratio is multiplied by 100, and the mean of all replicates is reported below as “normalized current.” The results of the [γ - 32 P]ATP PKA assays (Fig. 2A) suggest that if the effects of PKA on GluR6 were the result of phosphorylation of residues within the C-terminal tail domain, they were likely to be mediated by phosphorylation of at least one serine residue. To pinpoint specific serine residues, single serine-to-alanine mutations were introduced at S815, S825, S828 and S837. Examples of 2 and 6 min agonist applications are shown for WT and S815A, S825A, S828A, and S837A constructs (Fig. 4) to demonstrate that all of these single serine mutants could be potentiated in the presence of PKA (summarized in Fig. 6). Whole cell recordings of HEK293 cells transfected with WT rat GluR6 cDNA demonstrated potentiation in 64% of cells studied ($n=33$), with a normalized current of 131%. Exclusion of PKA from the pipette buffer resulted in a lack of potentiation in any cells studied ($n=5$), with a normalized current of 82%. That is, in the absence of PKA, current rundown was consistently observed. Whole cell current potentiation was retained despite serine-to-alanine mutations at either S815 (60% of cells potentiated, normalized current: 121%, $n=25$), S825 (60% of cells potentiated, normalized current: 121%,

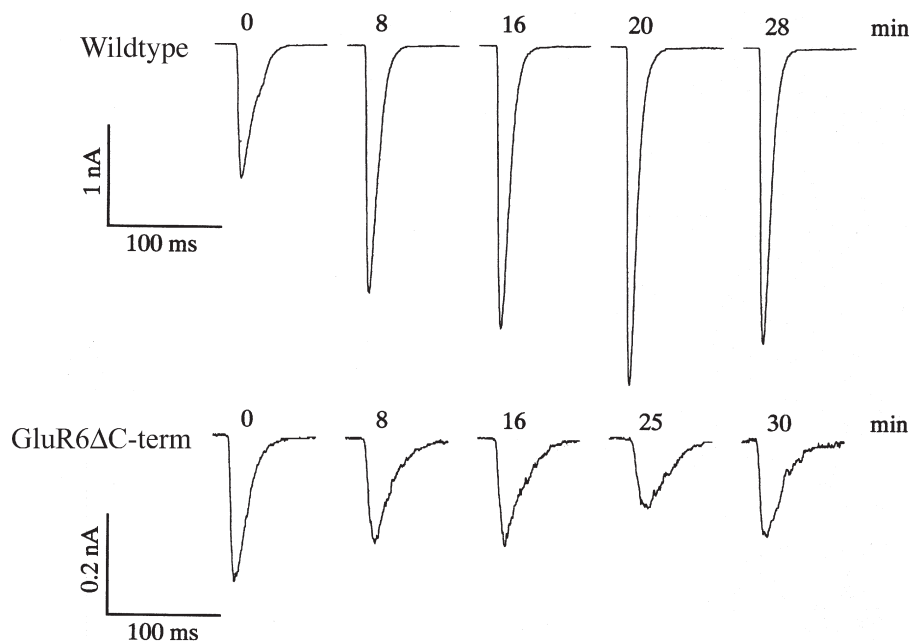


Fig. 3. The effect of truncation of the GluR6 C-terminus before S815. When PKA is included in the pipette, the peak current for WT GluR6 increases as a function of time. When the protein is truncated before S815 (removal of all serines and threonines from the C-terminal tail), current rundown is observed even in the presence of PKA.

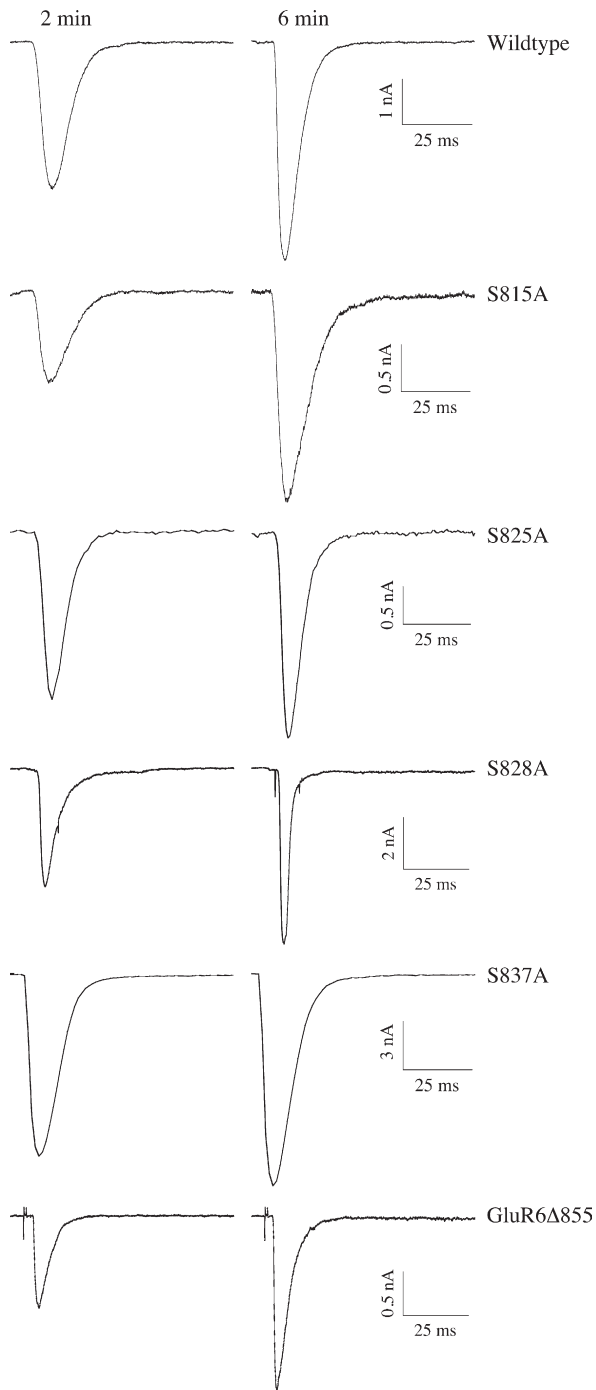


Fig. 4. Selected current traces from GluR6 WT, single serine to alanine mutations, and GluR6 Δ 855. In all cases, PKA was included in the pipette and measurements were taken 2 min and 6 min after formation of the whole cell patch.

$n=30$), S828 (83% of cells potentiated, normalized current: 158%, $n=12$) or S837 (52% of cells potentiated, normalized current: 121%, $n=27$), suggesting that these residues are not individually required for PKA-mediated potentiation in GluR6. Although the percent potentiation for S825A and S837A was numerically less than WT, the difference was not statistically significant; however,

these values differed significantly from currents in the absence of PKA (Fig. 6A).

To determine whether the C-terminal domain threonine residues are involved in PKA-mediated potentiation of GluR6, a truncation mutation was introduced into rat GluR6 immediately C-terminal to K855 (GluR6 Δ 855). This mutation, which removed all three threonine residues in the C-terminal tail domain, did not abolish potentiation (Fig. 4), which was seen in 78% of cells studied (normalized current: 160%, $n=18$), suggesting that the threonine residues are not essential for GluR6 potentiation by PKA.

Taken together, the whole cell recording results of the single serine and GluR6 Δ 855 mutations ruled out the possibility of either single serine residues or any combination of threonine residues being involved in mediating the phosphorylation-induced whole cell current potentiation. Instead, these results suggested a possibility that multiple serine residues may be required for PKA-mediated potentiation of GluR6. Initially, we engineered the S815A/S825A/S837A GluR6 (triple) mutant construct. In all but one case, the 6-min current amplitude was smaller than the 2-min current amplitude (normalized current: 78%, $n=8$; Fig. 5), suggesting that some combination of these serine residues (S815, S825, and S837) is required for PKA-mediated potentiation. To determine which combination of the three candidate serine residues was involved in potentiation, we engineered three double serine-to-alanine mutants on a GluR6 Δ 855 background. Examples of these whole-cell recording experiments are shown in Fig. 5. The S815A/S825A mutation failed to abolish potentiation (56% of cells potentiated, normalized current: 136%, $n=9$), as did the S815A/S837A mutation (57% of cells potentiated, normalized current: 176%, $n=7$), suggesting that neither of these combinations of serine residues is essential to the mechanism of PKA-mediated potentiation of GluR6; (Fig. 6). In contrast, all of the cells transfected with the S825A/S837A mutant construct failed to show potentiation (normalized current: 55%, $n=6$; Fig. 6), suggesting that the combination of both S825 and S837 was required for GluR6 potentiation by PKA. Consistent with these findings, both the S825A and S837A mutations significantly decreased the phosphorylation of a GST-C terminal peptide construct (Fig. 2B and C).

It is of interest to note that transfected HEK293 cells carrying multiple serine mutations on a GluR6 Δ 855 background were more likely to show either no response to glutamate application or unstable responses upon prolonged recording. Although the reason for this remains unclear, residues within the C-terminal domain of glutamate receptors have been identified as important trafficking motifs and as protein–protein contact domains with anchoring proteins such as GRIP and PSD-95 (Nishimune et al., 1998; Song et al., 1998; Hayashi et al., 2000; Standley et al., 2000; Scott et al., 2001; Shi et al., 2001; Malinow and Malenka, 2002; Hirbec et al., 2003; Yan et al., 2004; Salinas et al., 2006). It is possible that multiple serine-to-alanine and/or GluR6 Δ 855 mutations in the C-terminal domain of GluR6 disrupt important interactions with proteins that serve to localize and/or anchor the receptor in

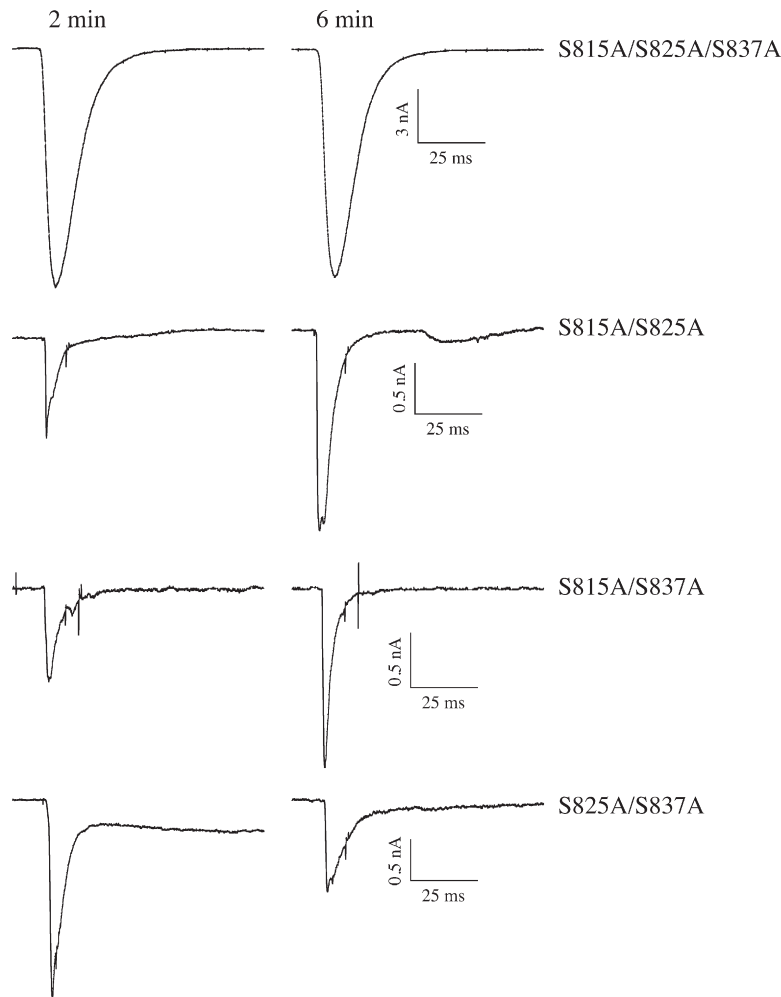


Fig. 5. Selected current traces from a GluR6 triple serine to alanine mutation and double serine to alanine mutations (on the GluR6 Δ 855 background). In all cases, PKA was included in the pipette and measurements were taken 2 min and 6 min after formation of the whole cell patch.

the plasma membrane, thereby destabilizing their normal function.

To determine if channel function was altered by the mutations alone, the rise time and desensitization rate were measured for the WT, Triple, and GluR6 Δ 855 constructs. These constructs were chosen to represent the extremes of serine (Triple) and threonine (GluR6 Δ 855) mutagenesis. Although rise times for GluR6 are difficult to measure accurately by the cell flow method (Li et al., 2003), no significant difference in apparent rise time or the desensitization rate was seen among these three constructs in the absence of PKA (data not shown). Thus, channel properties seemed to be similar. Consequently, the results obtained with PKA are likely to be a result of receptor phosphorylation.

DISCUSSION

Phosphorylation is an important mechanism of iGluR modulation (Raymond et al., 1993; Wang et al., 1993; Kohr and Seeburg, 1996; Roche et al., 1996; Lee et al., 1998; Zheng et al., 1998; Banke et al., 2000). A variety of phosphoki-

nases has been shown to phosphorylate iGluRs, and PKA-mediated phosphorylation of iGluRs has been demonstrated (Raymond et al., 1993; Wang et al., 1993; Roche et al., 1996). Although controversy regarding the transmembrane topology of iGluRs complicated the interpretation of early studies designed to determine specific sites of phosphorylation by PKA (Raymond et al., 1993; Wang et al., 1993), more recent work suggests that sites of physiological PKA-mediated phosphorylation of iGluRs are intracellular. Our study using [γ - 32 P]ATP kinase assays shows that the C-terminal domain of GluR6 can be phosphorylated by PKA, and that serine residues are the sites of phosphorylation. This is consistent with previous work in which residues within the C-terminal domain of iGluRs have been identified as likely sites of phosphorylation. The S845A mutation in the C-terminal domain of GluR1 abolished phosphorylation by PKA (Roche et al., 1996), and forskolin treatment increased phosphorylation of S845 in rat hippocampal slices (Mammen et al., 1997). Site-directed mutagenesis and antiphosphopeptide antibodies identified the C-terminal domain residue S831 as a site of phosphor-

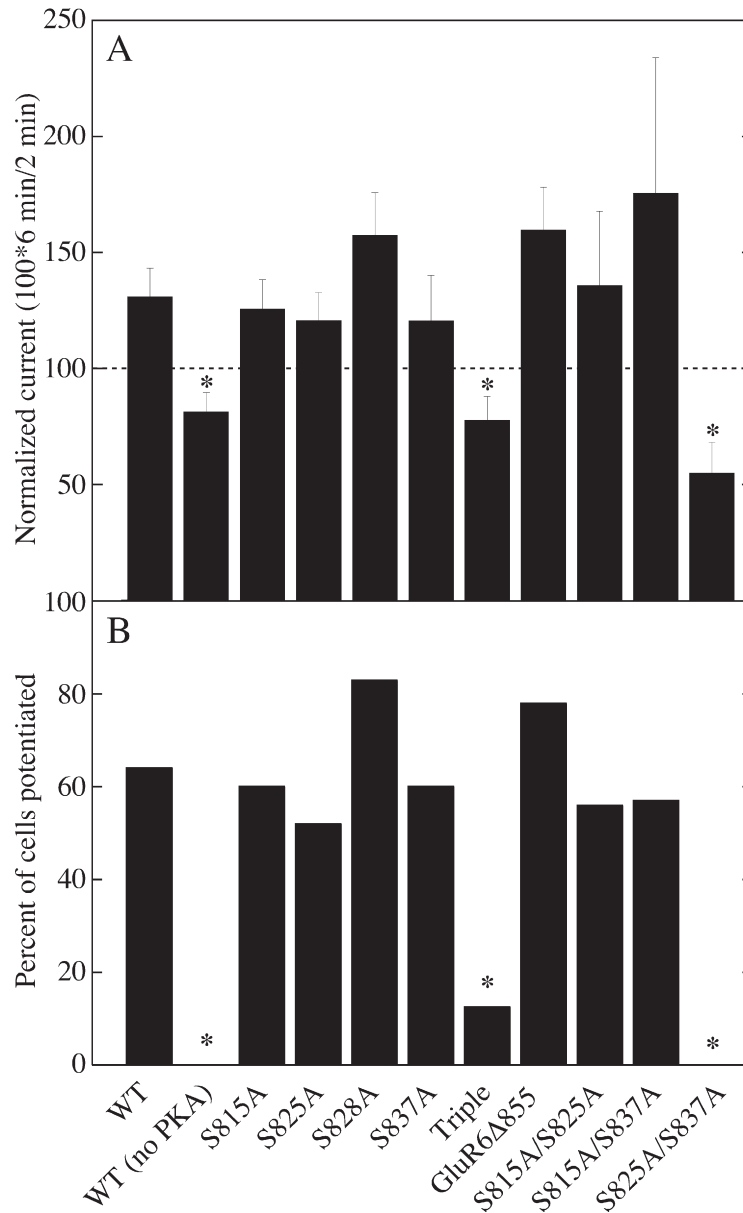


Fig. 6. (A) Average percent change in maximal current for 6 min following the formation of the whole cell patch versus 2 min following formation of the patch. The error bars represent standard errors. (B) Percent of cells that showed potentiation for each of the conditions tested. The asterisk in both (A) and (B) indicates a statistically significant difference from WT ($P < 0.05$). Triple refers to the S815A/S825A/S837A mutation, and GluR6Δ855 refers to the truncation before T856.

ylation by CaM kinase II in GluR1 (Roche et al., 1996; Barria et al., 1997; Mammen et al., 1997). This site is also a PKC target site and, along with the PKA phosphorylation site S845, has been shown to be basally phosphorylated in GluR1 (Mammen et al., 1997). It is interesting to consider that, like S831 in GluR1, which is not a consensus site for CaM kinase II or PKC, the serine residues in the C-terminal domain of GluR6 are not consensus sites for PKA. Both S845 and S831 of GluR1 have been implicated in long-term potentiation (LTP) and long-term depression (LTD). CaM kinase II phosphorylation of S831 has been reported to be required for LTP (Derkach et al., 1999; Lee et al., 2000; Whitlock et al., 2006) and dephosphorylation of

S845 has been implicated in LTD (Kameyama et al., 1998; Lee et al., 2000).

PKA has been shown to phosphorylate recombinant GluR6 expressed in HEK293 cells (Raymond et al., 1993). In the same study, PKA potentiated whole cell currents in GluR6, and mutation of S684 and S666 abolished potentiation. These residues were thought to be intracellularly located based upon the accepted transmembrane topology of glutamate receptors at that time (Hollmann et al., 1989; Keinänen et al., 1990). Subsequent studies, however, have shown that S684 and S666 are in fact extracellularly located (Hollmann et al., 1994; Wo and Oswald, 1994, 1995a; Fig. 1) and not translocated to the cytoplasm

(Basiry et al., 1999) and, thus, should not be accessible to intracellularly-applied PKA. Whether the functional effects of mutation of S864 and S666 are mediated by an allosteric mechanism remains unclear. One clue may come from accessibility studies which suggest that S684 in GluR6 (Basiry et al., 1999) and the corresponding residue in a goldfish kainate binding protein (S271; Wo et al., 1999) are exposed to solvent in the apo and antagonist-bound form but not in the agonist-bound form. This may suggest that this portion of the protein may undergo small changes upon activation and mutation of these residues could possibly have inhibited potentiation arising from the phosphorylation of cytoplasmic residues.

The potentiation of AMPA and kainate receptor current amplitude has been suggested to arise from an increased open channel probability (Knapp et al., 1990; Banke et al., 2000). Using nonstationary variance analysis, Banke et al. (2000) identified serine 845 in the C-terminal domain of GluR1 as an important component of the mechanism of potentiation by PKA in that phosphorylation by PKA increases the open probability of recombinant WT GluR1, but not that of the S845A mutant construct (Banke et al., 2000). The open probability of GluR6, measured by nonstationary variance analysis, is similarly increased by PKA, although specific residues involved in the mechanism of this increase have not been identified (Traynelis and Wahl, 1997). The open probability for GluR6 in the absence of PKA has been measured using laser-pulse photolysis to be approximately 0.96 (Li et al., 2003). Although the open probability of GluR6 in the absence of PKA would suggest that the potentiation due to an increase in open probability is unlikely, some potentiation would be possible (0.96–1.0) and changes in single channel conductance (or preferential population of higher conductance states; Derkach et al., 1999) cannot be ruled out.

In our studies, GluR6 Δ C-term abolished the PKA-mediated potentiation of whole cell currents seen in the WT construct (Fig. 3). This result supports the existence of sites within the C-terminal domain that are necessary for potentiation of GluR6 by PKA. The GluR6 Δ S855 mutation, which removes all three of the threonine residues (T856, T864, and T875) in the C-terminal domain, failed to abolish the potentiation of whole cell currents or phosphorylation of the C-terminal peptide, suggesting that these residues are not phosphorylated by PKA. The finding that the S825A/S837A mutation abolishes potentiation of the glutamate-induced GluR6 current by PKA and the S825A and S837A mutations decrease phosphorylation of the C-terminal peptide, suggests that S825 and S837 are involved in PKA-mediated potentiation of GluR6. The significance of the possible requirement for two serine residues in potentiation of whole cell current amplitude is unknown. It is possible that this requirement along with the fact that these sites are not strictly PKA consensus sequences may represent a physiological checkpoint in that a stronger stimulus for PKA recruitment may be required to achieve the degree of phosphorylation necessary for a functional effect (i.e. potentiation of current).

Our findings provide insight into the mechanism of potentiation of GluR6 by PKA. As the potentiation of GluR6 by PKA may play a role in a number of developmentally and clinically significant processes, it is hoped that an elucidation of this mechanism will enhance our understanding of the process of learning and memory and improve our ability to diagnose and treat a number of important neurological diseases. From a broader perspective, our findings may provide information regarding the molecular mechanism by which phosphorylation modulates the function of a variety of biologically important proteins.

Acknowledgments—This work was funded by a grant from the National Science Foundation (IBN-0323874) to R.E.O. and from the National Institutes of Health (K01 RR000155-04) to B.G.K. We thank Dr. Gregory Weiland for helpful discussions and assistance with manuscript preparation and Dr. Hollis Erb for statistical consultation.

REFERENCES

- Banke TG, Bowie D, Lee H, Haganir RL, Schousboe A, Traynelis SF (2000) Control of GluR1 AMPA receptor function by cAMP-dependent protein kinase. *J Neurosci* 20:89–102.
- Barria A, Derkach V, Soderling T (1997) Identification of the Ca²⁺/calmodulin-dependent protein kinase II regulatory phosphorylation site in the alpha-amino-3-hydroxy-5-methyl-4-isoxazole-propionate-type glutamate receptor. *J Biol Chem* 272:32727–32730.
- Basiry SS, Mendoza P, Lee PD, Raymond LA (1999) Agonist-induced changes in substituted cysteine accessibility reveal dynamic extracellular structure of M3-M4 loop of glutamate receptor GluR6. *J Neurosci* 19:644–652.
- Bennett JA, Dingledine R (1995) Topology profile for a glutamate receptor: Three transmembrane domains and a channel-lining re-entrant membrane loop. *Neuron* 14:373–384.
- Bettler B, Boulter J, Hermans-Borgmeyer I, O'Shea-Greenfield A, Deneris ES, Moll C, Borgmeyer U, Hollman M, Heinemann S (1990) Cloning of a novel glutamate receptor subunit, GluR5: expression in the nervous system during development. *Neuron* 5:583–595.
- Bettler B, Egebjerg J, Sharma G, Pecht G, Hermans-Borgmeyer I, Moll C, Stevens CF, Heinemann S (1992) Alignment of a total of 8 iGluR subunit sequences. *Neuron* 8:257–265.
- Blackstone C, Murphy TH, Moss SJ, Baraban JM, Haganir RL (1994) Cyclic AMP and synaptic activity-dependent phosphorylation of AMPA-preferring glutamate receptors. *J Neurosci* 14:7585–7593.
- Chen C, Okayama H (1987) High-efficiency transformation of mammalian cells by plasmid DNA. *Mol Cell Biol* 7:2745–2752.
- Chen L, Huang LYM (1992) Protein kinase C reduces Mg⁺⁺ block of NMDA-receptor channels as a mechanism of modulation. *Nature* 356:521–523.
- Cohen SN, Chang AC, Hsu L (1972) Nonchromosomal antibiotic resistance in bacteria: genetic transformation of *Escherichia coli* by R-factor DNA. *Proc Natl Acad Sci U S A* 69:2110–2114.
- Derkach V, Barria A, Soderling TR (1999) Ca²⁺/calmodulin-kinase II enhances channel conductance of alpha-amino-3-hydroxy-5-methyl-4-isoxazolepropionate type glutamate receptors. *Proc Natl Acad Sci U S A* 96:3269–3274.
- Dingledine R, Borges K, Bowie D, Traynelis S (1999) The glutamate receptor ion channels. *Pharmacol Rev* 51:7–61.
- Egebjerg J, Bettler B, Hermans-Borgmeyer I, Heinemann S (1991) Cloning of a cDNA for a receptor subunit activated by kainate but not AMPA. *Nature* 351:745–748.
- Francis MM, Cheng EY, Weiland GA, Oswald RE (2001) Specific activation of the alpha 7 nicotinic acetylcholine receptor by a quaternary analog of cocaine. *Mol Pharmacol* 60:71–79.

- Hamill OP, Marty E, Neher B, Sakmann B, Sigworth FJ (1981) Improved patch-clamp techniques for high-resolution current recording from cells and cell-free membrane patches. *Pflügers Arch* 391:85–100.
- Hayashi Y, Shi SH, Esteban JA, Piccini A, Poncer JC, Malinow R (2000) Driving AMPA receptors into synapses by LTP and CaMKII: requirement for GluR1 and PDZ domain interaction. *Science* 287:2262–2267.
- Herb A, Burnashev N, Werner P, Sakmann B, Wisden W, Seeburg PH (1992) The KA-2 subunit of excitatory amino acid receptors shows widespread expression in brain and forms ion channels with distantly related subunits. *Neuron* 8:775–785.
- Hirbec H, Francis JC, Lauri SE, Braithwaite SP, Coussen F, Mulle C, Dev KK, Coutinho V, Meyer G, Isaac JT, Collingridge GL, Henley JM (2003) Rapid and differential regulation of AMPA and kainate receptors at hippocampal mossy fibre synapses by PICK1 and GRIP. *Neuron* 37:625–638.
- Hollmann M, Maron C, Heinemann S (1994) N-Glycosylation site tagging suggests a three transmembrane domain topology for the glutamate receptor GluR1. *Neuron* 13:1331–1343.
- Hollmann M, O'Shea-Greenfield A, Rogers SW, Heinemann S (1989) Cloning by functional expression of a member of the glutamate receptor family. *Nature* 342:643–648.
- Kameyama K, Lee HK, Bear MF, Hugarir RL (1998) Involvement of a postsynaptic protein kinase A substrate in the expression of homosynaptic long-term depression. *Neuron* 21:1163–1175.
- Keinänen K, Wisden W, Sommer B, Werner P, Herb A, Verdoorn TA, Sakmann B, Seeburg PH (1990) A family of AMPA-selective glutamate receptors. *Science* 249:556–560.
- Kemp BE, Bylund DB, Huang TS, Krebs EG (1975) Substrate specificity of the cyclic AMP-dependent protein kinase. *Proc Natl Acad Sci U S A* 72:3448–3452.
- Kennelly PJ, Krebs EG (1991) Consensus sequences as substrate specificity determinants for protein kinases and protein phosphatases. *J Biol Chem* 266:15555–15558.
- Knapp AG, Schmidt KF, Dowling JE (1990) Dopamine modulates the kinetics of ion channels gated by excitatory amino acids in retinal horizontal cells. *Proc Natl Acad Sci U S A* 87:767–771.
- Kohr G, Seeburg PH (1996) Subtype-specific regulation of recombinant NMDA receptor-channels by protein tyrosine kinases of the src family. *J Physiol* 492 (Pt 2):445–452.
- Lee HK, Barbarosie M, Kameyama K, Bear MF, Hugarir RL (2000) Regulation of distinct AMPA receptor phosphorylation sites during bidirectional synaptic plasticity. *Nature* 405:955–959.
- Lee HK, Kameyama K, Hugarir RL, Bear MF (1998) NMDA induces long-term synaptic depression and dephosphorylation of the GluR1 subunit of AMPA receptors in hippocampus. *Neuron* 21:1151–1162.
- Leonard AS, Hell JW (1997) Cyclic AMP-dependent protein kinase and protein kinase C phosphorylate N-methyl-D-aspartate receptors at different sites. *J Biol Chem* 272:12107–12115.
- Lerma J (2006) Kainate receptor physiology. *Curr Opin Pharmacol* 6:89–97.
- Li G, Oswald RE, Niu L (2003) Channel-opening kinetics of GluR6 kainate receptor. *Biochemistry* 42:12367–12375.
- Lieberman DN, Mody I (1994) Regulation of NMDA channel function by endogenous Ca(2+)-dependent phosphatase. *Nature* 369:235–239.
- Malinow R, Malenka RC (2002) AMPA receptor trafficking and synaptic plasticity. *Annu Rev Neurosci* 25:103–126.
- Mammen AL, Kameyama K, Roche KW, Hugarir RL (1997) Phosphorylation of the alpha-amino-3-hydroxy-5-methylisoxazole-4-propionic acid receptor GluR1 subunit by calcium/calmodulin-dependent kinase II. *J Biol Chem* 272:32528–32533.
- Mayer ML (2005) Crystal structures of the GluR5 and GluR6 ligand binding cores: Molecular mechanisms underlying kainate receptor selectivity. *Neuron* 45:539–552.
- McGlade-McCulloh E, Yamamoto H, Tan SE, Brickey DA, Soderling TR (1993) Phosphorylation and regulation of glutamate receptors by calcium/calmodulin-dependent protein kinase II. *Nature* 362:640–642.
- Moss SJ, Blackstone CD, Hugarir RL (1993) Phosphorylation of recombinant non-NMDA glutamate receptors on serine and tyrosine residues. *Neurochem Res* 18:105–110.
- Nishimune A, Isaac JT, Molnar E, Noel J, Nash SR, Tagaya M, Collingridge GL, Nakanishi S, Henley JM (1998) NSF binding to GluR2 regulates synaptic transmission. *Neuron* 21:87–97.
- Omkumar RV, Kiely MJ, Rosenstein AJ, Min KT, Kennedy MB (1996) Identification of a phosphorylation site for calcium/calmodulin dependent protein kinase II in the NR2B subunit of the N-methyl-D-aspartate receptor. *J Biol Chem* 271:31670–31678.
- Plautz JD, Day RN, Dailey GM, Welsh SB, Hall JC, Halpain S, Kay SA (1996) Green fluorescent protein and its derivatives as versatile markers for gene expression in living *Drosophila melanogaster*, plant and mammalian cells. *Gene* 173:83–87.
- Raymond LA, Blackstone CD, Hugarir RL (1993) Phosphorylation and modulation of recombinant GluR6 glutamate receptors by cAMP-dependent protein kinase. *Nature* 361:637–641.
- Roche KW, O'Brien RJ, Mammen AL, Bernhardt J, Hugarir RL (1996) Characterization of multiple phosphorylation sites on the AMPA receptor GluR1 subunit. *Neuron* 16:1179–1188.
- Saiki RK, Gelfand DH, Stoffel S, Scharf SJ, Higuchi R, Horn GT, Mullis KB, Erlich HA (1988) Primer-directed enzymatic amplification of DNA with a thermostable DNA polymerase. *Science* 239:487–491.
- Salinas GD, Blair LA, Needleman LA, Gonzales JD, Chen Y, Li M, Singer JD, Marshall J (2006) Actinfilin is a Cul3 substrate adaptor, linking GluR6 kainate receptor subunits to the ubiquitin-proteasome pathway. *J Biol Chem* 281:40164–40173.
- Scott DB, Blanpied TA, Swanson GT, Zhang C, Ehlers MD (2001) An NMDA receptor ER retention signal regulated by phosphorylation and alternative splicing. *J Neurosci* 21:3063–3072.
- Shi S, Hayashi Y, Esteban JA, Malinow R (2001) Subunit-specific rules governing AMPA receptor trafficking to synapses in hippocampal pyramidal neurons. *Cell* 105:331–343.
- Smith CM, Radzio-Andzelm E, Madhusudan ?, Akamine P, Taylor SS (1999) The catalytic subunit of cAMP-dependent protein kinase: prototype for an extended network of communication. *Prog Biophys Mol Biol* 71:313–341.
- Song I, Kamboj S, Xia J, Dong H, Liao D, Hugarir RL (1998) Interaction of the N-ethylmaleimide-sensitive factor with AMPA receptors. *Neuron* 21:393–400.
- Songyang Z, Blechner S, Hoagland N, Hoekstra MF, Piwnicka-Worms H, Cantley LC (1994) Use of an oriented peptide library to determine the optimal substrates of protein kinases. *Curr Biol* 4:973–982.
- Standley S, Roche KW, McCallum J, Sans N, Wenthold RJ (2000) PDZ domain suppression of an ER retention signal in NMDA receptor NR1 splice variants. *Neuron* 28:887–898.
- Subramanian S, Srien F (1996) Quantitative analysis of transient gene expression in mammalian cells using the green fluorescent protein. *J Biotechnol* 49:137–151.
- Tingley WG, Ehlers MD, Kameyama K, Doherty C, Ptak JB, Riley CT, Hugarir RL (1997) Characterization of protein kinase A and protein kinase C phosphorylation of the N-methyl-D-aspartate receptor NR1 subunit using phosphorylation site-specific antibodies. *J Biol Chem* 272:5157–5166.
- Tingley WG, Roche KW, Thompson AK, Hugarir RL (1993) Regulation of NMDA receptor phosphorylation by alternative splicing of the C-terminal domain. *Nature* 364:70–73.
- Traynelis SF, Wahl P (1997) Control of rat GluR6 glutamate receptor open probability by protein kinase A and calcineurin. *J Physiol (Lond)* 503:513–531.
- Udgaonkar JB, Hess GP (1987) Chemical kinetic measurements of a mammalian acetylcholine receptor by a fast-reaction technique. *Proc Natl Acad Sci U S A* 84:8758–8762.
- Wang LY, Dudek EM, Browning MD, MacDonald JF (1994) Modulation of AMPA/kainate receptors in cultured murine hippocampal neurons by protein kinase C. *J Physiol* 475:431–437.

- Wang LY, Taverna FA, Huang XP, MacDonald JF, Hampson DR (1993) Phosphorylation and modulation of a kainate receptor (GluR6) by cAMP-dependent protein kinase. *Science* 259:1173–1175.
- Werner P, Voigt M, Keinänen K, Wisden W, Seeburg PH (1991) Cloning of a putative high-affinity kainate receptor expressed predominantly in hippocampal CA3 cells. *Nature* 351:742–744.
- Whitlock JR, Heynen AJ, Shuler MG, Bear MF (2006) Learning induces long-term potentiation in the hippocampus. *Science* 313:1093–1097.
- Wo ZG, Chohan KK, Chen H, Sutcliffe MJ, Oswald RE (1999) Cysteine mutagenesis and homology modeling of the ligand-binding site of a kainate-binding protein. *J Biol Chem* 274:37210–37218.
- Wo ZG, Oswald RE (1994) Transmembrane topology of two kainate receptor subunits revealed by N-glycosylation. *Proc Natl Acad Sci U S A* 91:7154–7158.
- Wo ZG, Oswald RE (1995a) A topological analysis of goldfish kainate receptors predicts three transmembrane segments. *J Biol Chem* 270:2000–2009.
- Wo ZG, Oswald RE (1995b) Unraveling the modular design of glutamate-gated ion channels. *Trends Neurosci* 18:161–168.
- Yan S, Sanders JM, Xu J, Zhu Y, Contractor A, Swanson GT (2004) A C-terminal determinant of GluR6 kainate receptor trafficking. *J Neurosci* 24:679–691.
- Zetterqvist O, Ragnarsson U, Humble E, Berglund L, Engstrom L (1976) The minimum substrate of cyclic AMP-stimulated protein kinase, as studied by synthetic peptides representing the phosphorylatable site of pyruvate kinase (type L) of rat liver. *Biochem Biophys Res Commun* 70:696–703.
- Zheng F, Gingrich MB, Traynelis SF, Conn PJ (1998) Tyrosine kinase potentiates NMDA receptor currents by reducing tonic zinc inhibition. *Nat Neurosci* 1:185–191.

(Accepted 7 February 2007)
(Available online 26 March 2007)

Mechanism of Inhibition of the GluR2 AMPA Receptor Channel Opening by 2,3-Benzodiazepine Derivatives[†]

Mark Ritz,[‡] Nicola Micale,[§] Silvana Grasso,[§] and Li Niu^{*;‡}

Department of Chemistry and Center for Neuroscience Research, University at Albany, State University of New York, Albany, New York 12222, and Dipartimento Farmaco-Chimico, Università di Messina, viale Annunziata, 98168 Messina, Italy

Received April 25, 2007; Revised Manuscript Received October 9, 2007

ABSTRACT: 2,3-Benzodiazepine derivatives are drug candidates synthesized for potential treatment of various neurodegenerative diseases involving the excessive activity of AMPA receptors. Here we describe a rapid kinetic investigation of the mechanism of inhibition of the GluR2_{Qnip} AMPA receptor channel opening by two 2,3-benzodiazepine derivatives that are structurally similar (BDZ-2 and BDZ-3). Using a laser-pulse photolysis technique with a time resolution of $\sim 60 \mu\text{s}$, we measured the effects of these inhibitors on both the channel opening rate and the whole-cell current amplitude. We found that both compounds preferably inhibit the open-channel state, although BDZ-2 is a more potent inhibitor in that it inhibits the open-channel state ~ 5 -fold stronger than BDZ-3 does. Both compounds bind to the same noncompetitive site. Binding of an inhibitor to the receptor involves the formation of a loose, partially conducting channel intermediate, which rapidly isomerizes to a tighter complex. The isomerization reaction is identified as the main step at which the receptor distinguishes the structural difference between the two compounds. These results suggest that addition of a bulky group at the N-3 position on the diazepine ring, as in BDZ-3, does not alter the mechanism of action, or the site of binding, but does lower the inhibitory potency, possibly due to an unfavorable interaction of a bulky group at the N-3 position with the receptor site. The new mechanistic revelation about the structure–reactivity relationship is useful in designing conformation-specific, more potent noncompetitive inhibitors for the GluR2 AMPA receptor.

Glutamate ion channels are classified into three subtypes: N-methyl-D-aspartic acid (NMDA), α -amino-3-hydroxy-5-methyl-4-isoxazolepropionic acid (AMPA),¹ and kainate receptors (1, 2). AMPA receptors mediate the majority of fast excitatory neurotransmission in the mammalian central nerve system and are essential in brain activities such as memory and learning (1, 2). Excessive activation of AMPA receptors is, however, known to induce calcium-mediated neurodegeneration, which underlies a variety of acute and chronic neurological disorders, such as post-ischemia cell death, Huntington's chorea, and amyotrophic lateral sclerosis (2). Developing AMPA receptor inhibitors to control the excessive receptor activity has been a long-pursued therapeutic approach to the treatment of these neurological disorders (3). To make new inhibitors more potent and selective for AMPA receptors, the mechanism of action of existing inhibitors needs to be investigated, and the structure–reactivity relationship for those structurally related compounds needs to be characterized.

2,3-Benzodiazepine derivatives, also known as GYKI compounds, represent one of the best classes of inhibitors in terms of their selectivity and affinity for AMPA receptors. GYKI 52466 [1-(4-aminophenyl)-4-methyl-7,8-methylenedioxy-5H-2,3-benzodiazepine] is the first inhibitor in this class discovered in the 1980s (4). Since then, hundreds of 2,3-benzodiazepine derivatives have been synthesized (5–7). GYKI compounds are considered allosteric regulators or noncompetitive inhibitors, a conclusion drawn largely from binding studies using radioactive agonists (6). However, the detailed mechanism by which 2,3-benzodiazepines inhibit AMPA receptors is not well documented. This deficiency can be mainly ascribed to the fact that an AMPA receptor opens its channel on the microsecond time scale following glutamate binding (8–10) but is desensitized or becomes inactivated while glutamate remains bound even on the millisecond time scale (11). As a result, the agonist binding assay is most relevant to characterization of the inhibitory effect on desensitized receptors. To assess the channel opening reaction for AMPA receptors, we have previously used a laser-pulse photolysis technique, together with a photolabile precursor of glutamate or the caged glutamate [i.e., γ -O-(α -carboxy-2-nitrobenzyl)glutamate] (12). We have shown that a channel opening reaction can be measured prior to the channel desensitization (8, 10, 13, 14).

Here we investigated the mechanism of inhibition of the opening of the GluR2_{Qnip} channel by two 2,3-benzodiazepine compounds, 1-(4-aminophenyl)-3,5-dihydro-7,8-methylenedioxy-4H-2,3-benzodiazepin-4-one (BDZ-2) and its 3-N-

[†] This work was supported in part by grants from the Department of Defense (W81XWH-04-1-0106), the ALS Association, and the American Heart Association (0130513T) (to L.N.).

* To whom correspondence should be addressed. Telephone: (518) 591-8819. Fax: (518) 442-3462. E-mail: lniu@albany.edu.

[‡] University at Albany, State University of New York.

[§] Università di Messina.

¹ Abbreviations: AMPA, α -amino-3-hydroxy-5-methyl-4-isoxazolepropionic acid; BDZ, 2,3-benzodiazepine compounds; GYKI 52466, 1-(4-aminophenyl)-4-methyl-7,8-methylenedioxy-5H-2,3-benzodiazepine; caged glutamate, γ -O-(α -carboxy-2-nitrobenzyl)glutamate; HEK cells, human embryonic kidney cells.

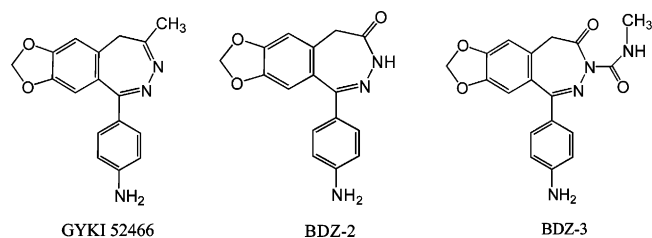


FIGURE 1: Chemical structures of GYKI 52466, BDZ-2, and BDZ-3. The chemical names for these compounds are given in the text.

methylcarbamoyl derivative (BDZ-3) (15) (Figure 1). BDZ-2 and BDZ-3 are structurally related to GYKI 52466, a template based on which many derivatives are synthesized (Figure 1). Compared to GYKI 52466, the 4-methyl group is replaced by a carbonyl group in both BDZ-2 and BDZ-3. The GluR2_{flip} channel was chosen for this study because the GluR2 subunit in the unedited or Q (glutamine) isoform is known to control the calcium permeability of heteromeric AMPA receptors (16, 17) and is thus considered a key subunit mediating excitotoxicity (18). The effect of an inhibitor on the channel opening and channel closing rate constants as well as the whole-cell current amplitude was determined with human embryonic kidney (HEK-293) cells that expressed the GluR2_{flip} AMPA channels. Our results show that BDZ-2 and BDZ-3 bind to the same site, and both preferably inhibit the open-channel state of the GluR2_{flip} receptor, although BDZ-2 is a stronger noncompetitive inhibitor. Furthermore, the inhibition of the receptor channel by these compounds likely involves the formation of a loose, partially conducting inhibitor–receptor intermediate, which rapidly isomerizes to a tighter, inhibitory complex. The implication of these results on the structure–reactivity relationship for developing more potent, conformation-specific 2,3-benzodiazepine derivatives is discussed.

EXPERIMENTAL PROCEDURES

Cell Culture and Receptor Expression. HEK-293S cells were cultured in Dulbecco's modified Eagle's medium supplemented with 10% fetal bovine serum and in a 37 °C, 5% CO₂, humidified incubator. GluR2_{flip} was transiently expressed in these cells using a calcium phosphate method (8). HEK-293S cells were also cotransfected with a plasmid encoding green fluorescent protein and a separate plasmid encoding large T-antigen (19). The weight ratio of the plasmid for GluR2 to that for green fluorescent protein and large T-antigen was 1:0.2:10, and the GluR2_{flip} plasmid used for transfection was ~5–10 μg/35 mm dish. After 48 h, the transfected cells were used for recording.

Whole-Cell Current Recording. A recording electrode was made from a glass capillary (World Precision Instruments, Sarasota, FL) and had a resistance of ~3 MΩ when filled with the electrode buffer. The electrode buffer was composed of 110 mM CsF, 30 mM CsCl, 4 mM NaCl, 0.5 mM CaCl₂, 5 mM EGTA, and 10 mM HEPES (pH 7.4, adjusted with CsOH). The external buffer contained 150 mM NaCl, 3 mM KCl, 1 mM CaCl₂, 1 mM MgCl₂, and 10 mM HEPES (pH 7.4, adjusted with NaOH). The whole-cell current was recorded with a cell voltage clamped at –60 mV, using an Axopatch-200B amplifier at cutoff frequency of 2–20 kHz by a built-in, eight-pole Bessel filter, and digitized at a sampling frequency of 5–50 kHz using an Axon Digidata

1322A instrument. The data were acquired using pCLAMP 8 (Molecular Devices, Sunnyvale, CA). All recordings were performed at room temperature. Unless otherwise noted, each data point was the average of at least three measurements collected from at least three cells.

Laser-Pulse Photolysis Measurements. The use of the laser-pulse photolysis technique to measure the channel opening kinetics has been described previously (8). Briefly, the caged glutamate (12) (Invitrogen, Carlsbad, CA) was dissolved in the external buffer and applied to a cell using a flow device (20) (see below). In the laser-pulse photolysis measurement of channel opening, a single laser pulse at 355 nm with a pulse length of 8 ns was generated from a pulsed Q-switched Nd:YAG laser (Continuum, Santa Clara, CA). The pulse energy varied in the range of 200–800 μJ, measured at the end of an optical fiber (300 μm core diameter) to which the laser beam was coupled. To calibrate the concentration of photolytically released glutamate, we applied two solutions of free glutamate with known concentrations to the same cell before and after a laser flash (9). The current amplitudes obtained from this calibration were compared with the amplitude from the laser measurement with reference to the dose–response relationship. These measurements also allowed us to monitor any damage to the receptors and/or the cell for successive laser experiments with the same cell (8).

To deliver an inhibitor to a cell, we used a “Ψ”-shaped flow device (21). The central tubing in the Ψ device was filled with an inhibitor solution for preincubation such that the solution was applied prior to the application of free glutamate as the control or free glutamate but mixed with the same inhibitor at the same concentration. In all experiments reported in this study, a 3 s preincubation flow protocol was required for both BDZ-2 and BDZ-3 to exert full inhibition of the receptor; a preincubation longer than 3 s caused no further current reduction. Furthermore, the 3 s preincubation for the ensuing inhibition was independent of glutamate concentration (and thus independent of the receptor form; see the explanation in the text). When the free glutamate was used to induce the receptor response in the absence and presence of an inhibitor, the amplitude of the whole-cell current observed using the flow device was corrected for receptor desensitization by a method previously described (20). The corrected current amplitude was used for data analysis.

Experimental Design and Data Analysis. To investigate the mechanism of inhibition, the effects of BDZ-2 or BDZ-3 on the channel opening rate constant (k_{op}) and channel closing rate constant (k_{cl}) were determined. These measurements were carried out at two glutamate concentrations by the following rationale. The observed rate constant (k_{obs}) of GluR2_{flip} channel opening is a function of ligand concentration (see eq 2; eq 2 and all other equations are in the Appendix), which includes both rate terms, k_{op} and k_{cl} . This is particularly true experimentally when the molar concentration of ligand or glutamate (L) is either comparable to or larger than the value of the intrinsic equilibrium constant for the ligand (K_1) (8). However, when the ligand concentration is lowered (i.e., $L \ll K_1$), the k_{obs} expression or eq 2 is reduced to $k_{obs} \approx k_{cl}$. Under such a condition, the effect of an inhibitor on, and its inhibition constant for, the open-

182 channel state can be determined (eq 4). At a higher ligand
 183 concentration, where $k_{obs} > k_{cl}$, the k_{op} value can be
 184 determined from the difference between k_{obs} and k_{cl} or by
 185 rearranging eq 2 in that $k_{obs} - k_{cl} = k_{op}[L/(L + K_1)]^2$.
 186 Accordingly, the effect of the inhibitor on k_{op} and the
 187 inhibition constant for the closed-channel state can be
 188 measured (eq 5). Previously, we measured k_{op} and k_{cl} for
 189 GluR2Q_{flip} (8) and also established the criteria under which
 190 k_{cl} can be determined from the measurement of k_{obs} (8, 9).
 191 For GluR2Q_{flip}, k_{cl} is numerically equal to the k_{obs} obtained
 192 at $\sim 100 \mu\text{M}$ glutamate, which corresponded to $\sim 4\%$ of the
 193 fraction of the open-channel form (8).

194 The experimental design of using current amplitude to
 195 determine the inhibition constant for both the open-channel
 196 and closed-channel states required varying concentrations of
 197 glutamate (see eqs 6a and 6b). Specifically, at low glutamate
 198 concentrations (i.e., $L \ll K_1$), the majority of the receptor
 199 was in the closed-channel state (see Figure 5; defined as the
 200 unliganded, singly liganded, and doubly liganded forms).
 201 Under this condition, the inhibition constant for the closed-
 202 channel state was determined from the ratio of the amplitude
 203 (see eqs 6a and 6b). Likewise, at a saturating ligand
 204 concentration (i.e., $L \gg K_1$), the majority of the receptor
 205 was in the open-channel state. Consequently, the inhibition
 206 constant associated with the open-channel state was mea-
 207 sured. The basis of using the two ligand concentrations that
 208 corresponded to ~ 4 and $\sim 95\%$ of the open-channel form
 209 (8) to determine the corresponding inhibition constant was
 210 a putative difference in affinity with which a compound
 211 inhibited the receptor as a function of agonist concentration.
 212 At those very low and very high ligand concentrations (8),
 213 the apparent inhibition constants were considered pertinent
 214 to the closed-channel and open-channel states, respectively.

215 In double-inhibitor experiments where two inhibitors were
 216 used at the same time, the concentration of one inhibitor was
 217 kept constant while the concentration of the other was varied
 218 (eqs 7 and 8). In these experiments, only the amplitude in
 219 the presence (A_1) and absence (A) of two inhibitors was
 220 determined. All of the other conditions were the same as
 221 described before.

222 Origin 7 (Origin Lab, Northampton, MA) was used for
 223 both linear and nonlinear regressions (Levenberg–Marquardt
 224 and simplex algorithms). The error reported refers to the
 225 standard error of the fits, unless noted otherwise.

226 RESULTS

227 BDZ-2 and BDZ-3 are previously known to inhibit
 228 endogenous AMPA receptors in native tissues (15). Whether
 229 they specifically inhibit the GluR2 AMPA receptor subunit
 230 is unclear. Here, we first determined that BDZ-2 and BDZ-3
 231 inhibited the GluR2Q_{flip} receptor, as evidenced, for example,
 232 by the reduction of the amplitude of the glutamate-induced
 233 whole-cell current via the GluR2 channel in the presence of
 234 an inhibitor (Figure 2). At all concentrations of inhibitors
 235 and glutamate that were tested, neither inhibitor affected the
 236 rate of receptor desensitization, consistent with earlier reports
 237 for this class of inhibitors in general (22, 23). We thus
 238 focused our investigation of the effect of an inhibitor on both
 239 the rate of the channel opening and the maximum current
 240 amplitude. For clarity, however, we present experimental data
 241 mostly for BDZ-2 since the BDZ-3 data are qualitatively
 242 the same.

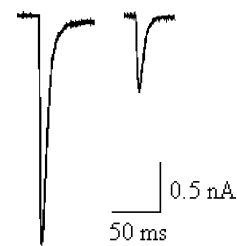


FIGURE 2: Representative whole-cell current traces via GluR2Q_{flip} channels expressed in HEK-293 cells in the absence (left) and presence (right) of BDZ-2. The concentrations of glutamate and the inhibitor were 3 mM and 10 μM , respectively. The whole-cell current was recorded at -60 mV , pH 7.4, and $22 \text{ }^\circ\text{C}$.

243 *Effect of BDZ-2 and BDZ-3 on the Channel Opening Rate*
 244 *Constants.* The rise of the whole-cell current via the
 245 GluR2Q_{flip} channel, initiated by laser photolysis of the caged
 246 glutamate, reflected channel opening (Figure 3A) (8). As
 247 compared to the control, the current rise was slowed and
 248 the amplitude was concomitantly reduced in the presence of
 249 BDZ-2 (Figure 3A), consistent with the notion that BDZ-2
 250 inhibited the channel opening of GluR2Q_{flip}. Furthermore,
 251 the observed rate constant in the absence (k_{obs}) and presence
 252 of BDZ-2 (k_{obs}') followed a first-order rate expression (eq
 253 1) for $\sim 95\%$ of the rising phase (Figure 3A). Such a
 254 monophasic rate process was observed at both 100 ± 10
 255 and $250 \pm 20 \mu\text{M}$ photolytically released glutamate and at
 256 all concentrations of either inhibitor, consistent with the
 257 assumption that (a) the binding of glutamate and/or inhibitors
 258 to the receptor was fast relative to channel opening and (b)
 259 the decrease of the rate of channel opening in the presence
 260 of inhibitor was a result of receptor inhibition. Furthermore,
 261 the rate of desensitization, seen as a current decay (Figure
 262 3A), at any given glutamate concentration in the absence
 263 ($8-10, 14$) and presence of an inhibitor at any concentration
 264 was at least 10-fold slower than the rate of current rise,
 265 suggesting that the channel opening rate could be measured
 266 as a distinct kinetic process in the presence of an inhibitor.
 267 Thus, the observed rate constant of the channel opening, i.e.,
 268 k_{obs} or k_{obs}' , was calculated (using eq 1) without the
 269 complication of desensitization. As such, the mechanism of
 270 inhibition of the receptor channel opening (in Figure 5) was
 271 formulated without desensitization.

272 The effects of BDZ-2 on k_{op} and k_{cl} were determined
 273 (Figure 3B,C; see also Experimental Procedures for the
 274 experimental design). As seen here, BDZ-2 affected k_{cl}
 275 (Figure 3B) and k_{op} (Figure 3C). These results indicated that
 276 BDZ-2 inhibited both the closed-channel and open-channel
 277 states (the inhibition constants for both inhibitors are
 278 summarized in Table 1). Our findings are consistent with a
 279 noncompetitive inhibition by these compounds (15) and
 280 suggest that there are regulatory sites to which these
 281 inhibitors can bind and inhibit the channel. The effect of
 282 BDZ-2 and BDZ-3 on the current amplitude, described
 283 below, is also consistent with this conclusion (Table 1).

284 *BDZ-2 and BDZ-3 Inhibited the Channel Opening by a*
 285 *Two-Step Process.* We now examine the reduction of the
 286 whole-cell current amplitude in the presence of inhibitor.
 287 BDZ-2, for instance, reduced the amplitude of the whole-
 288 cell response and concurrently slowed the rate of channel
 289 opening (Figure 3A). An inhibition constant was calculated
 290 from the ratio of the maximum current amplitude in the
 291 absence and presence of BDZ-2 as a function of its

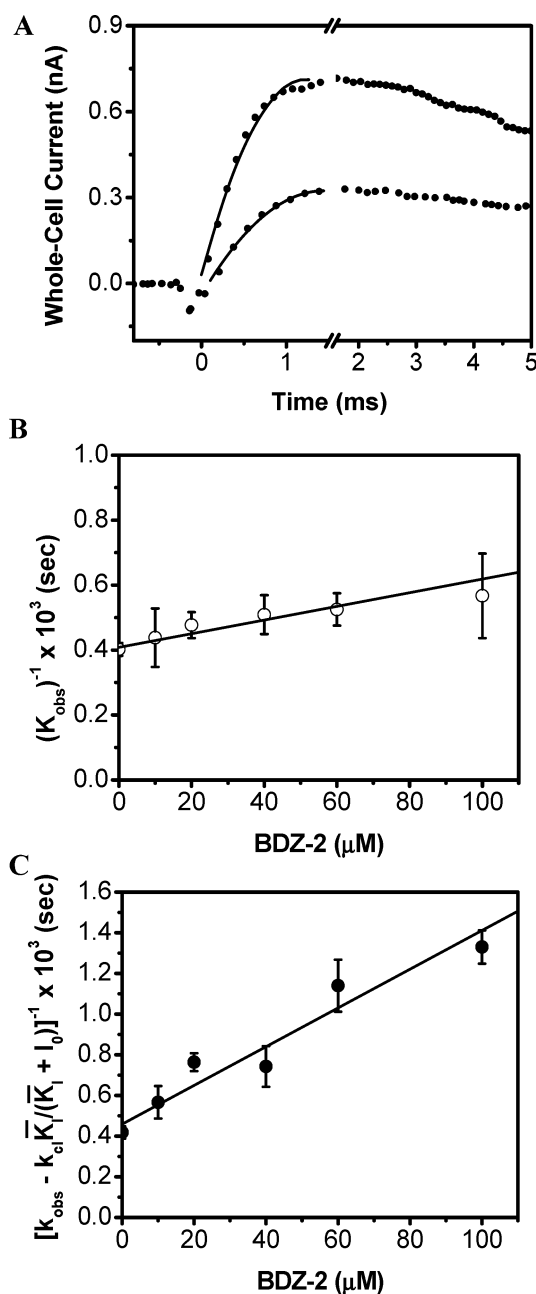


FIGURE 3: Effect of BDZ-2 on the channel opening rate constants. (A) Representative whole-cell current traces from the laser-pulse photolysis experiment showing that BDZ-2 inhibited both the rate and the amplitude of the opening of the GluR2Q_{flip} channel. The top trace is the control ($k_{\text{obs}} = 2519 \text{ s}^{-1}$; $A = 0.70 \text{ nA}$), and the bottom one included $20 \mu\text{M}$ BDZ-2 ($k_{\text{obs}} = 2114 \text{ s}^{-1}$; $A_I = 0.33 \text{ nA}$). In both traces, the concentration of the photolytically released glutamate was estimated to be $150 \mu\text{M}$. (B) Effect of BDZ-2 on k_{cl} obtained at $100 \mu\text{M}$ glutamate and as a function of BDZ-2 concentration. From this plot, a \bar{K}_1^* of $194 \pm 20 \mu\text{M}$ was obtained, using eq 4. (C) Effect of BDZ-2 on k_{op} obtained at $250 \mu\text{M}$ glutamate and as a function of BDZ-2 concentration. From this plot, a K_1^* of $48 \pm 5 \mu\text{M}$ was determined, using eq 5. All of the inhibition constants are summarized in Table 1.

292 concentration (eq 6 and Figure 4). However, the inhibition
 293 constant for both the open-channel and closed-channel
 294 states, obtained from the amplitude measurement, was
 295 always found to be smaller than the corresponding
 296 value obtained from the rate measurement (Table 1).
 297 A one-step inhibition model in which the binding of
 298 an inhibitor to the receptor directly led to a complete
 inhibition could not account for this

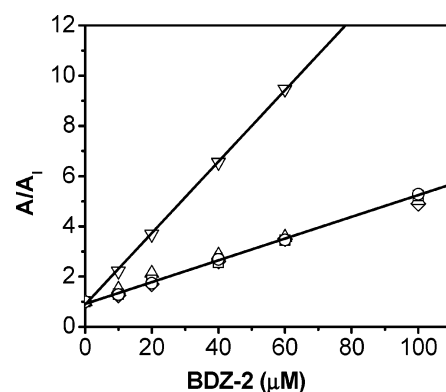


FIGURE 4: Effect of BDZ-2 on the amplitude of the whole-cell current in the absence (A) and presence (A_I) of BDZ-2. An inhibition constant was calculated from this plot using eq 6. At 3 mM glutamate (∇), a \bar{K}_1 of $6.9 \pm 1.0 \mu\text{M}$ was obtained, corresponding to the inhibition constant for the open state; a K_1 of $24.8 \pm 1.0 \mu\text{M}$ was obtained for the closed-channel state at a glutamate concentration of $100 \mu\text{M}$ (\diamond). In both cases, the amplitude was from the flow measurements. From laser-photolysis measurements, a K_1 of $25.2 \pm 1.0 \mu\text{M}$ was obtained from the data at $100 \mu\text{M}$ glutamate and varied concentrations of BDZ-2 (\triangle). At $250 \mu\text{M}$ glutamate (\circ), the \bar{K}_1 was determined to be $23.0 \pm 1.0 \mu\text{M}$.

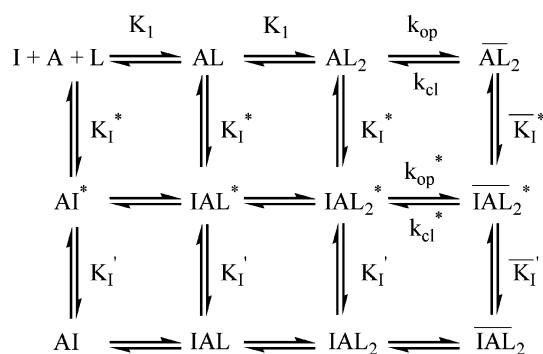


FIGURE 5: Minimal mechanism of the inhibition of the GluR2Q_{flip} receptor by BDZ-2 and BDZ-3 involving an intermediate state. L represents ligand or glutamate, and the number of ligands that bind to and open the channel is assumed to be two (8). Here, A represents the active, unliganded form of the receptor, and I represents an inhibitor. For simplicity and without contrary evidence, it is assumed that glutamate binds with equal affinity or K_1 , the intrinsic equilibrium dissociation constant, at all binding steps. All the species with an asterisk symbolize those at the intermediate state, whereas those species bound with inhibitor but without an asterisk represent those of the final state. All species related to A, AL, and AL_2 , including those bound with inhibitors, are in the closed-channel state, whereas those related to $\overline{AL_2}$ refer to the open-channel state.

299 discrepancy (24). With such a model, the inhibition constant
 300 obtained from the rate measurement would be the same as
 301 the one obtained from the current amplitude (24). However,
 302 the discrepancy could be ascribed to a minimal mechanism
 303 (in Figure 5) in which the binding of BDZ-2 or BDZ-3
 304 to the receptor initially formed an intermediate (e.g., $\overline{IAL_2^*}$)
 305 in the first step, and such an intermediate was partially
 306 conducting; in the second step, the intermediate isomerized
 307 rapidly to form an inhibitory complex ($\overline{IAL_2}$). The two-step
 308 inhibition process would apply to both the closed-channel
 309 and open-channel states, on the basis of our experimental
 310 results (Figure 3B,C).

311 Using this isomerization model (Figure 5), the discrepancy
 312 in the magnitude of the inhibition constant between the rate
 313 and the amplitude measurements can now be explained. First,

Table 1: Inhibition Constants of BDZ-2 and BDZ-3, Obtained from Rate and Amplitude Measurements, for the Closed-Channel and Open-Channel States of GluR2Q_{flip}

	rate measurement ^a			amplitude measurement		
	K_1^* (μM) ^b (closed channel)	\overline{K}_1^* (μM) ^b (open channel)	K_1 (μM) ^{b,d}	\overline{K}_1 (μM) ^{b,e}	K_1 (μM) ^{c,d} (closed channel)	\overline{K}_1 (μM) ^{c,f} (open channel)
BDZ-2	48 ± 5	194 ± 20	25.2 ± 1.0	23.0 ± 1.0	24.8 ± 1.0	6.9 ± 1.0
BDZ-3	514 ± 60	204 ± 18	200 ± 18	69 ± 4.0	210 ± 20	38 ± 10

^a The constants obtained from rate measurements represent those in the first step of inhibition as in Figure 5, whereas those obtained from the amplitude measurements represent the overall inhibition constants. ^b Laser-pulse photolysis measurement. ^c Cell-flow measurement. ^d Measurements at 100 μM glutamate for the closed-channel state. ^e Measurements at 250–350 μM glutamate. ^f Measurements at 3 mM glutamate.

the maximum current amplitude was related to the fraction of the open-channel form at the quasi-equilibrium level, which depended on glutamate concentration (see eq 6b). Therefore, a smaller inhibition constant or a stronger inhibition obtained from the amplitude measurement, as compared with the corresponding inhibition constant from the rate measurement at the same glutamate concentration, suggested that the magnitude of the receptor inhibition obtained from the rate measurement could not account for the total inhibition. An additional step, followed by the formation of the initial, partially conducting receptor–inhibitor intermediate, must be involved to presumably turn the intermediate into a tighter complex, thereby yielding additional inhibition. This assumption is supported by a ratio of inhibition constants being ~ 28 for the open-channel state (i.e., 194 $\mu\text{M}/6.9 \mu\text{M}$) in the case of BDZ-2 and a ratio of ~ 2 for the closed-channel state (i.e., 48 $\mu\text{M}/24.8 \mu\text{M}$) (in Table 1). BDZ-3 showed a similar, albeit less significant, reduction of the corresponding inhibition constant via the second step (Table 1). Second, a single-exponential current rise for the opening of the channel (Figure 3B) was always observed at all concentrations of the inhibitor (and glutamate), suggesting that the rate constants associated with the two steps in the presence of an inhibitor (Figure 5) were significantly different. If the two rates in the presence of an inhibitor were comparable, a double-exponential rate process would be expected at a certain concentration range of an inhibitor during the whole-cell current rise. Furthermore, the $1/k_{\text{obs}}$ increased linearly with an increase in inhibitor concentration, as predicted by eqs 3–5 derived from one-step inhibition (i.e., the scheme only involving the top and middle rows in Figure 5 with the assumption that the second step is much faster than the first step). Such a linear correlation remained at different glutamate concentrations where the effects of an inhibitor on both k_{cl} and k_{op} were determined (Figure 3B,C). As a result, this linearity allowed us to calculate K_1^* and K^* for the intermediate associated with the open channel and closed channel, respectively. If the second step were slow and were measured during the rising phase of the whole-cell current, then the one-step inhibition model should have fully accounted for the inhibition. Consequently, the inhibition constant obtained from the rate measurement would have been identical to the corresponding value obtained from the amplitude measurement (24).

Effect of BDZ-2 and BDZ-3 on the Whole-Cell Current Amplitude Determined in Flow Measurements. As an independent approach to evaluation of inhibition constants for both BDZ-2 and BDZ-3 based on the whole-cell current amplitude, we also used a solution flow technique with

known concentrations of free glutamate and measured the whole-cell current amplitude in the absence and presence of an inhibitor. The experimental design of using current amplitude to determine the inhibition constants for both the open-channel and closed-channel states required varying concentrations of glutamate (see Experimental Procedures and eqs 6a and 6b). Here, glutamate concentrations from 100 μM to 5 mM were chosen, which corresponded to the fraction of the open-channel form being from ~ 4 to $\sim 95\%$, respectively [note that the channel opening probability for this receptor is 96% (8)]. The apparent inhibition constants for both BDZ-2 and BDZ-3 were therefore determined at these glutamate concentrations (Figure 4 and Table 1).

Several conclusions can be drawn from these results. First, at a comparable glutamate concentration such as 100 or 250 μM , the A/A_1 ratios determined from the flow measurements were identical, within experimental error, to those obtained from the laser-pulse photolysis measurements for both inhibitors (Table 1). Second, at 3 mM glutamate where $\sim 93\%$ of the channels were in the open-channel state, the apparent inhibition constant was considered virtually a measure of the affinity of BDZ-2 for the open-channel state, \overline{K}_1 , of the GluR2Q_{flip} receptor (see eq 6). Thus, comparison of K_1 with K_1 , the inhibition constant for the closed-channel state, shows that BDZ-2 inhibits the open-channel state ~ 3.6 -fold more strongly (Table 1). BDZ-3, on the other hand, shows a 5-fold stronger inhibition for the open-channel state (Table 1). Third, BDZ-2 is a more potent inhibitor, because it has 5.5- and 8-fold higher affinities for the open-channel and closed-channel states of GluR2Q_{flip}, respectively, than BDZ-3 does.

BDZ-2 and BDZ-3 Bind to the Same Inhibitory Site on the GluR2Q_{flip} Receptor. On kinetic grounds (Table 1), BDZ-2 and BDZ-3 share essential functional similarities in that each inhibitor binds to a regulatory (i.e., inhibitory) site on the GluR2Q_{flip} receptor; both inhibit preferentially the open-channel state, although BDZ-2 is a stronger noncompetitive inhibitor. Given the structural similarity between these two compounds (Figure 1), we asked whether they competed for the same regulatory site or bound to two different sites on the receptor. The answer to this question shall have a meaningful implication in improving our understanding of the structure–reactivity relationship of the GYKI compound series, particularly in the prediction of the putative consequence of derivatization at the N-3 position of the diazepam ring.

To address whether the two compounds competed for one inhibitory site or bound separately to two sites, we carried out a double-inhibitor experiment (see Experimental Proce-

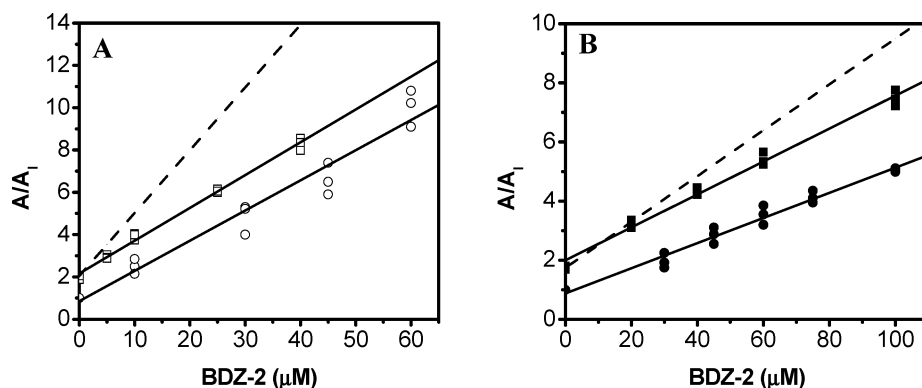


FIGURE 6: Double-inhibition experiments involving both BDZ-2 and BDZ-3. (A) Double inhibition of the open-channel state (3 mM glutamate) of the GluR2Q_{flip} receptor by both BDZ-2 and BDZ-3. The concentration of BDZ-3 was fixed at 40 μM , whereas the concentration of BDZ-2 was varied. The empty circles represent data for BDZ-2 only, and the empty squares represent data for double inhibition by both BDZ-2 and BDZ-3. The K_I of the double inhibition is $6.4 \pm 0.2 \mu\text{M}$ compared to the value of $6.9 \pm 0.5 \mu\text{M}$ for just BDZ-2 (Table 1). (B) Double inhibition of the closed-channel state (100 μM glutamate) of the GluR2Q_{flip} receptor by both BDZ-2 and BDZ-3. The concentration of BDZ-3 was fixed at 100 μM , whereas that of BDZ-2 was varied. The filled circles represent data for BDZ-2 only, while the filled squares represent data for both BDZ-2 and BDZ-3. The K_I of the double inhibition was found to be $19.0 \pm 1.0 \mu\text{M}$, compared to the K_I of 22.0 $\pm 2.0 \mu\text{M}$ for just BDZ-2 (Table 1). Note that all of the amplitudes used here were from solution-flow measurements. In both panels A and B, the top solid line represents the best fit to the data of the double-inhibition experiments, using eq 7, the one-site model (in the Appendix), compared to the bottom solid line which is the best fit to the data of the single-inhibitor experiment, using eq 6. The dashed line in both panels A and B is the simulated double-inhibition result from eq 8, assuming that the two inhibitors bind to two different sites.

dures and Appendix). The comparison of the ratio of the current amplitude in the absence and presence of two inhibitors with the ratio in the presence of just one inhibitor showed that the slope from which a $K_{I,\text{app}}$ value was determined (using eq 7) remained invariant even when the second inhibitor was additionally present (Figure 6). This result suggested that BDZ-2 and BDZ-3 bound to the same site (alternatively, they could bind to two sites, but the binding of the two sites would be mutually exclusive). This conclusion was mutually affirmed from the experiments at two different concentrations of glutamate (Figure 6), which correlated to the open-channel and closed-channel states. Conversely, if BDZ-2 and BDZ-3 bound to two different sites independently, the inhibition would be “additive” or stronger than that of either inhibitor alone, due to an effective increase in the overall concentration of inhibitors bound to the two sites (the dashed line in Figure 6A,B).

DISCUSSION

In this study, we investigated the mechanism of inhibition and the site of interaction for two structurally related inhibitors, BDZ-2 and BDZ-3 (Figure 1). Using the laser-pulse photolysis technique, which previously enabled us to characterize the channel opening rate process of GluR2Q_{flip} (8), we measured the effect of each inhibitor on k_{op} and k_{cl} as well as the whole-cell current amplitude. Our findings reveal new features for the mechanism of action and the structure–reactivity relationship of these compounds.

Site of Interaction of BDZ-2 and BDZ-3 with the GluR2Q_{flip} Receptor and Structure–Reactivity Relationship. Both BDZ-2 and BDZ-3 were found to inhibit the GluR2Q_{flip} channel noncompetitively. This conclusion was based on the finding that each of these compounds affected k_{op} and k_{cl} . If BDZ-2, for instance, inhibited the channel uncompetitively, commonly known as open-channel blockade, only the effect on k_{cl} , not that on k_{op} , would be expected; i.e., the $k_{\text{obs}} - k_{\text{cl}}'$ term in eq 5 would be independent of inhibitor concentration. On the other hand, if BDZ-2 inhibited the channel competitively, only the effect on k_{op} , not that on k_{cl} , would be

expected. Furthermore, it is equally important to note that, as observed in both the photolysis and flow measurements, BDZ-2 also inhibited the whole-cell current under the conditions where the open-channel and closed-channel states were measured. Therefore, the effects of BDZ-2 on both the rate constants and the current amplitude are all consistent with the conclusion that BDZ-2 is a noncompetitive inhibitor. The same conclusion can be drawn for BDZ-3.

BDZ-2 and BDZ-3 were also found to compete for the same noncompetitive site on GluR2Q_{flip}. Both inhibitors exhibit a higher affinity for the open-channel state of the receptor, although BDZ-2 is a stronger inhibitor. It seems that derivatizing BDZ-2 by addition of a methylcarbamoyl group at the N-3 position of the benzodiazepine ring, resulting in BDZ-3, preserves the same mechanism of action but decreases the overall potency for BDZ-3. One plausible explanation is that the same binding site on the receptor does not prefer to accommodate a bulky group at the N-3 position. We therefore hypothesize that addition of a bulky group at the N-3 position, based on the BDZ-2 template, will yield a compound that prefers to inhibit the open-channel conformation of GluR2Q_{flip} but with a weakened potency.

However, several issues remain. First, the kinetic evidence that enabled us to deduce the site of interaction for BDZ-2 and BDZ-3 with the receptor does not provide the clue for the location of this site (except it is distinct from the agonist binding site). In an attempt to address this question, we performed preliminary NMR experiments using ^{15}N -labeled S1S2 derived from the GluR2Q_{flip} receptor but found no change in chemical shifts when BDZ-2 was mixed with S1S2 (Jayaseelan, Shekhtman, and Niu, unpublished result). One possibility is that the S1S2 protein does not contain the noncompetitive site to which BDZ-2 binds (as a control, mixing of either glutamate or NBQX, a competitive antagonist, with S1S2 did show changes in chemical shifts). A previous study by Balannik et al. (25) with a different GYKI compound (i.e., GYKI 53655) suggested that the site of interaction is near the interface between the extracellular binding domain of S1S2 of an AMPA receptor and lipid

490 bilayer. Balannik and co-workers (25) also identified specific
491 amino acid residues affecting the receptor sensitivity to this
492 compound, which are part of the sequences linking the
493 C-termini of S1 and S2 to the transmembrane segments of
494 M1 and M4 or the S1–M1 and S2–M4 regions. However,
495 the linker sequences which cover these residues are not part
496 of the S1S2 construct (25). It should be further noted that
497 the C-terminus of S1S2 ends in the middle of the flip-flop
498 region as compared to the full-length receptor (26). Taken
499 together, the S1S2 construct is likely incomplete in forming
500 the site for noncompetitive inhibitors, as previously suggested
501 (25).

502 Second, it is not yet known what the structural feature(s)
503 confers the open-channel preferring property to both com-
504 pounds. What these compounds have in common, as
505 compared with the structure of the parent compound, GYKI
506 52466 (Figure 1), is the fact that the methyl group at position
507 4 in the benzodiazepine ring of GYKI 52466 is replaced by
508 a carbonyl group in both BDZ-2 and BDZ-3. Whether this
509 replacement makes a difference in conferring such a prefer-
510 ence awaits further study of additional inhibitors, such as
511 GYKI 52466.

512 *Mechanism of Action for BDZ-2 and BDZ-3.* Both BDZ-2
513 and BDZ-3 appear to operate in a two-step process to inhibit
514 the receptor channel. In the first step, an inhibitor forms a
515 loose complex with the receptor, resulting in a partially
516 inhibited channel. In the second step, the intermediate rapidly
517 isomerizes to a tighter complex. This two-step process is
518 evident in a comparison of the inhibition constants associated
519 with the first step and the overall reaction (Table 1). For
520 instance, the inhibition constant for the first step or \overline{K}_1^* is
521 $194 \mu\text{M}$ for BDZ-2, whereas the overall inhibition constant,
522 \overline{K}_1 , becomes $\sim 7 \mu\text{M}$, reflecting a 28-fold higher potency
523 after an isomerization reaction. This comparison suggests
524 that the initial step, resulting in the formation of an inhibitor–
525 receptor intermediate, is far from sufficient to account for
526 the full inhibition.

527 However, the incomplete inhibition through the initial
528 inhibitor–receptor channel is unlikely a result of inadequate
529 equilibration of an inhibitor with the receptor site, although
530 a 3 s preincubation was required for a full inhibition. Such
531 a preincubation time would be too long to be considered
532 relevant to a bimolecular rate process for the binding of these
533 compounds to the receptor site in this case. In one scenario
534 that can explain a long preincubation phenomenon for an
535 inhibitor with a fast binding reaction, a slow diffusional
536 access of an inhibitor to its site is required because the site
537 is covered by membrane or is a buried one. Given the results
538 from Balannik et al. (25) and our results from a NMR study
539 of the S1S2 binding domain, it is possible that the site to
540 which BDZ-2 and BDZ-3 bind is a buried one. However, in
541 spite of slow diffusional access, subsequent steps can be very
542 fast (but the inhibition can be measured only when the bound
543 activating ligand initiates the channel opening process). On
544 the other hand, if there were a slow inhibitor binding reaction
545 so that the binding could not be treated as a rapid equilibrium
546 on the time scale of channel opening, several phenomena
547 would be anticipated. First, on the time scale of channel
548 opening, we would have measured a bimolecular association
549 reaction, rather than an inhibition reaction. As a result, the
550 observed rate at a fixed glutamate concentration would have

551 been higher as the concentration of inhibitor had increased.
552 However, we observed just the opposite (i.e., k_{obs} was slower
553 when the inhibitor concentration increased). Second, could
554 the binding reaction be so slow that the inhibition occurred
555 on one of the two time scales, both of which were after the
556 channel opening: the inhibition occurred (a) in parallel to
557 the time course for desensitization or (b) after the channel
558 had desensitized or in a second time scale? In both cases,
559 the current amplitude would appear to be smaller or
560 “inhibited” because we would have measured the portion of
561 the receptors without any inhibitors bound. However, neither
562 the desensitization rate nor the rate of channel activity
563 recovery (after the channel was pre-exposed to inhibitor and
564 glutamate) was affected (data not shown); these are the same
565 phenomena reported by Balannik et al. (25) for other GYKI
566 compounds. We therefore conclude that the inhibition occurs
567 on the time scale of channel opening, after a full equilibra-
568 tion, consistent with the assumption that the decrease in the
569 rate of channel opening in the presence of an inhibitor was
570 due to inhibition.

571 Classical examples of a two-step inhibition involving
572 enzyme inhibitors are well documented (27, 28). Mechanisms
573 similar to the one proposed in this study (Figure 5), involving
574 a two-step inhibition process, have also been documented
575 with the muscle nicotinic acetylcholine receptor with several
576 inhibitors (29, 30). For the inhibition of the nicotinic
577 acetylcholine receptor by either cocaine (29) or MK-801 (30),
578 the first step yields a corresponding channel that is thought
579 to conduct cations as well as or even better than the channel
580 without an inhibitor, thus exhibiting no inhibition on k_{obs} at
581 either a low or a high ligand concentration. In the case of
582 MK-801, the second step, which yields the nonconducting
583 inhibitor–receptor complex, is thought to only occur through
584 the open-channel state (30). In the case of BDZ-2 and BDZ-
585 3, a two-step process occurs through both the closed-channel
586 and open-channel states, which is evidenced by the decrease
587 in k_{obs} at both low and high glutamate concentrations.

588 *Implication of Receptor Properties and Structure–*
589 *Reactivity Relationship.* The results of this study (Table 1)
590 reveal new features related to receptor properties and the
591 structure–reactivity relationship for these compounds. The
592 comparison of the overall inhibition constant between BDZ-2
593 and BDZ-3 shows that BDZ-2 inhibits the open-channel state
594 >5 -fold more strongly (see Table 1). However, the inhibition
595 constant for the initial receptor–inhibitor complex for the
596 open-channel state between the two inhibitors is identical
597 [i.e., \overline{K}_1^* is $194 \pm 20 \mu\text{M}$ for BDZ-2 as compared to $204 \pm$
598 $18 \mu\text{M}$ for BDZ-3 (Table 1)]. On the other hand, for the
599 closed-channel state, the \overline{K}_1 value associated with the initial
600 step for BDZ-2 is already 10-fold different from the value
601 for BDZ-3 (i.e., $48 \mu\text{M}$ for BDZ-2 vs $514 \mu\text{M}$ for BDZ-3).
602 Furthermore, when the overall inhibition for the closed-
603 channel state is compared, the difference between BDZ-2
604 and BDZ-3 is now 8-fold (i.e., $24.8 \mu\text{M}$ for BDZ-2 vs 210
605 μM for BDZ-3). This comparison suggests that the isomeri-
606 zation reaction for the *closed-channel state* has merely
607 resulted in ~ 2 -fold improvement for “tightening” the com-
608 plex for both inhibitors ($\overline{K}_1^*/\overline{K}_1 = 48/24.8$ for BDZ-2 and
609 $514/210$ for BDZ-3). In contrast, the receptor–inhibitor
610 complex in the *open-channel state* must undergo an ~ 5 -
611 fold change for BDZ-3 ($\overline{K}_1^*/\overline{K}_1 = 204/38$ (see Table 1)) and

612 a staggering ~ 28 -fold change for BDZ-2 (i.e., $\overline{K_1^*}/\overline{K_1} =$
 613 194/6.9). These results thus suggest that the closed-channel
 614 state bound with an inhibitor requires less conformational
 615 change to become a “tighter” complex than the open-channel
 616 state. One possible explanation is that the closed-channel
 617 forms are more “accommodating” to binding of inhibitors
 618 with different structures and are thus more “modifiable”, at
 619 least in the first step, than the open-channel form. Our results
 620 further suggest that the first step associated with the open-
 621 channel state is not the one to distinguish the structural
 622 difference between BDZ-2 and BDZ-3, although both
 623 compounds preferentially inhibit the open-channel state.
 624 Rather, it is the putative isomerization reaction involving the
 625 open-channel state that “sees” or discriminates the bulkier
 626 side chain at the N-3 position for BDZ-3, resulting in the
 627 overall difference in the inhibitory properties between the
 628 two compounds. Our results are further consistent with the
 629 notion by which, as compared with the initial intermediate,
 630 the isomerized receptor–inhibitor complex is tighter, thus
 631 making it possible for a closer interaction between the
 632 binding site and a binder so that the structural difference
 633 between the two inhibitors is distinguished.

634 Using the rapid kinetic techniques, we show that the
 635 mechanism of action and the structure–reactivity relationship
 636 of the two 2,3-benzodiazepine derivatives can now be
 637 characterized in a more detailed fashion than previously
 638 possible. The new findings provide useful clues for the future
 639 design and synthesis of 2,3-benzodiazepine inhibitors that
 640 are more potent and more specific toward a unique receptor
 641 conformation. Our finding that BDZ-3 acts mechanistically
 642 the same as BDZ-2 and binds to the same site as BDZ-2
 643 does, but is a weaker inhibitor, indicates that addition of a
 644 substituent to the N-3 position on the diazepine ring of BDZ-
 645 2, resulting in an increase in size at this position, is expected
 646 to generate a weaker inhibitor. However, our finding also
 647 suggests a possibility that a photolabel, for instance, can be
 648 attached to the N-3 position, and the resulting compound
 649 can serve as a site-directed reagent for labeling and mapping
 650 of the inhibitory site on the receptor. The location of the
 651 site, inferred from this study, is unknown. The location of
 652 this and any other regulatory site on any AMPA receptor
 653 subunit is in turn beneficial to the design and synthesis of
 654 newer 2,3-benzodiazepine derivatives.

655 APPENDIX

656 The channel opening rate process of GluR2Q_{flip}, initiated
 657 by a laser-pulse photolysis measurement with the caged
 658 glutamate, followed a single-exponential rate expression for
 659 $\sim 95\%$ of the rise time (8). This observation was without
 660 exception for all current traces induced by glutamate in the
 661 presence and absence of an inhibitor and was therefore
 662 consistent with the assumption that the binding of glutamate
 663 and/or inhibitor was fast relative to channel opening (8). An
 664 observed rate constant, k_{obs} , can be calculated from eq 1. In
 665 eq 1, I_t represents the current amplitude at time t and I_{max}
 666 the maximum current amplitude. Furthermore, using only
 667 the upper scheme in Figure 5 or the scheme without any
 668 inhibitor bound, k_{obs} can be formulated as in eq 2 to represent
 669 the channel opening reaction.

$$I_t = I_{\text{max}}(1 - e^{-k_{\text{obs}}t}) \quad (1)$$

$$k_{\text{obs}} = k_{\text{cl}} + k_{\text{op}} \left(\frac{L}{L + K_1} \right)^2 \quad (2)$$

670 When the channel opening rate was inhibited noncompeti-
 671 tively (as in Figure 5), the expression for the observed first-
 672 order rate constant was given by eq 3. The derivation of eq
 673 3 was based on the assumption that only the first step was
 674 observable (i.e., this step was assigned to the reaction
 675 involving the formation of the initial inhibitor–receptor
 676 complex) and the second step (i.e., the step leading to the
 677 formation of the final receptor–inhibitor complex via a
 678 presumed isomerization reaction) was faster than the first
 679 step and faster than the rate of channel opening. As such,
 680 the effect of an inhibitor on k_{cl} was determined using eq 4,
 681 where the inhibition constant associated with the open-
 682 channel state ($\overline{K_1^*}$) could be determined (at a low ligand
 683 concentration; see the text for further explanation). At higher
 684 ligand concentrations, the effect of an inhibitor on k_{op} was
 685 determined from the difference between k_{obs} and k_{cl} , as
 686 shown in eq 5, and K_1^* was determined (24).

$$k_{\text{obs}} = k_{\text{cl}} \left(\frac{\overline{K_1^*}}{\overline{K_1^*} + I} \right) + k_{\text{op}} \left(\frac{L}{L + K_1} \right)^2 \left(\frac{K_1^*}{K_1^* + I} \right) \quad (3)$$

$$\frac{1}{k_{\text{obs}}} = \frac{1}{k_{\text{cl}}} + \frac{1}{k_{\text{cl}}} \frac{I}{\overline{K_1^*}} \quad (4)$$

$$(k_{\text{obs}} - k_{\text{cl}})^{-1} = [k_{\text{op}}L/(L + K_1)^2]^{-1}(1 + I/K_1^*) \quad (5)$$

687 An inhibition constant was also independently estimated from
 688 the ratio of the maximum current amplitudes in the absence,
 689 A , and presence, A_I , of an inhibitor, given by eq 6a.

$$\frac{A}{A_I} = 1 + I \frac{(\overline{AL_2})_O}{K_1} \quad (6a)$$

690 where $(\overline{AL_2})_O$ represents the fraction of the open-channel
 691 form and is proportional to the current amplitude. In eq 6b,
 692 this fraction is expressed as a function of the fraction of all
 693 receptor forms.

$$(\overline{AL_2})_O = \frac{\overline{AL_2}}{A + AL + AL_2 + AL_2} = \frac{L^2}{L^2(1 + \Phi) + 2K_1L\Phi + K_1^2\Phi} \quad (6b)$$

694 Equation 6 permitted the calculation of the apparent overall
 695 inhibition constant at a defined agonist concentration. This
 696 is especially important for an inhibitor which exhibits a
 697 different affinity toward the open-channel and closed-channel
 698 states. In that case, the apparent inhibition constant, $K_{\text{I,app}}$,
 699 is further dependent on the agonist concentration.

700 To determine whether BDZ-2 and BDZ-3 bound to the
 701 same site or two different sites, the two inhibitors were used
 702 simultaneously to inhibit the channel activity (31). Specifi-
 703 cally, the amplitude was measured and used, as in eq 6, to
 704 plot $A/A_{\text{I,P}}$ versus one inhibitor concentration (see Figure 6).
 705 Here, one inhibitor was represented as I while the other was
 706 P , all at molar concentrations. Assuming that one inhibitor

707 bound per receptor and binding of one inhibitor excluded
 708 the binding of the other (i.e., one-site model or AI or AP
 709 was allowed but not API), the ratio of the current amplitude
 710 was given by eq 7 (31).

$$\frac{A}{A_{I,P}} = \left(1 + \frac{P}{K_P}\right) + \frac{I}{K_I} \quad (7)$$

711 On the other hand, for a two-site model in which there were
 712 two sites for I and P, respectively (i.e., both AI and AP and
 713 API were all allowed), the ratio of the current amplitude was
 714 given by eq 8.

$$\frac{A}{A_{I,P}} = \left(1 + \frac{P}{K_P}\right) + \left(1 + \frac{P}{K_P}\right) \frac{I}{K_I} \quad (8)$$

715 **ACKNOWLEDGMENT**

716 We thank Gang Li in the lab for collecting some data on
 717 BDZ-3 and Christof Grewer for critical reading of the
 718 manuscript.

719 **REFERENCES**

720 1. Hollmann, M., and Heinemann, S. (1994) Cloned glutamate
 721 receptors, *Annu. Rev. Neurosci.* 17, 31–108.
 722 2. Dingledine, R., Borges, K., Bowie, D., and Traynelis, S. F. (1999)
 723 The glutamate receptor ion channels, *Pharmacol. Rev.* 51, 7–61.
 724 3. Brauner-Osborne, H., Egebjerg, J., Nielsen, E. O., Madsen, U.,
 725 and Krogsgaard-Larsen, P. (2000) Ligands for glutamate recep-
 726 tors: Design and therapeutic prospects, *J. Med. Chem.* 43, 2609–
 727 2645.
 728 4. Tarnawa, I., Farkas, S., Berzensyi, P., Pataki, A., and Andrasi, F.
 729 (1989) Electrophysiological studies with a 2,3-benzodiazepine
 730 muscle relaxant: GYKI 52466, *Eur. J. Pharmacol.* 167, 193–
 731 199.
 732 5. Zappala, M., Grasso, S., Micale, N., Polimeni, S., and De Micheli,
 733 C. (2001) Synthesis and structure-activity relationships of 2,3-
 734 benzodiazepines as AMPA receptor antagonists, *Mini-Rev. Med.*
 735 *Chem.* 1, 243–253.
 736 6. Solyom, S., and Tarnawa, I. (2002) Non-competitive AMPA
 737 antagonists of 2,3-benzodiazepine type, *Curr. Pharm. Des.* 8,
 738 913–939.
 739 7. Zappala, M., Pellicano, A., Micale, N., Menniti, F. S., Ferreri,
 740 G., De Sarro, G., Grasso, S., and De Micheli, C. (2006) New
 741 7,8-ethylenedioxy-2,3-benzodiazepines as noncompetitive AMPA
 742 receptor antagonists, *Bioorg. Med. Chem. Lett.* 16, 167–170.
 743 8. Li, G., Pei, W., and Niu, L. (2003) Channel-opening kinetics of
 744 GluR2Q_{flip} AMPA receptor: A laser-pulse photolysis study,
 745 *Biochemistry* 42, 12358–12366.
 746 9. Li, G., and Niu, L. (2004) How fast does the GluR1Q_{flip} channel
 747 open? *J. Biol. Chem.* 279, 3990–3997.
 748 10. Li, G., Sheng, Z., Huang, Z., and Niu, L. (2005) Kinetic
 749 mechanism of channel opening of the GluRD_{flip} AMPA receptor,
 750 *Biochemistry* 44, 5835–5841.
 751 11. Trussell, L. O., and Fischbach, G. D. (1989) Glutamate receptor
 752 desensitization and its role in synaptic transmission, *Neuron* 3,
 753 209–218.
 754 12. Wieboldt, R., Gee, K. R., Niu, L., Ramesh, D., Carpenter, B. K.,
 755 and Hess, G. P. (1994) Photolabile precursors of glutamate:
 756 Synthesis, photochemical properties, and activation of glutamate
 757 receptors on a microsecond time scale, *Proc. Natl. Acad. Sci.*
 758 *U.S.A.* 91, 8752–8756.

13. Li, G., Oswald, R. E., and Niu, L. (2003) Channel-opening kinetics
 759 of GluR6 kainate receptor, *Biochemistry* 42, 12367–12375. 760
 14. Pei, W., Huang, Z., and Niu, L. (2007) GluR3 flip and flop:
 761 Differences in channel opening kinetics, *Biochemistry* 46, 2027–
 762 2036. 763
 15. Grasso, S., Micale, N., Zappala, M., Galli, A., Costagli, C.,
 764 Menniti, F. S., and De Micheli, C. (2003) Characterization of the
 765 mechanism of anticonvulsant activity for a selected set of putative
 766 AMPA receptor antagonists, *Bioorg. Med. Chem. Lett.* 13, 443–
 767 446. 768
 16. Jonas, P., and Spruston, N. (1994) Mechanisms shaping glutamate-
 769 mediated excitatory postsynaptic currents in the CNS, *Curr. Opin.*
 770 *Neurobiol.* 4, 366–372. 771
 17. Geiger, J. R., Melcher, T., Koh, D. S., Sakmann, B., Seeburg, P.
 772 H., Jonas, P., and Monyer, H. (1995) Relative abundance of
 773 subunit mRNAs determines gating and Ca²⁺ permeability of
 774 AMPA receptors in principal neurons and interneurons in rat CNS,
 775 *Neuron* 15, 193–204. 776
 18. Kwak, S., and Weiss, J. H. (2006) Calcium-permeable AMPA
 777 channels in neurodegenerative disease and ischemia, *Curr. Opin.*
 778 *Neurobiol.* 16, 281–287. 779
 19. Huang, Z., Li, G., Pei, W., Sosa, L. A., and Niu, L. (2005)
 780 Enhancing protein expression in single HEK 293 cells, *J. Neurosci.*
 781 *Methods* 142, 159–166. 782
 20. Udgaonkar, J. B., and Hess, G. P. (1987) Chemical kinetic
 783 measurements of a mammalian acetylcholine receptor by a fast-
 784 reaction technique, *Proc. Natl. Acad. Sci. U.S.A.* 84, 8758–8762. 785
 21. Niu, L., Grewer, C., and Hess, G. P. (1996) *Chemical kinetic*
 786 *investigations of neurotransmitter receptors on a cell surface in*
 787 *a microsecond time region*, Vol. VII, Academic Press, New York. 788
 22. Donevan, S. D., and Rogawski, M. A. (1993) GYKI 52466, a 2,3-
 789 benzodiazepine, is a highly selective, noncompetitive antagonist
 790 of AMPA/kainate receptor responses, *Neuron* 10, 51–59. 791
 23. Rammes, G., Swandulla, D., Spielmanns, P., and Parsons, C. G.
 792 (1998) Interactions of GYKI 52466 and NBQX with cyclothiazide
 793 at AMPA receptors: Experiments with outside-out patches and
 794 EPSCs in hippocampal neurones, *Neuropharmacology* 37, 1299–
 795 1320. 796
 24. Niu, L., and Hess, G. P. (1993) An acetylcholine receptor
 797 regulatory site in BC3H1 cells: Characterized by laser-pulse
 798 photolysis in the microsecond-to-millisecond time region, *Bio-*
 799 *chemistry* 32, 3831–3835. 800
 25. Balannik, V., Menniti, F. S., Paternain, A. V., Lerma, J., and Stern-
 801 Bach, Y. (2005) Molecular mechanism of AMPA receptor
 802 noncompetitive antagonism, *Neuron* 48, 279–288. 803
 26. Armstrong, N., and Gouaux, E. (2000) Mechanisms for activation
 804 and antagonism of an AMPA-sensitive glutamate receptor: Crystal
 805 structures of the GluR2 ligand binding core, *Neuron* 28, 165–
 806 181. 807
 27. Duggleby, R. G., Attwood, P. V., Wallace, J. C., and Keech, D.
 808 B. (1982) Avidin is a slow-binding inhibitor of pyruvate carboxy-
 809 lase, *Biochemistry* 21, 3364–3370. 810
 28. Kulmacz, R. J., and Lands, W. E. (1985) Stoichiometry and
 811 kinetics of the interaction of prostaglandin H synthase with anti-
 812 inflammatory agents, *J. Biol. Chem.* 260, 12572–12578. 813
 29. Niu, L., Abood, L. G., and Hess, G. P. (1995) Cocaine: Mech-
 814 anism of inhibition of a muscle acetylcholine receptor studied by
 815 a laser-pulse photolysis technique, *Proc. Natl. Acad. Sci. U.S.A.*
 816 92, 12008–12012. 817
 30. Grewer, C., and Hess, G. P. (1999) On the mechanism of inhibition
 818 of the nicotinic acetylcholine receptor by the anticonvulsant MK-
 819 801 investigated by laser-pulse photolysis in the microsecond-to-
 820 millisecond time region, *Biochemistry* 38, 7837–7846. 821
 31. Karpen, J. W., and Hess, G. P. (1986) Cocaine, phencyclidine,
 822 and procaine inhibition of the acetylcholine receptor: Character-
 823 ization of the binding site by stopped-flow measurements of
 824 receptor-controlled ion flux in membrane vesicles, *Biochemistry*
 825 25, 1777–1785. 826

Abstract for International Conference on Nucleic Acids, Membrane and Signal Transduction (Shujitsu University, Okayama, Japan, October 20 – October 23, 2004)

Rapid Kinetic Studies of Ion Channel Glutamate Receptors and Development of Novel Aptamers

Zhen Huang, Gang Li and Li Niu. Chemistry Department, Center for Neuroscience Research, State University of New York-Albany, Albany, NY 12222, USA

Ion channel glutamate receptors are ligand-gated transmembrane proteins and form cation-conducting channels upon binding to glutamate, a neurotransmitter in the brain. The function of these receptors is critically involved in brain activities such as memory and learning whereas receptor malfunction has been implicated in neurodegeneration and epilepsy. Development of specific receptor inhibitors has been a long pursued strategy in the treatment of neurological diseases. To study the function of the receptor and the mechanism of drug-receptor interaction, conventional kinetic techniques are not suitable because the time resolution is inadequate to resolve the glutamate-activated channel opening in the microsecond-to-millisecond time domain. We used a laser-pulse photolysis technique with a photolabile precursor of glutamate or caged glutamate (γ -O-(α -carboxy-2-nitrobenzyl)glutamate), which offers a 60 microsecond time resolution. Using this technique, we have characterized the channel-opening kinetic mechanism for glutamate receptors of the AMPA subtype, which is known as the fastest activating channel in the glutamate receptor family. We have investigated the mechanism of inhibition for some benzodiazepine compounds. We have also characterized some key questions in the structure and function relationship. Furthermore, using an iterative method (i.e, SELEX) and a combinatorial RNA library, we have identified a series of novel mechanism-based aptamers that are specific and high affinity towards the receptor. These aptamers are better inhibitors and drug candidates as compared to chemically synthesized inhibitors, because chemically synthesized inhibitors are poorly water soluble, and have cross activity in glutamate receptor family as well as low affinities.

Abstract for Albany 2005: Conversation 14 in Progress of Nucleic Acids and Proteins,
Albany, NY.

Selection and Characterization of Novel Aptamers for Ion channel Glutamate Receptors

Zhen Huang, Gang Li and Weimin Pei, and Li Niu

Chemistry Department, Center for Neuroscience Research, SUNY-Albany, Albany, NY
12222, USA

Ion channel glutamate receptors are ligand-gated transmembrane proteins and form cation-conducting channels upon binding of glutamate, a neurotransmitter. The glutamate receptors are involved in brain activities such as memory and learning whereas receptor malfunction has been implicated in neurodegenerative diseases and epilepsy.

Development of specific receptor inhibitors has been a long pursued strategy in the treatment of neurological diseases. Using an iterative method (i.e., systematic evolution of ligands by exponential enrichment or SELEX) and a combinatorial RNA library of a $\sim 10^{15}$ sequence variation, we have carried out SELEX against the GluR2Qflip glutamate receptor expressed in HEK-293 cells and identified a group of aptamers that are putative competitive inhibitors with nanomolar affinity. These aptamers are better inhibitors and drug candidates as compared with chemically synthesized inhibitors, because the synthetic inhibitors are generally water insoluble, and have cross activity in various subunits of the glutamate receptor family as well as low affinities. We are using rapid kinetic methods including a laser-pulse photolysis technique with a photolabile precursor of glutamate or caged glutamate, to characterize the structure-function relationship of the aptamers with the glutamate receptor in the microsecond-to-millisecond time domain. The novel mechanism of action of these aptamers on the GluR2Qflip glutamate receptor will be presented, together with the prediction of the unique, minimal aptamer structures.

Inaugural meeting of American Academy of Nanomedicine
Baltimore, MD (8/15-8/16, 2005)

Novel Glutamate Receptor Aptamers

Li Niu

Chemistry Department, Center for Neuroscience Research,
State University of New York (SUNY)-Albany, Albany, NY 12222

Ion channel glutamate receptors are ligand-gated transmembrane proteins and form cation-conducting channels upon binding to glutamate, a neurotransmitter in the brain. These receptors are critically involved in brain activities such as memory and learning whereas receptor malfunction has been implicated in epilepsy and neurodegeneration. Development of specific receptor inhibitors has been a long pursued strategy in the treatment of neurological diseases. The current methodology of inhibitor/drug development is based on chemical synthesis. The majority of synthetic inhibitors and drugs are poorly water soluble. The poor water solubility of these compounds has deleterious effects on kidney and liver in clinical trials. In addition, many inhibitors have cross reactivity between kainate and AMPA receptors, and low affinity. Using an *in vitro* iterative method (i.e., SELEX) and a combinatorial RNA library with $\sim 10^{14}$ sequence variations, we have identified a class of mechanism-based aptamers that have nanomolar affinity. These aptamers are water soluble by nature, and are novel in the mechanism of action on the receptor. For instance, we found two aptamer molecules that are identical in sequence but different in structure. Interestingly, the two structurally different aptamers must work as a pair to inhibit the receptor in a competitive fashion. Detailed discussion of these approaches and results shall be presented.

CHANNEL-OPENING KINETICS OF THE GluR3_{flip} AMPA RECEPTOR: A LASER-PULSE PHOTOLYSIS STUDY

Weimin Pei, Zhen Huang, and Li Niu

Department of Chemistry, and Center for Neuroscience Research, University at Albany, SUNY, Albany, NY 12222

Rapid opening of a ligand-gated ion channel receptor is the key step for the receptor to convert the binding of a chemical signal (i.e., neurotransmitters or ligands) into an electrical impulse at a chemical synapse of nervous systems. GluR3 is an AMPA receptor subunit of ionotropic glutamate receptors which are the major excitatory receptors involved in brain function and neurodegeneration. The kinetic properties of GluR3, relevant to the time scale of its channel opening, are not well understood. Using a laser-pulse photolysis technique, which permits glutamate to be liberated photolytically from γ -O-(α -carboxy-2-nitrobenzyl)glutamate (caged glutamate) with a time constant of ~ 30 μ s, we have characterized the receptor channel-opening, prior to the channel desensitization. We found that GluR3_{flip} opens the channel, following the binding of glutamate, with a rate constant of $\sim 9 \times 10^4$ s⁻¹, and closes its channel with a rate constant of $\sim 1 \times 10^3$ s⁻¹. The minimal kinetic mechanism for the channel opening is further consistent with binding of two glutamate molecules with the channel-opening probability being close to 1. As compared to other AMPA receptor homomeric channels, the GluR3_{flip} channel has the largest channel-opening rate constant and the smallest channel-closing rate constant. The results suggest a unique function of this AMPA receptor subunit.

This work was supported by the Department of Defense, American Heart Association, ALS Association, and Muscular Dystrophy Association to L.N.

One Aptamer Sequence, Two Structures: A Collaborating Pair that Competitively Inhibits AMPA Glutamate Receptors

Z. Huang, W.M. Pei, and L. Niu

Department of Chemistry, University at Albany, SUNY, Albany, NY 12211

The α -amino-3-hydroxy-5-methyl-4-isoxazole propionic acid (AMPA) receptor is a subtype of glutamate ion channel receptors. The AMPA receptors play essential role in the mammalian brain activities such as memory and learning, whereas the excessive activation of these receptors has been implicated in neurological diseases such as cerebral ischaemia, epilepsy, Alzheimer's diseases, and amyotrophic lateral sclerosis. Inhibitors against AMPA glutamate receptors are drug candidates for the treatment of these neurodegenerative diseases. Considerable research endeavors have consequently focused on developing glutamate receptor inhibitors to control the excessive receptor activity, as a therapeutic strategy to treat these neurological problems. However, chemically synthesized inhibitors generally have poor water-solubility and unwanted side effects. NBQX (6-nitro-7-sulfamoylbenzo[f]quinoxaline-2,3-dione), one of the most potent competitive inhibitors failed clinical trial due to its toxicity. Using systematic evolution of ligands by exponential enrichment (SELEX), we identified a group of water soluble RNA aptamer inhibitors against the recombinant GluR2Q AMPA receptor channels embedded in the membrane fragments of HEK-293S cells. Using whole-cell recording as a functional assay, we found an aptamer that competitively inhibits the AMPA receptor with nanomolar affinity, rivaling NBQX. Unlike NBQX, however, the aptamer is water soluble, and maintains the same potency in inhibiting the GluR2 AMPA receptor even at clinically relevant acidic pH. Surprisingly, the same sequence of the aptamer assumes two stable structures, both of which are required for competitive inhibition. The intrinsic inhibition constant of one structure was found to be 63 ± 10 nM while the other was 66 ± 18 nM. A mechanism of action is proposed for this collaborating pair. With the nanomolar affinity and water solubility, this aptamer serves as a promising template for the design of novel AMPA receptor inhibitors.

MECHANISM-BASED DESIGN OF APTAMERS FOR GLUTAMATE ION CHANNELS

Li Niu

Chemistry Department, Center for Neuroscience Research,
State University of New York (SUNY) – Albany
Albany, New York, USA

Excitotoxicity is one of the leading pathogenic mechanisms ascribed to a number of neurodegenerative diseases such as amyotrophic lateral sclerosis (ALS). Excitotoxicity is induced largely by the excessive activation of AMPA-type ionotropic glutamate receptors through which Ca^{2+} enters the cell and builds up to a toxic level. Using inhibitors to block the AMPA receptor-mediated excitotoxicity has been a long-pursued therapeutic strategy. However, making and using inhibitors specific for AMPA receptors currently suffers two major problems. The first problem is water solubility. For instance, NBQX, a classical competitive inhibitor for the AMPA/kainate glutamate receptors, failed clinically due to, at least in part, its poor water solubility. Second, the inhibitors are routinely characterized with the desensitized receptor form because the kinetic methods commonly used have insufficient time resolutions to assay the receptor that, upon binding glutamate, opens its channel in the microsecond time region and desensitizes even within a few milliseconds. These problems have hampered the development of effective anti-excitotoxic compounds as potential drugs for the associated neurodegenerative diseases.

We identified a novel class of aptamers or RNA inhibitors against the GluR2Qflip receptor, a key AMPA receptor subunit that controls the calcium permeability and mediates excitotoxicity. An aptamer is a single-stranded nucleic acid that directly inhibits a protein's function. It does so by folding into a specific three-dimensional structure that dictates high-affinity binding to the target protein. Aptamers are water soluble by nature and the majority have nanomolar affinity against the protein target.

A molecular biology approach called systematic evolution of ligands by exponential enrichment (SELEX) was used to evolve these aptamers from a combinatorial RNA library containing 10^{15} sequences. Furthermore the laser-pulse photolysis technique was used as a critical method of screening to identify more specific and more potent aptamers against GluR2Qflip. The latter technique offers a microsecond time resolution so that we can measure the inhibitory effect on the receptor channel-opening process that occurs in the microsecond time region. Such a functional assay has not been previously possible. In running SELEX for aptamer discovery, NBQX, a competitive inhibitor, was used as the selection pressure. The aptamers we identified indeed competitively inhibit the AMPA receptor. We found that the synthetic version of the same sequence for one aptamer has K_d value of 4 nM, rivaling any other inhibitors prepared so far, including NBQX. Unlike NBQX, however, the aptamer is water soluble, and maintains the same potency even at clinically relevant acidic pH.

The aptamer reported here represents a unique, water-soluble lead compound for future design of nanomolar affinity inhibitors with potential therapeutic values in the diagnosis and the treatment of neurodegenerative disorders.

DEVELOPMENT OF APTAMERS AS ANTI-EXCITOTOXIC DRUGS FOR ALS THERAPY

Li Niu

State University of New York (SUNY) - Albany

BACKGROUND: Excitotoxicity is one of the leading pathogenic mechanisms ascribed to amyotrophic lateral sclerosis (ALS). Excitotoxicity is induced largely by the excessive activation of AMPA-type ionotropic glutamate receptors through which Ca^{2+} enters the cell and builds up to a toxic level, causing motor neuron death in ALS. Using inhibitors to block the AMPA receptor-mediated excitotoxicity, which is controlled by the GluR2 subunit, has been a long-pursued therapeutic strategy. However, making and using inhibitors specific for AMPA receptors currently suffers two major problems. First, the number of existing AMPA inhibitors is limited and so is their water solubility. For instance, NBQX, a classical competitive inhibitor for the AMPA/kainate glutamate receptors, failed clinically due to its poor water solubility. Second, the inhibitors are routinely characterized with the desensitized receptor form because the kinetic methods commonly used have insufficient time resolutions to assay the receptor that, upon binding glutamate, opens its channel in the microsecond time region and desensitizes even within a few milliseconds. These problems have hampered the development of effective anti-excitotoxic compounds as potential drugs for ALS therapy.

PURPOSE: We wanted to develop a novel class of powerful aptamer-based drugs against the GluR2Qflip receptor, a key AMPA receptor subunit that controls the calcium permeability and mediates excitotoxicity. An aptamer is a single-stranded nucleic acid that directly inhibits a protein's function. It does so by folding into a specific three-dimensional structure that dictates high-affinity binding to the target protein. Aptamers are water soluble by nature and the majority have nanomolar affinity against the protein target. Aptamers have been increasingly explored clinically as useful reagents.

METHODS: Our research employs a combination of two novel approaches to develop better glutamate inhibitors or RNA aptamers. First, a molecular biology approach called systematic evolution of ligands by exponential enrichment (SELEX) was used to evolve RNA inhibitors from a combinatorial RNA library containing 10^{15} sequences. Second, the laser-pulse photolysis technique was used as a critical method of screening to identify more specific and more potent aptamers against GluR2Qflip. The latter technique offers a microsecond time resolution so that we can measure the inhibitory effect on the receptor channel-opening process that occurs in the microsecond time region. Such a functional assay has not been previously possible.

RESULTS: We have thus far successfully identified a class of aptamers with nanomolar affinity against the GluR2Qflip AMPA receptor subunit, using NBQX, a competitive inhibitor, as the selection pressure. The aptamers we identified, as anticipated, competitively inhibit the AMPA receptor, rivaling NBQX, one of the most potent inhibitors. Unlike NBQX, however, the aptamer is water soluble, and maintains the same potency even at clinically relevant acidic pH. Surprisingly, the same aptamer sequence assumes two structures, and both must bind to inhibit the receptor (with individual $K_I = \sim 65$ nM) as a collaborating pair. The aptamer we described is an excellent template for design of better inhibitors against AMPA glutamate receptors.

CONCLUSION: As an initial proof of principle experiment, our results suggest the possibility of developing competitive inhibitors specific to AMPA receptor subunits. Our results further demonstrate the possibility of evolving useful RNA molecules from a regular, unmodified RNA library using SELEX directed against a total, functional membrane protein from a recombinant source. The aptamer reported here represents a unique, water-soluble lead compound for future design of nanomolar affinity inhibitors with potential therapeutic values in the diagnosis and the treatment of ALS and other neurodegenerative disorders.

TECHNOLOGY (PRODUCT) DESCRIPTION: Inhibitors of AMPA receptors are promising anti-excitotoxic drug candidates. Here we show the excellent properties of the novel aptamers we identified. We are further developing these aptamers into unique, powerful new lead compounds as a novel class of drugs for ALS therapy.

2007- Biophysical Society Meeting
Baltimore, MD (March 3-March 7, 2007)

One Aptamer Sequence, Two Structures: A Collaborating Pair that Competitively Inhibits AMPA Glutamate Receptors

Zhen Huang*, Weimin Pei*, and Li Niu*[‡]

*Department of Chemistry, and Center for Neuroscience Research, University at Albany, Albany, New York 12222; [‡]Corresponding author

The α -amino-3-hydroxy-5-methyl-4-isoxazole propionic acid (AMPA) subtype of glutamate ion channel receptors plays an essential role in the mammalian brain activities such as memory and learning, whereas the excessive receptor activation has been implicated in neurological diseases such as cerebral ischaemia, epilepsy, and amyotrophic lateral sclerosis. Inhibitors acting on AMPA glutamate receptors are drug candidates for potential treatment of these neurological diseases. Using systematic evolution of ligands by exponential enrichment (SELEX), we identified an RNA aptamer, named as AN58, which competitively inhibits the AMPA receptor with nanomolar affinity. Surprisingly, the *in vitro* transcription of the DNA sequence of AN58 produces two stable RNA structures, M1 and M2, both of which are required for competitive inhibition in a 1:1 stoichiometry. The intrinsic inhibition constant of M1 and M2 was found to be 63 ± 10 nM and 66 ± 18 nM respectively. M1 and M2 are formed independently during the same *in vitro* transcription, but are thermodynamically stable and inconvertible even after they are subject to freezing, ethanol precipitation, and boiling in ~50% formamide denaturing buffer containing 7 M urea. Using reverse transcription, we show M1 and M2 can be reversely transcribed into the full-length 58-nt cDNA. However, the reverse transcription reaction also generates distinct, shorter reverse transcripts, suggesting M1 and M2 have different structures. Sequencing of M1 and M2 using primer extension dideoxy chain termination reaction suggests that they have indeed the same sequence. These findings indicate that the same DNA sequence can be transcribed into two RNA structures that are structurally and functionally distinct. Furthermore, with the nanomolar affinity and water solubility, AN58 serves as a useful template for design of novel AMPA receptor inhibitors.

ABSTRACT

2007- Biophysical Society Meeting
Baltimore, MD (March 3-March 7, 2007)

Channel-Opening Kinetics of GluR1Q_{flip} L497Y: A Laser-Pulse Photolysis Study

Weimin Pei, Zhen Huang, and Li Niu

Department of Chemistry, and Center for Neuroscience Research, University at Albany, SUNY, Albany, NY 12222

A single leucine-to-tyrosine substitution in the ligand binding domain S1 of AMPA glutamate receptors is known to turn the corresponding mutant subunits (i.e., L497Y for GluR1, L483Y for GluR2 and L507Y for GluR3) into virtually non-desensitizing homomeric receptor channels, whereas the wild type receptor channels desensitize rapidly in response to the binding of glutamate. Crystallographic studies show that the mutation is located in the interface of two extracellular binding domains and thus causes interference in domain movement, once agonist is bound, which is thought to trigger the channel desensitization. Using a laser-pulse photolysis technique with a caged glutamate, we measured the glutamate-induced channel-opening rate process for GluR1Q_{flip} L497Y mutant channels expressed in HEK-293 cells. We found that the channel-opening rate constant for the mutant channel or k_{op} of $(1.9 \pm 0.1) \times 10^4 \text{ s}^{-1}$ is 1.5-fold smaller than that of the wild type, whereas the channel-closing rate constant of the mutant or k_{cl} of $(140 \pm 26) \text{ s}^{-1}$ is 15-fold smaller than the k_{cl} of the wild type channel. These results suggest that the leucine-to-tyrosine mutation in GluR1Q_{flip} is largely responsible for stabilizing the open-channel conformation. The kinetic results further suggest that the channel-closing rate constant or the lifetime of the open-channel likely controls the channel desensitization.

MAY 19 – MAY 21, 2007. MILAN, ITALY

RNA APTAMERS TARGETTING GLUTAMATE ION CHANNELS AS ANTIEXCITOTOXIC DRUG CANDIDATES

Li Niu

Chemistry Department, Center for Neuroscience Research,
State University of New York (SUNY) – Albany
Albany, New York, USA

Telephone: 518-591-8819; Fax: 518-442-3462; E-mail: lniu@albany.edu

Excitotoxicity is a leading pathogenic mechanism ascribed to a number of neurodegenerative diseases such as amyotrophic lateral sclerosis (ALS). Excitotoxicity is induced largely by the excessive activation of AMPA-type glutamate ion channels. Using inhibitors to block the AMPA receptor-mediated excitotoxicity is a long-pursued therapeutic strategy. However, the majority of existing inhibitors of AMPA channels are small organic molecules and are poorly water soluble. NBQX, for instance, is a classical competitive inhibitor for the AMPA/kainate glutamate receptors but failed clinically mainly due to its poor water solubility. Furthermore, inhibitors are routinely assayed with the desensitized receptor form, because conventional kinetic techniques have insufficient time resolutions to study an AMPA receptor, which, upon binding glutamate, opens its channel in the microsecond time domain and desensitizes in the millisecond time region. These problems have hampered the development of anti-excitotoxic compounds as effective drugs.

Using systematic evolution of ligands by exponential enrichment (SELEX), we identified a class of aptamers or RNA inhibitors, from a RNA library containing $\sim 10^{15}$ sequences, against GluR2Qflip, a key AMPA receptor subunit that controls the calcium permeability and mediates excitotoxicity. An aptamer is a single-stranded nucleic acid that inhibits a protein's function. It does so by folding into a specific three-dimensional structure that dictates high-affinity binding to the target. Furthermore, using a laser-pulse photolysis technique, we screen these aptamers against GluR2Qflip with a microsecond time resolution, sufficient to measure the inhibitory effect of an aptamer with a functional AMPA channel. One of our aptamers was found to have K_d of 4 nM, and this affinity rivals any existing inhibitors, including NBQX. Unlike NBQX, the aptamer is water soluble, and maintains the same potency even at clinically relevant acidic pH. The aptamer represents a unique, water-soluble lead compound with nanomolar affinity for future design of better AMPA receptor inhibitors/drugs for potential therapy of various neurodegenerative disorders. The methods we have developed during this study should be also applicable in general to selection of high affinity inhibitors targeting membrane proteins.

2008 ALS Workshop:
Accelerating ALS Research: Translating Basic Discoveries into Therapies for ALS
January 13 -- January 16, Tampa, FL.

Research Interest

Li Niu, Ph.D.

Department of Chemistry, Center for Neuroscience Research
University at Albany, SUNY
Phone: 518-591-8819; Fax: 518-442-3462; e-mail: lniu@albany.edu

We study glutamate ion channel receptors, and are interested in developing compounds and biological molecules to regulate the receptor activity quantitatively and selectively. Glutamate ion channels mediate synaptic neurotransmission and are indispensable in the brain activity, such as memory and learning. Excessive receptor activation, however, leads to neurodegeneration. Inhibitors of glutamate receptors are thus promising agents to treat neurodegenerative diseases such as ALS. One of the major efforts in my research group is to develop better inhibitors that are more potent, more selective towards AMPA receptor subtype and the subunits involved in the selective motor neuron degeneration in ALS.

We are investigating how synthetic inhibitors block the receptor channel opening in the μ s-to-ms time region. In order to test these compounds on the receptor activity we use a laser-pulse photolysis technique with a caged glutamate to measure the channel opening and the effect of an inhibitor on the channel-opening process in the μ s time domain. At the present, we focus on characterization of 2,3-benzodiazepine compounds, a class of the most potent noncompetitive inhibitors. We are trying to establish the structure-reactivity relationship, based on the high time resolution data, so that better inhibitors can be designed and synthesized.

We are also using these compounds as structural probes to investigate the location and properties of the sites of interaction between inhibitors and receptors. For this purpose, we are also using NMR to determine the structures of chemical inhibitors and nucleic acid inhibitors in the absence and presence of the S1S2 AMPA receptors (the S1S2 receptor is a partial receptor protein containing the extracellular binding domain, amenable to structural studies).

We also attempt to develop nucleic acid-based inhibitors or aptamers as drug candidates. This approach is different from conventional drug design strategy mostly based on organic synthesis. Using a molecular biology approach called SELEX, we have identified some aptamers, from a RNA library ($\sim 10^{15}$ sequences), with nanomolar affinity and novel mechanisms of action. These aptamers are novel templates for design of drugs and diagnostic reagents with higher affinity and selectivity.

List of personnel in my laboratory who have received salary support from this grant

Li Niu

Dr. **Gang Li**, Research Scientist.

Dr. **Zhen Huang**, Research Scientist

Dr. **Jae Seon Park**, Research Scientist

Dr. **Zhenyu Shen**, postdoctoral fellow

Mr. **Sabarinath Jayaseelan**, graduate student who has passed all qualifying exams and working towards his Ph.D. degree

Ms. **Yan Han**, a graduate student working towards her Ph.D. degree

Mr. **Joe Wang**, a graduate student working towards her Ph.D. degree

The following people have received pay from this grant and who have also received degrees.

Dr. **Weimin Pei**, a graduate student in my lab who completed his Ph.D. thesis study in December 2006. He returned China early this year.

Mr. **Mark Ritz**, a graduate student who completed his MS degree and is now working in a chemical company in Albany, NY.

Mr. **Leivi A. Sosa**, an undergraduate who got his research training in my lab. He was awarded a BS and is now in Downstate Medical College in New York City. He has been enlisted as a navy officer subsequently.

Ms. **Jamie Cohen**, an undergraduate student who was a chemistry major, and got her research training in my lab. She is now a medical student in SUNY-Buffalo.